The repair of a site-specific DNA double-strand break during meiosis

Rebecca Anna Johnson

A thesis submitted for the degree of:
Doctor of Philosophy

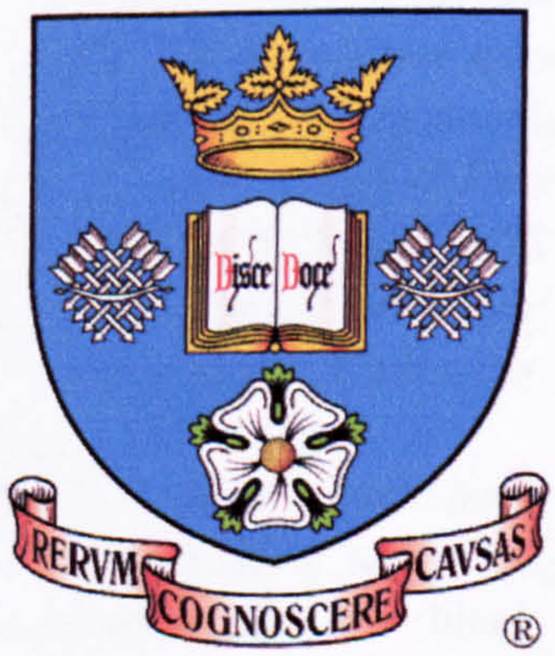

July 2007

The University of Sheffield

Department of Molecular Biology and Biotechnology

Summary

The repair of a site-specific DNA double-strand break during meiosis

Rebecca Anna Johnson

Meiotic recombination is initiated by DNA double strand breaks (DSBs), catalysed by the protein Spo11 (Spo11p-DSBs). In meiotic cells, repair of the Spo11p-DSBs is directed towards the homologous chromosome, establishing physical connections between homologous chromosome pairs. It is these physical connections, visualised genetically as chiasmata that facilitate appropriate segregation of chromosomes during the first meiotic division, and thus prevent aneuploid progeny.

A reporter cassette that suffers a Spo11p-independent DSB, VDE-DSB, was utilised through out this study. This reporter cassette can be used to examine many facets of meiotic DSB repair; including template choice, repair kinetics and the genetic regulation of 5´ to 3´ resectioning of DNA.

In cells mutant for *DMC1* repair of the VDE-DSB was prevented; this was not dependent upon cell cycle. The *dmc1Δ* block was relieved when made doubly mutant with certain recombination genes, leading to the development of a Dmc1p-dependent pathway for repair.

A correlation was identified between the prevention of VDE-DSB repair and the amount of ssDNA within a cell, leading to the hypothesis that sequestration of repair machinery was responsible for the block of repair in *dmc1Δ* cells. Chromatin immunopreciptation (ChIP) was utilised to identify that Rfa-1, a subunit of RPA, was in limited supply at the VDE-DSB when compared to a Spo11p hotspot, in *dmc1Δ* cells. This data suggests that sequestration of ssDNA binding proteins is be responsible for the block of repair found in *dmc1Δ* cells.

Mre11p and Exo1p function during VDE-DSB repair was also assayed. Mre11p was found to have a direct role in regulation of resectioning at VDE-DSB - a role downstream of its accepted involvement in removal of Spo11p from the break site. *exo1Δ* cells were found to have a very severe phenotype with an almost total lack of repair. This study has implicated Exo1p in the initiation and processivity of resectioning at the VDE-DSB.

Acknowledgements

First and foremost I would like to thank my supervisor, Alastair. For the opportunity, guidance and support during the last three years and for the knowledge that the door to your office was always open. Thank you.

To the members of the Goldman and Sudbury Groups past and present. I would like to thank in particular Anna and Madhu for guidance when I was a fresh faced first year, Sheils for our chats and Matt for help with all things technical. A big thank you to all the other members of the group for making my time in the lab so special and for advice whenever needed: Pete, Bernardo, Muhammed, Kay, Andrew (thanks for the proof reading!), Slava, Adam and Hannah. Many thanks also to my collaborators throughout this thesis – Matt Neale, Valerie Borde, Sheila Harris and to people who provided plasmids: Beth Rockmill and Stefan Milson. I'd also like to say a special thanks to the fabulous Janet for making the lab such a smooth running ship, your holidays were always dreaded! Of course to my fellow members of the Hydra (no longer four headed!): Hel Belle, Rachy (thanks for all the help with protein work), Lyds (best bay partner ever) and Laura. You girls are fab, I'll miss our time together so much. Big thank you to all my friends in the Department (especially Ab and Sam, two really great friends), too many ace people to mention. You make Firth Court such a special place. Not forgetting my Lincoln Girls: Kimmy (will always be our Sheffield), Joey and Jules.

To my amazing family: my Mother, Father, Grandparents, Trix, Kieron and my divine baby nephew Joseph. Thank you so much for all of the love and unstinting support over the past four years in particular. This thesis would not have been possible without you. Finally, a great big thank you to Al. Thank you for being lovely and for never complaining during my write up, even though I'm know I was difficult to live with at times. You have provided me with some fabulously glamorous distractions throughout this PhD and a very exciting goal to work towards – here's to New York!

Abbreviations

ADE	adenine
AE	axial element
Ade+	adenine prototrophic
amp	ampicillin
amp^R	ampicillin resistance
BLM	Bloom Syndrome
BSA	bovine serum albumin
C. elegans	*Caenorhabditis elegans*
° C	degrees Celsius
CE	central element
ChIP	chromatin immunoprecipitation
Chr. Coord	chromosomal coordinates
CTAB	hexadecyltrimethylammonium bromide
C-terminal	carboxy-terminal
D. melanogaster	*Drosophila melanogaster*
dAG	diploid strain number
DAPI	4′,6′–diamidino–2–phenylindoline
dH_20	deionised water
DNA	deoxyribonucleic acid
dNTP	deoxynucleotide triphosphate
DSB(s)	double strand break(s)
ds	double stranded
E. coli	*Escherichia coli*
EDTA	ethylene-diaminetetraacetic acid
FISH	fluorescence *in situ* hybridisation
5-FOA	5-fluoroorotic acid
G418	G418 Disulphate

hAG	haploid strain number
HO	homothallic
HR	homologous recombination
hr	hour
IR	ionising radiation
KAc	potassium acetate
kb	kilobases
l	litre
LE	lateral element
µg	microgram
µl	microlitre
M	mole
mM	millimolar
mbar	millibar
mg	milligram
min	minute
ml	millilitre
MI/II	first/second meiotic division
MMS	methyl methanesulphonate
MNase	micrococcal nuclease
MRX	Mre11p/Rad50p/Xrs2p complex
OD_x	optical density$_{wavelength}$
ORF	open reading frame
pAG	plasmid strain number
PAGE	Polyacrylamide Gel Electrophoresis
PCR	polymerase chain reaction
PEG_{3500}	polyethylene glycol $_{3500}$
rpm	revolutions per minute
RT	Room Temperature
S. cerevisiae	*Saccharomyces cerevisiae*

S. pombe	*Schizosaccharomyces pombe*
Sc	synthetic complete (medium)
SC	synaptonemal complex
SDSA	synthesis dependent strand annealing
sec	seconds
ss	single stranded
SSA	single strand annealing
SPB	spindle pole body (microtubule organising centre)
2TY	2x tryptone, yeast extract
Unpub.	unpublished
URA	uracil
UV	ultraviolet
UP-H_20	ultra pure water
VDE	*VMA1*–derived endonuclease
v/v	volume by volume
w/o	without
w/v	weight by volume
w/w	weight by weight
WT	wildtype
YEPD	Yeast extract peptone D-glucose

Nomenclature

Wildtype genes are referred to in italicised capitals, e.g. *SPO11*

Mutant genes are referred to in lowercase italics, e.g. *spo11*

Δ indicates that a gene has been deleted from a strain

Proteins are referred to in non–italic, with first letter capitalised, e.g. Spo11

For emphasis, the suffix, p, is added to proteins, e.g. Spo11p

Full Latin names of organisms are italicised, e.g. *Saccharomyces cerevisiae*

TFP1/TFP1 indicates homozygosity at the *TFP1* allele

TFP1::VDE/TFP1 indicates heterozygosity at the *TFP1* allele

spo11f represents the *spo11–Y135F–HA3His6::KanMX* allele

Δproduct refers to the deletion product in figure legends

Contents

Chapter One

Introduction

1.1 *Saccharomyces cerevisiae*

Saccharomyces cerevisiae (S. cerevisiae), known also as baker's yeast, is a single celled eukaryote that has been established as an organism of immense importance in the understanding of eukaryotic molecular genetics. *S. cerevisiae* organises its small 14 Mb genome into 16 linear chromosomes. This genome has been fully sequenced and annotated, greatly assisting the advance of molecular biology techniques and the subsequent understanding of higher eukaryotic organisms.

S. cerevisiae is an ideal model organism for the study of meiosis, as changes in the environment, e.g. the deprivation of glucose and nitrogen, and the presence of a non-fermentable carbon source (e.g. potassium acetate) can activate meiosis. The production of spores following meiosis greatly facilitates the examination of meiotic products, as they remain tightly associated thanks to the spore coat.

1.2 Meiosis – An introduction

Meiosis is the process of cell division that results in the halving of chromosome number. It is the mechanism by which gametes are formed; hence it is essential for sexual reproduction. In a manner analogous to that of mitosis, initially the chromosomes are replicated, resulting in the production of two identical sister chromatids. The meiotic cell then undergoes two successive rounds of division, in stark contrast to mitosis in which only one divisional event occurs. The first of the meiotic divisions (MI) separates the homologous chromosomes, referred to as reductional division. This is followed by a second round of division (MII) that serves to separate the sister chromatids, which is termed equational division. It is the tightly regulated control of the segregation events that prevents aneuploid

progeny. The process of meiosis results in the production of genetically distinct daughter cells, all four of which have a haploid genotype containing one copy of each sister chromatid. Figure 1.1 is a comparison of divisional events during the mitotic and meiotic cell cycles.

Meiosis is a highly controlled and ordered event, which if allowed to proceed without the necessary tight regulation, can result in the production of aberrant chromosome numbers. Aneuploid meiotic progeny, as a result of meiosis I non-disjunction, is a rare event in unicellular organisms. Only approximately 1 in 10,000 meioses result in aneuploid spores (e.g. monosomic diploid or disomic haploid). In *S. cerevisiae* disomy is tolerated (Sears *et al.*, 1992), but inviable *S. cerevisiae* cells occur when a haploid lacks one of the 16 chromosomes, as all 16 chromosomes encode essential genes. Conversely, in multicellular organisms the frequency of meiosis I non-disjunction is widely varied. Studies using murine models have shown a much higher frequency with 1 % - 2 % of all fertilisations containing an aneuploidy (Hassold and Hunt, 2001). In humans, aneuploidy is the most commonly identified chromosomal abnormality, with an estimated 10 - 25 % of all fertilisations containing an aberrant chromosome number. Among liveborns, the most common forms of aneuploidy is trisomy chromosome 21 (Down's Syndrome), trisomy chromosome 13 (Patau Syndrome), and a number of sex chromosome disorders (XXX syndrome in females; XXY – Klinefelter's Syndrome, and XYY syndrome in males) (Hassold *et al.*, 1995).

1.2.1 Meiotic prophase

The process of meiosis I is a far lengthier event than that of meiosis II or mitosis. This is thought to be due to the increased complexity of the event and the formation of the Synaptonemal Complex (Synaptonemal Complex; SC), a meiosis I specific structure. Throughout the first stage of prophase I: leptotene, the chromosomes are observed as thread-like structures in which no single chromosome is perceptible to be separate from the others. As of yet, no

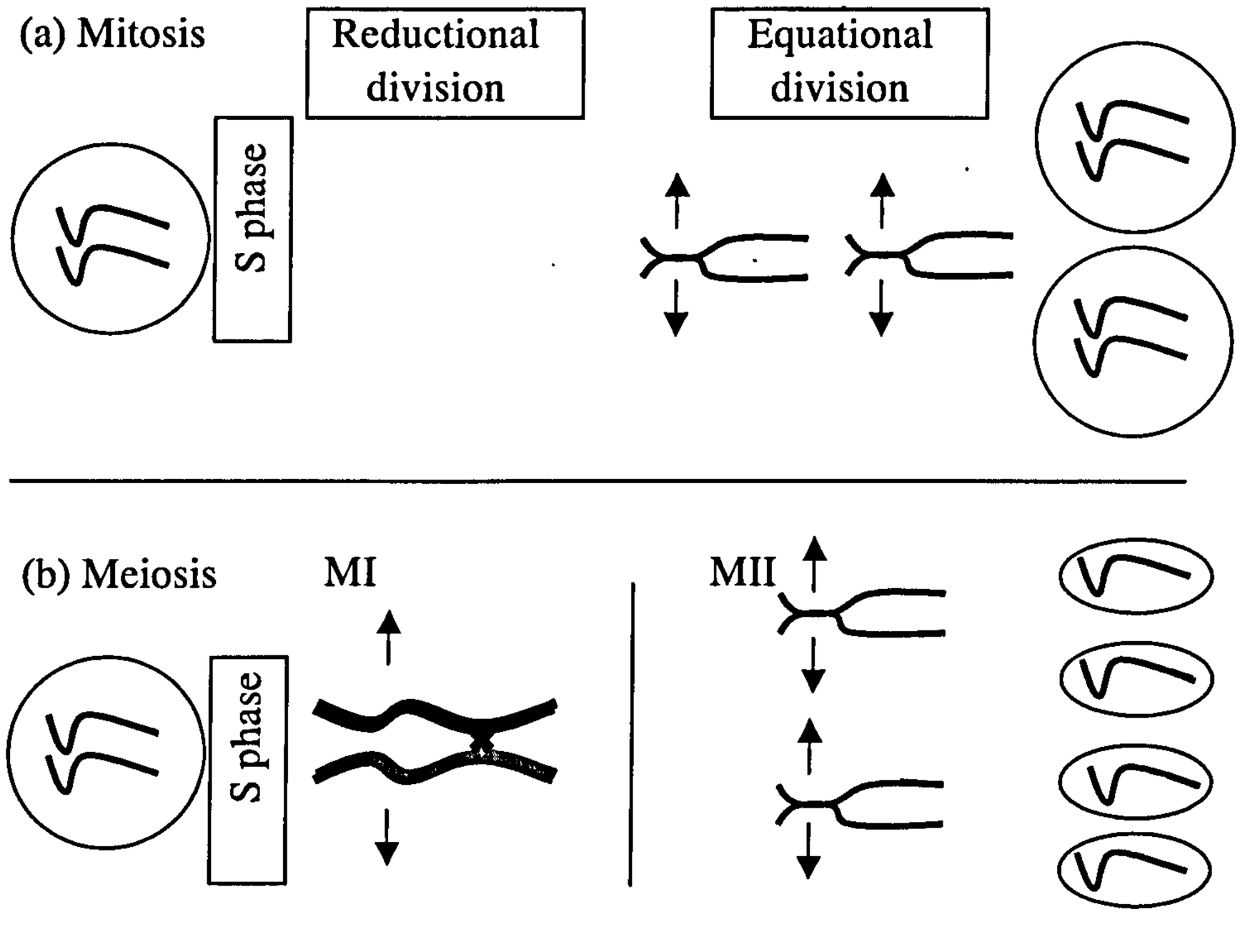

Figure 1.1: Comparison of Mitosis and Meiosis. Prior to the one mitotic and two meiotic nuclear division(s), the chromosomes are replicated to create sister chromatids. (a) During mitosis, sister chromatids are associated through sister chromatid cohesion to ensure bipolar orientation on the metaphase plate. Spindle fibers from opposite poles become attached to the sister kinetochores, and via pole-ward forces, the chromosomes become appropriately orientated. At anaphase, loss of sister chromatid cohesion along the chromatid arms, permits sister chromatid disjunction to opposite poles (b) Prior to the first meiotic division, homologous chromosomes become aligned and recombine, creating crossovers. Connected homologues undergo bipolar orientation on the MI spindle (analogous to sister chromatids in mitosis). At anaphase I, loss of sister chromatid cohesion along the chromosomal arm regions permits the homologue kinetochores to move to opposite poles, while maintenance of sister chromatid cohesion at the centromeric regions ensures that the segregation is reductional. For the second meiotic division, sister chromatids become aligned. Loss of sister chromatid cohesion in the centromeric regions marks anaphase II, permitting the disjunction of sister chromatids (figure adapted from Zickler and Kleckner, 1998).

underlying organisation or structure has been identified (Zickler and Kleckner, 1999). During zygotene the chromosomes can then be seen to pair with their homologue and synapse along their length. The homologues themselves are brought together in separate processes. Firstly, the chromosomes colocalise to the same physical space. After co-localisation the chromosomes co-align, this results in the structural axis. During the first meiotic division, it is the homologues and not the sister chromatids that are separated. At the onset of zygotene, the chromosomes begin to condense and can be visualised individually. As this condensation event takes place, the chromatin structure of the chromosomes is simultaneously altered, resulting in a highly ordered array of loops. It is the underside of these loops that go on to form the chromosomal axes (Zickler and Kleckner, 1999). Figure 1.2 shows the MI and MII events and divisions in *Secale cereale* microsporocytes.

1.3 Prophase in detail

During prophase I striking modifications to chromosome organisation in the meiotic nucleus occur. Gross conformational changes occur including: chromosome condensation, pairing, and synapsis. Recombination occurs preferentially between homologous chromosomes and alters chromosomal conformation at the nucleotide level, in the generation of gene conversions, and at the structural level, in the formation of chiasmata.

1.3.1 Sister chromatid cohesion

Sister chromatid cohesion is established during S-phase as shown through *in situ* hybridisation experiments (Guacci *et al.*, 1994). Sister chromatid cohesion prevents the precocious separation of sister chromatids during attachment on the mitotic spindle. In mitotic cells a multisubunit complex is required for cohesion between sister chromatids, comprising of cohesion proteins: Smc1p, Smc3p, Scc1p

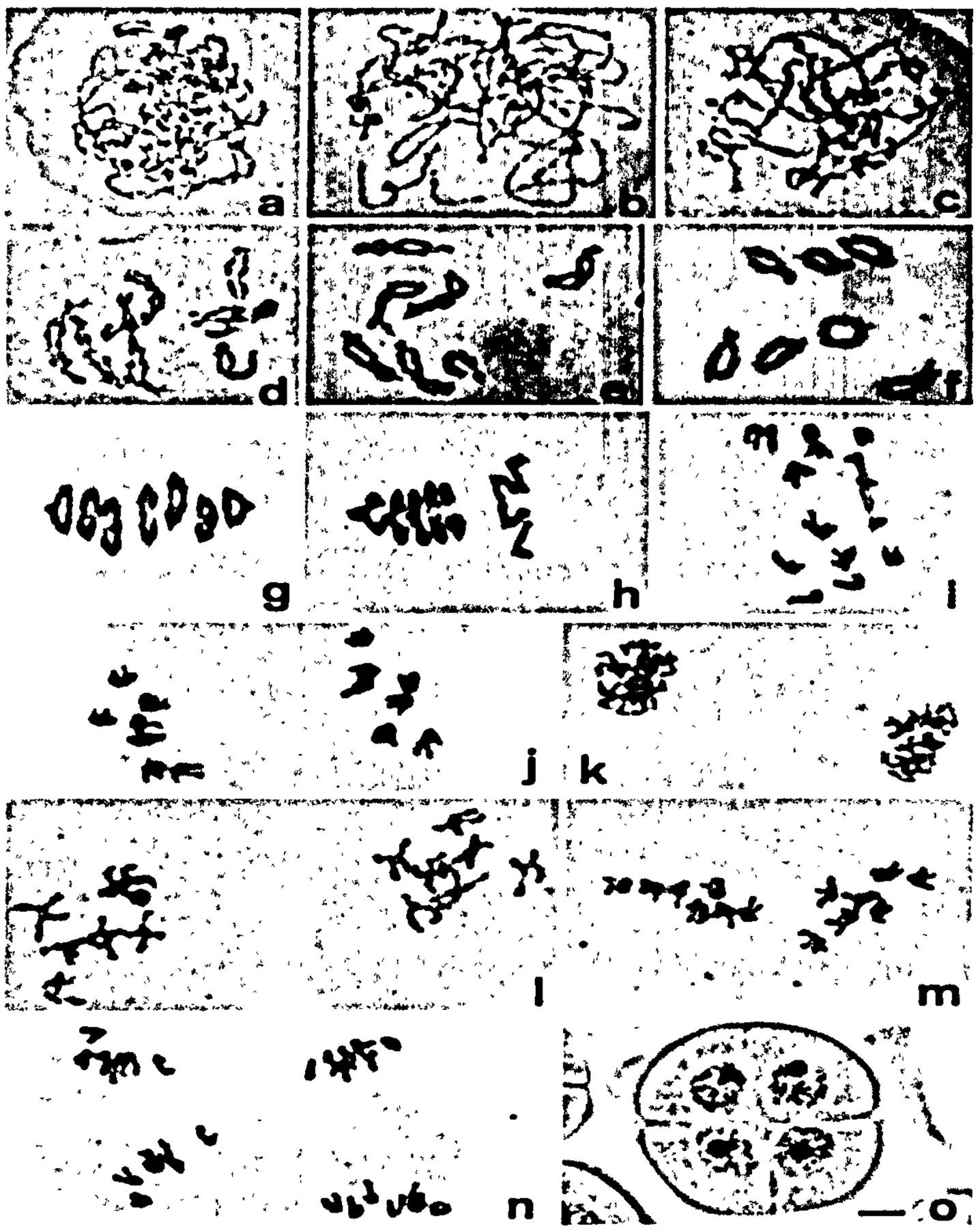

Figure 1.2: Meiotic divisions I and II in the rye *Secale cereale* microsporocytes. (a-f) Prophase I, (a) early zygotene; chromosomal condensation and early pairing. (b-d) early to late pachytene; continued chromosomal condensation and homologue pairing, followed by synapsis. (e) Diplotene; progressive loss of sister chromatid cohesion. (f) Diakinesis; homologous chromosomes are distinguishable, connected by chiasmata. (g, h) Metaphase I; homologous chromosomes align on the MI spindle. (i, j) Anaphase I; reductional segregation of homologues. (k) Telophase I. (l) Prophase II. (m) Metaphase II; sister chromatids align along the MII spindle. (n) Anaphase II; equational segregation of sister chromatids. (o) Four haploid pollen cells (Bar = 5μm) (Figure taken from Zickler and Kleckner, 1998).

and Ssc3p. In meiotic cells, this sister chromatid cohesion is mediated through the Scc1p orthologue Rec8p (Klein *et al.*, 1999) (Miyazaki and Orrweaver, 1994), although Scc1p cannot substitute for Rec8p in meiosis, probably due to Rec8p's additional involvement in recombination and SC formation (Yokobayashi *et al.*, 2003). At the first meiotic division the sister chromatids remain tightly associated with cohesion only lost distal to the crossover (Reviewed in (Nasmyth *et al.*, 2000)). Sgo1p (shugoshin), from *S. cerevisiae*, has recently been shown to have sequence similarity to MEI-S332p of *Drosophila melanogaster*, a protein required for the persistence of cohesion at the centromeres at meiosis I (Lee and Orr-Weaver, 2001). Studies have shown that Sgo1p is required for maintenance of Rec8p at centromere locations during meiosis I (Katis *et al.*, 2004).

1.3.2 Genetic control of homologous chromosome alignment

The bringing together of homologous pairs is achieved by three concurrent processes: pairing, recombination and synapsis. It has been recently proposed that these three processes are mechanistically related, as discussed by Agarwal and Roeder (Agarwal and Roeder, 2000; Tsubouchi and Roeder, 2003; Henderson and Keeney, 2004; Petukhova *et al.*, 2005). This hypothesis has been forwarded as proteins functioning in all three processes are shared, which would explain how the three processes could be so intimately linked (Agarwal and Roeder, 2000; Chen *et al.*, 2004). Furthermore, if proteins were shared amongst these processes, once pairing is initiated, synapsis and recombination would be automatically activated.

Although the mechanism of homologue pairing is not fully understood, there appears to be a link with recombination. FISH (Fluorescent *in situ* hybridisation; FISH) studies in *S. cerevisiae* have shown that the number of pairing sites is similar to the number of recombination events. An observation that supports the hypothesis that early pairing events later serve as initiation of recombination sites (Weiner and Kleckner, 1994).

In yeast both Hop2p and Mnd1p are known to be involved in homologue pairing; it has recently been suggested that they are specifically involved in facilitating homologue recognition. *hop2Δ* cells fail to pair and possess an inability to repair DSBs; this persistence of unrepaired DSBs triggers the pachytene checkpoint and the cells arrest. *hop2Δ* cells are found to have a complement of SCs that have formed between non-homologous chromosomes (Leu *et al.*, 1998). *mnd1Δ* cells also arrest at the pachytene stage, with arresting cells lacking a mature SC complement. Interestingly, Hop2p and Mnd1p are known to act in concert as they form a heterodimer termed H_2M_1, (Tsubouchi and Roeder, 2002). A putative role of the heterodimer is in that of homologue pairing (Chen *et al.*, 2004; Petukhova *et al.*, 2005).

1.3.3 Formation of the bouquet

The term 'bouquet' is given to the structure formed during the organisation of the telomeres to a distinct nuclear lamina location, occurring at the leptotene/zygotene transition, concurrent with the formation of DNA Double Strand Breaks (Double Strand Breaks; DSBs). The formation of a bouquet results in the anchoring of chromosome ends to the inner membrane of the nuclear membrane, close to the Spindle Pole Body (Spindle Pole Body; SPB) (Zickler and Kleckner, 1999). The bouquet is a meiosis specific structure, however, its precise role is still unknown. It has been suggested that the bouquet may have a role in chromosome pairing, as *ndj1* mutant cells, which do not form the bouquet, have been shown to exhibit a two hour delay in alignment, suggesting that Ndj1p promotes homologue pairing but is not essential (Trelles-Sticken *et al.*, 2000). Ndj1p (Tam1p in mammals) is a meiosis specific protein, which localises to the telomeres (Conrad *et al.*, 1997; Trelles-Sticken *et al.*, 2000). An increase in ectopic recombination (recombination between homologous inserts on non-homologous chromosomes) is also seen in *ndj1* cells (Goldman and Lichten, 2000). This suggests that Ndj1p and by

inference the bouquet, functions to restrict deleterious homologous recombination between repeated sequences (Goldman and Lichten, 2000).

Currently, how the bouquet formation facilitates pairing is not fully known. In a number of organisms including Silkworms and Mouse, the first chromosome regions to undergo synapsis are the telomeres (Rasmussen, 1986; Scherthan *et al.*, 1996). However, detailed examination in human spermatocytes reveals that telomeric synapsis may precede bouquet formation (Rasmussen, 1986). If the hypothesis that pairing initiates in the telomeres is correct, (present in, or prior to the bouquet), as these studies suggest, zippering up of paired contacts in a telomere to interstitial direction would increase the likelihood of producing interlocks between heterologous chromosomes (A possibility discussed in Zickler and Kleckner, 1998). Even though interlocks are rare during the late stages of prophase I (discussed in Zickler and Kleckner 1998), there is evidence that they occur frequently during zygotene, suggesting that synapsis does indeed proceed in a telomere to interstitial direction (Rasmussen, 1986). However, as interlocks are rare in pachytene, some authors suggest that the formation of the bouquet, or entry into and out of the bouquet facilitates only the juxtaposition of telomeric regions, which would otherwise associate poorly (Zickler and Kleckner, 1998)

Additional chromosome movements take place during the meiotic cell cycle; rotational chromosome movements during prophase have been detected in the fission yeast *Schizosaccharomyces pombe* (*S. pombe*) - a period of dramatic nuclear movement occurs during meiotic prophase. For two to three hr, the telomeres move back and forth between the cell poles (Svoboda *et al.*, 1995; Hiraoka *et al.*, 2000). These chromosome movements have been shown to be sensitive to microtubule inhibitors, suggesting the reorganisation is dependent upon microtubule polymerisation and depolymerisation (Svoboda *et al.*, 1995). It has been suggested that these chromosome movements may serve to increase the probability (per specified unit of time) that homologous sequences are in contact, and thus benefit the pairing of homologous sequences (Zickler and Kleckner, 1998)

In essence, the role of the bouquet is thought to be in the facilitation of the reorganisation of the chromosomes, thus assisting in the juxtaposition of the homologues. After the bouquet structure breaks down, movements of the chromosomes appears to cease. As the cells enter pachytene the SC links the homologues to one another.

1.3.4 The synaptonemal complex

The synaptonemal complex is a meiosis-specific, tripartite proteinaceous structure that functions to assist the exchange of genetic material between homologues (reviewed in (Heyting, 1996)). The SC is an important feature of the meiotic chromosome, perhaps illustrated by its presence in a wide range of unrelated organisms from *S. cerevisiae* to *D. melanogaster*, though there may be subtle differences at the ultra-structure level. In *S. pombe* and *Aspergillus nidulans* there is no SC formation, although in *S. pombe* Lateral Elements, components of mature SCs similar to those formed in *S. cerevisiae*, are found.

1.3.5 The structure of the SC

The detailed knowledge of the SC has been possible due to the identification of several protein subunits form purified SCs. Formation of the SC begins as the chromosomes condense in early leptotene. The establishment of the SC is progressive and initiates with the production of the Axial Elements (Axial elements; AEs) - an assembly of rod like structures, which extend down the length of the chromosomes and go on to form the Lateral Elements (Lateral Elements; LEs). So far, three proteins have been identified as components of the LEs: Hop1p, Red1p and Zip1p, with Hop1p and Red1p both localising to the AEs, and Zip1p localising to the Central Element (Central element; CE) (Smith and Roeder, 1997). The CE is the name given to the structure that runs down the length of the SC, at an equal distance from the LEs. The LEs are then connected to the CE via

an additional component termed the transverse filament (the 'zip') (Zickler and Kleckner, 1999). The assembly of the SC was determined by Electron Microscopy of meiotic spreads and sectioning techniques (Moses and Solari, 1976) and more recently, the 3–D structure of the SC was revealed by Electron Tomography (Schmekel *et al.*, 1993). Figure 1.3 shows a proposed model for the structure of the SC, and its relative position on the chromatin of the homologous chromosomes.

The relationship between chromosome synapsis and recombination appears to vary, depending on the organism being studied. In *S. cerevisiae*, mutants blocked for SC formation, still create Spo11p-DSBs, whilst in cells mutant for *SPO11*, where meiotic DSBs are prevented, SC formation is also blocked. This implies that in yeast, Spo11-DSBs are not only initiated before synapsis, but they are also a necessity for the formation of the SC. Hence, synapsis is not required for the initiation of recombination. This is in unity with studies of the timing of recombination and synapsis in *S. cerevisiae*, where it was described that meiotic DSBs were initiated in early prophase, prior to the appearance of the SC (Padmore *et al.*, 1991). However, this is not true for *Caenorhabditis elegans* or *D. melanogaster* females where full SCs form in cells lacking *SPO11* orthologues (Dernburg *et al.*, 1998; McKim and Hayashi-Hagihara, 1998). Conversely, in *A. nidulans* and *S. pombe,* organisms that do not form SCs, recombination still occurs. In *Coprinus comatus* cells lacking functional Spo11p, synapsis can be restored if artificial DSBs are introduced (Celerin *et al.*, 2000).

Events downstream of the initiation of recombination can also be influenced by the start of synapsis in *S. cerevisiae*. Mutants that form WT levels of Spo11p-DSBs but are defective in DSB repair, e.g. *dmc1Δ* and therefore accumulate recombination intermediates, form only partial SCs (Prinz *et al.*, 1997).

The breakdown of the SC leads to homologue separation over much of the length of the previously synapsed bivalent. It is at this stage, diplotene that the only remaining homologue contacts are at a few points known as a chiasma. Chiasmata are visible cytologically because they mark the site of non-sister chromatid

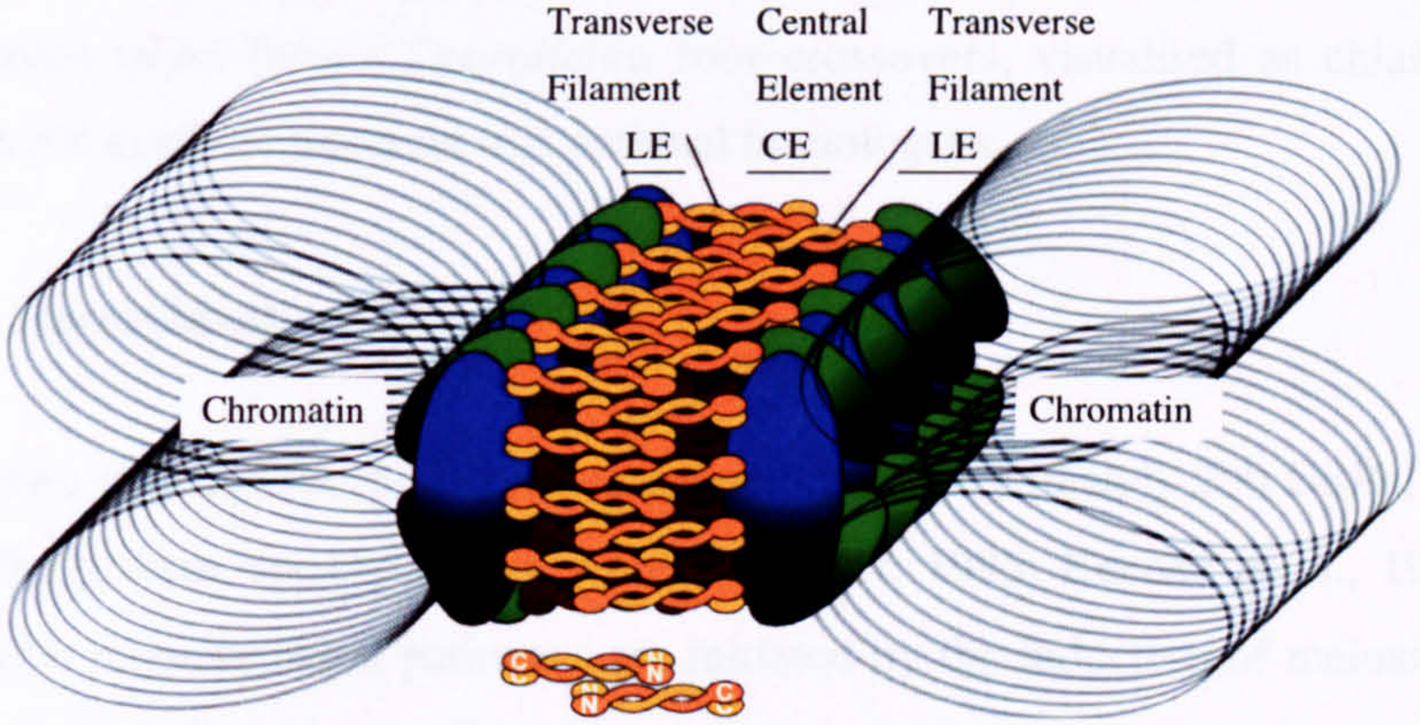

Figure 1.3: Proposed model of the structure of the synaptonemal complex. A model in cross section taken through the synaptonemal complex, and its relative position on the chromatin of homologous chromosomes. The position of the Lateral Elements (LE), the Transverse Filaments, the Central Element (CE), the cohesin/condensin complexes (blue) and the additional proteins of the Lateral Elements (green) (figure taken from Page and Hawley, 2004.)

exchange between the homologues of a bivalent. In organisms with large, well-defined chromosomes (e.g. Grasshopper, *Chorthippus parallelus*) the four sister chromatids become visible at diplotene. This permits the visualisation of chromatid exchange at the point of each chiasma. Figure 1.4 shows a diplotene bivalent taken from *C. parallelus,* four crossovers, visualised as chiasmata, are seen between the maternal and paternal homologues.

1.4. Recombination

In yeast meiosis, recombination is initiated by approximately 200 DSBs, catalysed by the protein Spo11p (Keeney and Kleckner, 1995; Keeney *et al.*, 1997). All meiotic recombination pathways are initiated by the induction of meiosis-specific DSBs; these breaks were first observed in genomic regions that recombine at high frequencies (Nicolas *et al.*, 1989). Evidence to support the proposal that DSBs are the catalyst for meiotic recombination, includes the observed increase in recombination frequency when DSBs are introduced into WT cells (Kolodkin *et al.*, 1986; Malkova *et al.*, 1996) and the correlation shown between DSB formation and recombination kinetics (Cao *et al.*, 1990; Padmore *et al.*, 1991; Goyon and Lichten, 1993).

1.4.1 Formation of the Spo11p double strand break

Meiotic DSB formation in *S. cerevisiae* has an absolute requirement for the protein products of at least 11 genes, *MEI4, MER1, MER2, REC102, REC104, REC114, MRE2* and *SPO11,* which are all meiosis-specific, plus *MRE11, RAD50* and *XRS2.* Null mutations of any of these genes abolish both DSB formation and meiotic recombination (comprehensively reviewed Krogh and Symington, 2004).

Spo11p shares homology with TOP6A, the catalytic subunit of archeal type II topoisomerase from *Sultalobus shibatare* (Bergerat *et al.*, 1997). In *S. cerevisiae*, DSBs, Holliday Junctions (Holliday Junctions; HJ) – recombination intermediates,

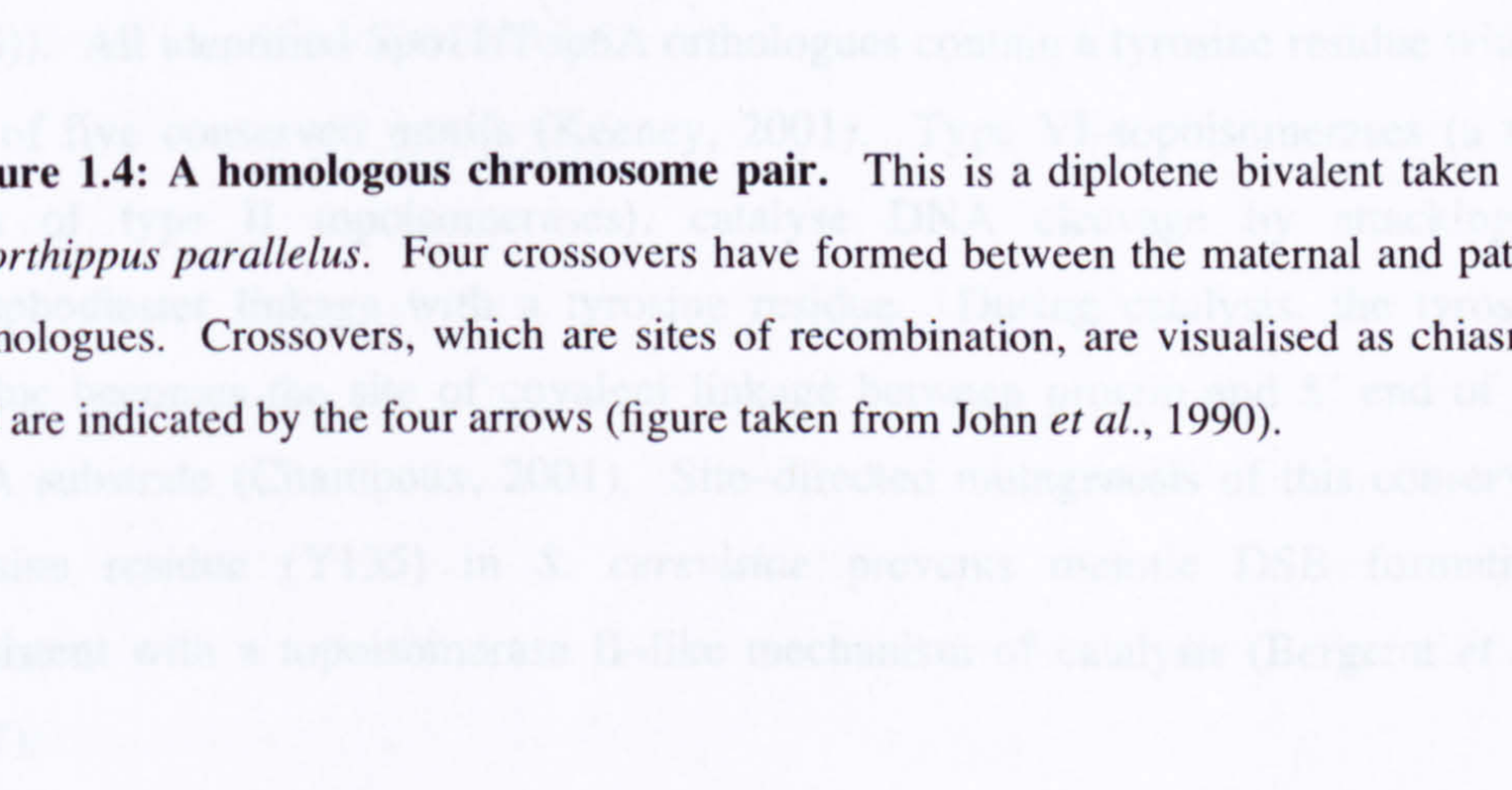

Figure 1.4: A homologous chromosome pair. This is a diplotene bivalent taken from *Chorthippus parallelus*. Four crossovers have formed between the maternal and paternal homologues. Crossovers, which are sites of recombination, are visualised as chiasmata, and are indicated by the four arrows (figure taken from John *et al.*, 1990).

and mature recombination products, do not form in the absence of Spo11p (Cao *et al.*, 1990; Schwacha and Kleckner, 1994). Homologous chromosomes also fail to synapse, as is also true for mouse cells (Baudat *et al.*, 2000).

In mammalian cells, meiotic DSB formation has been inferred from Spo11p–dependent phosphorylation of H2AX (Mahadevaiah *et al.*, 2001); a hallmark of DNA damage in mitotic cells (Rogakou *et al.*, 1998; Rogakou *et al.*, 1999; Downs *et al.*, 2000). Furthermore, Spo11p orthologues have been identified in many species, where, like in *S. cerevisiae*, they are essential for meiotic recombination (*S. pombe*, (Lin and Zakian, 1994); *C. comatus*, (Celerin *et al.*, 2000), (McKim and Hayashi-Hagihara, 1998); *C. elegans*, (Dernburg *et al.*, 1998); mice, (Keeney *et al.*, 1999; Baudat *et al.*, 2000); *Arabidopsis thaliana*, (Hartung and Puchta, 2000)). All identified Spo11/Top6A orthologues contain a tyrosine residue within one of five conserved motifs (Keeney, 2001). Type VI–topoisomerases (a sub class of type II topoisomerases), catalyse DNA cleavage by attacking a phosphodiester linkage with a tyrosine residue. During catalysis, the tyrosine residue becomes the site of covalent linkage between protein and 5′ end of the DNA substrate (Champoux, 2001). Site–directed mutagenesis of this conserved tyrosine residue (Y135) in *S. cerevisiae* prevents meiotic DSB formation, consistent with a topoisomerase II–like mechanism of catalysis (Bergerat *et al.*, 1997).

1.4.2 Location of the DSB

The location and quantity of DSBs are influenced by chromatin structure. This can be demonstrated by the positive correlation between sites of DSBs and *in vitro* nuclease hypersensitivity, indicative of open regions of chromatin. These areas of hypersensitivity also undergo a meiosis specific structural change within the chromatin (Keeney and Kleckner, 1995). Little is known with certainty about the determining factors for the location of Spo11p-DSBs, though work carried out by Gerton *et al.*, (2000). It has been shown that DSBs are located preferentially in

chromosomal regions that are at least three percent more GC–rich than the chromosome average. One promising rationalisation for hotspot activity in GC rich regions could be indirect, and due to absence of cohesion complexes, which bind AT rich regions (Blat and Kleckner, 1999); this could facilitate recombination machinery gaining access to the hotspot (Gerton *et al.*, 2000). DSB hotspots may also be related to chromatin loop structure, with DSBs only forming in axis–associated sequences. However, in the *S. cerevisiae* study carried out by Gerton *et al.*, (2000), the average distance between hotspots (54 kb) is greater than the average chromatin loop size 20 kb; (Moens *et al.*, 1998) indicating that not all loops are DSB hotspots.

Even though Spo11p-DSBs do not appear to be sequence specific, they do occur with a high prevalence in potential transcription promoter regions (Baudat and Nicolas, 1997). This again supports the hypothesis that chromatin structure influences DSB location.

A hallmark of DSB formation is the phosphorylation of histone H2A. This modification spreads up to 40 kb each side of the DSB. Tsukuda and colleagues have shown that in close proximity to a DSB there is a phosphorylation event of H2A, followed by loss of the histones H2B and H3. After this histone modification the chromatin shows an increased sensitivity to micrococcal nuclease (Usui *et al.*, 2001).

1.4.3 Removal of the covalently bound Spo11p

For many years, it was unknown how the Spo11 protein was released form the break site. There were two theoretical models proposed for the release of Spo11p, firstly by a single stranded nucleolytic cleavage reaction downstream of the cleavage site, releasing a Spo11p monomer bound to an oligonucleotide, and a resected DSB. The second model involves the hydrolysis of a tyrosine residue; this would then release Spo11p monomers with a 5′-phosphate terminus on the cleaved strand of the DNA (Keeney *et al.*, 1997; Neale *et al.*, 2005). Figure 1.5 illustrates

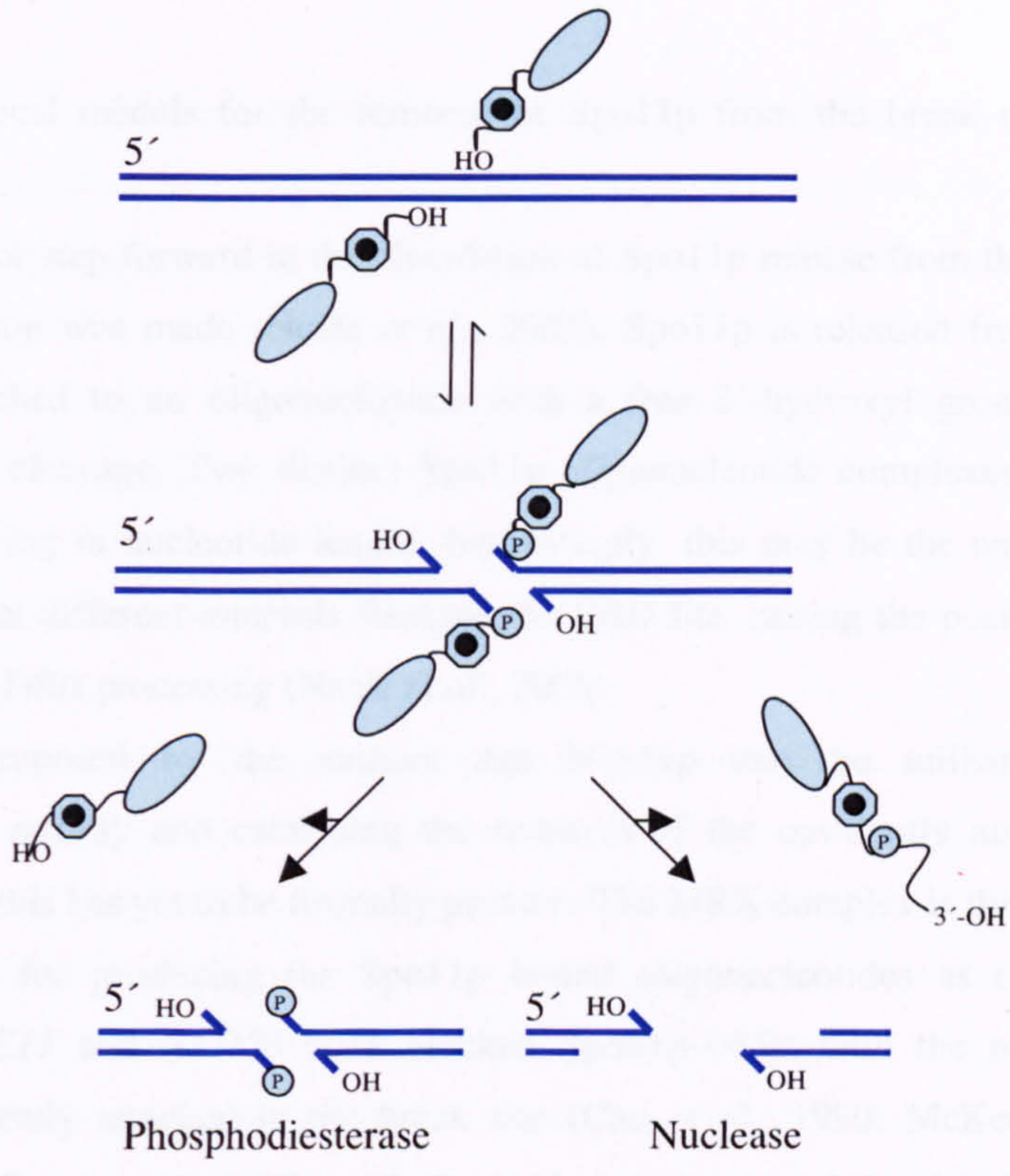

Figure 1.5: Alternative Mechanisms for Spo11p Protein Release. Spo11 protein creates meiotic DSBs via a reversible transesterase reaction. Covalently-bound Spo11p attacks the DNA backbone via a tyrosine side chain, generating a phosphodiester linkage between the 5´ terminus and Spo11 protein. Previously, Spo11p was thought to be released from the break site by either direct hydrolysis of the protein-DNA linkage via a phosphodiesterase, or single-stranded endonuclealytic cleavage. It has recently been confirmed that the Spo11 protein is released via a nuclease action, covalently attached to an oligonucleotide with a free 3´ -hydroxyl group (figure adapted from Neale *et al.*, 2005).

the two theoretical models for the removal of Spo11p from the break site, as described above.

Recently, a major step forward in the elucidation of Spo11p release from the sites of DSB formation was made (Neale *et al.*, 2005). Spo11p is released from the break site, attached to an oligonucleotide with a free 3´-hydroxyl group, via endonucleolytic cleavage. Two distinct Spo11p-oligonucleotide complexes were identified, differing in nucleotide length. Interestingly, this may be the result of strand cleavage at different intervals flanking the DSB site, raising the possibility of asymmetrical DSB processing (Neale *et al.*, 2005).

It has been proposed by the authors that Mre11p may be utilising its endonucleolytic activity and catalysing the removal of the covalently attached Spo11p, though this has yet to be formally proven. The MRX complex is the most likely candidate for producing the Spo11p bound oligonucleotides as certain mutants of *MRE11* and *RAD50* have blocked Spo11p-DSBs with the protein remaining covalently attached to the break site (Cao *et al.*, 1990; McKee and Kleckner, 1997; Prinz *et al.*, 1997). Neale *et al.*, have proposed that Mre11p is creating single strand breaks in close proximity to the Spo11p catalysed DSB, which results in the release of the Spo11p-oligonucleotide (Neale *et al.*, 2005).

The DSBs are then rapidly resected at the 5´ end to reveal 3´ single stranded tails. If certain mutations occur in the genes *RAD50, MRE11* or *SAE2*, this resectioning step is blocked (McKee and Kleckner, 1997; Prinz *et al.*, 1997).

1.4.4 Repair of the DSB in meiotic cells

As a result of the danger a DSB poses to a cell, there have evolved several sophisticated mechanisms with which to combat this threat. There are two main categories of DBS repair: homologous and non-homologous repair, of which there are several different forms within each category. Homologous recombination, HR, is characterised by utilising a homologous sequence as the repair template, and typically requires many hundred bases of homology, in contrast to non-

homologous repair, which can be efficient with as little as a couple of bases. The mechanisms of DSB repair are well conserved between *S. cerevisiae* and higher eukaryotes, though there is some variation depending upon organism and stage of the cell cycle. In *S. cerevisiae,* HR is the principal mechanism of break repair whilst non-homologous recombination is the predominant mechanism in mammalian cells (Pastink *et al.*, 2001).

1.4.5 Homologous recombination

Studies with recombination deficient and radiation sensitive strains have led to the elucidation of many genes involved in DSB repair, including the *RAD52* epistasis group, members of which are: *MRE11, XRS2, RAD51, RAD52, RAD54, RAD55, RAD57* and *RAD59.* There are several different forms of homologous recombination, single-strand annealing (single-strand annealing; SSA), gene conversion (gene conversion; GC) and break-induced replication (break-induced replication; BIR). All of which are initiated in the same manner - resectioning of the DNA in a 5′ to 3′ direction, to reveal 3′ ended ssDNA tails (Haber, 2000).

1.4.6 Canonical DSB repair model

Figure 1.6 illustrates the DSB repair model forwarded by Szostak in 1983; a general over-view of this mechanism is as follows; 5′ to 3′ resectioning of the DSB results in 3′ ssDNA tails. These 3′ tails are highly recombinogenic and go on to invade the repair template, be it a homologous chromosome, sister chromatid or at an alternative ectopic location, which serves as a primer for initiation of novel DNA synthesis. The invasion of the repair template generates a characteristic four-stranded branch structure, an HJ. Subject to how the two ensuing double HJs are resolved, a crossover could or could not be associated with a gene conversion event. If there is cleavage of non-crossed strands from one HJ, and of crossed strands from the other, this causes the crossover of flanking

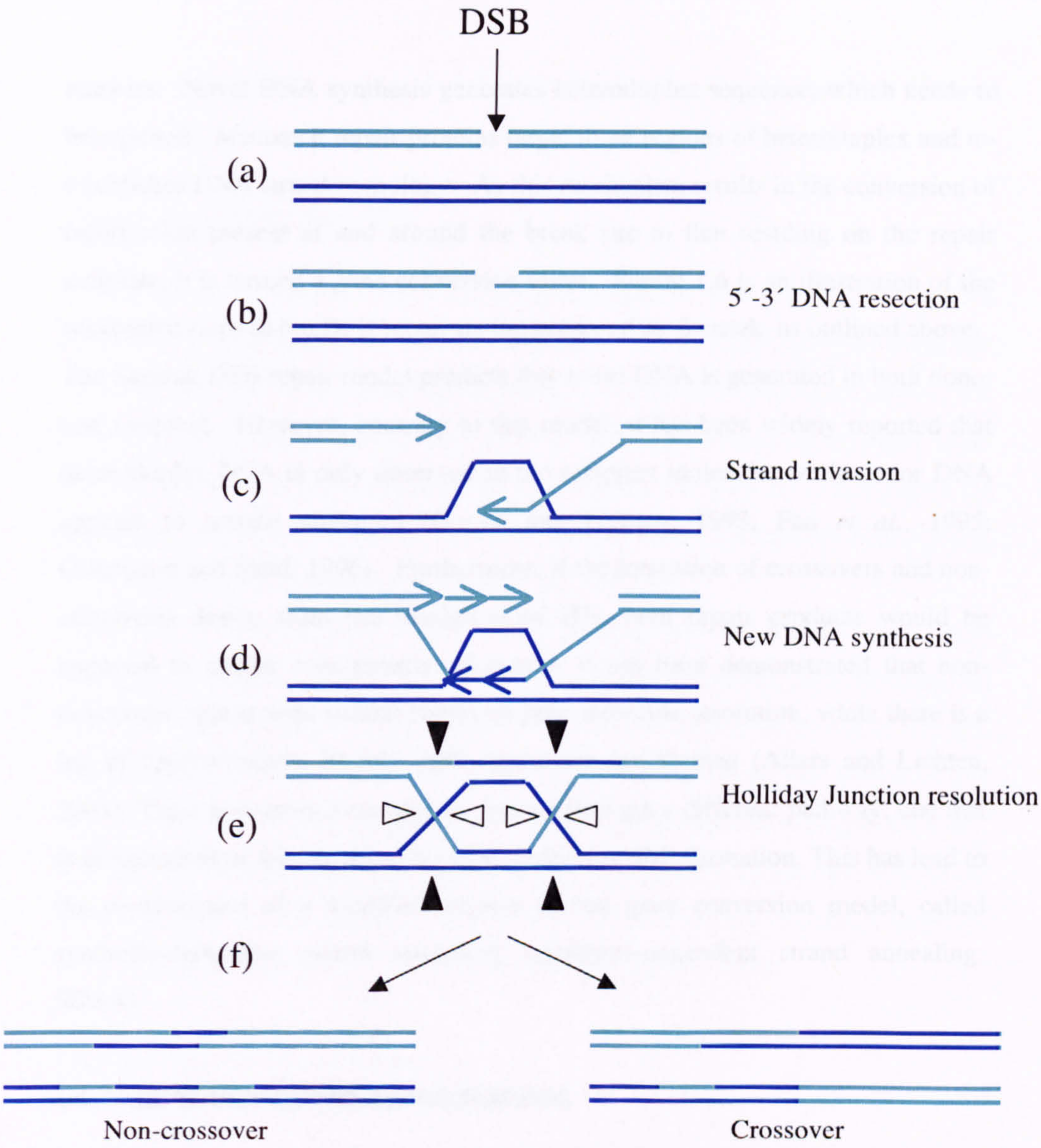

Figure 1.6: Szostak DSB Repair Model: (a) DSB formation is followed by (b) 5´-3´ resection of the DNA termini. (c) The resulting 3´ ssDNA tails are highly recombinogenic and can invade a homologous template, (d) to initiate novel DNA synthesis. (e) A double Holliday-Junction forms and is resolved via the alternative cleavage of (f) crossed (open arrowhead) or non-crossed (closed arrowhead) strands (figure adapted from Paques and Haber, 1999).

markers. Novel DNA synthesis generates heteroduplex sequence, which needs to be repaired. Mismatch repair proteins target these regions of heteroduplex and re-establishes DNA strand homology. As this mechanism results in the conversion of information present at and around the break site to that residing on the repair template, it is termed a gene conversion event. Figure 1.6 is an illustration of the successive steps in the DSB repair model proposed by Szostak, as outlined above. The Szostak DSB repair model predicts that novel DNA is generated in both donor and recipient. However, contrary to this model, it has been widely reported that heteroduplex DNA is only observed in the recipient molecule, while donor DNA appears to remain unaltered (Goyon and Lichten, 1993; Fan *et al.*, 1995; Gilbertson and Stahl, 1996). Furthermore, if the formation of crossovers and non-crossovers derive from the resolution of HJs, both repair products would be expected to appear concurrently. However, it has been demonstrated that non-crossovers appear with similar timing to joint molecule resolution, while there is a lag of approximately 30 min until crossovers are formed (Allers and Lichten, 2001). Thus, non-crossovers may be formed through a different pathway, one that is independent of joint molecules (joint molecules; JM) formation. This has lead to the development of a modified version of the gene conversion model, called synthesis-dependent strand annealing (synthesis-dependent strand annealing; SDSA).

1.4.7 Synthesis-dependent strand annealing

SDSA predicts that the two DNA termini of a DSB act independently of each other in the homology search, and that stable heteroduplex intermediates between the 3´ ssDNA tails and the template regions, do not form. Following strand invasion, the HJ does not enlarge, but instead migrates into the gap created. After DNA synthesis, the newly synthesised strands are displaced and anneal to the 5´ ends of the DSB. SDSA has been shown to be involved in mating-type switching in *S.*

cerevisiae and more recently in meiotic gene conversion (Allers and Lichten, 2001b). Figure 1.7 illustrates the successive steps during SDSA.

1.4.8 Single-strand annealing

SSA is one of the possible repair mechanisms employed by the cell when repeated regions of homologous sequence flank the site of the DSB, and was first identified following studies in *Xenopus laevis* oocytes. As figure 1.8 demonstrates, the homologous sequences are revealed when 5′ to 3′ resectioning of the DNA takes place. The homologous sequences are then ligated, resulting in a deletion of the intervening DNA. SSA requires the nucleotide excision repair proteins Rad1p and Rad10p to remove the non-homologous 3′ ssDNA tails.

Studies in *S. cerevisiae* of mitotic cells, utilising the HO-endonuclease, have revealed that repair practically always takes place between the most proximal of the homologous repeats. This guarantees that the minimum amount of DNA is lost (Sugawara and Haber, 1992b). The efficiency of SSA is dependent upon both the length and the sequence identity of the flanking repeat sequences (Sugawara *et al.*, 2000). The process is approximately 100 % efficient with around 400 bp of homology, but can be initiated with as little 30 bp (however efficiency drops to 5 %) (Sugawara and Haber, 1992a) (Reviewed in (Haber, 2000).

1.4.9 Break-induced replication

In this mechanism of DSB repair, the 3′ended single stranded tail invades the homologous duplex, and following strand invasion it is this 3′ end that is extended by DNA synthesis, resulting in a unidirectional replication fork. This fork is able to extend the entire length of a chromosome, or until it encounters a second replication fork. If the 3′ end of the other side of the DSB is captured, termed second end capture, a double Holliday junction is formed, the resolution of which is described above (Haber, 2000a; Signon *et al.*, 2001).

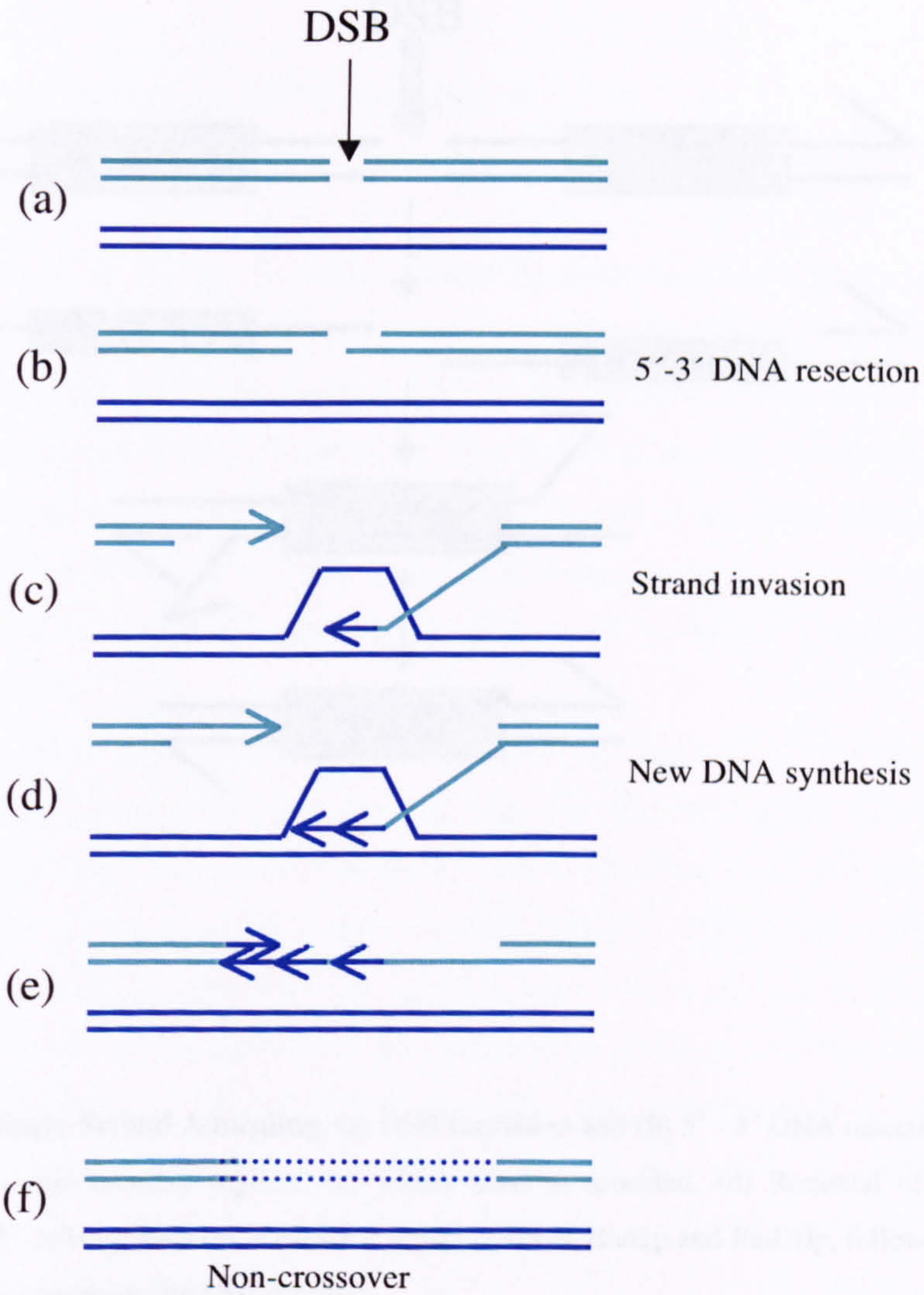

Figure 1.7: Synthesis-Dependent Strand Annealing Model: (a) Following DSB creation, there is (b) 5´-3´ DNA resection, (c) one DNA terminal end invades the donor and (d) novel DNA synthesis occurs. The newly synthesised strand is displaced until it meets the other end, (e) which is then used as a primer for the replicated second strand. (f) The repaired DNA represents a non-crossover (figure adapted from Haber, 2000).

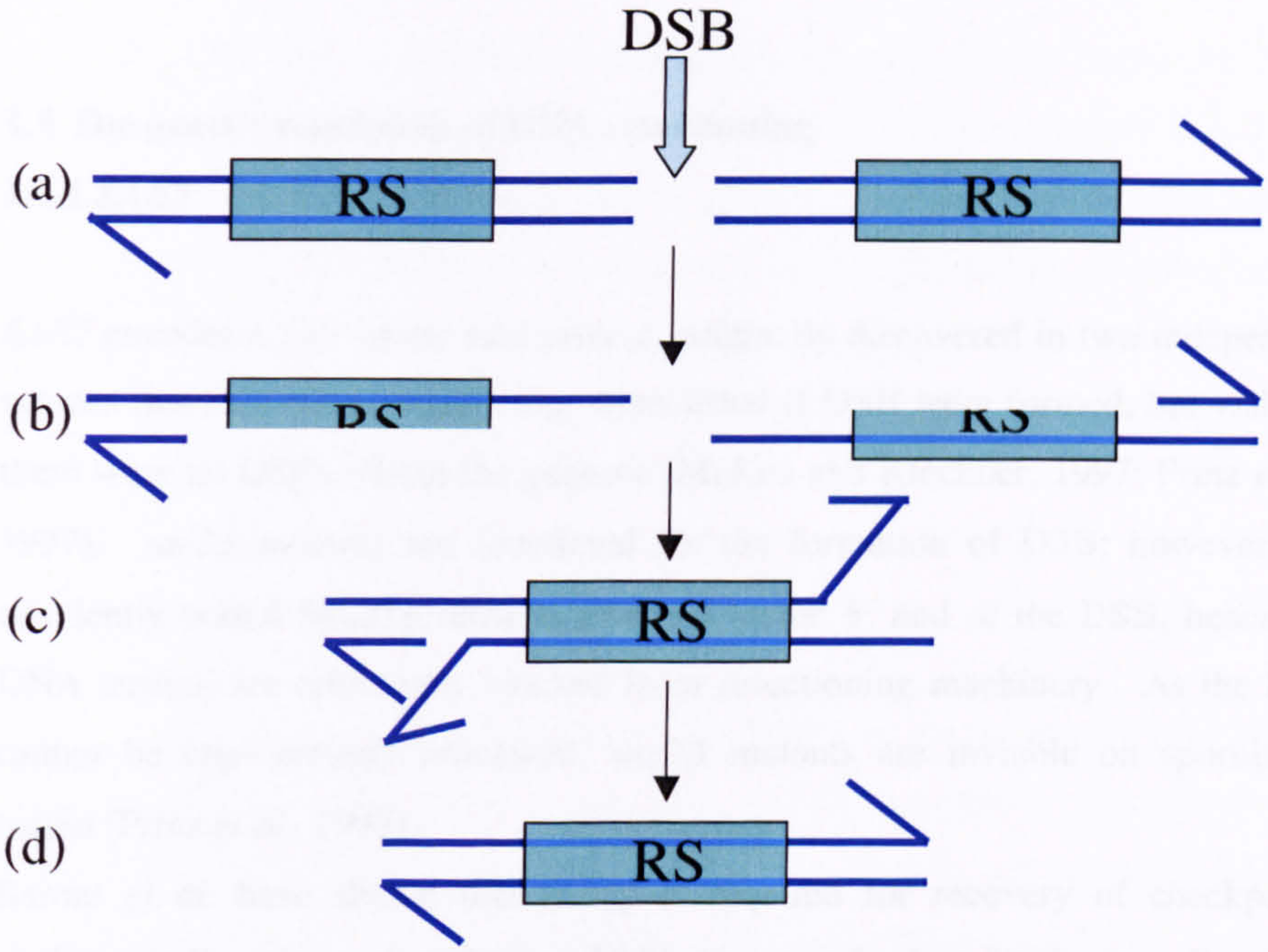

Figure 1.8: Single-Strand Annealing. (a) DSB formation and (b) 5´ - 3´ DNA resectioning exposes the complementary regions, (c) which become annealed. (d) Removal of non-homologous 3´ tails by nucleotide excision repair proteins, Rad1p and Rad10p, followed by strand ligation completes the SSA process

1.5 The genetic regulation of DNA resectioning

1.5.1 *SAE2*

SAE2 encodes a 345 amino acid protein, originally discovered in two independent screens that identified mutants that were lethal if DSB were formed, but viable if there were no DSBs within the genome (McKee and Kleckner, 1997; Prinz *et al.*, 1997). *sae2Δ* mutants are functional for the formation of DSB; however, the covalently bound Spo11p remains attached to the 5′ end of the DSB, hence the DNA termini are effectively blocked from resectioning machinery. As the DSB cannot be appropriately processed, *sae2Δ* mutants are inviable on sporulation media (Prinz *et al.*, 1997).

Baroni *et al.* have shown that Sae2p is required for recovery of checkpoint-mediated cell cycle arrest following DNA damage. In their 2004 paper, Baroni *et al.* also demonstrated that Sae2p of budding yeast is phosphorylated periodically through out the cell cycle, and in response to DNA damage. This phosphorylation of Sae2p is dependent upon the checkpoint kinase Mec1p and its associated upstream effectors, and an additional phosphorylation pathway involving Tel1p and the MRX complex. If both *MEC1* and *TEL1* are simultaneously deleted, phosphorylation of Sae2p cannot be detected and meiotic DSBs accumulate (Cartagena-Lirola *et al.*, 2006). This phosphorylation is a periodic event during the cell cycle, with initiation concurrent with the onset of S phase, reaching a maximum concomitant with Spo11p-DSB formation and Mek1p phosphorylation, decreasing as the DSBs are repaired. If the Spo11p-DSBs are unrepaired, phosphorylated Sae2p accumulates (Cartagena-Lirola *et al.*, 2006). Continued activation of meiotic recombination checkpoint, as seen in *dmc1Δ*, prevents Sae2p dephosphorylation, implying that its phosphorylation is associated with activation of the checkpoint. Further evidence for this is that site directed mutagenesis of the five canonical ATM/ATR phosphorylation sites of Sae2p results in an increase in sensitivity to the mutagen MMS, a synthetic lethality with *RAD27* and

accumulation of unresected DSBs - all of which are indicative of a role for Sae2p in recombination and DNA repair (Baroni *et al.*, 2004; Cartagena-Lirola *et al.*, 2006). Clerici *et al.* have recently shown that *sae2Δ* cells do not turn off the Mec1p and Tel1p mediated checkpoints, which are activated by an unrepairable DSB, and also demonstrate a delay in the disassembly of Mre11p foci at DSB sites. This suggests that Sae2p may negatively regulate checkpoint signalling via MRX and DSB association (Clerici *et al.*, 2006).

1.5.2 Mre11p-Rad50p-Xrs2p complex

Several genes control the resectioning of the DNA, in all mechanisms of repair. The genes of the budding yeast *S. cerevisiae RAD50* and *MRE11* are orthologues of the *E. coli* genes *sbcC* and *sbcD*. Rad50p and Mre11p are known to form a complex with Xrs2p, Nsb1p in mammals, collectively termed the MRX complex, when mutated cells exhibit defects in mitotic DSB repair (Cao *et al.*, 1990). Chromosomal instability syndromes are caused by mutations in the mammalian MRX complex; Nijmegen breakage syndrome is the result of truncations in *hNBS1*, and Ataxia-telangiectasia-like disorder is caused by hypomorphic mutations of *hMRE11* (Varon *et al.*, 1998; Stewart *et al.*, 1999). Cells derived from sufferers of these disorders are characterised by common DNA damage response defects: hypersensitivity to ionising radiation and defective checkpoint responses. Both of these disorders cause genome instability, predisposing affected individuals to cancer (Petrini, 1999; D'Amours and Jackson, 2002).

The MRX complex is of paramount importance for the maintenance of chromosome stability, telomere integrity, sister chromatid interactions and homologous recombination. There have been three distinct functions of Mre11p so far elucidated: DNA hairpin opening, ssDNA endonuclease activity and dsDNA exonuclease activity with 3′ to 5′ polarity. All of these activities require the presence of Mn^{2+} ions, with the latter two requiring ATP and Rad50p (Furuse *et al.*, 1998; Trujillo and Sung, 2001; Yu *et al.*, 2004)

Structural analysis of $(Mre11)_2/(Rad50)_2$ has revealed two Rad50p α-helical coiled-coil domains projecting from the globular head of each heterotetramer. A conserved sequence Cys-X-X-Cys, is found at the apex of the coiled coil forming a molecular zinc-hook that allows two heterotetramers to dimerise. As Mre11p localises to DSB hotspots prior to DSB formation, it has been proposed M_2R_2 bridging has a role in sister chromatid interactions (Hopfner *et al.*, 2002). Additionally, M_2R_2 bridging may allow DSB ends to physically interact and prepare them for joining. Xrs2p is required to target Rad50p and Mre11p to DNA ends and for the DSB end-bridging function of the MRX complex (Trujillo *et al.*, 2003).

After the formation of the DSB, the MRX complex remains on the chromosome where it forms foci, and is then termed the post DSB complex. There are discrete roles for the pre and post DSB complexes, even though they share the same components. The different functions of the complex have been established as a result of different binding positions of Mre11p and associations with different proteins. The complex that participates in the formation of the break does not require the Mre11p protein to act as a binding core, whereas the formation complex does (Usui *et al.*, 1998; Usui *et al.*, 2001a).

The processing of a DSB occurs rapidly after it has been formed. The implication of this is that the pre-DSB complex must be rapidly converted into the post-DSB complex. The post-DSB complex cannot be formed without the prior formation of the pre-DSB complex (Usui *et al.*, 1998).

The processing of the DSB requires the functions of a nuclease, demonstrated by the observation that cells harbouring mutation *mre11*-58S, which has lost the nuclease activity, are deficient in the processing of DSBs (Tsubouchi and Ogawa, 1998).

Notwithstanding the amount of evidence that has accumulated, the exact role of the MRX complex in Spo11p-DSB processing remains unclear, due to a significant anomaly. The 3′ to 5′ polarity of the exonuclease activity displayed by the MRX complex *in vitro*, is opposite to that observed in meiotic DSB

resectioning *in vivo* (Furuse *et al.*, 1998; Trujillo *et al.*, 1998). An attractive prospect therefore, is that the ssDNA endonuclease activity of MRX, in concert with a helicase, degrades the 5′ ssDNA termini at Spo11p-DSB sites (Moreau *et al.*, 1999). Alternatively, the MRX complex may have a more indirect role in DSB resectioning, by recruiting other 5′ to 3′ polarised exonucleases to the sites of Spo11p-DSBs, possibly Exo1p.

1.5.3 Tel1p activates the MRX complex

Tel1p is a member of the ATM family of protein kinases. This protein is known to have a role in telomere maintenance and DSB repair, in concert with the MRX complex (Ritchie and Petes, 2000). During the meiotic cycle of *S. cerevisiae,* Mre11p and Xrs2p are both phosphorylated in a Tel1p-dependent manner, more specifically, in response to DNA damage as shown in cells exposed to MMS (Usui *et al.*, 2001b). Furthermore, both Tel1p and Mre11p are essential for cell cycle delay of a *rad50S* cell in which the repair of Spo11p-DSBs is blocked due to a failure to remove the covalently bound Spo11p dimer. The checkpoint that is triggered in *rad50S* cells is termed the TM checkpoint (Usui *et al.*, 2001b). The triggering of this TM checkpoint in response to a blocked DSB, and the requirement for the MRX complex at the break site, implicates the MRX complex in Spo11p-DSB repair that is some manner positively regulated by Tel1P, most probably through phosphorylation. In essence, the Spo11p-DSB is proposed to act as a signal to initiate Tel1p-dependent phosphorylation of the MRX complex, which when activated, then proceeds to remove the covalently bound Spo11p dimer and initiate resectioning of the DNA. There are several observations that have been made that support this hypothesis: Tel1p has been shown to physically interact with DSBs in an Xrs2p-dependent manner (Nakada *et al.*, 2003). *In vivo,* Tel1p directly interacts with the C-terminus of Xrs2p; it is the C-terminus of Xrs2p that is not required for formation of the MRX complex. These observations were further confirmed when Nakada *et al.*, showed that Tel1p can be identified at

an artificial DSB site in an Xrs2p dependent manner. Nakada and colleagues detected the presence of Tel1p at DSB sites through a method called Chromatin Immunoprecipitation (ChIP) - an immunoprecipitation technique coupled with PCR, so the specific DNA site where the protein is bound can be identified (Nakada *et al.*, 2003). Usui and co-workers have also shown that Tel1p is not required for Dmc1p arrest that is triggered due to hyper-resected DSB, but is required for Rad50p induced arrest, triggered by Spo11p remaining covalently bound to the break site (Usui *et al.*, 2001).

1.5.4 *EXO1*

Exo1p is a member of the Rad2p family of structure-specific endonucleases, possessing 5′ to 3′ exonuclease and 5′ flap endonuclease activities *in vitro* (Fiorentini *et al.*, 1997). In *S. cerevisiae* cells, the *exo1Δ* mutation has been shown to be synthetically lethal with *top1Δ* and exhibits a synthetic growth defect with members of the *RAD27* family, suggesting an important role within the cell (Tong *et al.*, 2004). This importance extends to mammalian orthologues, as *exo1Δ* mice have been shown to have increased cancer susceptibility and male, female sterility (Wei *et al.*, 2003).

Exo1p is known to be involved in many different cellular functions including: UV resistance, Okazaki fragment processing, telomere maintenance and homologous recombination. Exo1p was first isolated and purified from *Schizosaccharomyces pombe,* by Szankasi and Smith (1995). When cells were made to enter meiosis Exo1p activity was found to increase 5-fold, with the transcript increasing by approximately 10-fold. Supportive of a role in DNA maintenance, the *EXO1* transcript is induced on exposure to UV, and further evidence has come from Fiorentini *et al.* (2002) who have shown that recombination between direct *ade2* repeats was decreased 6-fold in *exo1Δ*. In *S. cerevisiae,* the *exo1Δ* mutation reduces spore viability to around 80 %, believed to be due to reduced intergenic crossing over, resulting in increased Meiosis I non-disjunction, suggesting that

Exo1p may act to promote crossing over (Wang *et al.*, 1999; Tsubouchi and Ogawa, 2000; Khazanehdari and Borts, 2000)).

As mentioned earlier, it is thought that the MRX complex functions in the removal of Spo11p from the 5′ end of a DSB, possibly catalyzed by the endonuclease activity of Mre11p. Whilst this activity of Mre11p may be enough to produce long 3′ single stranded tails, an attractive model suggests that Mre11p removes Spo11p, leaving the ends to be resected by an alternative nuclease, possibly Exo1p. Supportive of this hypothesis is that *exo1Δ* cells of *S. cerevisiae* are found to have DSBs that are processed to form a heterogeneous population of molecules, indicative of active resectioning. However in mutants that accumulate DSBs e.g. *dmc1Δ*, the excessive degradation of breaks is reduced by *exo1Δ* mutation, suggesting that Exo1p does function in DNA resectioning *in vivo* (Tsubouchi and Ogawa, 2000).

Mutants of *MRE11*, *XRS2* or *RAD50*, as mentioned earlier, suffer form high sensitivity to ionizing radiation and radiomimetic chemicals. This phenotype can be suppressed by overexpression of *EXO1* (Chamankhah *et al.*, 2000). The *exo1Δ* mutant itself does show weak MMS sensitivity, which is greatly exaggerated when combined with an *mre11Δ* mutation, suggesting that Mre11p and Exo1p have overlapping functions in DNA damage repair (Tsubouchi and Ogawa, 2000).

If Exo1p is involved in active resectioning of meiotic DSBs it would be expected that *exo1Δ* mutants would show a decrease in gene conversion at distant markers. Although this has been shown at several loci, it has not been observed at all (Khazanehdari and Borts, 2000).

The Mre11p complex acts in concert with Exo1p to activate the Mec1p signalling pathway in response to replication block or following DNA damage. This is thought to be achieved through the production of long ssDNA tails at the DSB break site, produced by both Mre11p and Exo1p, which in turn promotes the association of Mec1p with the break site (Nakada *et al.*, 2004).

Exo1p has also been specifically implicated in SSA; Exo1p was isolated form mitotic *S. cerevisiae* as a result of its ability to process DNA duplex to substrates for the SSA pathway of repair (Fiorentini *et al.*, 1997).

In essence, Exo1p is understood to have many varying and subtle roles within the cell, including DNA end processing and mitotic recombination. Exo1p also appears to have a redundant role with one or more other nucleases, possibly regulated by the MRX complex. A homology search of the sequenced and annotated genome of *S. cerevisiae* has revealed that there are four proteins predicted to share sequence similarity with *EXO1: RAD2, RAD27, DIN7* and *YEN1*. This raises the possibility that there could be functional redundancy amongst these proteins (Tishkoff *et al.*, 1997). Din7p functions specifically in mitochondria, so it is unlikely that it would share any functional redundancy with Exo1p (Fikus *et al.*, 2000). Rad27p is a better candidate for redundancy, as an *exo1Δrad27Δ* mutant exhibits synthetic lethality (Tishkoff *et al.*, 1997). Tran and colleagues have postulated that the synthetic lethality of *exo1Δrad27Δ* mutants is due to Exo1p flap endonuclease activity and not its dsDNA 5′ to 3′ exonuclease activity, shown by work with mutants with deficiencies in both activities (Tran *et al.*, 2002).

1.6 Repair template choice

When a DSB is repaired by HR, a homologous template is required. If the repair takes place in a diploid cell, there are two options for the homologous template: homologous chromosome or sister chromatid. Rather than a decision based on chance, the choice between inter- or intra-homologue repair is believed to be a highly regulated selection. The preferential direction of DSB repair towards the homologous chromosome in a meiotic cell is purposeful, allowing crossover formation exclusively between homologous chromosomes, ensuring their tight association until the reductional division at MI.

In certain circumstances, when a DSB occurs, it is desirable for no recombination to take place during its repair, for example in mitotic cells. In such situations, the decision as to which template should be used is pushed to the direction of the sister chromatid.

There are several proteins known to regulate the choice of template partner in *S. cerevisiae*, including Dmc1p and Rad51p, orthologues of the bacterial strand invasion protein RecAp. These genes are believed to have arisen due to an ancient gene duplication event, prior to the divergence of eukaryotes. The amino acid sequences of both Rad51p and Dmc1p are strongly conserved with RecAp at C-terminal regions, however there is substantial difference along the N-terminus. Orthologues of *S. cerevisiae RAD51* have been elucidated in many organisms ranging from *X. laevis* to *A. thaliana,* however, there are no *DMC1* orthologues in certain organisms including *C. elegans* and *D. melanogaster* (Villeneuve, 2001).

1.6.1 *RAD51*

During yeast meiosis, *rad51Δ* mutants accumulate DSBs that are unable to convert to JMs. There are additional phenotypes in *rad51Δ* mutants, typical of a defect in a recombination gene, including reduced pairing and synapsis of homologues, and a decreased spore viability (Nag *et al.*, 1995; Rockmill *et al.*, 1995). Immunofluorescence studies of Rad51p have shown that it localises to specific foci with other recombination proteins during meiotic prophase - the stage of the cell cycle at which the interactions between homologues are occurring.

The protein product of *RAD51* is not limited to use within meiotic recombination, it is also involved in the repair of DSBs in vegetative cells. Vegetative cells are programmed to use the *RAD51* dependent pathway in which the sister chromatid is the repair partner of choice (Paques and Haber, 1999).

Accessory factors of Rad51p have been well characterised. RPAp, a single strand DNA binding protein, is necessary for effective strand exchange catalysed by Rad51p (Sung *et al.*, 2003). RPAp is believed to minimise secondary structures

within the DNA, thus encouraging Rad51p filament formation. Additionally, Rdh54p has also been implicated assisting Rad51p. *RDH54* is an orthologue of *RAD54* and it has been shown to be necessary for the transformation of DSB lesions into mature recombination products, specifically by promoting D-loop formation by Rad51p, *in vitro* at least (Shinohara *et al.*, 1997; Petukhova *et al.*, 2000). One possible role of Rad54p, which gives an insight into abundance of proteins being a limiting factor in reaction kinetics, is in promoting disassembly of Rad51p-dsDNA complexes.

1.6.2 *DMC1*

In the SK1 strain background of *S. cerevisiae,* a *dmc1Δ* mutation results in accumulation of processed DSBs, reduction in homologue synapsis and abnormalities in reciprocal recombination (Bishop *et al.*, 1992). The primary role of Dmc1p is thought to be when the search for homology is occurring - in *dmc1Δ* mutants, the search for homology ceases and inappropriate interactions occur. The importance of the role Dmc1p plays within the meiotic cell is illustrated in the murine model, in which mutants are sterile and show characteristics of poorly repaired DSBs (Di Giacomo *et al.*, 2005).

rad51Δ mutants are unable to produce JMs between sister chromatids, whilst *dmc1Δ* mutants are unable to form JMs between homologues (reviewed in (Haber, 2000)). Dmc1p and Rad51p have both been implicated in operating in recombination pathways that, to some extent at least, overlap as overexpression in *S. cerevisiae* of Rad51p or Rad54p can suppress the *dmc1Δ* phenotype (Bishop *et al.*, 1999; Tsubouchi and Roeder, 2003).

An additional role of Dmc1p is thought to be in crossover interference. In most organisms, crossovers are not randomly distributed along a chromosome, instead, the bias for a crossover is dependent upon the number of crossovers present locally. This bias is such that if there is a crossover situated in close proximity,

that crossover makes it less probable that a crossover will form at the position in question.

Until recently, little has been known about the accessory factors of Dmc1p, however more is known about those of the strand exchange protein Rad51p (as outlined in section 1.6.1). One can therefore postulate whether the same factors have a similar effect on the activity of Dmc1p. Recent studies have suggested that Mei5p and Sae3p form a complex that in some way assists Dmc1p during meiotic recombination. Cells singularly and doubly mutant for *mei5*, *sae3* and *dmc1* have been identified as having identical phenotypes, including defects in meiotic DSB repair and formation of the SC. Further evidence for a real interaction between the proteins has come from Chromatin Immunoprecipitation experiments, which have demonstrated that Mei5p, Sae3p and Dmc1p colocalise with one another at DSB sites and that there is a mutual interdependence for this localisation (Hayase *et al.*, 2004; Tsubouchi and Roeder, 2004).

One important observation that has ramifications identifying how Rad51p and Dmc1p carry out their specific roles in meiosis, is that whilst Mei5p and Sae3p are required for the formation of Dmc1p complexes at DSB sites, they are not required for Rad51p complexes. Whilst it is not known conclusively what the function of the Mei5p-Sae3p complex is, one current thought is that the complex may promote Dmc1p filament formation on ssDNA, as Dmc1p is known to poorly form these filaments in the absence of Mei5p or Sae3p. This is not the only hypothesis: Shinohara and colleagues have implicated the Mei5p-Sae3p-Dmc1p complex in increasing the formation of helical filaments over ring structures. Reviewed in (Neale and Keeney, 2006).

Hop2p and Mnd1p have been shown to form a chromosome-associated, heterodimeric complex. If either *MND1* or *HOP2* are deleted, chromosomes synapsis occurs in a non-homologous manner and DSBs fail to repair (Gerton and DeRisi, 2002; Tsubouchi and Roeder, 2002; Petukhova *et al.*, 2005). Zierhut *et al.*, (2004) has hypothesised that the Hop2p-Mnd1p complex functions by indirectly promoting Dmc1p by influencing the chromatin structure (reviewed in Neale *et*

al., 2006). The human Dmc1p requires ATP and is strongly dependent upon RPA for its function in strand exchange (Sehorn *et al.*, 2004).

Whilst some detail is known about the functions of Rad51p and Dmc1p, and their associated accessory factors, still unknown is whether inter-homologue bias displayed by meiotic cells is the result of active promotion of inter-homologue recombination or active suppression of inter-sister recombination.

1.6.3 Mek1p-Red1p-Hop1p complex

In addition to the bias to homologous repair directed through Dmc1p, a second mechanism has also been identified. Mek1p, Red1p and Hop1p, all meiosis-specific chromosomal core proteins, are involved in establishing inter-homologue bias. Mek1p is a kinase and its activation and subsequent phosphorylation of downstream targets is believed to mediate inhibition of proteins required for inter-sister repair, e.g. Rad54p (Wan *et al.*, 2004). The mechanism of inter-homologue bias for budding yeast, proposed by Niu *et al.*, (2005) appears to be evolutionarily conserved. Chromosome core components analogous to Hop1p have been found in organisms ranging from plants to nematodes (Zetka *et al.*, 1999). Comparison of *hop1Δ* mutants in other organisms suggests that the mechanism is present in higher eukaryotes.

1.7 Crossover formation

The repair of a break by homologous recombination does, or doesn't result in a crossover event. For correct segregation to occur, a crossover event between homologues must occur. Therefore, to ensure correct segregation, not only does the repair pathway have to be pushed down the inter-homologue route, it also has to result in a crossover.

The preference for crossovers in meiotic cells is strong; between 30 - 50 % of recombination events in meiotic cells are associated with a crossover, as opposed

to 5 - 20 % in vegetative cells of budding yeast (Paques and Haber, 1999). This striking difference suggests that meiotic cells may positively regulate crossovers. The number of crossovers per chromosome is of critical importance, as many will result in chromosome entanglement, and none will result in increased incidences of non-disjunction. A recently forwarded model has resulted from a collection of work and proposes that crossovers and non-crossovers of DSB repair are products of different pathways of repair. In 1999, Paques and Haber proposed that ssDNA each side of the DSB invades the template in an independent rather than a simultaneous manner. This hypothesis was further strengthened by work of Hunter and Kleckner (2001), who identified the presence of strand exchange intermediates that only contain one of the DSB ends.

It has been also demonstrated by Allers and Lichten, that the canonical double Holliday junction intermediates mainly result in crossover products (Allers and Lichten, 2001), suggesting that non-crossover products result from an alternative pathway, which diverges prior to double Holliday junction formation. According to this revised model, the majority of non-crossovers are believed to result from SDSA (Villeneuve and Hillers, 2001).

Data from Beth Rockmill and colleagues has suggested that the protein Sgs1p may play a significant role in the control of crossovers (Rockmill *et al.*, 2003). This protein is a member of the *RECQ* family of DNA helicases that includes the human orthologues associated with Bloom's Syndrome (BLM), symptoms of which include: predisposition to cancer, spontaneous mutations and an increase in the frequency of sister-sister recombination (Enomoto, 2001). *sgs1Δ* mutants undergo full chromosome synapsis, which occurs at a rate faster than WT. In addition, the amount of crossing over is increased, as shown by tetrad dissection - the only mutant isolated so far to do this (Rockmill *et al.*, 2003). Rockmill *et al.* have proposed that Sgs1p may act on recombination intermediates that have not yet been committed to a crossover or non-crossover fate, more specifically they have speculated that the Sgs1p helicase may act on a strand invasion intermediate. Taken together, Rockmill and colleagues' data has led to the suggestion that Sgs1p

acts as a negative regulator of inter-chromosomal interactions, and thus is an important determinant of the number of crossovers present in a meiotic cell (Rockmill *et al.*, 2003).

Crossover control is the term coined to describe the decision a cell makes as to whether a DSB is repaired to a crossover or a non-crossover. Martini *et al.* have recently been working with Spo11p hypomorphs in an attempt to understand this phenomenon. They have discovered that the level of crossovers present within a cell is generally maintained to a certain threshold, to the detriment of non-crossover events. Their results have shown that a reduction in the number of DSBs does not have a concomitant reduction in the number of crossovers, which they have termed a 'buffering' mechanism. The work of Martini further supports previous findings of the Keeney lab, who observed that a decrease in the activity of Spo11p in *S. cerevisiae* (through a combination of mutant alleles with and without HA tags) does not show a linked decrease in the abundance of Zip3p complexes, a mark of a crossover site (Fung *et al.*, 2004; Henderson and Keeney, 2004; Martini *et al.*, 2006).

1.8 Cell cycle monitoring of recombination events

Meiotic recombination and progression through the first nuclear division are directly linked with one another; many recombination deficient mutants, for example *dmc1Δ*, arrest at the pachytene stage of meiosis (Bishop *et al.*, 1992). It is the pachytene checkpoint that serves to prevent the segregation of homologues that have failed to undergo successful recombination, thus preventing aneuploid progeny. Pachytene is an appropriate stage for a checkpoint as beyond this point, the cell is committed to undergo reductional division of chromosomes (Leu *et al.*, 1998).

A cyclin-dependent kinase, Cdc28p, is believed to control the cell cycle at pachytene, as loss of this kinase results in arrest of the cell at this stage (Shuster and Byers, 1989). Specifically, it is believed that pachytene cell cycle arrest is the

result of accumulation of hyper-phosphorylated Swe1p, which is thought to inactivate Cdc28p (Leu and Roeder, 1999).

The transcription factor Ndt80p is also essential for the completion of meiosis. Many essential genes required for sporulation after pachytene are dependent upon *NDT80* for transcription, including *CLB1*, which encodes the major cyclin of MI, essential for exit from pachytene (Hepworth *et al.*, 1998). When the pachytene checkpoint is activated, the target genes of Ndt80p are not transcribed, however, if the checkpoint is rendered in an inactive state, the genes are once again transcribed (Chu *et al.*, 1998).

The detection of recombination intermediates is most likely mediated through some or all of the DNA damage proteins, e.g. Mec1p, Tel1p, Rad24p, Rad17, Ddc1p and Mec3p (Lydall *et al.*, 1996; Roeder and Bailis, 2000). In mitotic cells, when damaged DNA is sensed, these proteins are involved in the activation of downstream targets such as Rad9p and Rad53p. These activated proteins then impose cell–cycle arrest, orchestrated perhaps through the repression of cyclin transcription (Longhese *et al.*, 1998). Several protein complexes are formed by the DNA damage proteins; Rad24p complexes with Rfc2p, Rfc3p, Rfc4p, and Rfc5p (Shimomura *et al.*, 1998), and thus resembles the pentameric replication factor C (RFC), required to load PCNA (proliferating cell nuclear antigen) onto primer templates during replication (Waga and Stillman, 1998). Recently, the equivalent human checkpoint proteins (Rad17p–Rfc2-5p, and Rad1p–Rad9p–Hus1p, respectively) have been shown to form complexes that are very similar to RFC and PCNA (Shiomi *et al.*, 2002), supporting such a loading mechanism. Mutations in genes from the *RAD24* group show decreased levels of recombination, erroneous chromosome synapsis and low spore viability - phenotypes that cannot be attributed to defects in checkpoint functions alone (Lydall *et al.*, 1996), suggesting that checkpoint genes also play roles in recombination (Hong and Roeder, 2002).

There are a number of *S. cerevisiae* mutants that either delay or arrest at the pachytene checkpoint, including *zip1Δ*, *zip2Δ*, *hop2Δ* and *dmc1Δ*. It is believed

that these mutants arrest at pachytene as a result of a build up of recombination intermediates; *dmc1Δ* cells process their DSB to produce extended tracts of ssDNA, *zip1Δ* cells arrest with a large number of delayed Holliday junctions and around 10 % unrepaired DSBs whilst *hop2Δ* cells have an accumulation of single stranded tails (Leu *et al.*, 1998). Several mutants, which prevent the initiation of recombination, e.g. *spo11f* cells, in which no Spo11p-DSBs are formed, can alleviate this arrest (Bishop *et al.*, 1992b; Leu *et al.*, 1998).

The pachytene checkpoint also requires Mek1p, Red1p and Hop1p. Deletion of *MEK1, RED1* or *HOP1* restores WT levels of meiotic nuclear division in mutants that are subjected to an arrest at pachytene e.g. *zip1Δ* or *dmc1Δ*. In these arresting mutants Mek1p is found to be active, whilst Red1p remains in a phosphorylated state. It was speculated by Bailis and Roeder (2000) that phosphorylation of Red1p inhibits exit from pachytene, and that in a WT cell, the completion of recombination sets off dephosphorylation of Red1p in a Glc7p-dependent manner. The arrest at pachytene in a *zip1Δ* mutant can be bypassed by deletion of *RED1* or *MEK1* leading to the suggestion that both Red1p and Mek1p are necessary for the production of a recombination structure that is subject to monitoring by the pachytene checkpoint machinery (Xu *et al.*, 1997). Figure 1.9 is an illustration of the genetic pathway of the pachytene checkpoint.

Pch2p is a meiosis-specific protein that has a nuclear ribosomal DNA localisation, dependent upon silencing factor Sir2p. In *S. cerevisiae*, there are three nuclear regions that are caused to undergo silencing, areas of repressed chromatin structure that is both gene-independent and position-dependent. The three regions are: the telomeres, the mating type loci and the rDNA. Whilst telomere and mating loci silencing is due to Sir2p and Sir3p, the rDNA silencing is only dependent upon Sir2p (Lustig, 1998). In a WT state, both Sir2p and Pch2p are found mostly in the nucleolus in addition to foci on meiotic chromosomes (San-Segundo and Roeder, 1999). Pch2p is only present in the nucleolus in *zip1Δ* cells, in which the checkpoint is successfully operating, where as Pch2p is not present in the nucleolus in *sir2Δ* mutants where the checkpoint is non-functional. This

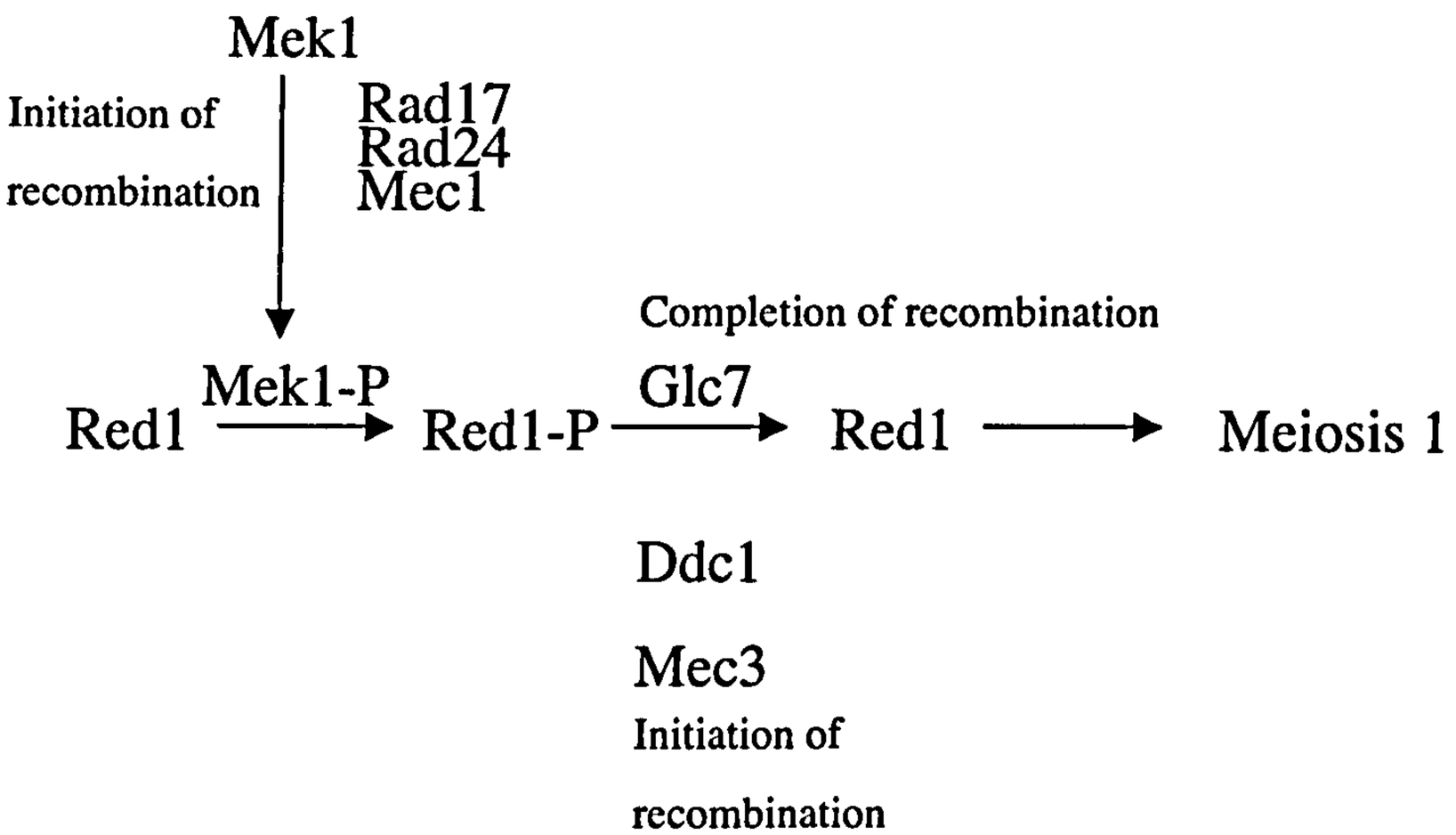

Figure 1.9: Model for the Pachytene Checkpoint Pathway. The Pachytene checkpoint is not triggered by the absence of recombination, but by the absence of an inhibitory signal that must be eliminated in order to exit from Pachytene. It would appear that this signal is generated by the initiation of recombination. Mek1p and Red1p both become phosphorylated and remain so until recombination is complete. In mutants that fail to undergo recombination, for example *spo11*; Mek1p and Red1p do not become phosphorylated, therefore this signal is not produced. Bailis and Reoder (2000) have postulated that Mek1p and Red1p become phosphorylated in response to DSBs and remain so until recombination is completed. The successful completion triggers the dephosphorylation of Red1p and exit from Pachytene. The phosphorylation of Red1p is believed to act as a signal that coordinates meiotic recombination with cell cycle progression (figure adapted from Roeder and Bailis, 2000).

observation has led to the suggestion that the localisation of Pch2p is central in checkpoint function. One interesting finding of San-Segundo *et al.* (2000) has shown that in certain circumstances Sir-dependent localisation of Pch2p to telomeres can impart checkpoint function, thus connecting the nucleolus and chromatin silencing with the pachytene checkpoint. A model forwarded by San-Segundo (2000) implicated chromatin silencing in the pachytene checkpoint, however, the precise mechanism of this involvement remains unclear. An important consideration for this model would be that the nucleolar and non-nucleolar forms of Pch2p differ form one another by a yet unknown modification.

There are several other checkpoints that operate during the meiotic cycle at pachytene. One such checkpoint is the *RAD9*-dependent arrest, induced in cells that have been subjected to chromosome damage early in meiosis. Specifically, this checkpoint arrests cells after replication of DNA, but before recombination.

Correct orientation of chromosome pairs on the metaphase spindle is a further meiotic checkpoint. Tension across the spindle is created when homologues, joined via chiasmata, are pulled to opposite spindle poles. This tension is sensed by a checkpoint, and unpaired chromosomes trigger a delay in the meiotic cycle (reviewed in (Roeder, 1997)).

1.8.1 *TEL1/MEC1*-mediated checkpoint pathway

DNA damage checkpoint pathways are mediated by highly conserved protein kinases; ataxia-telangiectasia mutated (ATM) and ATM-Rad3-related (ATR) of higher eukaryotes. In budding yeast, *TEL1* and *MEC1* encode the homologues of these kinases, respectively.

Mec1p physically interacts with Ddc2p to form a complex that localises to sites of replication block and DNA damage (Rouse and Jackson, 2002). A recently proposed model suggests that Ddc2p identifies DNA damage by interacting with RPAp-associated ssDNA, facilitating the association of the Mec1p-Ddc2p complex with sites of DNA damage (Zou and Elledge, 2003). It is not yet known

whether Tel1p localisation requires RPAp association. Mec1p and Tel1p have effects downstream of their DNA association; after the production of DNA DSBs or damage, Mec1p and Tel1p are known to phosphorylate and activate Rad53p, a yeast homologue of the mammalian Chk2p. Rad53p has been shown to play an important role in DNA damage checkpoints – its activation results in cell cycle arrest and the transcription of genes required for the repair of the DNA damage (Longhese *et al.*, 1998).

The Rad53p checkpoint activity appears approximately 1 hr after DSB induction and fades shortly after repair of the damage. Cells mutant for the helicase Sgs1p do not recover, even though they appear to have successfully finished DNA repair, with Rad53p kinase remaining activated. This mutant phenotype is abolished in *mec1Δ* strains that lack the checkpoint, or when the repair of the break is completed before checkpoint activation. Taken together, this suggests that Sgs1p is required to turn off the DNA damage checkpoint (Vaze *et al.*, 2002).

1.9 Origins of the assay in this study

Repair of a meiosis-specific DSB has been previously studied using a Spo11p-independent reporter assay (Neale *et al.*, 2002). In that study, a DSB created by VDE endonuclease was flanked by WT and mutant *URA3* alleles. VDE; *VMA1* derived homing endonuclease is a meiosis specific endonuclease that cleaves at a specific recognition site with timing approximately equal to that of Spo11p. Following formation of the VDE-DSB, four repair outcomes were possible: a gene conversion event using the *arg4-bgl* allele as repair template, yielding *ARG4* or *arg4-bgl* alleles or a SSA event between the flanking *URA3* homologous sequences, yielding deletion products *ura3::Ty* or *URA3* alleles. This reporter cassette used by Neale *et al.*, (2002) is the same as the reporter cassette used in this study. Neale *et al.*, (2002) reported that WT levels of Spo11p-DSBs are required for normal regulation of resectioning, even at a DSB created by another protein. The authors postulated that WT control over resectioning could be important for

directing repair to be inter-chromosomal, increasing the chance of creating inter-homologue connections essential to meiotic segregation.

1.10 Initial aims of this study

Characterise the genetic requirements for VDE-DSB repair

Examine repair of the VDE-DSB in the context of Spo11p-DSB formation

Examine whether repair machinery abundance is a limiting step in VDE-DSB repair

Characterise the genetic regulation of resectioning at Spo11p-independent VDE-DSB

Chapter Two

Materials and Methods

Table 2.1 *E. coli* strains

Name	Genotype	Source
DH5α	*supE*44, *ΔlacU*169 (*ϕ80lacZΔM15*), *hsdR*17, *rec*A1, *end*A1, *gyr*A96, *thi*-1, *rel*A1	Laboratory Source

Table 2.2 Plasmids

Name	Description	Source
pAG326	Based on pUC18. 1.5kb *Bam*H1-*Acc*I fragment of pSS50 containing most of *PCH2* ORF replaced with *Bam*H1-*Cla*1 of R1333 containing *URA3*	B. Rockmill
pAG336	pUG34 *CEN6 AmpR MET25-P yEGFP3 CYC1-T HIS3* 627bps Yeast expression vector for *MET25* induced expression of GFP fusion proteins	D. Hegemann
pAG337	pUG34 vector has been digested with *Xba*I and re-ligated to remove GFP section.	S. Milson
pAG338	pUG34 *AmpR CEN6 HIS3 MET25-P Exo1-6xHIS yEGFP3* sequence was excised with an *Xba*1-*Xho*1 digest. Ligated in was *EXO1* ORF- 6x*HIS* with *Xba*1 and *Xho*1 ends respectively.	This study

2.3 *S. cerevisiae* strains

Table 2.3.1 Haploid strains

All haploid strains are derivatives of SKI (Kane and Roth, 1974), unless stated otherwise. All haploid strains are *ura3 lys2 ho::LYS2 leu2 nuc1::LEU2*, unless stated otherwise. Only mutant alleles are shown.

Name	Genotype	Source
hAG2	*MAT***a** *trp1::hisG*	S55, M. Lichten
hAG3	*MAT***a** *trp1::hisG*	S56, M. Lichten
hAG7	*MAT***a** *ura3 lys2 ho::LYS2 leu2-R arg4-nsp,bgl*	S105, M.Lichten
hAG55	*MAT***a** *ura2*	H317, M.Lichten
hAG56	*MATα ura2*	H317, M.Lichten
hAG251	*ura3::URA3-[arg4-bgl] spo11(Y135F)-HA3His6::KanMX ade2 dmc1::ADE2 TFP1::VDE*	(Neale *et al.*, 2002)
hAG354	*ura3::URA3-[arg4-VDE] TFP1::TFP1*	M. J. Neale (Unpub.)
hAG408	*MATα leu2-R arg4-nsp,bgl trp1::hisG ade2 his3::TRP1 K.lac*	M. J. Neale (Unpub.)
hAG1301	hAG354 transformed with pAG326	This study
hAG1387	hAG251 transformed with Exo1p-6xHIS	This study
hAG1389	hAG408 transformed with pAG338	This study
hAG1307	hAG3 transformed with pAG326	This study

2.3.2 Diploid strains

All diploid strains are SK1, *MAT***a**/α and homozygous for *ura3 lys2 ho::LYS2 arg4-nsp,bgl leu2 nuc1::LEU2* unless stated otherwise. Only mutant alleles shown.

Name	Genotype	Source
dAG205	*ura3::URA3-[arg4-VDE]/ura3::URA3[arg4-bgl] spo11(Y135F)-HA3His6::KanMX/spo11(Y135F)-HA3His6::KanMX TFP1::VDE/TFP1::TFP1*	(Neale *et al.*, 2002)
dAG206	*ura3::URA3-[arg4-VDE]/ura3::URA3[arg4-bgl] spo11(Y135F)-HA3His6::KanMX/Spo11 TFP1::VDE/TFP1::TFP1*	(Neale *et al.*, 2002)

dAG277	*ura3::URA3-[arg4-VDE]/ura3::URA3[arg4-bgl] spo11(Y135F)-HA3His6::KanMX/Spo11 sae2::KanMX/ sae2::KanMX TFP1::VDE/TFP1::TFP1*	(Neale *et al.*, 2002)
dAG287	*ura3::URA3-[arg4-VDE]/ura3::URA3[arg4-bgl] spo11(Y135F)-HA3His6::KanMX/ spo11(Y135F)-HA3His6::KanMX dmc1::ADE2/ dmc1::ADE2 TFP1::VDE/TFP1::TFP1*	M.J.N (Unpub.).
dAG288	*ura3::URA3-[arg4-VDE]/ura3::URA3[arg4-bgl] spo11(Y135F)-HA3His6::KanMX/Spo11 dmc1::ADE2/ dmc1::ADE2 TFP1::VDE/TFP1::TFP1*	M.J.N (Unpub.).
dAG291	*ura3::URA3-[arg4-VDE]/ura3::URA3[arg4-bgl] spo11(Y135F)-HA3His6::KanMX/spo11(Y135F)-HA3His6::KanMX ndt80::ADE2/ ndt80::ADE2TFP1::VDE/TFP1::TFP1*	(Neale *et al.*, 2002)
dAG292	*ura3::URA3-[arg4-VDE]/ura3::URA3[arg4-bgl] spo11(Y135F)-HA3His6::KanMX/Spo11 ndt80::ADE2/ ndt80::ADE2 TFP1::VDE/TFP1::TFP1*	(Neale *et al.*, 2002)
dAG484	*ura3::URA3-[arg4-VDE]/ura3::URA3[arg4-bgl] spo11(Y135F)-HA3His6::KanMX/Spo11hop1::LEU2/ hop1::LEU2 dmc1::ADE2/ dmc1::ADE2 TFP1::VDE/TFP1::TFP1*	M.J.N (Unpub.).
dAG534	*ura3::URA3-[arg4-VDE]/ura3::URA3[arg4-bgl] spo11(Y135F)-HA3His6::KanMX/ spo11(Y135F)-HA3His6::KanMX dmc1::ADE2/ dmc1::ADE2 TFP1::VDE/TFP1::TFP1*	M.J.N (Unpub.).
dAG702	*ura3::URA3-[arg4-VDE]/ura3::URA3[arg4-bgl] spo11(Y135F)-HA3His6::KanMX/Spo11 mek1::LEU2/mek1::LEU2 TFP1::VDE/TFP1::TFP1*	M.J.N (Unpub.).
dAG744	*ura3::URA3-[arg4-VDE]/ura3::URA3[arg4-bgl] spo11(Y135F)-HA3His6::KanMX/Spo11 tel1::ADE2/ tel1::ADE2 TFP1::VDE/TFP1::TFP1*	M.J.N (Unpub.).

dAG806	*ura3::URA3-[arg4-VDE]/ura3::URA3[arg4-bgl] spo11(Y135F)-HA3His6::KanMX/Spo11 dmc1::ADE2/ dmc1::ADE2 ndt80::ADE2/ndt80::ADE2 TFP1::VDE/TFP1::TFP1*	M.J.N (Unpub.).
dAG835	*ura3::URA3-[arg4-VDE]/ura3::URA3[arg4-bgl] mre11-58s/mre11-58s TFP1::VDE/TFP1::TFP1*	M. Ramachandran (Unpub.).
dAG1110	*ura3::URA3-[arg4-VDE]/ura3::URA3[arg4-bgl] mre11-H125N/mre11-H125N TFP1::VDE/TFP1::TFP1*	M. Ramachandran (Unpub.).
dAG1235	*ura3::URA3-[arg4-VDE]/ura3::URA3[arg4-bgl] mre11Δ::KanMX/mre11Δ::KanMX TFP1::VDE/TFP1::TFP1*	This study
dAG1237	*ura3::URA3-[arg4-VDE]/ura3::URA3[arg4-bgl] Spo11 /Spo11 dmc1::ADE2 / dmc1::ADE2 mek1::LEU2/ mek1::LEU2 TFP1::VDE/TFP1::TFP1*	This study
dAG1309	*ura3::URA3-[arg4-VDE]/ura3::URA3[arg4-bgl] Spo11/Spo11 mek1::LEU2 ade2-bgl::GST-(mek1-K199R)-ADE2/ mek1::LEU2 ade2-bgl::GST-(mek1-K199R)-ADE2 dmc1::ADE2 / dmc1::ADE2 TFP1::VDE/TFP1::TFP1*	This study
dAG1371	*ura3::URA3-[arg4-VDE]/ura3::URA3[arg4-bgl] spo11(Y135F)-HA3His6::KanMX/spo11(Y135F)-HA3His6::KanMX sae2::KanMX/sae2::KanMX TFP1::VDE/TFP1::TFP1*	This study
dAG1384	*ura3::URA3-[arg4-VDE]/ura3::URA3[arg4-bgl] Spo11 /Spo11 dmc1::ADE2/ dmc1::ADE2 pch2::URA3/pch2::URA3 TFP1::VDE/TFP1::TFP1*	This study
dAG1432	*leu2-R/leu2-R arg4-nsp,bgl/arg4-nsp,bgl trp1::hisG/trp1::hisG ade2 his3::TRP1/his3::TRP1 MET25-EXO1-6xHIS::HIS/MET25-EXO1-6xHIS::HIS*	This study

Relevant mutation strains containing either the *ura3*::*arg4*–vde cassette were made by mating and dissection with relevant congenic haploids.

2.4 Primers

Oligonucleotides used in primer extension and PCR were synthesised by MWGBiotech with the high–purity salt free (HPSF) purification method.

Name	Sequence	Description
Exo1F	ctagtctagaATGGGTATCCAAGGTCTTCTT	To 6xHIS tag Exo1p
Exo1R	ccgctcgagCTAATGATGATGATGATGATGACCT TTACCTTTATAAACAAATTGGGAAAGCAA	To 6xHIS tag Exo1p
MN03	GGTACAATCACTTGGATTGCTCC	*TFP1* locus
MN04	AAGCTTCTCTGGCTGCAACCGGC	*TFP1* locus
MN11	AAAGGAACTATCCAATACCTCGCC	Downstream of *URA3* locus
MN12	AAGGATCCCCACCTATGGGC	Downstream of *URA3* locus
VDE01	CCATACTGCGAATGAAAGACGTCTTGG	*ARG4* locus
VDE02	ATGACCAGCAAGAGCGCCTGCACCC	*ARG4* locus
VDE03	GAGTTGTTAAGAGGTAAATCCGG	*ARG4* locus
VDE04	GATCTTGTCCGAATCTCGAATCG	*ARG4* locus
VDE05	GCCCTGCACCATTATGTTCCGG	pBR322 specific
VDE06	AGCTGCGGTAAAGCTCATCAGCG	pBR322 specific

2.5 Media and stock solutions

2.5.1 Media

YPD: 1 % (w/v) yeast extract (Difco); 2 % (w/v) peptone (Difco); 2 % (w/v) D-glucose (BDH); 40 μg/ ml adenine; solid media included 2 % (w/v) agar (Oxoid).

Minimal: 0.67 % (w/v) yeast nitrogen base free of amino acids (Difco); 2 % (w/v) D-glucose (BDH); 2 % (w/v) agar (Oxoid).

SC: Made up as minimal plates above, but with 0.85 g/ l of dropout mastermix, and 1 μl/ ml of 2 M NaOH. Complete SC mastermix contained: 0.8 g adenine; 0.8 g arginine; 4.0 g aspartic acid; 0.8 g histidine; 2.4 g leucine; 1.2 g lysine; 0.8 g methionine; 2.0 g phenylalanine; 8.0 g threonine; 0.8 g tryptophan; 1.2 g tyrosine; 0.8 g uracil. Dropout mastermix was as complete mastermix with the exclusion of one or more supplements.

PSP2: 0.67 % (w/v) yeast nitrogen base free from amino acids (Difco); 0.1 % (w/v) yeast extract (Difco); 1 % (w/v) potassium acetate; 50 mM K-biphthalate (Sigma); pH 5.0

Potassium acetate: 1 % (w/v) potassium acetate; supplemented with 10 μg/ ml adenine, plus appropriate amino acid supplements (e.g. adenine, arginine) at 10 μg/ ml for the auxotrophies of the strain under study. Solid media included 2 % (w/v) agar (Difco); 0.05 % (w/v) yeast extract (Difco) and 0.1 % (w/v) D-glucose (BDH).

5FOA: 1.4 % (w/v) nitrogen base without amino acids; 4 % (w/v) Bacto agar, 4 % (w/v) glucose; 0.01 % (w/v) uracil; 0.006 % (w/v) argnine; 0.018 % (w/v) leucine; 0.006 % (w/v) adenine (and any other amino acids that the *S. cerevisiae* strains are mutant for) in 500 ml of water is autoclaved. 0.2 (w/v) % 5-FOA dissolved in 500 ml water filter sterilised in the autoclaved media.

2TY: 1% (w/v) tryptone; 1 % (w/v) yeast extract; 0.5 % (w/v) sodium chloride; 1.5 % (w/v) Bacto agar (in solid media); pH 7.4

2.5.2 Stock Solutions

20 X SSPE: 3.6 M NaCl; 200 mM NaH_2PO_4; 20 mM EDTA; pH 7.4

50 X TAE: 2 M Tris.acetate; 50 mM EDTA, pH 8.0

10 X TE: 100 mM Tris.HCl; 10 mM EDTA, pH 8.0

10 X TNE: 100 mM Tris.HCl; 2M NaCl; 10 mM EDTA, pH 7.4

5 X Neutral loading buffer: 0.25 % (w/v) bromophenol blue; 0.25 % (w/v) xylene cyanol; 20 % (w/v) ficoll 400

6 X Alkaline loading buffer: 300 mM NaOH; 6 mM EDTA; 0.15 % (w/v) bromocresol green; 0.25 % (w/v) xylene cyanol; 18 % (w/v) ficoll 400

4 X TCA Loading dye: 250 mM Tris (6.8); 8 % (w/v) SDS; 20 % (w/v) glycerol; 20 % (v/v) β-mercaptoethanol; 0.4 % (w/v) bromophenol blue

RNase: 10 mg/ ml RNaseA in 10 mM Tris.HCl (pH7.5); 22.5 mM NaCl. Heated to 100 °C for 15 min, and slowly cooled to RT. Storage at –20 °C

Proteinase K: 20 mg/ ml proteinase K, in 10 mM Tris.HCl; 2 mM $CaCl_2$, 50 % (v/v) glycerol. Filter sterilise before addition of proteinase K. Storage at –20 °C

Genomic TENS: 2 % (w/v) Triton-x100; 1 % (w/v) SDS; 100 mM NaCl; 10 mM Tris.HCl pH 8; 1 mM EDTA

Spheroplasting solution (with or without glycerol): 1 M sorbitol; 50 mM KPO_4 pH 7.5; 10 mM EDTA pH 7.5 (20 % (v/v) glycerol).

CTAB Extraction solution: 100 mM Tris.HCl pH7.5; 25 mM EDTA; 2 M NaCl; 2 % (w/v) PVP40. 10 % (w/v) solutions of PVP40 and 10 % (w/v) CTAB were made and dissolved in a 55 °C water bath before addition to the other chemicals in solution.

CTAB Dilution solution: 20 ml 10 % (w/v) CTAB; 10 ml 1 M Tris.HCl pH 7.5; 4 ml 0.5 M EDTA pH 8 in 200 ml

2.6 Growth, culture and storage of *S. cerevisiae* and *E. coli*

All strains of *S. cerevisiae* used for experimental work in this study are SK1 background. Diploid SK1 strains sporulate rapidly following nitrogen starvation when placed in the presence of the non–fermentable carbon source: Potassium acetate (Kane and Roth, 1974).

2.6.1 *S. cerevisiae* growth conditions

All *S. cerevisiae* strains were grown on for 48 hr at 30 °C on YPD plates. Yeast cultures were grown in 5 ml of YPD broth in sterile glass culture tubes for 24 hr at 30 °C with constant agitation on a rotor wheel.

2.6.2 *S. cerevisiae* storage conditions

S. cerevisiae strains were stored in 50 % (v/v) glycerol at –80 °C

2.6.3 *E. coli* growth conditions

All *E. coli* strains were grown on 2TY plates containing plasmid selection drug, mostly ampicillin (50 μg/ ml), for 24 hr at 37 °C. *E. coli* cultures were grown in 2TY broth with 50 μg/ ml of ampicillin for 24 hr at 37 °C with constant agitation.

2.6.4 *E. coli* storage conditions

E. coli containing plasmids were stored in 50 % (v/v) glycerol at –80 °C

2.7 *E. coli* techniques

2.7.1 Transformation of chemically competent DH5α cells

1 μl of DNA is mixed by gentle pipetting with 50 μl chemically competent cells (DH5α). Cells were incubated on ice for 15 min, followed by a heat shock of 90

seconds at 37 °C. 450 µl of 2TY broth (with 25 ng of ampicillin) was added to the cells and incubated at 37 °C. 220 µl of cells were plated out on 2TY solid media containing the plasmid selection drug, predominantly ampicillin (30 µg/ ml), and incubated at 37 °C overnight.

2.7.2 Small-scale isolation of plasmid DNA (Minipreps)

All minipreps were carried out using the QIAprep Miniprep Kit (Qiagen) according to manufacturer's guidelines.

2.7.3 Large-scale isolation of plasmid DNA (Midipreps)

All midipreps were carried out using the Wizard *Plus* Midipreps DNA Purification System kit (Promega) according to manufacturer's guidelines.

2.8 *S. cerevisiae* techniques

2.8.1 Production of single colonies

S. cerevisiae strains were streaked onto YPD plates from –80 °C stock using a 10 μl loop. After one day at 30 °C single colonies could be seen, after two they could be used.

2.8.2 Mating haploid strains

Single colonies of opposite mating type (a or α) were patched together onto YPD plates. After 24 hr growth at 30 °C, it was possible to streak these patches for single colonies. After a further 24 hr at 30 °C these single colonies could be tested to check they were diploid by mating type testing (see below) and for sporulation on KAc plates (see below).

2.8.3 Mating type testing

Single colonies (all strains used are *URA3*) were mated with both tester strains (hAG 55, Mat a and hAG 56, Mat α), which have a mutation in *ura3*. After 24 hr at 30 °C the YPD plates were replica plated onto minimal media plates and

incubated at 30 °C for an additional 24 hr. When a diploid strain is created, all nutritional requirements of the cell are satisfied and the cell is able to grow on minimal media. A cell, which is able to grow when mated with hAG 55, is of the α mating type, and one that grows when mated with hAG 56 is of the a mating type.

2.8.4 Diploid strain sporulation (Solid media)

Single diploid colonies were patched onto YPD plates. Following 24 hr at 30 °C, they were replica plated onto 1 % (w/v) KAc plates and left for a further 24 hr at 30 °C. After 24 - 48 hr incubation, almost 100 % sporulation is observed (For sporulation competent cells).

2.8.5 Tetrad dissection

Diploid cells were grown on 1 % (w/v) KAc plates for 24 hr at 30 °C. Cells were incubated in 20 μl β-glucooronidase for 20 min at 30 °C on a rotor wheel. This process breaks down the spore wall, allowing the tetrads to be isolated. 20 tetrads were dissected per plate of YPD by a micromanipulator. Plates were incubated at 30 °C for 48 hr.

2.8.6 *S. cerevisiae* transformation (Lithium acetate)

Haploid yeast were transformed with plasmids or linear DNA fragments using the lithium acetate (LiAc) procedure. A 5 ml overnight culture of cells were diluted in fresh YPD to an OD_{600} of 0.2, and grown for 3 hr – 5 hr, to an OD of 0.8 - 1.0, to allow time for at least two divisions to take place. Following this growth, cells were harvested, washed in 1 ml 100 mM LiAc, and resuspended in 160 μl 100 mM LiAc. Cells were then vortexed and 50 µl of cells per transformation aliquoted into fresh 1.5 ml tubes. The aliquoted cells were then centrifuged at 14000 x g for 15 seconds and the excess LiAc removed. Following this, 240 µl of 50 % (w/v) filter sterilised PEG_{3500}, 36 µl 1M LiAc, 100 µg of salmon testis ssDNA that has been boiled and cooled on ice, 0.1 - 10 µg of DNA, and sterile water to make

volume up to 360 µl, was added to the cells. Chemicals were added in this order so the cells were shielded from the detrimental effects of the LiAc by the PEG_{3500}, thus reducing potential cellular damage.

Cells were incubated at 30 °C for 30 min, then heated to 42 °C in a water bath for 30 min (heat–shock). Transformants were selected for by plating on appropriate selective plates and incubated for 2-3 days at 30 °C.

2.8.7 *S. cerevisiae* transformation (Electroporation)

5 ml YEPD cultures were incubated overnight at 30 °C and then pelleted at 3000 x g for 2 min. The pellets were washed three times in 5 ml 1.2 M ice-cold sorbitol, centrifuged as before, and then resuspended in a minimum volume (less than 20 µl). 5 - 10 µg of transforming DNA was ethanol precipitated with 5 µl heat denatured salmon testis ssDNA (10 mg/ ml), and resuspended in 5 µl of 1 x TE. 40 µl of washed cells was mixed with the DNA and gently pipetted into a Gene Pulser cuvette (BioRad) and placed inside an EasyjecT+ electroporator, where the cells were exposed to an electrical pulse of 1.5 kV, 25 μF and 200 Ω. 400 µl of ice-cold 1.2 M sorbitol was added to the electroporated cells to buffer the cells. The cells were plated out onto selective media containing 1.2 M sorbitol, and incubated at 30 °C for 72 hr. Sizeable colonies were streaked out onto selective media and incubated at 30 °C for a further 48 hr to select for true transformants.

2.8.8 Synchronous meiotic time course

The yeast strains of desired phenotype were streaked onto YPD plates from –80 °C glycerol stock. The plates were then incubated at 30 °C for 48 hr. 5 ml of YPD broth was then inoculated with a single colony and kept at 30 °C on a rotor wheel overnight. The OD_{600} of the overnight culture was taken after 16 hr is an OD_{600} of between 16 and 20 was achieved, the culture was used to inoculate 300 ml of PSP2 with dilutions ranging from 1 in 100 to 1 in 500 depending upon the OD_{600} of the overnight culture. The PSP2 is inoculated into 2 l conical flasks. After 24 hr at 30 °C, the OD_{600} of the PSP2 cultures is taken. An OD_{600} reading of between 1.6 and

2.0 can be used in a time course. The PSP2 cultures are centrifuged at 4500 x g for 2 min. The subsequent pellet was then washed in 1 % (w/v) KAc and centrifuged at 4500 x g for 2 min. Finally, the pellet is resuspended in 300 ml 1 % (w/v) KAc, supplemented with 3 mg adenine, 3 mg arginine and 300 µl 1 % (w/v) PPG. The KAc cultures were left in a 3 l baffled flasks, shaking at 300 rpm. The first time point was taken immediately; subsequent time points were taken hourly.

2.8.9 Cell harvesting following meiotic time course

At each time point, 40 ml of synchronously sporulating cells were taken for DNA extraction. 400 μl of 10 % (w/v) sodium azide and 8 ml of 50 % (v/v) glycerol (ice-cold) were added to the cells. The cells were placed in an ice slurry for 5 min. Following this, cells were pelleted at 3000 x g for 3 min then washed in 5 ml of spheroplasting solution with glycerol and transferred into round-bottomed glass tubes. The spheroplasting solution was removed after a further pelleting. Cells were then snap frozen in liquid N_2 for 5 min and transferred to –80 °C for storage.

2.8.10 Cell harvesting following meiotic time course for chromatin immunoprecipitation (ChIP)

At each time point, 25 ml of synchronously sporulating cells were taken for immunoprecipitation. Formaldehyde was added to a final concentration of 1 % (v/v). Samples were incubated for 20 min at RT. Glycine was then added to a final concentration of 125 mM and samples were incubated for a further five min at RT. Samples were then centrifuged at 14000 rpm for 5 min, the pellets were then washed in 10 ml 1 x TBS. Samples were again centrifuged at 14000 rpm for 5 min and resuspended in 1 ml of 1 x TBS. Finally, the samples were transferred to screw capped micro-centrifuge tubes and the supernatant removed. Samples could then be stored at –80 °C.

2.8.11 DAPI staining

500 µl of culture is added to 500 µl of 100 % (v/v) ethanol and stored at –20 °C for staining with 4′,6-Diamidino-2-phenylindole (DAPI, to 0.5 μl/ml). This enables the nuclei to be visualised. Stained cells were visualised on a Leica DMLB Epifluorescence Microscope at magnification of x 40. The number of cells with 1, 2, 3 or 4 nuclei was recorded for each time point. More than 200 cells per time point were counted.

2.9 Molecular biology techniques

2.9.1 Ethanol precipitation of DNA

One-tenth volume of 3 M sodium acetate pH 5.2 was added to the DNA (in solution), and then mixed by gentle vortexing. Following this; 2 volumes of 100 % ethanol were added. The DNA precipitated following storage at –20 °C for approximately 16 hr, or 30 min at –70 °C. A DNA pellet formed following centrifugation at 14000 rpm for 30 min. Finally, the DNA pellet was washed in 1 ml of 70 % ethanol, twice and air-dried. The DNA was then resuspended in 1 x TE.

2.9.2 DNA digests

DNA was digested with restriction enzymes under the conditions recommended by the manufacturer. Analytical digests were carried out for 1 hr in a water bath at temperature specified. Digests for Southerns were carried out for 3 hr. All digests were made up to final volume with dH_20.

2.9.3 DNA ligations

Plasmid–insert ligations were performed with a 5–fold molar excess of insert molecule relative to linearised plasmid. Plasmids linearised with a single enzyme were treated with shrimp alkaline phosphatase (USB) for 30 min at 37 °C, heated to 65 °C for 20 min, then concentrated by precipitation prior to use in the ligation. This treatment minimised recircularisation of the plasmid molecule. Typical

ligation reactions were 50 – 100 ng plasmid, 5–fold molar excess of insert molecules, 1 x reaction buffer (40 mM Tris.HCl, 10mM $MgCl_2$, 10mM DTT, 5 mM ATP, pH 7.8), 1 μl T4 DNA ligase (MBIFermentas). Ligations were made up with UP–H_20 in the minimum volume possible (usually 10 - 20 μl), and incubated at RT for 2 hr.

2.9.4 Polymerase chain reaction (PCR)

For amplification of regions less than 3.5 Kb, 2 x PCR Master Mix (ABgene) was used with 100 pM each of the forward and reverse primers. Yeast genomic DNA (300 – 500 ng) or plasmid DNA (300 – 500 ng) was used as template. Typical PCR cycling was 96 °C for 1 min, followed by 30 cycles of: 94 °C for 30 sec, x °C for 30 sec, and 72 °C for y–sec, where x is the primer–specific annealing temperature and y is proportional to the length of DNA product to be obtained (1 min per Kb). Reactions were terminated with a final extension of 72 °C for 2 min.

2.9.5 Long range PCR

For amplification of regions greater than 3.5 Kb or when high fidelity polymerase was required, 2 x concentration of Extensor Master Mix (ABgene) was used. The same concentrations of primers as standard PCR were used. For long range PCR, all amplification steps were carried out at 68 °C not 72 °C as for standard.

2.9.6 Yeast colony PCR

A single colony of yeast was added to 20 μl of 20 T zymolyase (5 mg/ ml, ICN) and incubated at 37 °C for 30 min. The zymolyase mix was then incubated at 100 °C for 5 min to inactivate any nucleases. 1 μl of this zymolyase mix was then added to the PCR reaction.

2.9.7 *E. coli* colony PCR

A single colony of *E. coli* was added to 50 μl of dH_20 and incubated at 100 °C for 5 min. The waster/colony mix was then centrifuged at maximum speed for one 1

min then resuspended in 20 µl of dH_20. 1 µl of this mix was then added to the PCR reaction..

2.9.8 Glass beads method of DNA extraction

An overnight YPD culture of 1.5 ml was centrifuged in a sterile micro-centrifuge tube at 14000 x g for 2 min. Following this, the cell pellet was resuspended in 200 μl of genomic TENS. Sterile glass beads were then added to the mix, up to the level of the meniscus, with vigorous vortexing for 2 min. After vortexing, 100 μl of isoamyl:phenol:chloroform (1:25:24) was added with an additional 2 min vortexing. The micro-centrifuge tube was then centrifuged for 2 min at 14000 x g and the top layer was transferred to a fresh sterile micro-centrifuge tube. To this new micro-centrifuge tube, 200 μl of phenol was added and vortexed for an additional 2 min, then centrifuged for 2 min at 14000 x g. Again, the top layer was transferred into a fresh sterile micro-centrifuge tube and the DNA was precipitated using standard ethanol precipitation.

2.9.9 CTAB method of DNA extraction

40 ml of meiotic cells from a time course was pelleted and transferred into a sterile micro-centrifuge tube. The cells were then washed in 1 ml of spheroplasting solution and again pelleted. The cell pellet was then resuspended in 100 μl of spheroplasting solution, 0.25 mg of 100 T zymolyase (ICN) and 5 μl of β-mercaptoenthanol. The mix was then incubated at 37 °C for 5 - 7 min, inverted once during incubation. After incubation, cells were then pelleted once again at 4000 x g for 5 min (well-zymolyased cells can be hard to pellet) and resuspended in 200 μl CTAB extraction solution, 2 μl proteinase K and 0.5 μl RNaseA and gently vortexed. The mix was then incubated at 37 °C for 15 min, inverted twice. Following this incubation, 50 μl of chloroform:isoamylalcohol (1:24) was added to the cell mix, vortexed for 20 seconds, rested for 2 min, then vortexed for an additional 20 secs. After vortexing, cells were centrifuged at 14000 x g for 5 min. The top layer was then transferred to a fresh micro-centrifuge tube, with 900 μl of

CTAB dilution solution layered very gently on top, precipitating the DNA away from the CTAB complex. Gentle mixing of the micro-centrifuge tube precipitated the DNA as white solids. The CTAB dilution solution was then carefully removed from the micro-centrifuge tube and the DNA washed twice in 1 ml of ice cold 0.4 M NaCl in 1 x TE then resuspended in 300 μl ice cold 1.4 M NaCl in 1 x TE. The DNA was then precipitated by adding 600 μl 100 % ethanol and left at RT for 15 - 20 min. Following precipitation of the DNA, the DNA was then washed twice with 70 % (v/v) ethanol. All traces of ethanol were then removed and the DNA was resuspended in 30 - 100 μl of 1 x TE, depending upon size of DNA pellet.

2.9.10 Liquid DNA concentration - Fluorometer

DNA concentration was determined by flourometry using a Hoefer DyNA Quant 200 Fluorometer. 1.5 ml of 1 x TNE buffer was filtered sterilised into the glass 2 ml cuvette. To this 1 x TE, 2 µl of 0.5 mg/ ml DAPI was added and mixed thoroughly with a pipette. The machine was zeroed and then calibrated using 50 ng/ µl λ*BSTE*II as a concentration standard. Each DNA sample was measured twice to obtain an average reading.

2.9.11 Gel purification of DNA fragments

DNA bands were separated by gel electrophoresis and the band of interest was excised from the agarose. DNA was extracted from the agarose using a DNA gel extraction kit (Qiagen) following the manufacturers instructions. This was followed by ethanol precipitation of the DNA.

2.9.12 Native DNA electrophoresis

For standard analysis, DNA was fractionated in 1 % (w/v) agarose gels (made up to volume with 1 x TAE) in 1 x TAE, run at 70 v for the desired length of time. Ethidium bromide (200 μg/ l) was added to the 1 x TAE running buffer prior to running the gel. For Southern blotting, DNA is fractionated in 250 ml 0.5 % (w/v)

agarose gels in 1 x TAE in a 25 cm x 15 cm tray. Electrophoresis was carried out at 70 v for 11 – 13 hr with constant buffer circulation.

2.9.13 Alkaline DNA electrophoresis

For analysis of single stranded DNA, DNA was fractionated in 0.7 % (w/v) alkaline agarose gels (50 mM NaOH, 1 mM EDTA, made up to volume with degassed water). Gels were run with alkaline running buffer (50 mM NaOH, 1 mM EDTA made up to volume with degassed water, chilled in an ice bath). After digestion with appropriate enzyme, 100 mM EDTA was added to a final concentration of 10 mM and mixed. Prior to loading the appropriate amount of 6 x Alkaline loading dye was added to the samples.

Restriction–site–loss assays make use of the fact that type–II restriction endonucleases only cleave double stranded DNA. Thus restriction enzyme digestion will occur at sites flanking an *in vivo* DSB only if the DNA has not undergone resectioning of the 5´–ending strand. Increased length of single–strand resectioning will lead to the restriction enzyme cleaving the DNA at sites further away from the DSB. The longer restriction fragments that are produced can be detected using Southern blotting techniques, following electrophoresis. For this analysis, the type II restriction endonuclease used is *Hae*II. *Hae*II cleaves DNA at sites closely flanking the VDE–DSB site and at a further seven locations within 10 kb downstream of the *arg4–VDE* allele. VDE–DSB formation at *arg4–VDE* creates a unique 358 bp–long, truncated form of the parental molecule. Subsequent 5´ to 3´ resectioning will render *Hae*II restriction sites single–stranded, and thus prevent their cleavage. If a VDE–DSB molecule becomes resected beyond the site of the closest *Hae*II site (+358 bp), cleavage will occur at the next nearest *Hae*II site, ~ 1.8 kb downstream. Similarly, resectioning beyond 1.8 kb but less than ~ 2.2 kb will lead to cleavage at the *Hae*II site + 2.2 kb downstream. In the same way, products of increasing molecular weight will be liberated as resectioning becomes more extensive.

2.9.14 Southern Blot

After electrophoresis, the agarose gels were washed three times in dH_20 for 5 min removing any running buffer or Ethidium bromide. Following the washes in dH_20, the gels were then depurinated in 1 l of 0.25 M HCl for 20 min, then soaked in 1 l 0.4 M NaOH for a further 20 min, denaturing the DNA. Following the washes, the DNA was transferred onto a nylon membrane, Zetaprobe (BioRad) using a blotting system, VacugeneXL (Pharmacia), at 50 mbar for 2 hr in 1 l 0.4 M NaOH. After the blotting, the membrane was washed in 2 x SSPE for 15 min to remove any remaining agarose and to neutralise the NaOH. Finally, the DNA was cross-linked to the membrane using a UV lamp.

2.9.15 Southern analysis to assess VDE cleavage

Standard Southern analysis can assess the rate of VDE cutting by using an *Eco*RV/*Bgl*II-double digest that separates the parental *arg4-VDE* allele from the other molecules (Neale *et al.*, 2002). DNA, isolated from synchronously sporulating (synchrony of cells and entry into the meiotic divisions was monitored by recording nuclear divisions through DNA staining with DAPI) cells at hourly intervals, was restriction digested with *Eco*RV and *Bgl*II, and fractionated on 0.5 % agarose gels. The DNA was transferred to nylon membrane and hybridised with a 386 bp *ARG4*-specific probe (made by PCR using primers VDE 03 and VDE 04) identical to the region directly downstream of the *Eco*RV site (or VDE–cutsite in *arg4–VDE*). This restriction digest makes it possible to separate *arg4–VDE* parental molecules from all other species (see figure 3.4 for details). This digest is a useful way of measuring the rate of VDE–induced cleavage as the amount of DNA present in the *arg4–VDE* band will reduce relative to a loading control, as more cleavage occurs. All error bars presented in quantification of Southern blots are the standard deviations from the mean data values.

2.9.16 Southern analysis to visualise VDE-DSB and deletion product formation

When meiotic DNA is extracted and digested with *Spe*I and then probed on a Southern blot with chromosome *V*-specific probe made from PCR using primers MN11 and MN12, the VDE-DSB is visible as a truncated form of the parental band, with a molecular weight of ~ 7.8 kb. In a WT cell, the VDE-DSB peaks at time point 5 hr, and then decreases as the VDE-DSB is repaired.

To determine the level of VDE-DSB and the proportion of the deletion product formed in the strains, the quantity of probe hybridising to the VDE-DSB and the deletion bands was calculated as the proportion of total DNA in the lane. The total DNA that is probed in each lane consists of two *arg4–VDE* chromatids, and two *arg4–bgl* chromatids. Therefore, values, as the proportion of total DNA, were doubled to express data as the percentage of *arg4–VDE* chromatids (see figure 3.9). All error bars presented in quantification of Southern blots are the standard deviations from the mean data values.

2.9.17 Slot blot

Meiotic DNA isolated at hourly time points was blotted with and without heat denaturation onto a nylon membrane using a slot–blot apparatus. Blots were hybridised with ^{32}P–labelled single–stranded DNA probes complementary to the unresected strand (3 kb downstream of the VDE–DSB). Single–stranded probes were made by primer extension using gel purified PCR products as templates (primers for PCR: VDE 05 and VDE 06). Scanning densitometry was used to determine the amount of probe hybridising to each of the DNA samples. The single–stranded probe is able to hybridise to the denatured DNA samples independently of there being any single–stranded resectioning. By contrast, the probe is only able to hybridise to the native DNA samples if resectioning has passed the site of the probe (see Figure 4.4). The quantity of hybridisation signal to native DNA was normalised to the denatured DNA hybridisation signal from

the same time point. This allows an estimate to be made of the extent of single–strandedness at the site of the probe at each hour in meiosis.

2.9.18 Generation of double stranded ^{32}P probes

Probe DNA templates were produced by PCR using genomic DNA as a template. The subsequent PCR products were then gel purified to remove any genomic DNA, then used as a template in a second round of PCR. The PCR products were then ethanol precipitated and resuspended in 1 x TE to a final concentration of 50 ng/ μl. Labelling reactions included 50 ng of probe, 0.1 ng of λ*BstE*II digested DNA, 9 μl dH_20 and 4 μl HighPrime (Roche) random primer. This mix was then incubated at 100 °C for 2 min than put onto ice for 5 min. To this 5 µl of ^{32}P labelled dCTP was added incubated at 37 °C for 20 min. BioRad chromatography columns were used to remove any unincorporated nucleotides from the probe mix. The labelled probe was added to a spin column and centrifuged at 4000 x g for 4 min. 250 µl of salmon sperm ssDNA (10 mg/ ml) was added and placed at 100 °C for 2 - 3 min.

2.9.19 Pre-hybridisation, hybridisation and washes

DNA cross-linked membranes were prehybridised for 4 hr – 24 hr at 65 °C in prehybridisation solution (2 x SSPE, 1 % SDS, 0.5 % non-fat dry milk, 5 µg/ ml boiled salmon sperm ssDNA). Hybridisation took place at 65 °C for 16 hr in hybridisation solution (2 x SSPE, 1 % SDS, 0.5 % non-fat dry milk, 5 % dextran sulphate (Sigma-Aldrich)), with the ^{32}P-incorporated probe. After incubation, membranes were washed at RT with agitation in 250 ml of the following solutions: 2 x SSPE, 1 % SDS; 0.5 x SSPE, 1 % SDS. Each wash took 15 min. Membranes were wrapped in watertight plastic wrap, and exposed to a blanked phosphor screen (Kodak), with a screen guard between the two (BioRad).

2.9.20 Generation of single stranded ^{32}P probes

Gel purified PCR products were used as a DNA template in a linear PCR reaction. A typical PCR reaction would include 10 ng DNA template, 40 μM dATP, 40 μM dGTP, 40 μM dTTP , 1 μM dCTP and 100 pM of primer. This reaction mix was denatured at 100 °C for 2 min followed by ice chilling for 5 min. Following this, 1 μl Taq polymerase (5 U/ μl, buffer B, Promega), 1 μl 10 x Mg^{2+} free Buffer, 1 μl $MgCl_2$ and 5 μl ^{32}P-labelled dCTP (ICN, 3000Cio/mmol, frozen) was added. The PCR cycle was as follows; 94 °C for 30 sec, 57 °C for 30 sec, 72 °C for 45 sec (15 cycles). Labelled probes were purified from unincorporated ^{32}P–labelled nucleotides using a chromatography spin column (BioRad).

2.9.21 Scanning densitometry

A Personal FX phosphorimager (BioRad) was used to scan the screen to determine the density of radiation emitted from the hybridised filter. Quantification of the hybridisation signal released was assayed using the quantification software, Quantity One (BioRad). In essence, borders were placed around the upper and lower limits of each band to be measured in each lane of the gel; the removal of lane background was also used so that background signals were not incorporated into the quantification of the bands. The quantity of signal within each band was determined by calculating the signal form the area under each peak minus the background signal.

2.9.22 Chromatin immunoprecipitation (ChIP)

Meiotic time courses were carried out and samples were taken for DNA extraction and DNA-protein cross-linking. Southern analysis was carried out on the meiotic time courses to ensure that the VDE allele had undergone efficient cutting. Cleavage at *arg4-VDE* was found to be as WT (data not shown).

Chromatin Immunoprecipitation time courses were performed that cross-linked all proteins bound to DNA. Protein cross-linked time course samples were sent to V. Borde who carried out all ChIP experiments. Immunoprecipitation using anti

Rfa-1 antibody was used to pull down all DNA sequences with Rfa-1 bound. Quantitative multiplex PCR was used using primers specific to Spo11p coldspot YCR013C, Spo11p hotspot YCR048W and the *URA3* repeat region of the VDE construct.

Primers VDE E and VDE F anneal to the *URA3* region of the reporter cassette on chromosome *VIII* (see figure 5.8). Primers 13C F and R anneal to the region YCR013C of chromosome *III*, with a product size of 220 bp, which is a dubious ORF, unlikely to encode a protein. This region is used as a Spo11p coldspot. The primers 48W F and R anneal to the region YCR048W on chromosome *III* (see figure 5.8), with a product size of 164 bp, and encoding an endoplasmic reticulum enzyme that contributes to the major sterol esterification activity in the absence of oxygen. This region is used as a Spo11p hotspot, with 9% of all chromosomes receiving a break.

PCR reactions were run on polyacrylaminde gels and quantified using the BioRad QuantityOne package. Output PCR samples (PCR reactions using DNA from immunoprecipitation reactions as a template) were calculated relative to input PCR samples (PCR reactions not associated with an immunoprecipitation reaction). The Output/Input ratios at the Spo11p-hotspot were calculated as fold enrichment over the Output/Input ratio at the Spo11p-coldspot (Borde *et al.*, 2004). The use of a ratio between input and output figures allows the background PCR product to be subtracted from the PCR product coupled with the immunoprecipitation.

2.9.23 Generation of 6xHIS tagged Exo1p and promoter replacement

EXO1 was amplified using primers Exo1F and Exo1R. The amplified *EXO1* ORF contained an *Xba*I restriction site 5′ of the START codon. At the 3′ end of the ORF, the STOP codon was removed and cloned in was a glycine linker followed by six histidine residues. Following on from the histidine residues, an *Xho*I-restriction site was cloned into frame (see figure 6.12). pAG336 was digested with *Xba*I and *Xho*I, which excised the *yEGFP3* fragment (see figure 6.11). The amplified *EXO1-6xHIS* ORF was ligated in between the *Xba*I and *Xho*I-restriction

sites. The *EXO1-6xHIS* ORF was under control of the highly expressed and regulatable promoter, *MET25*. The new plasmid was designated pAG338. pAG338 was transformed into competent DH5α *E. coli* cells and transformants were screened by colony PCR. Correct transformants were selected and the plasmid was isolated. hAG407 was transformed with pAG336 and transformants were again screened by PCR. A correct transformant was selected and designated hAG1389.

2.10 Biochemistry techniques

2.10.1 Method of soluble protein extraction

Cells were grown to mid log phase (1 x 10^7). Cultures were then centrifuged at 3000 rpm for 5 min. The pellet was then resuspended in 1 ml 20 % TCA (w/v) and transferred to a screw capped micro-centrifuge tube. Cells were then again centrifuged at 14000 rpm for 1 min. This pellet was then resuspended into 200 µl 20 % TCA. Glass beads were then added up to the meniscus and the samples were then Ribolysed at speed 6 for 25 secs, a total of three times. It was then checked to see how well the cells had lysed under the light microscope. If sufficient, an additional 200 µl of 5 % TCA was added to the sample. The sample was then centrifuged at 3000 rpm for 5 min to remove the glass beads. The supernatant was then transferred to a fresh micro-centrifuge tube and centrifuged for an additional 5 min at 14000 rpm. Finally, the pellet was then resuspended in 1 ml of TCA loading dye and stored at –80 °C if necessary.

2.10.2 Method of total protein extraction

200 ml of synchronous meiotic culture was harvested at each time point by centrifugation at 3000 rpm for 5 min, washed in sterile water and transferred to a 2 ml screw capped micro-centrifuge tube. Cells were pelleted by brief centrifugation and the supernatant was removed. To the cell pellet was added an approximately equal volume of acid washed beads (Sigma, 425 - 600 microns) and enough protein lysis buffer to cover the beads was added. Cells were disrupted by

agitation using a Mini Beadbeater for 30 sec, followed by 30 sec on ice, then a final 30 sec of agitation. Beads and cellular debris were removed by centrifugation at 11,000 rpm for 5 min at 4 °C.

2.10.3 Determination of protein concentration

Protein concentrations were determined using Bio-Rad protein determination kit and bovine serum albumin as standard. Both standard and unknown protein concentrations were assayed under manufacturers conditions.

2.10.4 Immuno-precipitation of 6xHIS tagged protein

20 μg of protein lysate was incubated with 1 μl of a 1 in 10 dilution of the secondary antibody (DakoCytomation, polyclonal goat anti-mouse HRP) and 20 μl of IgG agarose (Santa Cruz) beads at 4 ° C for 30 min, with constant agitation. Following incubation, samples were centrifuged at 11,000 rpm for 5 min and the supernatant removed. To the supernatant, 5 μl of primary antibody (tetra-His α-mouse HRP, Sigma) was added and incubated at 4 °C for 1 hr. Following incubation, 20 μl of IgG agarose beads was added and incubated at 4 °C for 2 hr. Following incubation, samples were centrifuged at 11,000 rpm for 5 min and the supernatant was discarded. The agarose beads were then washed twice in 1 x PBS pH 7.4.

2.10.5 Phosphatase treatment of protein lysate

20 μg of protein lysate was incubated at 37 °C for 45 min with 2 units of Calf Intestinal Phosphatase (CIP, 1 U/ μm, Roche) and an appropriate amount of 10 x buffer with and without the presence of phosphatase inhibitors (0.1 M Sodium Phosphate, 0.2 mM Sodium Orthovanadate, 1 mM Sodium Floride) before diluting with 4 x protein sample buffer and boiling for 10 min.

2.10.6 Protein lysate buffer

50 mM Tris (pH 7.5), 50 mM NaF, 5 mM EDTA, 25 mM NaCl, 0.1 mM Na_3VO_4, 17.28 mg/ ml β-glycerophosphate, 6.92 mg/ ml p-nitrophenylphosphate, 0.4 mM DTT, 1 µl/ ml IGPALCA-630, 1.6 µl/ ml PMSF (10 mg/ ml in isopropanol) 4 µl/ ml complete EDTA free protease inhibitor cocktail tablet (Roche, made up according to manufacturers instructions.)

2.10.7 SDS-Polyacrylamide gel electrophoresis

Proteins were separated by SDS-PAGE in a Mini-Protean II system (BioRad). The appropriate percentage of SDS-PAGE separating gel was determined by calculation of the molecular weight of the protein of interest. Proteins of high molecular weight (>150 kD) were usually run on 6 % (v/v) gels, whilst lower molecular weight proteins (<40 kD) were run on 14 % (v/v) gels. Prior to loading, protein samples were boiled for 4 min in sample buffer. These samples were loaded into wells formed within the stacking gel, and electrophoresis proceeded at a constant current of 300 mA until the appropriate level of protein separation had occurred. Molecular standard markers (New England BioLabs) were run beside the samples to indicate protein size.

2.10.8 SDS-PAGE solutions

30 % (v/v) Acrylamide stock (BDH): 29.2 % (v/v) acrylamide and 0. 8 % (v/v) Bis-acrylamide

Ammonium persulphate: 10 % (w/v) solution made fresh

Stacking gel: 125 mM Tris pH 6.8; 0.1 % SDS, 4 % (v/v) polyacrylamide

Resolving gel: 500 mM Tris pH 8.8; 0.1% SDS, (x%) polyacrylamide

Running buffer pH 8.3: 0.025 M Tris ; 0.192 M glycine and 0.1 % (w/v) SDS

Transfer buffer: 25 mM Tris; 192 mM glycine; 20 % methanol

4x protein sample buffer: 0.125 M Tris.HCl (pH 6.8); 10 % (v/v) glycerol; 5 % (v/v) β-mercaptoenthanol; 2 % (w/v) SDS; 0.015 % (w/v) bromophenol blue

Block: 5 % (w/v) non-fat dried milk powder in 1 x TBS

1xTBS: 24 g/ l Tris; 80 g/ l NaCl

2.10.9 Western blotting

SDS-PAGE separated proteins can be blotted onto a nitrocellulose membranes by means of electrophoretic transfer. The electrophoresed gel, transfer membrane, 6 pieces of Whatmann filter paper were pre-equilibrated in transfer buffer (25 mM Tris and 192 mM glycine with 20 % (v/v) methanol). A gel-blot sandwich was constructed of 3 pieces of filter paper, the gel, the membrane and the remaining sheets of paper. The sandwich was immersed within a buffer-filled Western blotting tank, with gel towards the cathode and membrane towards the anode. The electrophoretic transfer proceeded at 300 mA, for 1 hr. Efficiency of protein transfer was verified by staining the membrane with Ponceau-S (Sigma). The transient stain was water-soluble and did not affect further analysis of blotted proteins.

2.10.10 Immuno-detection of proteins on blotted membranes

All immuno-detection steps were carried out at RT with constant agitation. 1 x TBS-T20 (1 x TBS, 0.1 % (v/v) Tween 20) was used as both a base for blocking agent (5 % (w/v) non-fat dried milk powder dissolved in TBS-T20, and as between-step washes. After Ponceau–S staining, the remaining protein-binding sites on the blot were blocked by incubation in blocking agent for 1 hr. Primary antibody was diluted in blocking agent at a final volume of 0.1 ml/ cm of

membrane and used to probe the blot for 1 hr. The blot was washed 3 times with TBS-T20, following this, the secondary antibody was diluted in blocking agent and applied to the membrane for a further hour. Again surplus antibody was removed by washing 3 times with TBS-T20. Antibody binding was visualised by means of enhance chemiluminessence (ECL), (Amersham). Appropriate volume of reagents A and B were mixed and applied to the blot for 1 min, and then excess was removes.

2.10.11 Development of membranes

The fluorescence was detected by exposure to Kodak X-ray film and developed using Compact X4 Developer (Xograph Imaging Systems Ltd).

2.11 Description of *S. cerevisiae* strains used

2.11.1 Strain nomenclature

In diploid strains *spo11f* indicates homozygosity of the *spo11–Y135F–HA3His6::KanMX* allele. In diploid strains *SPO11* indicates *SPO11/spo11–Y135F–HA3His6::KanMX* heterozygosity. For all other genes, all of the experimental diploid strains were homozygous for the defined mutation, for example *dmc1Δ* indicates homozygous *dmc1Δ::ADE2* alleles. *TFP1/TFP1* indicates homozygosity at the *TFP1* allele. *TFP1::VDE/TFP1* indicates heterozygosity at the *TFP1* allele.

2.11.2 Inclusion of strain information

The haploid strain list (Table 2.3.1) contains only the yeast strains from which specific alleles originate, rather than the manifold intermediate strains used to create the experimental diploids. The diploid strain list (2.3.2) contains all of the experimental diploids used in this study.

2.11.3 General methods for creating yeast strains of the desired genotype

Where a deletion or disruption cassette was available, appropriate haploid strains were directly transformed via the lithium acetate method or electroporation method, to achieve the desired genotype. To create the experimental diploids, intermediate strains were routinely made by mating haploids with appropriate genotypes, followed by sporulation and tetrad dissection. The haploid genotype of spores was determined largely by identifying mutant alleles marked with amino acid biosynthetic genes, or antibiotic resistance genes.

The requisite and non-requisite phenotypes of each mating cross were scored to confirm the expected marker segregation. To ensure haploid ploidy, colonies were selected from four spore viable tetrads only. When alleles disrupted by the same marker were required in a haploid strain, diploids heterozygous for the markers were made and dissected. Only marker+ haploids from 2 + : 2 - segregations were selected, thus ensuring the presence of both alleles in the haploid. When no protrophic or antibiotic resistance markers were available, (e.g. VDE insertion at the *TFP1* locus, creating *TFP1::VDE*), locus-specific primers were used to amplify the appropriate region via PCR. The size of the PCR product, and/or the presence or absence of restriction sites (relative to a reference PCR), was indicative of the genotype.

Chapter Three

An assay for Spo11p-independent DSB repair in meiosis

3.1 Introduction

In this study a meiosis specific and site-specific endonuclease, VDE, was employed to induce a DSB. VDE is a good candidate to drive recombination in yeast, as an approximation to Spo11p-induced recombination for the following reasons; Firstly, VDE recognises a complex cleavage sequence equivalent to at least 18 bp in length (Bremer *et al.*, 1992; Gimble and Thorner, 1992), ensuring that DSB formation is site–specific. Secondly, the endonuclease activity of VDE is meiosis–specific, and equally important, creates DSBs during meiosis at about the same time that Spo11p–DSBs form (Gimble and Thorner, 1992). Finally, gene conversion is efficiently induced by VDE-DSB formation (Gimble and Thorner, 1992), indicating that VDE should be a competent tool for use in this study. A self–homing endonuclease causes conversion of an endonuclease$^-$ allele (e.g. *TFP1*) into a endonuclease$^+$ allele (e.g. *TFP1*::*VDE*). Figure 3.1 is an illustration of self-propagation by VDE. This reaction is unidirectional as the cutsite is only present in the endonuclease$^-$ allele, and the only available homology to repair the induced DSB is the endonuclease$^+$ allele. Thus subsequent conversion of endonuclease$^-$ allele causes the endonuclease cutsite to be lost in the cell and subsequent generations. SK1 strains do not naturally express VDE (they contain a *TFP1* allele). All SK1 strains expressing the VDE endonuclease in this study have been made to do so experimentally with the VDE allele being integrated into the yeast genome.

The cut site for VDE is located within an inserted copy of a modified *ARG4* gene, creating the *arg4-VDE* allele. This is a heterozygous cassette with a second modified *ARG4*, *arg4-bgl* residing on the homologous chromosome *V*. Repeated

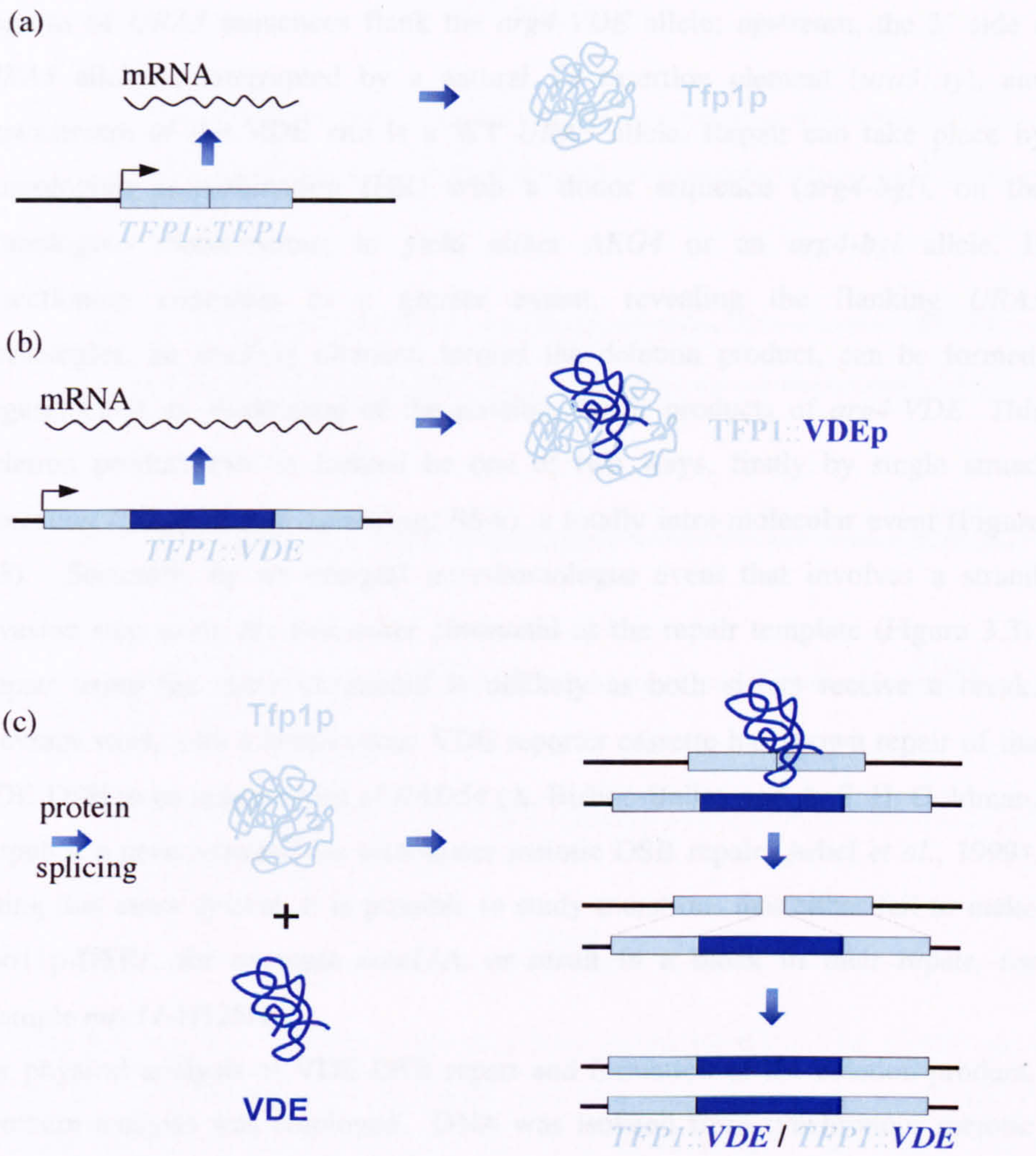

Figure 3.1: Self propagation by VDE. (a) Transcription and translation of *TFP1* creates the Tfp1p. (b) Transcription and translation of *TFP1*::*VDE* forms the transient Tfp1::VDE protein. (c) Mature Tfp1p and VDE proteins are produced through a splicing reaction. Homing of the VDE reading frame is mediated by VDE–induced DSB formation within *TFP1*, followed by GC using the *TFP1*::*VDE* locus as the repair template.

regions of *URA3* sequences flank the *arg4-VDE* allele; upstream, the 5´ side a *URA3* allele is interrupted by a natural Ty insertion element (*ura3::ty*), and downstream of the VDE site is a WT *URA3* allele. Repair can take place by homologous recombination (HR) with a donor sequence (*arg4-bgl*), on the homologous chromosome, to yield either *ARG4* or an *arg4-bgl* allele. If resectioning continues to a greater extent, revealing the flanking *URA3* homologies, an *ura3::ty* element, termed the deletion product, can be formed. Figure 3.2 is an illustration of the possible repair products of *arg4-VDE*. This deletion product can be formed be one of two ways, firstly by single strand annealing (Single strand annealing; SSA), a totally intra-molecular event (Figure 3.3). Secondly, by an unequal inter-homologue event that involves a strand invasion step using the non-sister chromatid as the repair template (Figure 3.3). Repair using the sister chromatid is unlikely as both sisters receive a break. Previous work with a hemizygous VDE reporter cassette has shown repair of the VDE-DSB to be independent of *RAD54* (A. Bishop-Bailey and A. S. H. Goldman, Unpub.), a gene required for inter-sister meiotic DSB repair (Arbel *et al.*, 1999). Using this assay system, it is possible to study mutations that either fail to make Spo11p-DSBs, for example *mre11Δ*, or result in a block in their repair, for example *mre11*-H125N.

For physical analysis of VDE-DSB repair and formation of the deletion product, Southern analysis was employed. DNA was isolated from synchronous meiotic cultures and following appropriate restriction digest, was fractionated under native agarose conditions. Following transfer of DNA onto membranes, DNA was radio–labelled with specific probes and exposed to a Kodac Phosphor screen.

Phosphor screens were then scanned on a BioRad Phosphoimager following appropriate exposure. All work published in Neale *et al.*, (2002) involved transfer of the Kodak phosphor screen from lead cassette to Personal FX phosphoimager under the light conditions of a standard laboratory. During 2003, the laboratory was refurbished and central lighting was replaced. All scanned images were found to have dramatically reduced signals when scanned in the refurbished laboratory.

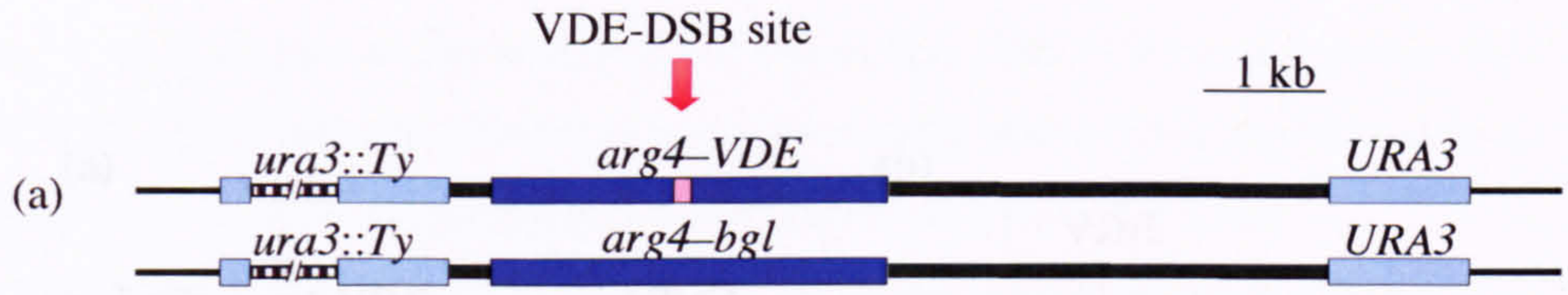

Figure 3.2: Reporter construct and associated repair products. (a) Diploid strains contained *arg4–VDE* and *arg4–bgl* alleles (dark blue boxes) inserted along with pBR322 plasmid DNA (dark lines) at the *ura3*::*Ty* loci of chromosome *V* (thin lines). The *Ty* disruption of *ura3* (striped box) is ~ 6 kb long. The insertions created flanking repeats of *URA3* homology (light blue boxes). (b) VDE cleaves specifically the *arg4–VDE* allele during meiosis at the 73 bp VDE–cutsite cloned into the *Eco*RV site of *ARG4*. (c–e) Each *arg4–VDE* chromatid is able to repair the VDE–DSB in four different ways. Gene conversion via an interaction with the *arg4–bgl* allele can result in production of (c) an *ARG4*, or (d) an *arg4–bgl* allele. The VDE–DSB can also be repaired by deletion of the inserted DNA via interaction between the flanking *URA3* homology. (e) Deletion to *ura3*::*Ty* involves interaction between the 2nd and 3rd regions of *URA3* sequence. (f) Deletion to *URA3* involves interaction between the 1st and 3rd regions of *URA3*, this is a very rare (< 3 % total repair events) repair event.

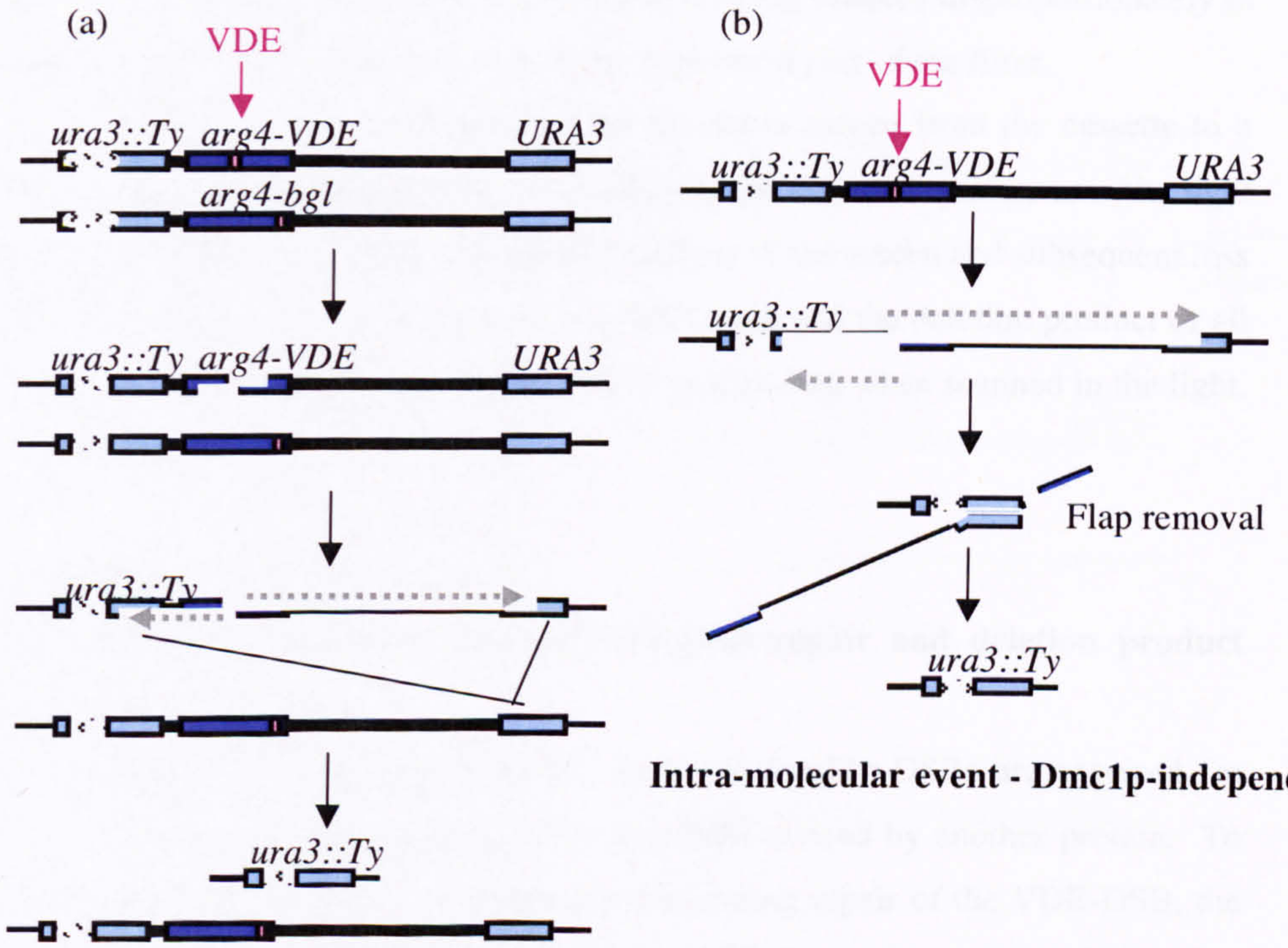

Figure 3.3: The two routes for deletion product formation at the VDE-DSB: (a) Long resection tracts lead to repair using flanking repeated *URA3* sequence, and formation of the deletion product *ura3::Ty*. The repair event uses the homologous chromosome as the repair template, involving a strand invasion event. (b) A single–strand annealing event, which is expected to be independent of Dmc1p activity and of a strand invasion event.

Due to the position of the bands on the radioactive filter it became apparent that the VDE-DSB band and deletion product were being blanked disproportionately in comparison with the Parental band on the uppermost part of the filter.

It was decided that the movement of the Phosphor screen from the cassette to a phosphoimager should be carried out entirely in the dark as exposure to white light prior to scanning would result in partial blanking of the screen and subsequent loss of signal. When scanned in the dark, the DSB band and the deletion product of all strains was found to be approximately 20 % higher than when scanned in the light, as described below.

3.2 Results

3.2.1 Redefining the base level of VDE-DSB repair and deletion product formation

Neale *et al.*, (2002) reported that WT levels of Spo11p-DSBs are required for normal regulation of resectioning, even at a DSB created by another protein. To characterised the functions of further proteins during repair of the VDE-DSB, the original experiments reported in Neale *et al.*, (2002) had to be repeated. Repeating the original experiments produced new repair profiles for WT, *spo11f*, *sae2Δ* and *hop1Δ*, with which the newly investigated mutants could be compared to.

To confirm the kinetics of VDE-DSB repair and the level of deletion products formed in the WT, *spo11f*, *hop1Δ* and *sae2Δ* cells and to investigate the kinetics of VDE-DSB repair and the level of deletion products formed in *mek1Δ* and *mek1*-K199R strains, meiotic time courses were performed and DNA was isolated from each time point.

Standard Southern analysis can assess the rate of VDE cutting by using an *Eco*RV/*Bgl*II double digest that makes it possible to separate *arg4–VDE* parental molecules from all other species (see Materials and Methods section 2.9.16 and illustrated in figure 3.4). This digest is a useful way of measuring the rate of VDE–induced cleavage as the amount of DNA present in the *arg4–VDE* band will reduce relative to a loading control, as more cleavage occurs.

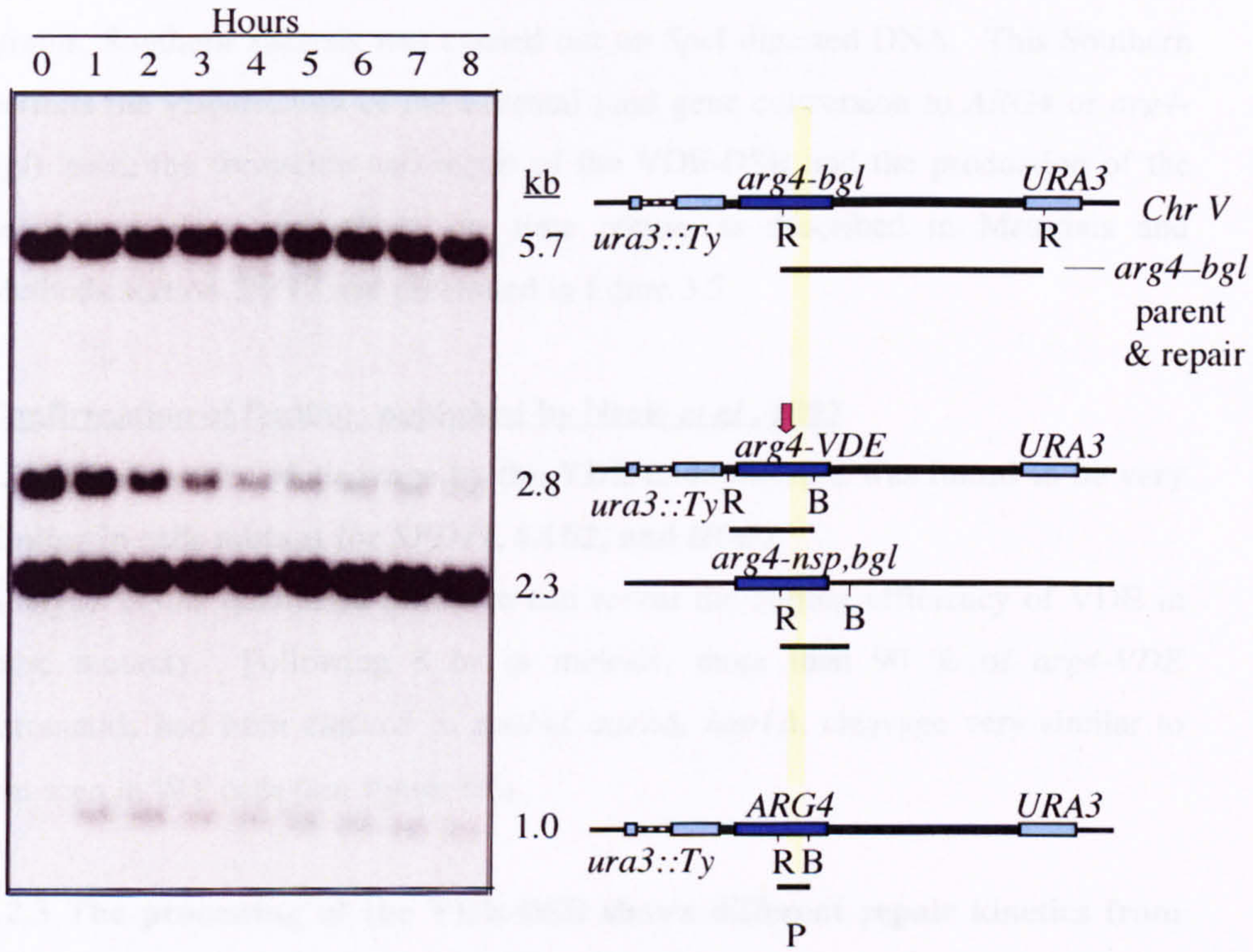

Figure 3.4: Physical analysis of *arg4–VDE* cleavage and *ARG4* formation. *Eco*RV- and *Bgl*II-digested DNA extracted from a synchronous meiotic time course was fractionated in a 0.5 % 1 x TAE agarose gel and hybridised with a probe (P) specific to the region of *ARG4*. The 2.8 kb band represents *arg4-VDE* chromatids *(Chr V)*, which disappear with time and VDE action. The 2.3 kb band represents the natural *arg4* locus (*Chr VIII*), used as a loading control. The 5.7 kb band contains both parental *arg4-bgl* and gene conversion molecules *(Chr V)*. The 1 kb band represents the *ARG4* repair product and the VDE-DSB *(Chr V)*. Neither the 5.7 kb nor the 1 kb bands are used in this study.

To determine whether the VDE-DSB is processed differently in different mutant strains, Southern analysis was carried out on *Spe*I digested DNA. This Southern permits the visualisation of the Parental (and gene conversion to *ARG4* or *arg4-bgl*) band, the formation and repair of the VDE-DSB and the production of the deletion product, throughout the time course as described in Materials and Methods section 2.9.17 and illustrated in figure 3.5.

<u>Confirmation of findings published by Neale *et al.*, 2002</u>

3.2.2 The kinetics of cleavage by the VDE-endonuclease was found to be very similar in cells mutant for *SPO11*, *SAE2*, and *HOP1*

Analysis of the quantified Southern can reveal the cutting efficiency of VDE in these mutants. Following 8 hr in meiosis, more than 90 % of *arg4-VDE* chromatids had been cleaved in *spo11f*, *sae2Δ*, *hop1Δ*, cleavage very similar to that seen in WT cells (see figure 3.6).

3.2.3 The processing of the VDE-DSB shows different repair kinetics from WT cells, in cells mutant for *SPO11*, and *HOP1*.

The *Eco*RV/*Bgl*II digest of meiotic DNA has confirmed that the cleavage at the *arg4-VDE* is independent of all mutations so far studied. To determine whether the VDE-DSB is processed differently in *spo11f* or *hop1Δ* cells, Southern analysis was carried out to quantify the VDE-DSB throughout the time course as described in Materials and Methods section 2.9.17 and illustrated in figure 3.5. Results obtained were compared with those published in Neale *et al.*, 2002.

In WT cells, the VDE-DSB peaks at 45 % of chromatids that had received a break at 5 hr of meiosis, and has approximately 10 % DSBs remaining unrepaired by the end of the time course (see figure 3.7). In *spo11f* cells, the VDE-DSB peaks approximately two hr earlier than in WT. Furthermore, the VDE-DSB accumulates to a lower level in the *spo11f* strain reaching a maximum of approximately 15 %. The 2 hr earlier peak of maximum VDE-DSB peak, coupled with a reduced value suggests that the VDE-DSB is repaired with faster kinetics in

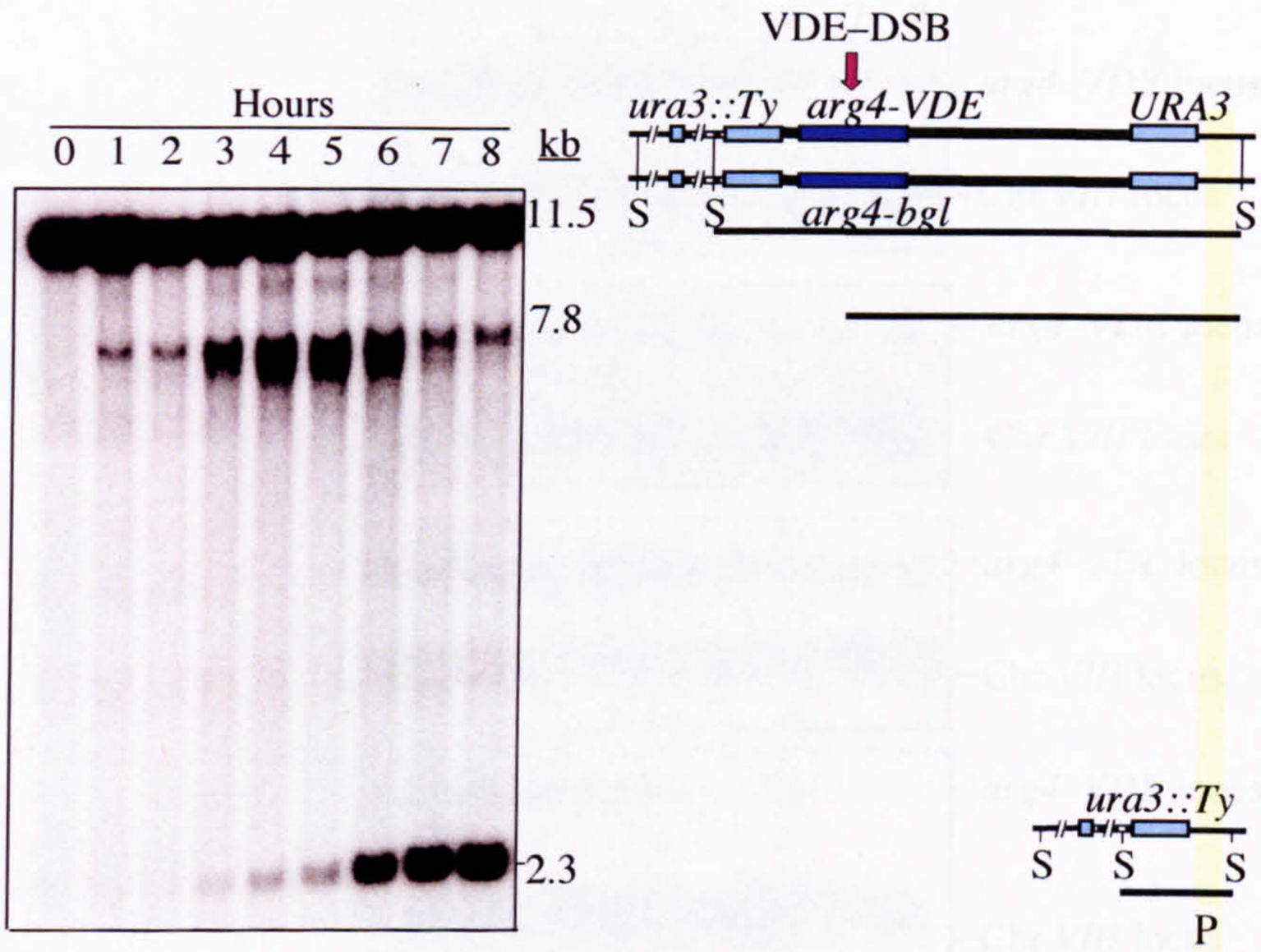

Figure 3.5: Physical analysis of DNA events at the *arg4–VDE* locus. *Spe*I (S)-digested DNA extracted from meiotic time course was fractionated on 0.5 % 1 x TAE gels, hybridised with a 1 kb probe (P) specific to the region of chromosome *V*, 200 bp downstream of *ura3*::*Ty*. The 2.3 kb and 11.5 kb bands represent the fragments derived from the chromosome *V ura3*::*Ty* natural and insert–containing loci, respectively. The 11.5 kb band corresponds to the parental *arg4–VDE* and *arg4–bgl* constructs as well as gene conversion (GC) repair products to *ARG4* and *arg4–bgl*. The transient ~7.8 kb band shows the VDE-DSB. Limited 5´– 3´ single–stranded resectioning leads to shortening of some molecules in the population causing the smeared appearance of the VDE–DSB. The 2.3 kb band represents the deletion product.

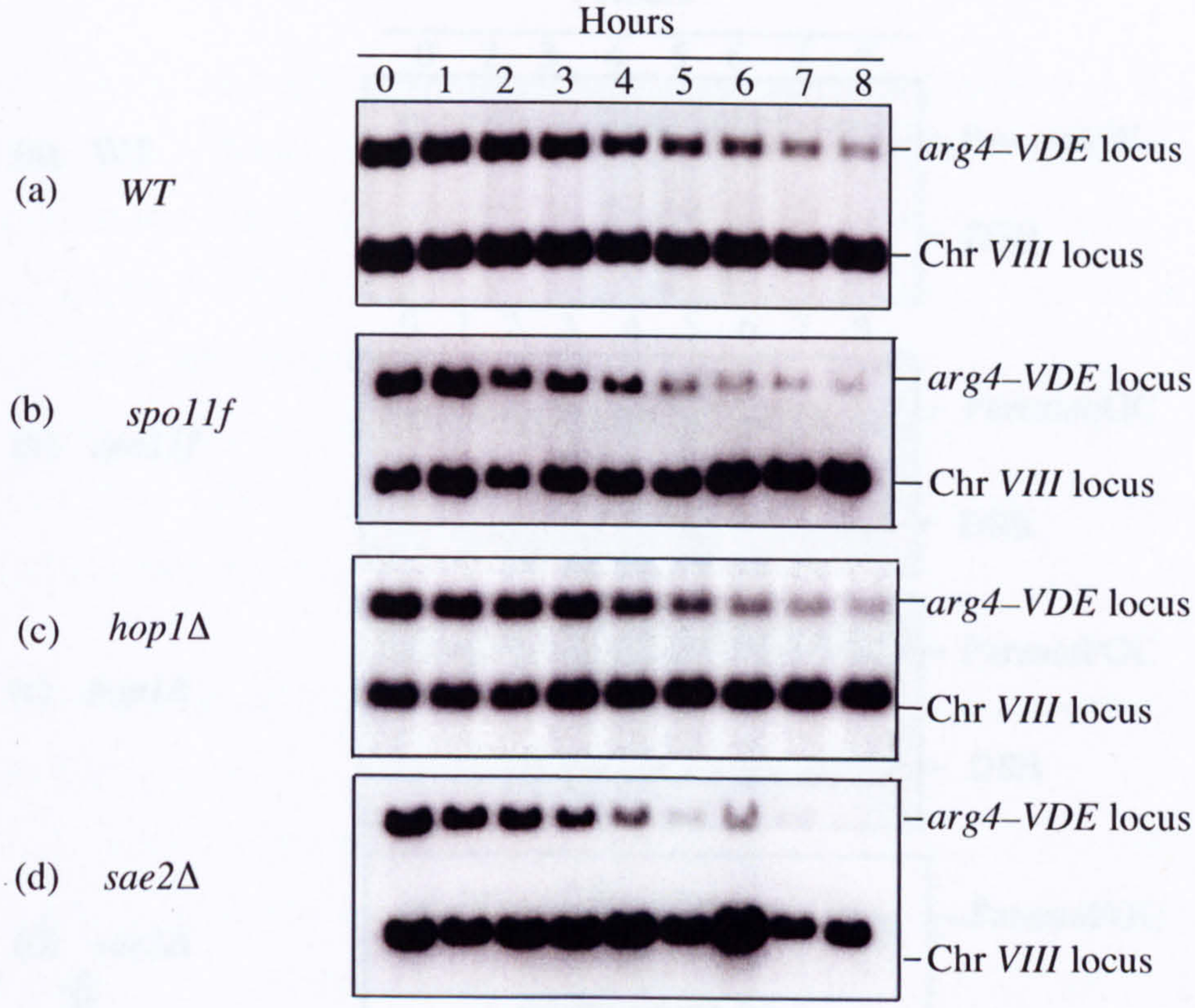

Figure 3.6: Physical analysis and quantification of *arg4–VDE* cleavage in WT, *spo11f*, *hop1Δ* and *sae2Δ* cells. Southern analysis using *Bgl*II/*Eco*RV-digested DNA extracted from synchronous meiotic time course of (a) WT, (b) *spo11f* (c) *hop1*Δ and (d) *sae2*Δ, and processed as for figure 3.4. The scanned images have been cropped to show only the *arg4–VDE* and *arg4–nsp,bgl* (loading control) band. (e), The extent of VDE cleavage was similar in all strains.

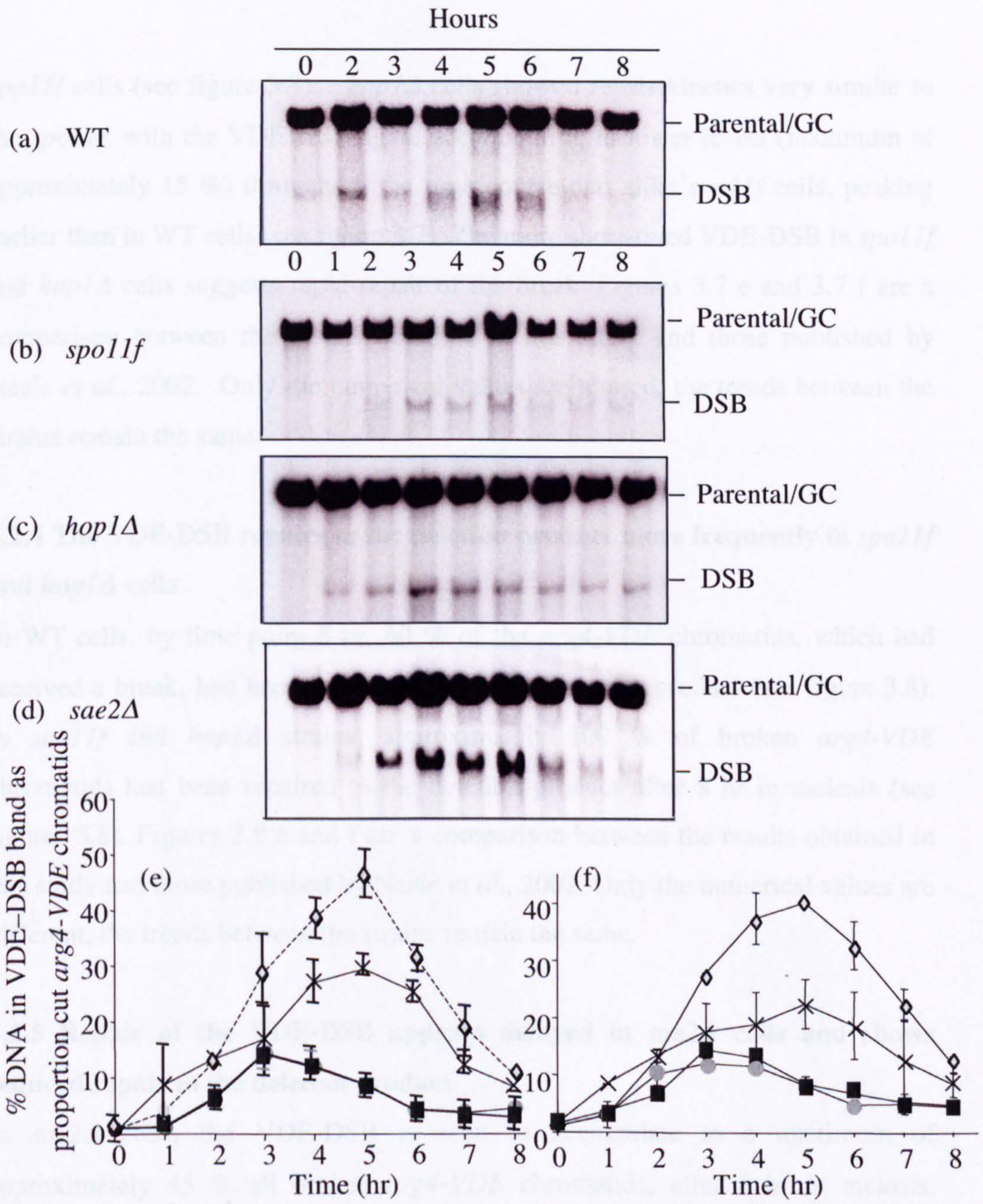

Figure 3.7: Comparison between the physical analysis of the VDE–DSB in experiments reported by Neale *et al.*, (2002) and in this study. Southern analysis using *Spe*I-digested DNA of (a) WT, (b) *spo11f,* (c) *hop1*Δ and (d) *sae2Δ* and processed as for figure 3.5. The scanned images have been cropped to show just the parental/GC and VDE-DSB bands. (e) The VDE-DSB in *hop1Δ* and *spo11f* cells peaks two hours earlier, at time point 3 hr, than in WT cells and peaks to a lower maximum level, at just ~ 15 %. *sae2*Δ cells show an increase in the maximum value of the DSB in comparison to WT cells. (f) Data presented in Neale *et al.,* 2002, when scanning of Phosphor screens occurred in the light, for comparative purposes. —×—WT —■—*hop1Δ* —●—*spo11f* -◇-*sae2Δ*

spo11f cells (see figure 3.7). *hop1Δ* cells showed repair kinetics very similar to the *spo11f,* with the VDE-DSB again accumulating to lower levels (maximum of approximately 15 %) throughout the time course and alike *spo11f* cells, peaking earlier than in WT cells (see figure 3.7). The more short-lived VDE-DSB in *spo11f* and *hop1Δ* cells suggests rapid repair of the break. Figures 3.7 e and 3.7 f are a comparison between the results obtained in this study and those published by Neale *et al.*, 2002. Only the numerical values are altered, the trends between the strains remain the same.

3.2.4 The VDE-DSB repairs to the deletion product more frequently in *spo11f* and *hop1Δ* cells

In WT cells, by time point 8 hr, 60 % of the *arg4-VDE* chromatids, which had received a break, had been repaired to form the deletion product (see figure 3.8). In *spo11f* and *hop1Δ* strains, approximately 100 % of broken *arg4-VDE* chromatids had been repaired to the deletion product after 8 hr in meiosis (see figures 3.8). Figures 3.8 e and f are a comparison between the results obtained in this study and those published by Neale *et al.*, 2002. Only the numerical values are different, the trends between the strains remain the same.

3.2.5 Repair of the VDE-DSB appears delayed in *sae2Δ* cells and shows reduced repair to the deletion product

In *sae2Δ* cells, the VDE-DSB is seen to accumulate to a maximum of approximately 45 % all broken *arg4-VDE* chromatids, after 5 hr in meiosis, compared to around 30 % in WT cells. This increase in the maximum value of VDE-DSB is indicative of delayed kinetics for break repair (see figure 3.7).

Approximately 40 % of broken *arg4-VDE* chromatids are repaired to the *URA3* repeat regions in cells lacking Sae2p, compared to 60 % in WT (see figure 3.8). This data supports the observation that the VDE-DSB has a delayed turnover in *sae2Δ* cells (see figure 3.7).

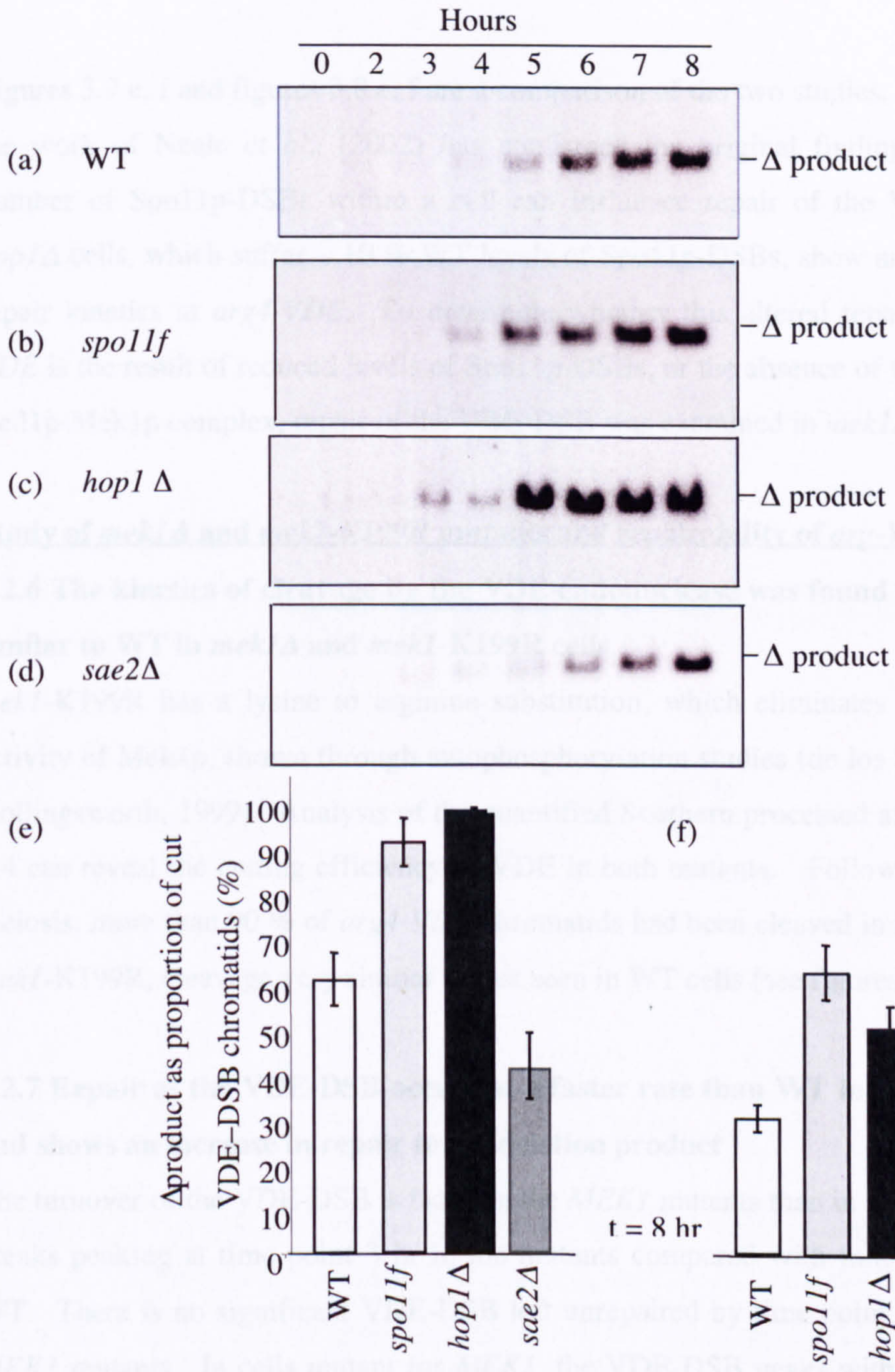

Figure 3.8: Physical analysis and quantification of deletion product formation in WT, *spo11f*, *hop1Δ*, and *sae2Δ* cells. Southern analysis using *Spe*I-digested DNA extracted from synchronous meiotic time course of (a) WT, (b) *spo11f* , (c) *hop1*Δ and (d) *sae2*Δ cells and processed as for figure 3.5 The scanned images have been cropped so only the deletion product is seen. (e) By time point 8 hr, repair of the VDE-DSB to the deletion product is increased in *spo11f* and *hop1*Δ cells in comparison to WT and decreased in *sae2*Δ cells. (f) Data presented in Neale *et al.*, (2002) when scanning of Phosphor screens occurred in the light, for comparative purposes.

Figures 3.7 e, f and figures 3.8 e, f are a comparison of the two studies. Repeating the work of Neale *et al.*, (2002) has confirmed the original findings that the number of Spo11p-DSBs within a cell can influence repair of the VDE-DSB. *hop1Δ* cells, which suffer ~ 10 % WT levels of Spo11p-DSBs, show an enhanced repair kinetics at *arg4-VDE*. To determine whether this altered repair at *arg4-VDE* is the result of reduced levels of Spo11p-DSBs, or the absence of the Hop1p-Red1p-Mek1p complex, repair of the VDE-DSB was examined in *mek1Δ* cells.

Study of *mek1Δ* and *mek1-K199R* mutants and repairability of *arg-VDE*

3.2.6 The kinetics of cleavage by the VDE-endonuclease was found to be very similar to WT in *mek1Δ* and *mek1*-K199R cells

mek1-K199R has a lysine to arginine substitution, which eliminates the kinase activity of Mek1p, shown through autophosphorylation studies (de los Santos and Hollingsworth, 1999). Analysis of the quantified Southern processed as for figure 3.4 can reveal the cutting efficiency of VDE in both mutants. Following 8 hr in meiosis, more than 90 % of *arg4-VDE* chromatids had been cleaved in *mek1Δ* and *mek1*-K199R, cleavage very similar to that seen in WT cells (see figures 3.9).

3.2.7 Repair of the VDE-DSB occurs at a faster rate than WT in *mek1Δ* cells and shows an increase in repair to the deletion product

The turnover of the VDE-DSB is faster in the *MEK1* mutants than in WT, with the breaks peaking at time point 3 hr in the mutants compared with time point 5 in WT. There is no significant VDE-DSB left unrepaired by time point 8 hr in the *MEK1* mutants. In cells mutant for *MEK1*, the VDE-DSB peaks with a value of ~ 15 % (see figure 3.10), similar to *spo11f* and *hop1Δ*.

In *mek1Δ*, by time point 8 hr, 80 % of the *arg4-VDE* chromatids, which had received a break, had been repaired to form the deletion product (see figure 3.11), compared with 60 % in WT cells.

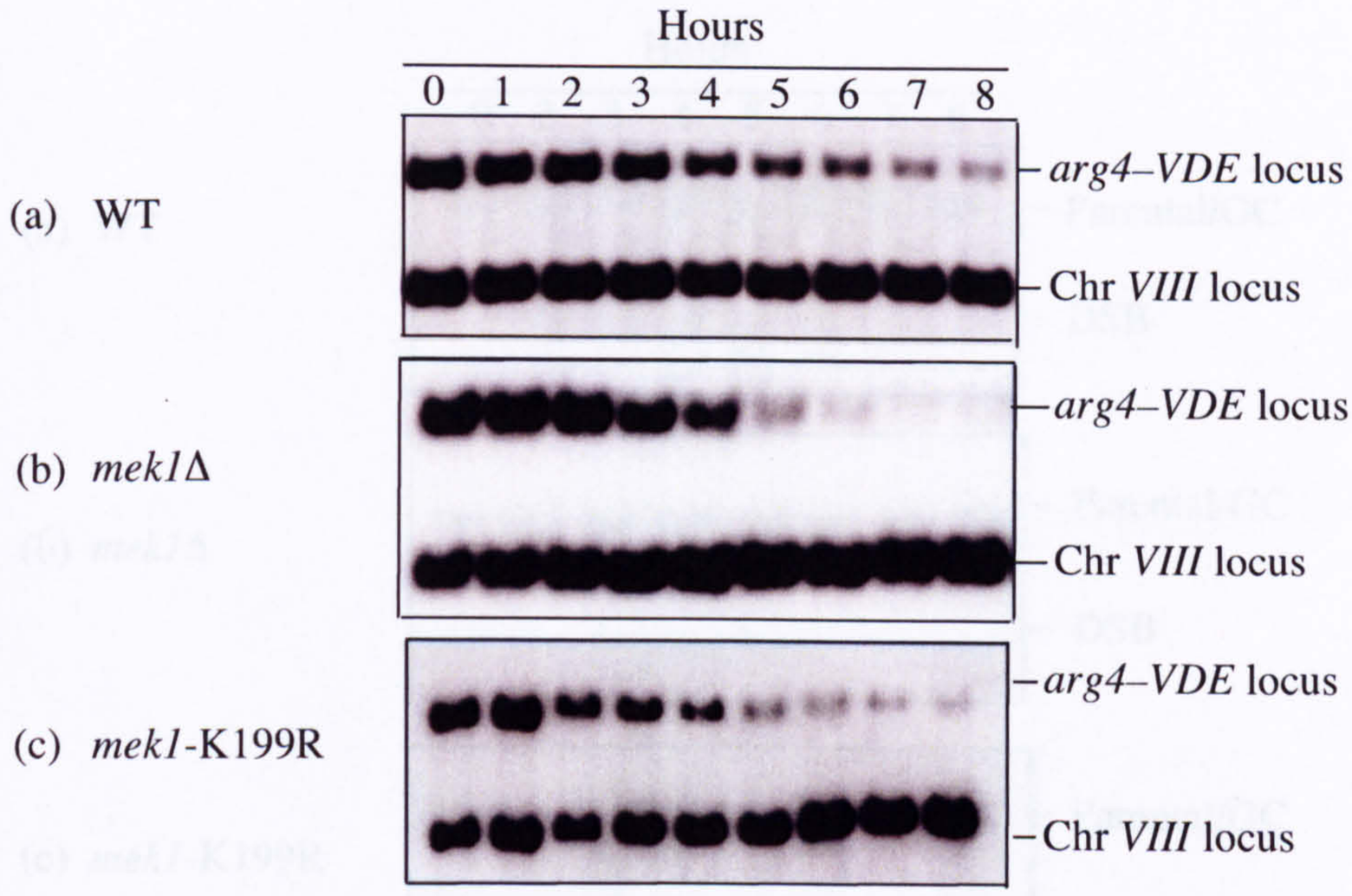

Figure 3.9: Physical analysis and quantification of *arg4–VDE* cleavage in WT, *mekΔ* and *mek1*-K199R cells. Southern analysis using *Bgl*II/*Eco*RV-digested DNA extracted from synchronous meiotic time course of (a) WT (b) *mek1*Δ and (c) *mek1*-K199R cells, and processed as for figure 3.4. Images were cropped to show only the *arg4–VDE* and *arg4–nsp,bgl* (loading control) band. (d) At t = 0 hr nearly all *arg4–VDE* alleles are uncut. The extent of VDE cleavage was similar in all three strains,

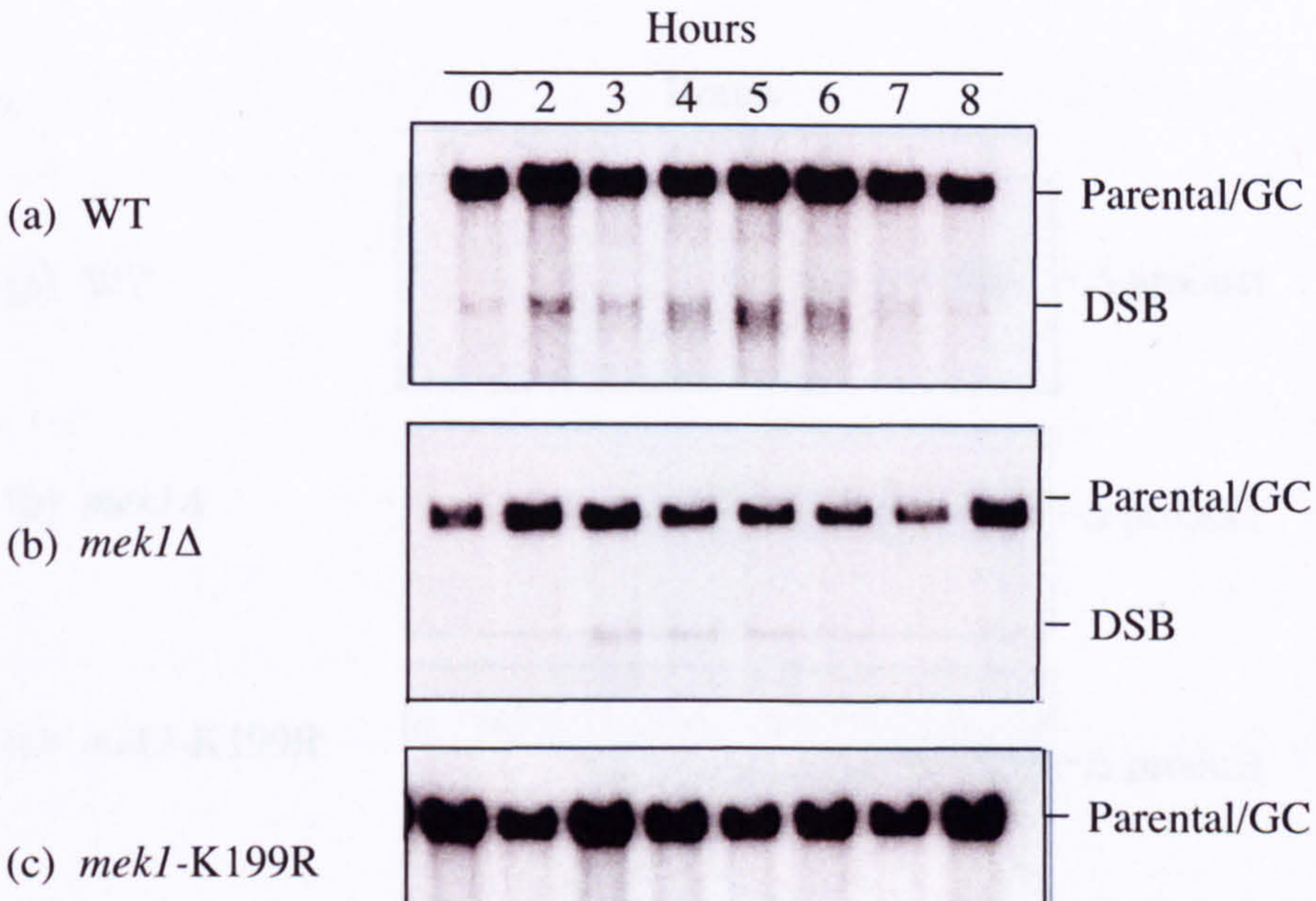

Figure 3.10: Physical analysis and quantification of the VDE–DSB in WT, *mek1Δ* and *mek1*-K199R cells. Southern analysis using *Spe*I-digested DNA from extracted synchronous meiotic time course of (a) WT, (b) *mek1Δ* and (c) *mek1*-K199R cells and processed as for figure 3.5. Scanned images were cropped so only Parental/GC and VDE-DSB bands were visualised. (d) Both *MEK1* mutant alleles showed an earlier peak of VDE-DSB, and showed a lower maximum value for the DSB than WT cells.

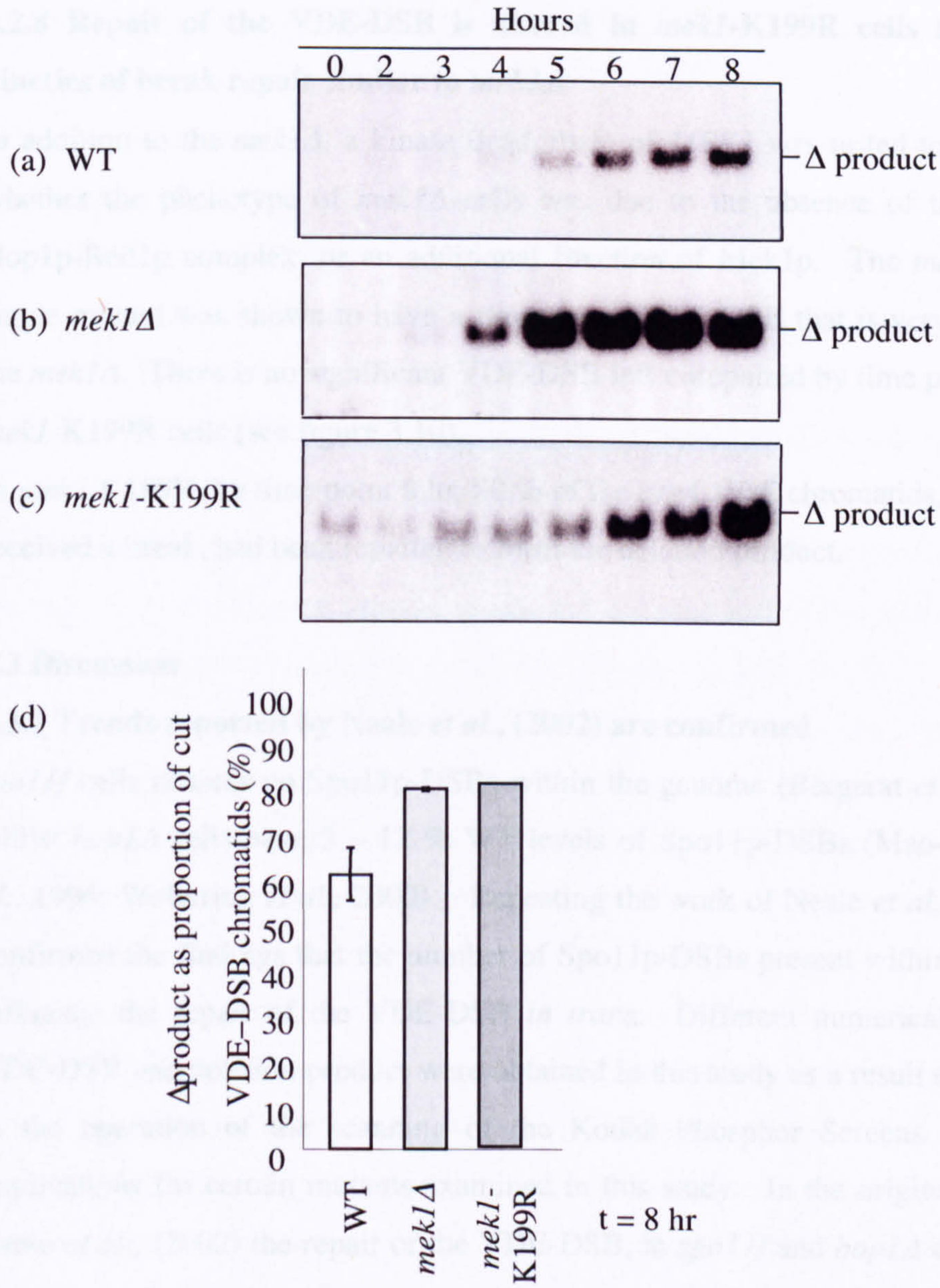

Figure 3.11: Physical analysis and quantification of deletion product formation in WT, *mek1Δ* and *mek1*-K199R cells. Southern analysis using *Spe*I-digested DNA extracted from synchronous meiotic time course of (a) WT, (b) *mek1Δ* and (c) *mek1*-K199R cells and processed as for figure 3.5. Scanned images were cropped to only show the deletion product. (d) At time point 8 hr, both *MEK1* mutants showed an increase in repair of the VDE-DSB to the deletion product relative to WT cells.

3.2.8 Repair of the VDE-DSB is altered in *mek1*-K199R cells and shows kinetics of break repair similar to *mek1Δ*

In addition to the *mek1Δ*, a kinase dead allele of *MEK1* was tested to determine whether the phenotype of *mek1Δ* cells was due to the absence of the Mek1p-Hop1p-Red1p complex, or an additional function of Mek1p. The *mek1*-K199R single mutant was shown to have a turnover of VDE-DSB that is very similar to the *mek1Δ*. There is no significant VDE-DSB left unrepaired by time point 8 hr in *mek1*-K199R cells (see figure 3.10).

In *mek1*-K199R, by time point 8 hr, 80 % of the *arg4-VDE* chromatids, which had received a break, had been repaired to form the deletion product.

3.3 Discussion

3.3.1 Trends reported by Neale *et al.,* (2002) are confirmed

spo11f cells possess no Spo11p-DSBs within the genome (Bergerat *et al.*, 1997), whilst *hop1Δ* cells have 5 – 12 % WT levels of Spo11p-DSBs (Mao-Draayer *et al.*, 1996; Woltering *et al.*, 2000). Repeating the work of Neale *et al,* 2002., has confirmed the findings that the number of Spo11p-DSBs present within a cell can influence the repair of the VDE-DSB *in trans*. Different numerical values of VDE-DSB and deletion product were obtained in this study as a result of a change in the operation of the scanning of the Kodak Phosphor Screens. This has implications for certain mutants examined in this study. In the original study by Neale *et al.*, (2002) the repair of the VDE-DSB, in *spo11f* and *hop1Δ* cells, to the deletion product accounted for 80 % of total repair. However, on repeating this experiment, it was discovered that nearly 100 % of all repair of the VDE-DSB utilised the long resectioning tracts required to reveal the flanking *URA3* repeat regions.

spo11f and *hop1Δ* cells show an increase in resectioning at VDE-DSB shown through an increased rate of VDE-DSB turnover, with a reduced maximum level of break, and peaking three hr earlier than in WT cells. Taken together, the work outlined in this chapter supports the findings of Neale *et al.,* (2002) that the

number of Spo11p-DSBs present within a cell can influence the rate of resectioning, *in trans*.

Work presented in this chapter supports the original suggestion of Neale *et al*, that Sae2p has a role in promoting resectioning as when it is mutated, the kinetics of break repair are retarded and repair to the deletion product is reduced. The trends between *sae2Δ* and WT were the same as presented in the original study, only the absolute values were altered. Is the phenotype of *sae2Δ* cells the result of blocked Spo11p-DSBs present within the genome? If Spo11p-DSBs are not correctly processed, does this influence repair at the Spo11p-independent break VDE? An alternative hypothesis is that Sae2p is a positive regulator of resectioning, as when the protein is absent from the cell there is a reduced level of resectioning at the VDE-DSB. This would be a novel role for the protein Sae2p, as to date its primary role in meiotic Spo11p-DSB has been in permitting the removal of the covalently bound protein Spo11p. This assay has allowed the separation of the roles Sae2p plays in break repair, a fete impossible directly at Spo11p-DSBs. The putative involvement of Sae2p in the regulation of resectioning is further tested in Chapter five.

3.3.2 Mek1p acts as a negative regulator of resectioning at *arg4-VDE*

It has been shown that loss of *MEK1* (or *RED1)* can reduce the presence of Spo11p-DSBs up to 4-fold and furthermore, can enforce recombination down a Dmc1p independent route (Schwacha and Kleckner, 1997; Xu *et al.*, 1997). However, following further research, it was discovered that *mek1Δ* cells do not form fewer Spo11p-DSBs, the breaks in question appear to be resected at a greater rate than in WT, so much so that the apparent number of breaks appears significantly reduced. The evidence for this comes from studies with *mek1Δrad50S* cells, which show WT levels (*rad50S* cells have blocked break ends, which cannot be resected) (Xu *et al.*, 1997).

mek1Δ cells show increased repair kinetics and exhibit an increase in repair of the *arg4-VDE* to the deletion product, suggesting that *mek1Δ* cells have increased

levels of 5′ to 3′ resectioning at the VDE-DSB as more repair of the VDE-DSB utilises the long resectioning tracts required to reveal the flanking *URA3* repeat sequences. The phenotype of repair at the *arg4-VDE* in *mek1Δ* cells is similar to that seen in *hop1Δ* cells. *mek1Δ* and *hop1Δ* cells show different steady states of Spo11p-DSBs; *mek1Δ* cells show a faster turnover of Spo11p-DSBs, whilst *hop1Δ* cells receive ~ 10 % of WT levels of Spo11p-DSBs. The phenotype of VDE-DSB repair in *mek1Δ* cells could be the result of altered processing of Spo11p-DSBs *in trans,* the absence of the Mek1p-Red1p-Hop1p complex, or an additional function of Mek1p. To test this theory, VDE-DSB repair was assayed in cells lacking Mek1p kinase activity: *mek1*-K199R. *mek1*-K199R cells were found to repair the VDE-DSB with repair kinetics similar to *mek1Δ*, suggesting that the kinase activity of Mek1p is necessary for WT-like repair of *arg4-VDE.* One possibility is that the kinase activity of Mek1p is required to enable inter-homologue recombination to be promoted, reducing resectioning at a meiotic DSB to allow the search for homology to proceed.

Chapter Four

The establishment of a Dmc1p dependency for repair of the *arg4-VDE* allele

4.1 Introduction

In meiosis, in order to prevent aneuploid progeny, it is critical to form inter-homologue joints. The inter-homologue joints, known as crossovers, are the end product of the repair of a programmed DSB, catalysed by the protein Spo11. When repair of the Spo11p-DSBs is directed towards the homologue as opposed to the sister, these crossovers, which are visualised as chiasmata, are formed. Hence, in meiosis there is a strong drive to direct repair of a Spo11p-DSB towards the homologous chromosome (Zickler and Kleckner, 1999).

There are several proteins that have been implicated in establishing this drive towards repair using the homologue as template. One such group of proteins are related to the *RAD52* epistasis group, which includes the meiosis-specific *recA* homologue of *E. coli*: *DMC1*. Dmc1p has been implicated in the establishment of repair directed towards the homologue as *dmc1Δ* cells show an absence of joint molecules (JMs) formed between homologous chromosomes (Schwacha and Kleckner, 1997). A supporting group of proteins is the Mek1p complex: Mek1p, Hop1p, Red1p (Hollingsworth and Ponte, 1997; Thompson and Stahl, 1999). Mek1p is a kinase with an as yet unknown substrate. When Mek1p is disrupted there is an increase in the proportion of inter-sister recombination over inter-homologue, characterised by an increase in *RAD54*-dependent repair (Niu *et al.*, 2005).

4.2 Results

The previously described reporter cassette (Chapter Three, section 3.1 and figures therein) has been utilised in order to identify if the requirement for Dmc1p-dependent repair is specific to gene conversion or whether it extends to different methods of repair. Earlier analysis from other labs has assumed that SSA is Dmc1p independent, as the mechanism does not involve a strand invasion event. This assumption was tested using the heterozygous VDE reporter cassette.

4.2.1 The kinetics of cleavage by the VDE-endonuclease was found to be very similar in WT cells and in cells mutant for *DMC1*

The previously described *Eco*RV/*Bgl*II-double digest (see Materials and Methods section 2.9.15 and figure 3.4), which permits the separation of the *arg4–VDE* parental molecules from all other species, was carried out on WT and *dmc1Δ* meiotic DNA. The cleavage at *arg4-VDE* was found to occur in a WT manner, with approximately 95 % of chromatids having received a break by 8 hr in meiosis (see figure 4.1).

4.2.2 The VDE-DSB accumulates in the absence of Dmc1p

Southern analysis of *Spe*I-digested DNA that permits visualisation of the broken *arg4-VDE* allele, reveals that the turnover of the VDE-DSB in *dmc1Δ*, cells is significantly different from WT (see Materials and Methods section 2.9.16 and figure 3.5).

The amount of DNA in the VDE-DSB is normalised to the proportion of *ura3::arg4-VDE-URA3* chromatids that have been cut prior to the time point. Figure 4.2 shows that 35 % of the chromatids that receive a VDE-DSB remain visible in the VDE-DSB band from time point 4 hr, and remain at this level to the 8 hr time point. This differs from WT cells in which the VDE-DSB is seen to accumulate up to five hr after meiotic induction and reduces as the break is repaired.

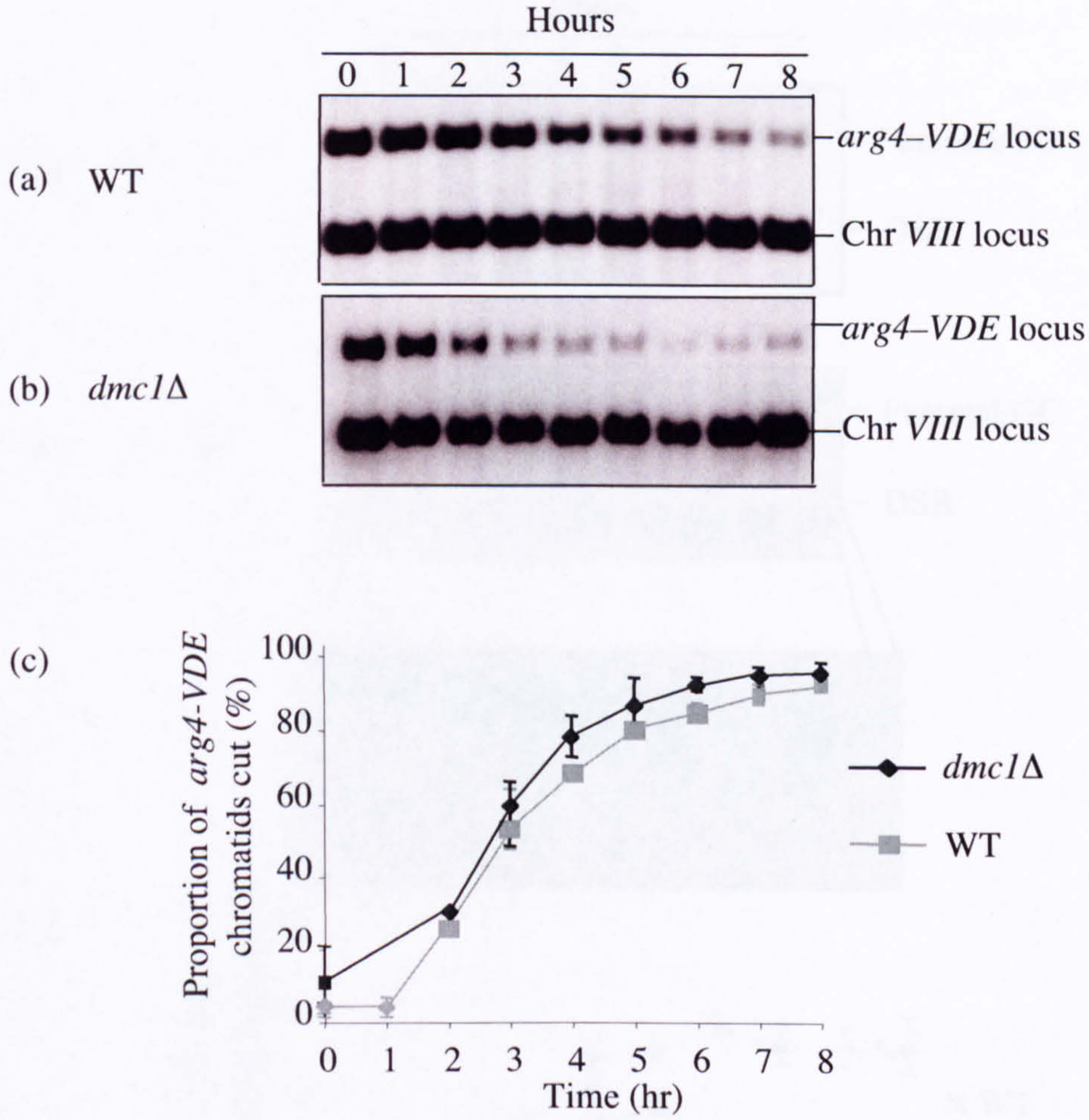

Figure 4.1: Physical analysis and quantification of *arg4–VDE* cleavage in WT and *dmc1Δ* cells. Southern analysis using *Bgl*II/*Eco*RV-digested DNA from synchronous meiotic time course (a) WT and (b) *dmc1*Δ cells and processed as for figure 3.4. WT data is shown for comparison. The scanned images have been cropped to show only the *arg4–VDE* and *arg4–nsp,bgl* (loading control) band. (c) The extent of VDE cleavage was similar in both WT and *dmc1*Δ cells.

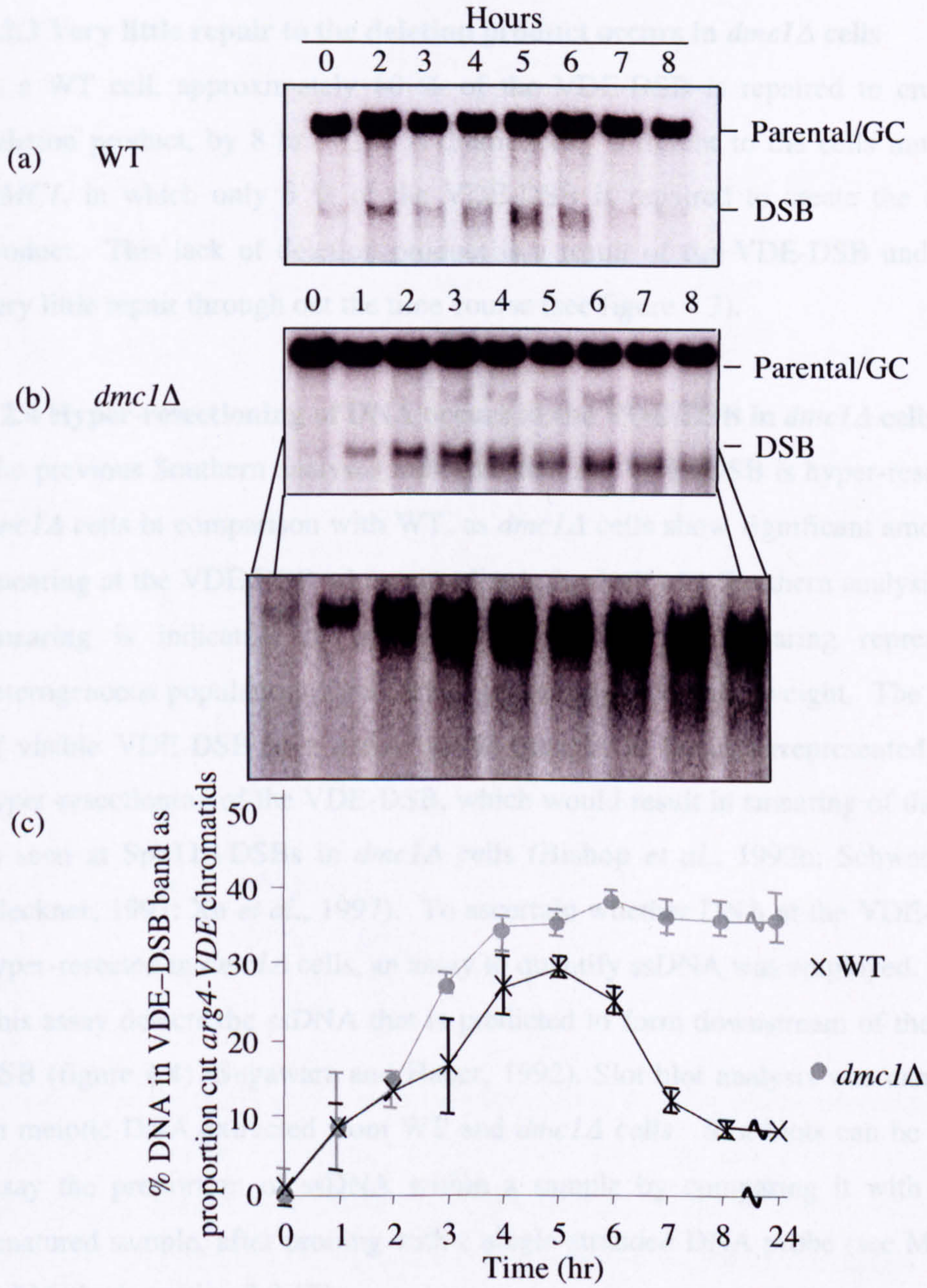

Figure 4.2: Physical analysis and quantification of the VDE–DSB in WT and *dmc1Δ* cells. Southern analysis using *Spe*I-digested DNA extracted from synchronous meiotic time course of (a) WT and (b) *dmc1*Δ cells and processed as for figure 3.5. The scanned images have been cropped to show only the parental/GC and VDE-DSB bands. WT data is shown for comparison. When the contrast is increased, smearing is visible at the VDE–DSB, indicative of hyper-resectioning. (c) The repair of the VDE-DSB is blocked in *dmc1*Δ cells.

4.2.3 Very little repair to the deletion product occurs in *dmc1Δ* cells

In a WT cell, approximately 60 % of the VDE-DSB is repaired to create the deletion product, by 8 hr. This is dramatically different to the cells mutant for *DMC1*, in which only 5 % of the VDE-DSB is repaired to create the deletion product. This lack of deletion product is a result of the VDE-DSB undergoing very little repair through out the time course (see figure 4.3).

4.2.4 Hyper-resectioning of DNA occurs at the VDE-DSB in *dmc1Δ* cells

The previous Southern analyses indicated that the VDE–DSB is hyper-resected in *dmc1Δ* cells in comparison with WT, as *dmc1Δ* cells show significant amounts of smearing at the VDE-DSB when visualised physically by Southern analysis. This smearing is indicative of hyper-resectioning as the smearing represents a heterogeneous population of molecules of varying molecular weight. The amount of visible VDE-DSB in a native gel is thought to be underrepresented due to hyper-resectioning of the VDE-DSB, which would result in smearing of the DNA, as seen at Spo11p-DSBs in *dmc1Δ* cells (Bishop *et al.*, 1992b; Schwacha and Kleckner, 1997; Xu *et al.*, 1997). To ascertain whether DNA at the VDE-DSB is hyper-resected in *dmc1Δ* cells, an assay to quantify ssDNA was employed.

This assay detects the ssDNA that is predicted to form downstream of the VDE–DSB (figure 4.4) (Sugawara and Haber, 1992). Slot blot analysis was carried out on meiotic DNA extracted from WT and *dmc1Δ* cells. Slot blots can be used to assay the proportion of ssDNA within a sample by comparing it with a fully denatured sample, after probing with a single-stranded DNA probe (see Materials and Methods section 2.9.17).

When the filters were hybridised with a single–stranded probe 3 kb distal to the VDE–DSB, the maximum signal to native DNA was reached 1 hr earlier in *dmc1Δ*, than in WT (see figure 4.4). Furthermore, in WT cells, the signal to native DNA decreased following its maximum value, indicative of the resected molecules being repaired. In contrast, the signal for DNA from *dmc1Δ* cells does not decrease, persisting with a similar signal from 5 hr in meiosis to the completion of

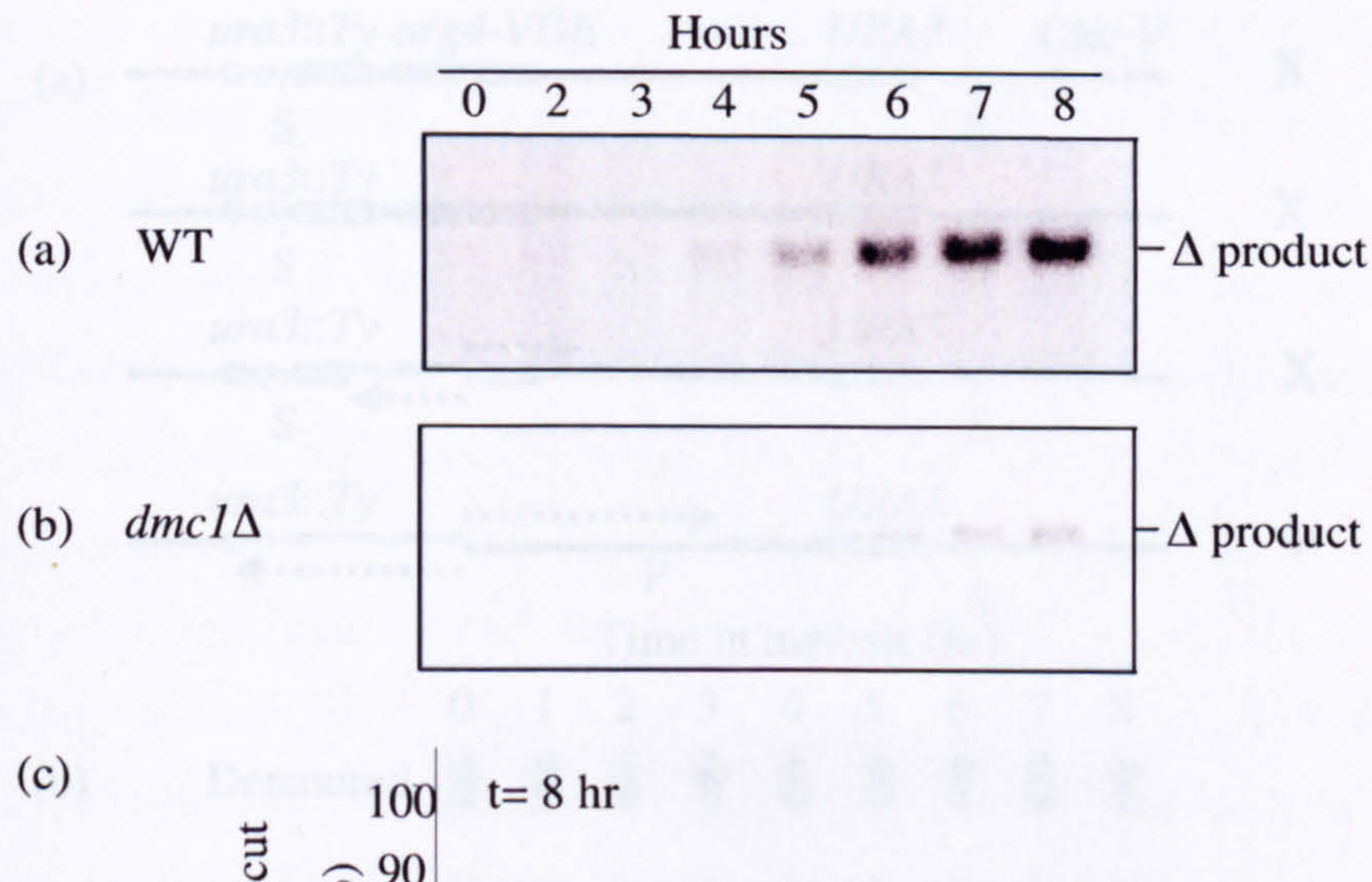

Figure 4.3: Physical analysis and quantification of deletion product formation in WT and *dmc1Δ* cells. Southern analysis using *Spe*I-digested DNA extracted from synchronous meiotic time course of (a) WT and (b) *dmc1*Δ cells and processed as for figure 3.5 with WT data being shown for comparative purposes. The images have been cropped to show only the deletion product. (c) 60 % of VDE-DSB repairs to the deletion product in WT cells, where as there is very little (< 10 %) repair to the deletion product formed in *dmc1*Δ cells.

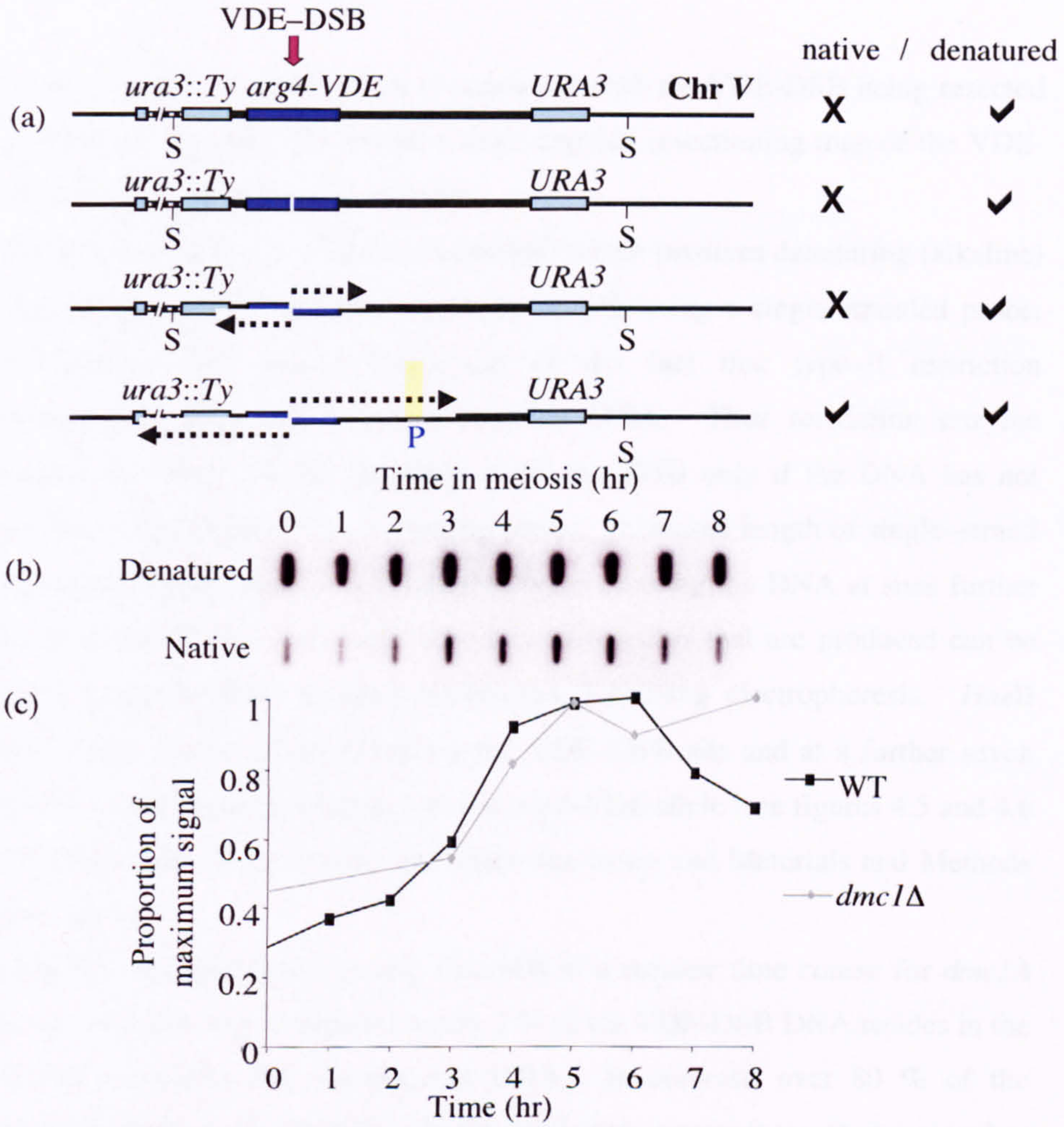

Figure 4.4: Slot blot analysis of single–stranded resection intermediates in WT and *dmc1Δ* cells. DNA extracted from synchronous meiotic time course and digested with (S) *Spe*I, and blotted directly to nylon membrane using a slot blot apparatus under vacuum pressure, with or without prior denaturation, and hybridised with a single–stranded DNA probe complementary to the unresected strand 3 kb away from VDE–DSB. (a) Illustration showing that a signal in the slot blot assay is only possible in the native samples when the VDE–DSB has formed and has been resected (dotted arrows) beyond the position of the probe. (b) Example WT slot–blot . (c) Densitometry was used to calculate the quantity of signal in each sample when hybridised Total signal was normalised to the denatured signal (which gives 100 % hybridisation) and expressed as the proportion of maximum signal. ssDNA is seen to persist longer I *dmc1Δ* cells than in WT.

the time course at t = 8 hr. This is consistent with the VDE-DSB being resected and not being repaired. To obtain a more detailed resectioning map of the VDE-DSB, a second physical assay was used.

A loss-of-restriction site assay was employed which involves denaturing (alkaline) gel electrophoresis followed by Southern analysis using a single-stranded probe. Restriction–site–loss assays make use of the fact that type–II restriction endonucleases only cleave double stranded DNA. Thus restriction enzyme digestion will occur at sites flanking an *in vivo* DSB only if the DNA has not undergone resectioning of the 5′–ending strand. Increased length of single–strand resectioning will lead to the restriction enzyme cleaving the DNA at sites further away from the DSB. The longer restriction fragments that are produced can be detected using Southern blotting techniques, following electrophoresis. *Hae*II cleaves DNA at sites closely flanking the VDE–DSB site and at a further seven locations within 10 kb downstream of the *arg4–VDE* allele (see figures 4.5 and 4.6 for an illustration of the loss-of-restriction site assay and Materials and Methods section 2.9.13).

Analysing DNA taken from hourly intervals of a meiotic time course for *dmc1Δ* cells, showed that by 8 hr approximately 2 % of the VDE-DSB DNA resides in the band that represents the non-resected DNA. In contrast, over 80 % of the *arg4::VDE* DNA of *dmc1Δ* cells is in the bands that represent resected molecules. If the proportion of VDE chromatids that have not received a VDE-DSB (i.e. between 5 - 10 %) is taken into account, virtually all cut *arg4::VDE* chromatids remain in a resected state. This data is considerably different from that obtained in WT cells, in which only 11 % of DNA resided in the bands representing resected DNA by t = 8 hr. The loss-of-restriction site assay was carried out in collaboration with M. J. Neale and A. S. H. Goldman.

The Dmc1p dependency for repair of the VDE-DSB was a surprise, as the repair can take place via SSA; a mechanism thought to be independent of Dmc1p function. To further test this dependency, the *dmc1Δ* mutant was coupled with

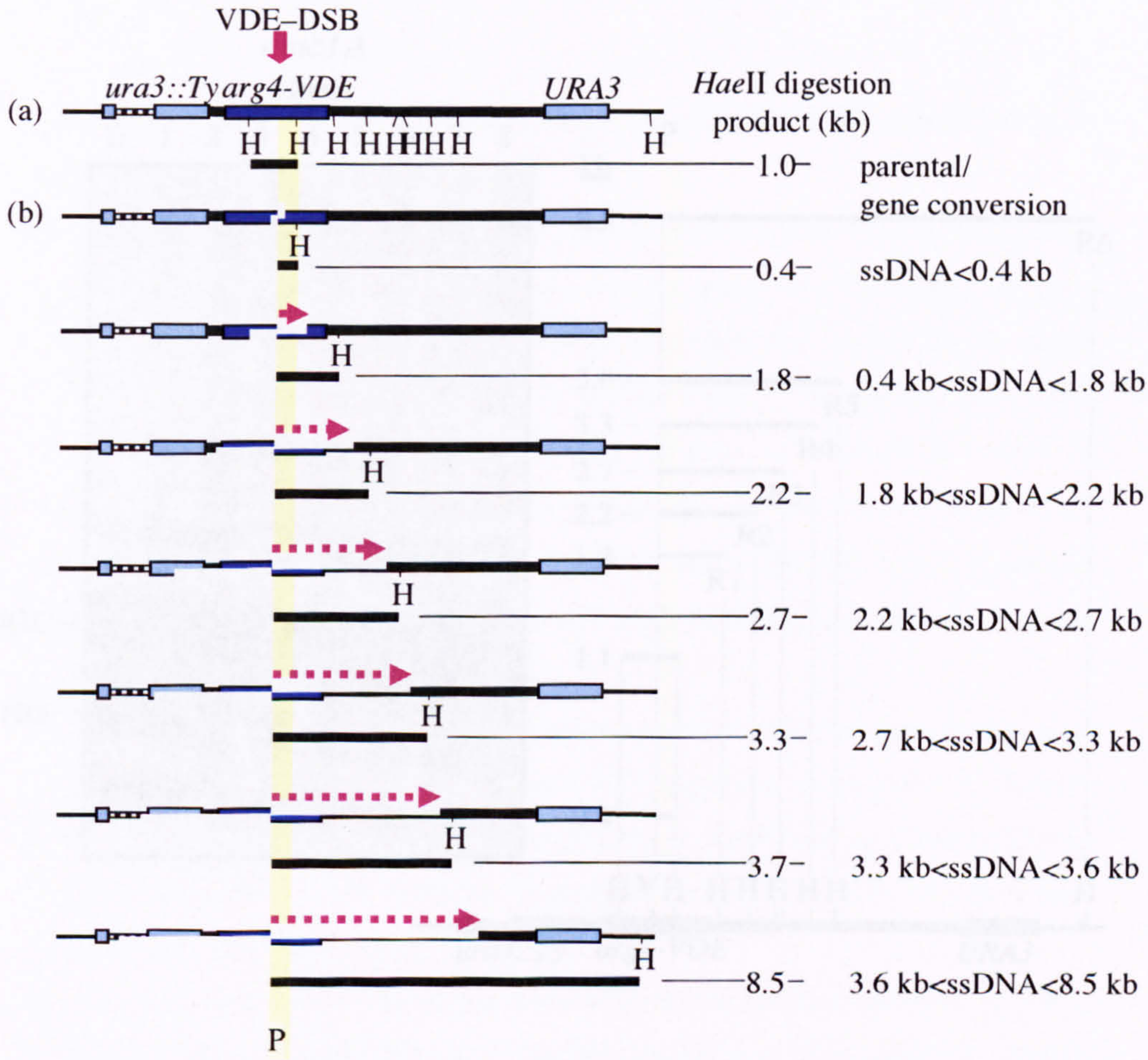

Figure 4.5: Scheme for measuring the extent of resection at the VDE–DSB. The restriction endonuclease (H) *Hae*II cleaves double–stranded DNA only. (a) *Hae*II sites flank the VDE–DSB site, and are present at a further seven locations within 10 kb downstream of the *arg4–VDE* allele. (b) Single–stranded (ss) 5′–3′ resectioning (red dotted arrows) through the *Hae*II sites prevents their cleavage. Following digestion with *Hae*II, DNA is fractionated on alkaline gels. ssDNA fragments proportional to the length of ssDNA that has resected can be detected using (P) a ssDNA probe specific to the 3′–end of the unresected strand.

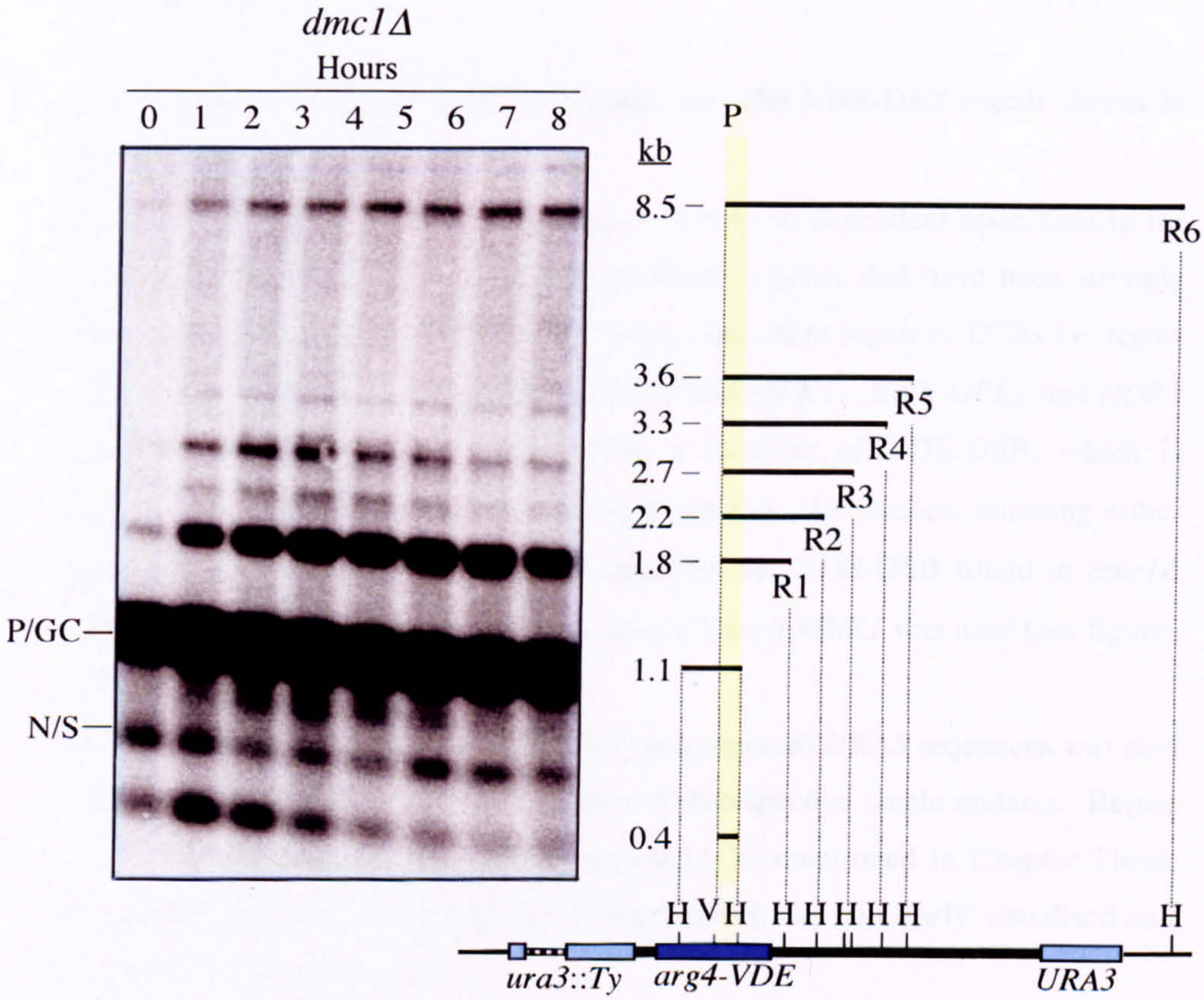

Figure 4.6: Physical analysis of resection at the VDE–DSB in *dmc1Δ* cells. Following digestion with *Hae*II (H), *dmc1*Δ cells and digested DNA was fractionated in an alkaline 0.7 % agarose gel and hybridised with (P), a ssDNA probe specific to the 3´–end of the unresected strand. (P/GC) parental and gene conversion band (N/S) non–specific hybridisation. Bands corresponding to the sequential loss of *Hae*II cleavage at sites downstream of the (V) VDE–DSB were detected at later time points. Such bands indicate the passage of single–stranded resectioning through an earlier *Hae*II site. This work was carried out in collaboration with M.J. Neale.

mutations in genes previously reported to be involved in Dmc1p-dependent repair pathway.

4.2.5 Mutation of *MEK1* or *HOP1* suppresses the VDE-DSB repair defect in *dmc1Δ* cells

So far, repair of the VDE-DSB has been shown to be dependent upon Dmc1p for repair. To confirm the dependence upon Dmc1p, genes that have been strongly implicated in being in the pathway of Dmc1p-dependent repair of DSBs i.e. repair towards the homologue, were mutated: *HOP1* and *MEK1*. Both *MEK1* and *HOP1* when doubly mutant with *dmc1Δ*, show a turnover of VDE-DSB, which is comparable to the *mek1Δ* and *hop1Δ* single mutants. In essence, mutating either *MEK1* or *HOP1* relieves the block in repair of the VDE-DSB found in *dmc1Δ* cells. In addition to the *mek1Δ* a kinase dead allele of *MEK1* was used (see figures 4.7).

The repair of the VDE-DSB using the flanking repeated *URA3* sequences was also examined in double mutants and compared with respective single mutants. Repair of the VDE-DSB using these repeat sequences, as mentioned in Chapter Three, Section 3.3, yields a 2.3 kb deletion product, which can be clearly visualised and quantified by Southern analysis.

dmc1Δ cells repair very little of the VDE-DSB to the deletion product (< 5 %), however, the *mek1Δdmc1Δ*, *mek1*-K199R*dmc1Δ and hop1Δdmc1Δ* double mutants are all able to efficiently repair the VDE-DSB to form the deletion product. The amount of deletion product formed in all three of the double mutants is very similar to the respective single mutants *mek1Δ*, *mek*-K199R or *hop1Δ*, (see figure 4.8). These findings suggest that both Mek1p and Hop1p are involved in establishing the Dmc1p-dependent repair of the VDE-DSB. Both Mek1p and Dmc1p have been implicated in directing repair of a Spo11p-DSB to use the homologous chromosome as repair template (Niu *et al.*, 2005). One possibility for the rescuing of the *dmc1Δ* block of repair when made doubly mutant with *hop1Δ*

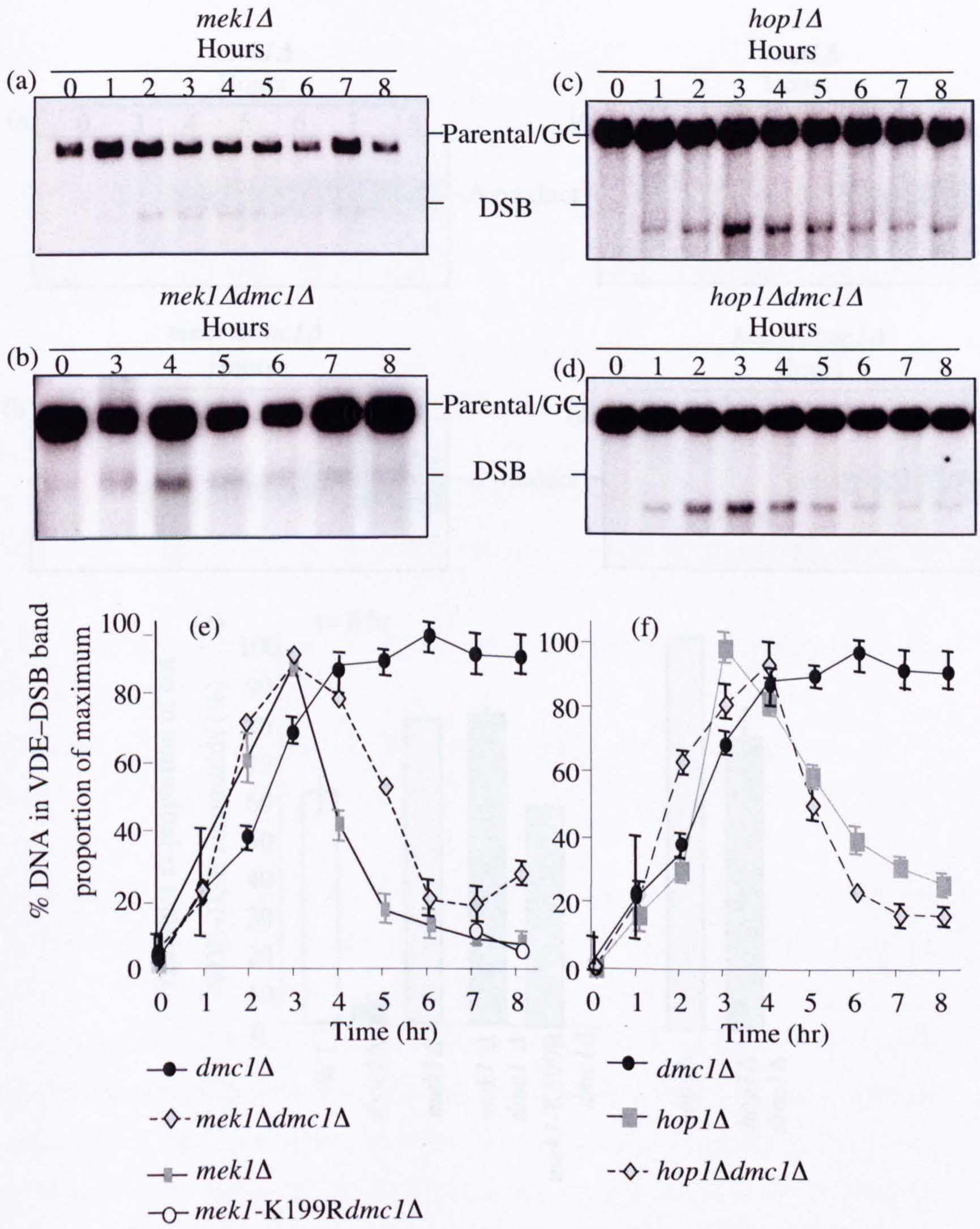

Figure 4.7: Physical analysis and quantification of the VDE–DSB. in *dmc1Δ, mek1Δ, mek1*-K199R, *mek1Δdmc1Δ, hop1Δ* and *hop1Δdmc1Δ* cells. Southern analysis using *Spe*I-digested DNA extracted from synchronous meiotic time course of (a) *mek1*Δ, (b) *mek1*Δ*dmc1*Δ (c) *hop1*Δ and (d) *hop1*Δ*dmc1*Δ cells and processed as for figure 3.5. *mek1*Δ, *dmc1Δ* and *hop1*Δ single data is shown for comparative purposes (see Chapter Three). Scanned images were cropped to show only Parental/GC and VDE-DSB bands. (e) Repair of the VDE–DSB is largely blocked by *dmc1*Δ, but this is restored by *mek1*Δ mutation. (f) Repair of the VDE–DSB is largely blocked by *dmc1*Δ, but this is restored by *hop1*Δ mutation.

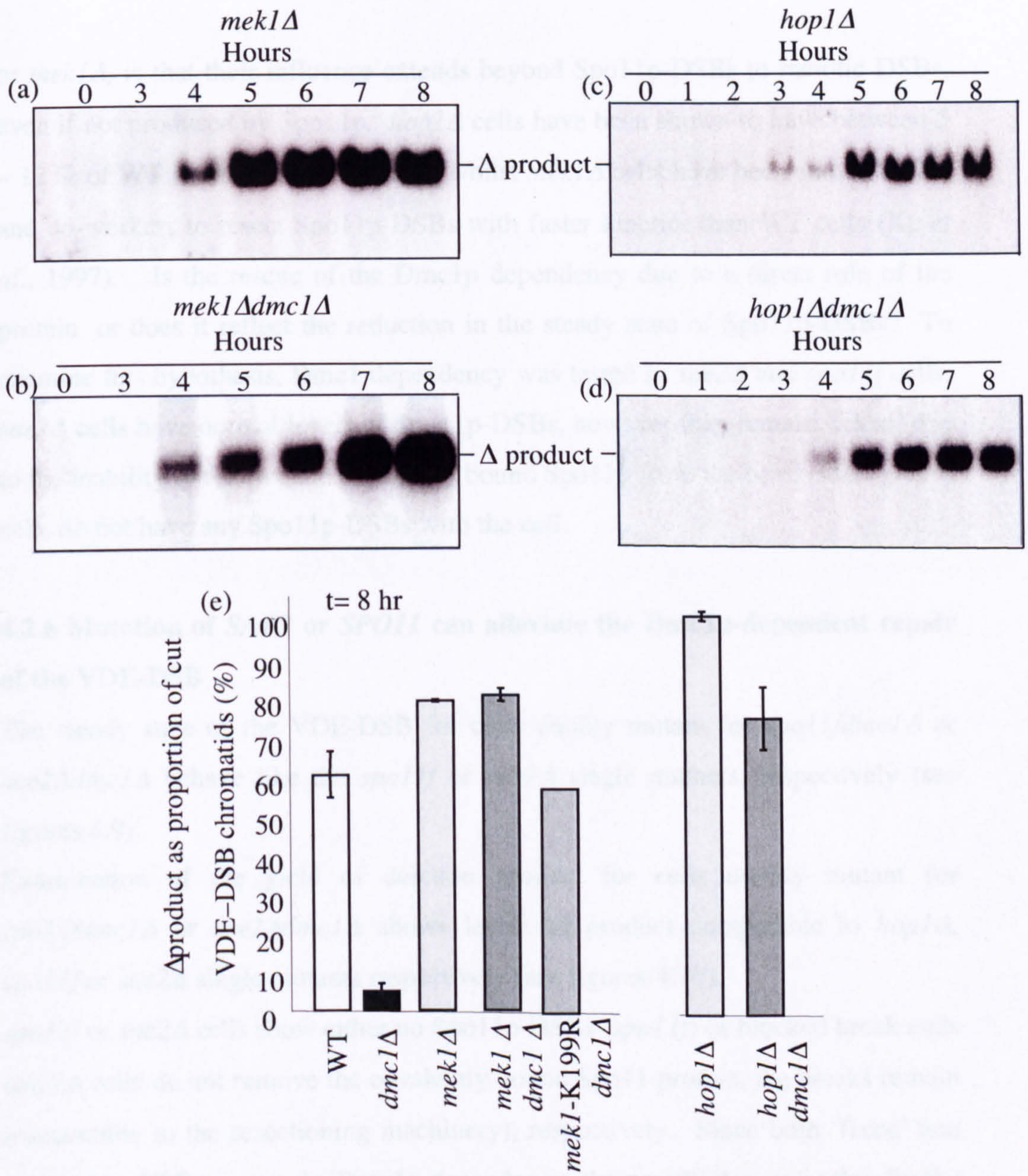

Figure 4.8: Physical analysis and quantification of deletion formation in *dmc1Δ*, *mek1Δ*, *mek1*-K199R, *mek1Δdmc1Δ*, *hop1Δ* and *hop1Δdmc1Δ* cells. Southern analysis using *Spe*I-digested DNA extracted from synchronous meiotic time course of (a) *mek1*Δ, (b) *mek1*Δ*dmc1*Δ, (c) *hop1*Δ and (d) *hop1*Δ*dmc1*Δ cells and processed as for figure 3.5. *mek1*Δ, *hop1*Δ and *dmc1*Δ data is shown for comparative purposes (see Chapter Three). The scanned images have been cropped to show only the deletion product. (e) The block of VDE-DSB in *dmc1*Δ cells is relieved when made doubly mutant with *mek1*Δ, *mek1*-K199R or *hop1*Δ. By time point 8 hr, the amount of repair to the deletion product in the double mutants reflects that of *mek1*Δ, *mek1*-K199R or *hop1*Δ respectively.

or *mek1Δ*, is that their influence extends beyond Spo11p-DSBs to meiotic DSBs, even if not produced by Spo11p. *hop1Δ* cells have been shown to have between 5 – 12 % of WT levels of Spo11p-DSBs whilst *mek1Δ* cells have been shown by Xu and co-workers to resect Spo11p-DSBs with faster kinetics than WT cells (Xu *et al.*, 1997). Is the rescue of the Dmc1p dependency due to a direct role of the protein, or does it reflect the reduction in the steady state of Spo11p-DSBs? To examine this hypothesis, Dmc1 dependency was tested in *sae2Δ* and *spo11f* cells; *sae2Δ* cells have normal levels of Spo11p-DSBs, however they remain 'fixed' due to the inability to remove the covalently bound Spo11p from the break site. *spo11f* cells do not have any Spo11p-DSBs with the cell.

4.2.6 Mutation of *SAE2* or *SPO11* can alleviate the Dmc1p-dependent repair of the VDE-DSB

The steady state of the VDE-DSB for cells doubly mutant for *spo11fdmc1Δ* or *sae2Δdmc1Δ* behave like the *spo11f* or *sae2Δ* single mutants, respectively (see figures 4.9).

Examination of the yield of deletion product for cells doubly mutant for *spo11fdmc1Δ* or *sae2Δdmc1Δ* shows levels of product comparable to *hop1Δ*, *spo11f* or *sae2Δ* single mutants respectively (see figures 4.10).

spo11f or *sae2Δ* cells show either no Spo11p-DSBs (*spo11f*) or blocked break ends (*sae2Δ* cells do not remove the covalently bound Spo11 protein, the breaks remain inaccessible to the resectioning machinery), respectively. Since both 'fixed' and no Spo11p-DSBs rescue the Dmc1p dependency, the possibilities exist that firstly; Sae2p and Spo11p have *bone fide* roles in VDE-DSB repair. Secondly, this *dmc1Δ* rescue could reflect the change in the steady state of Spo11p-DSBs.

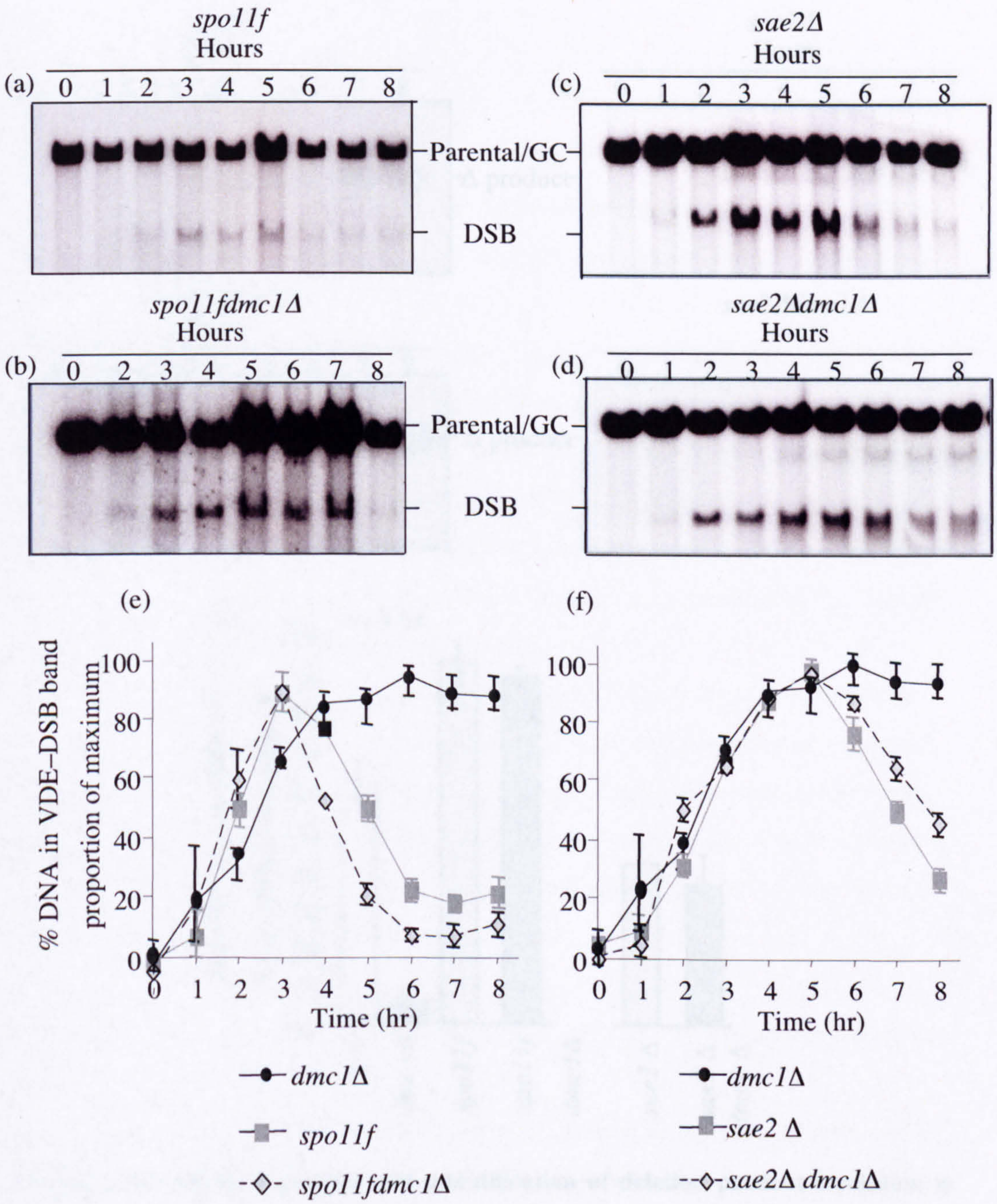

Figure 4.9: Physical analysis and quantification of the VDE–DSB in *spo11f*, *dmc1*Δ, *spo11fdmc1*Δ, *sae2*Δ and *sae2*Δ*dmc1*Δ cells. Southern analysis using *Spe*I-digested DNA extracted from synchronous meiotic time course of (a) *spo11f*, (b) *spo11fdmc1*Δ, (c) *sae2*Δ and (d) *sae2*Δ*dmc1*Δ cells and processed as for figure 3.5. *dmc1*Δ, *sae2*Δ *and spo11f* (See Chapter Three) data is shown for comparison purposes. Scanned images were cropped to only show Parental/GC and deletion product bands. (e), (f) Repair of the VDE–DSB is largely blocked by *dmc1*Δ, but this is restored by *spo11f* and *sae2*Δ.

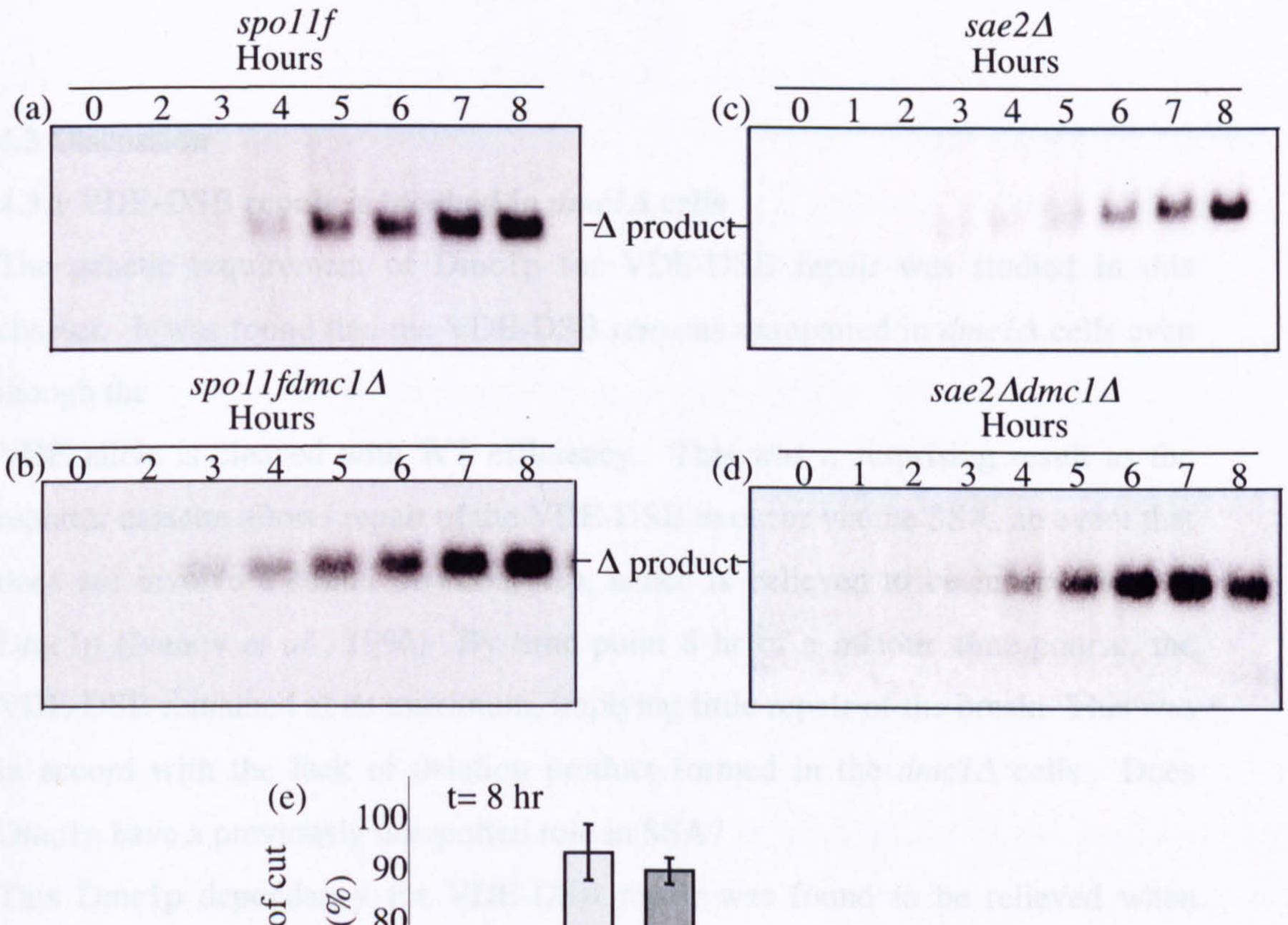

Figure 4.10: Physical analysis and quantification of deletion product formation in WT, *spo11f*, *dmc1*Δ, *spo11fdmc1*Δ, *sae2*Δ and *sae2*Δ*dmc1*Δ cells. Southern analysis using *Spe*I-digested DNA extracted from synchronous meiotic time course of (a) *spo11f*, (b) *spo11fdmc1*Δ, (c) *sae2*Δ and (d) *sae2*Δ*dmc1*Δ cells, and processed as for figure 3.5. Scanned images were cropped to show only Parental/GC and VDE-DSB bands. *spo11f*, *sae2*Δ and *dmc1*Δ data (See Chapter Three) is shown for comparative purposes. (e) The block of VDE-DSB repair in *dmc1*Δ cells is relieved when made doubly mutant with *spo11f* or *sae2*Δ. By time point 8 hr, the amount of repair to the deletion product in the double mutants reflects that of *spo11f* or *sae2*Δ cells respectively.

4.3 Discussion

4.3.1 VDE-DSB repair is blocked in *dmc1Δ* cells

The genetic requirement of Dmc1p for VDE-DSB repair was studied in this chapter. It was found that the VDE-DSB remains unrepaired in *dmc1Δ* cells even though the

VDE allele is cleaved with WT efficiency. This was a surprising result as the reporter cassette allows repair of the VDE-DSB to occur via the SSA, an event that does not involve a strand invasion step, hence is believed to be independent of Dmc1p (Ivanov *et al.*, 1996) By time point 8 hr of a meiotic time course, the VDE-DSB remained at its maximum, implying little repair of the break. This was in accord with the lack of deletion product formed in the *dmc1Δ* cells. Does Dmc1p have a previously unreported role in SSA?

This Dmc1p dependency for VDE-DSB repair was found to be relieved when made doubly mutant with specific mutations in genes already implicated in certain facets of meiotic DSB repair. Mutations in *SPO11, SAE2, HOP1* and *MEK1* were found to relieve the *dmc1Δ* block in repair of the break with double mutants showing repair kinetics and deletion product formation similar to the *spo11f, sae2Δ, hop1Δ* and *mek1Δ* single mutants.

4.3.2 Proposed model for the establishment of a Dmc1p-dependant mechanism of VDE-DSB repair

One hypothesis for this Dmc1p dependency and alleviation when made doubly mutant is that there is a pathway present within a meiotic cell that establishes the meiotic characteristics of break repair i.e. Dmc1p-dependent repair using the homologous chromosome as the repair template.

Overall, the data has lead to one suggestion that the presence of Spo11p–DSBs, and their normal processing, are significant contributors to the regulation of the outcome meiotic DSB repair *in trans*. The establishment of Dmc1p dependence

for repair at a given break requires the presence of Spo11p–DSBs, but not that Spo11p created the break studied.

In addition, while the presence of Spo11p–DSBs is required to create Dmc1p dependency, they are not sufficient. Moreover, the VDE-DSB must be processed by Sae2p for either activation or commitment to the Dmc1p repair route, which is mediated by the Mek1p complex (Mek1p, Red1p and Hop1p). Figure 4.11 is an illustration of the proposed Dmc1 dependent pathway of meiotic DSB repair.

The proposed model of Dmc1p-dependency suggests that in a WT situation, the repair of the VDE-DSB is dependent upon Dmc1p and hence is an inter-homologue event. When *DMC1* is mutated, the VDE-DSB cannot be repaired as the Dmc1p-dependency has already been established by the upstream members of the dependency pathway (Spo11p, Sae2p, Mek1p complex). According to this model, repair of the VDE-DSB in mutants such as *dmc1Δ*, *spo11f* and *hop1Δ* is now a Dmc1p independent event, and so is repaired by an intra molecular SSA mechanism. In the *dmc1Δ* double mutants, the Dmc1p dependency has not been established as upstream members of the pathway are missing, so the break can be repaired, even in the absence of Dmc1p.

4.3.3 Mutants that prevent the accumulation of large amounts of single-stranded DNA relieve the requirement for Dmc1p to repair the VDE-DSB

The possibility became apparent that in place of an active signalling pathway that results in the establishment Dmc1p-dependent repair. The reason repair of the VDE-DSB is sensitive to the presence of Dmc1p is the effect of the large amount of single-stranded DNA that accumulates at Spo11p-DSBs in *dmc1Δ* cells. In *dmc1Δ* cells there is a defect in the conversion of Spo11p-DSBs into the recombination intermediates required for inter-homologue repair. This causes an accumulation of meiotic DSBs, the broken DNA termini then undergo 5′- 3′ resectioning, which generates large amounts of ssDNA (Bishop *et al.*, 1992). In order to test this hypothesis, we looked at experiments in which the amount of ssDNA present in the genome was different from WT. The requirement for

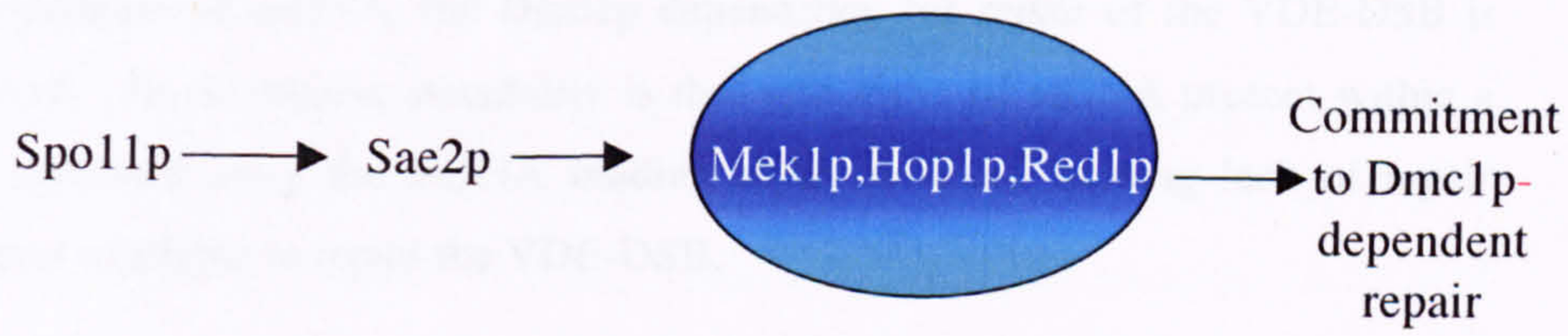

Figure 4.11: Proposed model for the establishment of Dmc1p-dependent DSB repair in meiotic cells. The establishment of Dmc1p-dependence for repair at a given break requires the presence of Spo11p–DSBs but not that Spo11p created the break studied. While the presence of Spo11p–DSBs is required to create Dmc1p-dependency, they are not sufficient. We suggest that Spo11p–DSBs must be processed by Sae2p for either activation or commitment to Dmc1p-dependent repair, which is almost certainly mediated by the Mek1p complex.

Dmc1p for repair of the VDE-DSB in cells was established in cells with reduced levels of Spo11p-DSBs (*hop1Δ* with 5 – 12 % of WT level of Spo11p-DSBs) or no Spo11p-DSBs (*spo11f*) and cells with WT levels of Spo11p-DSBs but where the Spo11 protein remains covalently bound to the break site, hence no accumulation of ssDNA (*sae2Δ*). When the *dmc1Δ* mutation is coupled with a mutation that prevents the formation of WT levels of Spo11p-DSBs and hence prevents the accumulation of ssDNA, the Dmc1p dependency for repair of the VDE-DSB is relieved. An alternative possibility is that vast tracts of ssDNA present within a cell sequester away the ssDNA binding repair proteins, causing lack of repair proteins available to repair the VDE-DSB.

4.3.4 Is repair of the VDE-DSB dependent upon progression of the meiotic cell cycle?

There also exists the possibility that in place of an active pathway for Dmc1p-dependent repair, or a limited supply of repair proteins, the pachytene arrest found in *dmc1Δ* cells could be responsible for the lack of repair at VDE-DSB (Bishop *et al.*, 1992). Chapter five aims to identify whether repair proteins are in limited supply in *dmc1Δ* cells or whether the pachytene arrest is responsible for block in repair.

Chapter Five

The testing of the proposed Dmc1p-dependent pathway for repair of the *arg4-VDE* allele

5.1 Introduction

In the previous chapter the repair of the VDE-DSB was assayed in cells singularly mutant for *DMC1* and in combination with other proteins implicated in Spo11p DSB formation and repair. The data identified an absolute necessity for Dmc1p for the repair of the VDE-DSB unless Spo11p-DSBs were absent or resectioning at Spo11p-DSBs was inhibited.

Three possible explanations for this Dmc1p dependency have been considered. Firstly, lack of repair of the VDE-DSB could be the result of pachytene arrest of *dmc1Δ* cells. Secondly, Dmc1p could have a *bone fide* influence on DSB repair with a proposed Dmc1p-dependent pathway. Thirdly, there is a positive correlation between a block of repair of the VDE-DSB and an accumulation of ssDNA within the cell, raising the possibility that the availability of ssDNA binding proteins is a limiting factor in VDE-DSB repair. This chapter aims to identify why *dmc1Δ* cells have such a severe phenotype at the VDE-DSB.

5.2Results

5.2.1 Repair of the VDE-DSB is not dependent upon progression of the meiotic cell cycle

Two mutants that influence cell cycle progression have been used to test the possibility that *dmc1Δ* cell arrest influences repair of the VDE-DSB. Firstly, *ndt80Δ;* Ndt80p is a transcription factor that is required for progression from the first meiotic prophase. *ndt80Δ* cells experience normal Spo11p-DSB formation and normal chromosome pairing and synapsis up until the point of arrest. The

repair of the VDE-DSB was found to be very similar to WT in *ndt80Δ* cells, even though the cells cannot pass through the first meiotic prophase. Thus a block in the cell cycle is per sé does not influence VDE-DSB repair, suggesting that the block of repair found in *dmc1Δ* cells is not the result of cell cycle arrest (see figure 5.1).

5.2.2 Removal of the pachytene arrest in *dmc1Δ* cells does not restore VDE-DSB repair

To further test whether the cell cycle arrest in *dmc1Δ* cells was responsible for the block of repair, a second approach was taken to remove the arrest found in *dmc1Δ* cells. Pch2p is required for the meiotic checkpoint that prevents chromosome segregation when recombination and chromosome synapsis are defective. Mutation of *PCH2* relieves the checkpoint-induced pachytene arrest of the *zip1Δ*, *zip2Δ*, and *dmc1Δ* mutants, resulting in chromosome mis-segregation and low spore viability (San-Segundo and Roeder, 1999). If the block of repair found in a *dmc1Δ* strain is due to the arrest, removing the arrest should be able to rescue repair of the VDE-DSB.

The *pch2Δ* mutation relieves the pachytene arrest of *dmc1Δ* as observed by staining with DAPI. The majority of *dmc1Δ* cells remain mononucleate after 10 hr in sporulation medium whilst WT cells show nearly complete entry into MI or MII. *pch2Δdmc1Δ* cells show rescue of the *dmc1Δ* block with approximately WT levels of entry into MI or MII by time point 10 hr (figure 5.2).

The cleavage at *arg4-VDE* was found to occur in a WT level in *pch2Δdmc1Δ* cells with approximately 95 % of chromatids having received a break by 8 hr in meiosis (figure 5.3).

Standard Southern analysis of *Spe*I-digested DNA reveals *pch2Δdmc1Δ* double mutant to have a VDE-DSB repair phenotype that is intermediate between WT and *dmc1Δ* (Figure 5.4). The *pch2Δdmc1Δ* mutant is seen to accumulate large levels of VDE-DSBs, which argues that the pachytene arrest of the *dmc1Δ* cells is not the cause of the block of repair. Interestingly, there is significantly more repair of the

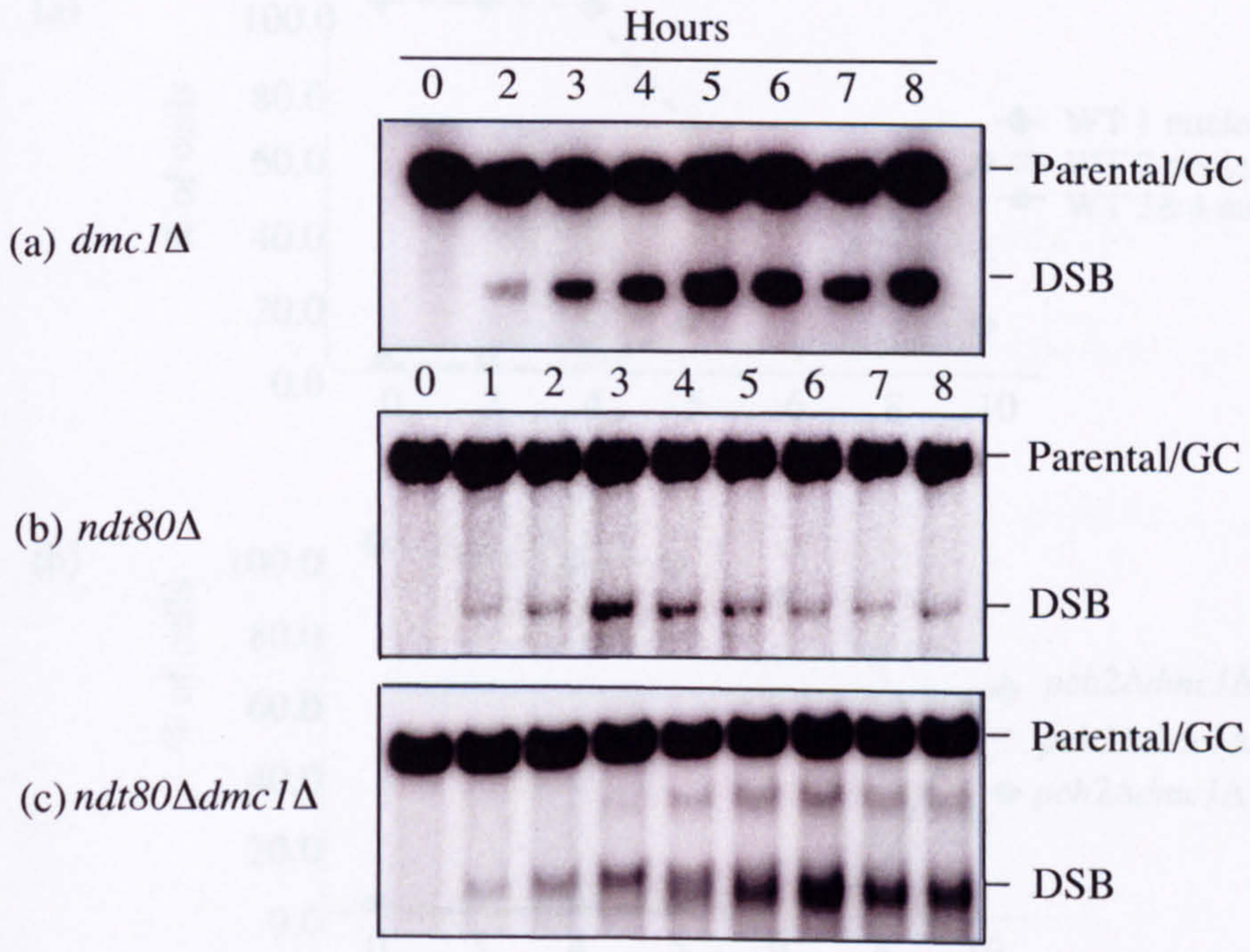

Figure 5.1: Physical analysis and quantification of the VDE–DSB in WT, *ndt80Δ*, *dmc1Δ*, and *ndt80Δdmc1Δ* cells. Southern analysis using *Spe*I-digested DNA extracted from synchronous meiotic time course of (a) WT, (b) *ndt80*Δ and (c) *ndt80*Δ*dmc1*Δ cells and processed as for figure 3.5. (d) *ndt80*Δ cells do not show a block in the repair of the VDE-DSB. This implies that the block in *dmc1*Δ cells is not dependent upon the pachytene arrest.

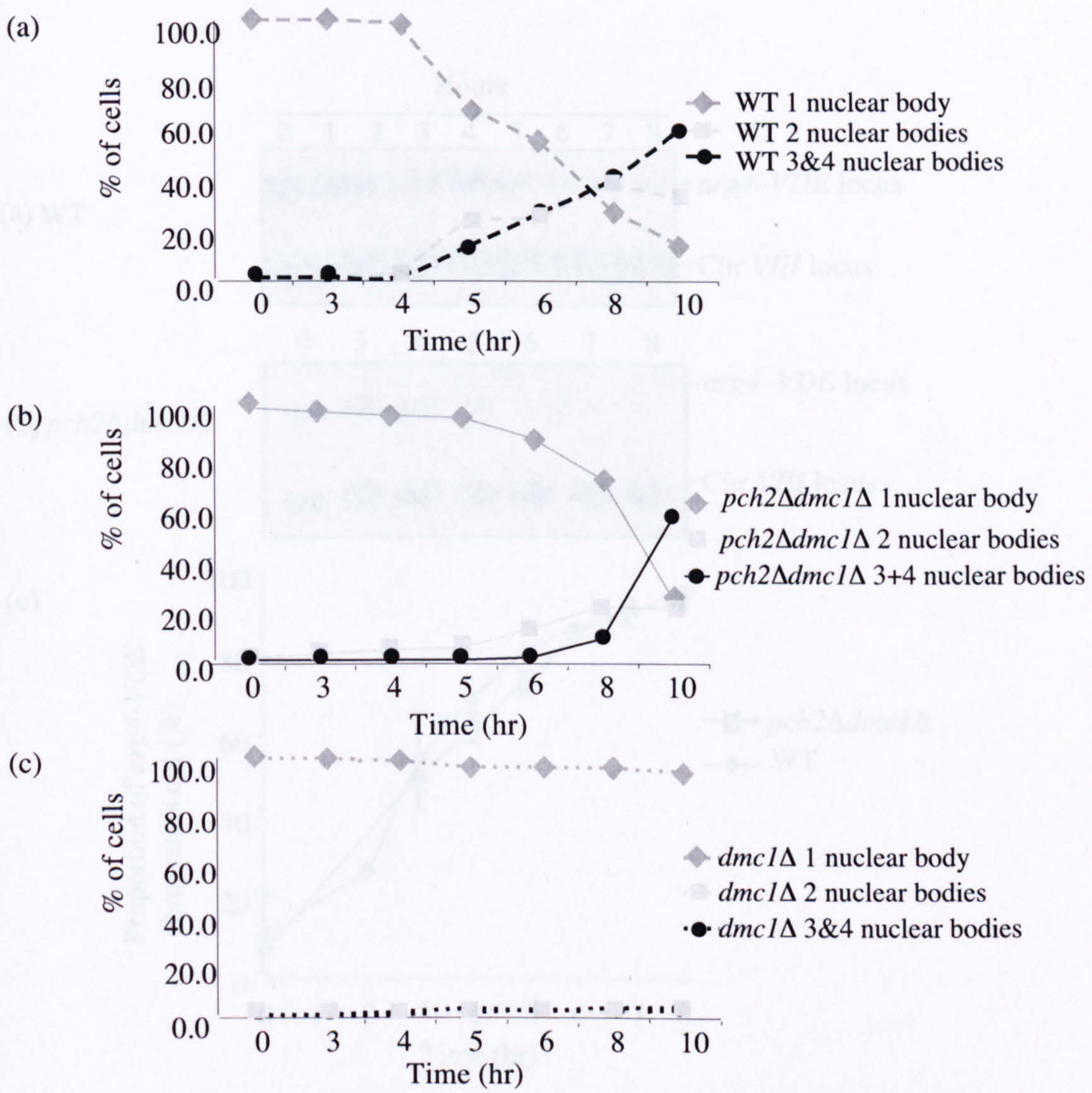

Figure 5.2: Passage of WT, *pch2Δ* and *pch2Δdmc1Δ* cells into the meiotic divisions as assessed by DAPI staining. Cells from synchronous meiotic cultures of (a) WT, (b) *dmc1*Δ and (c) *pch2*Δ*dmc1*Δ cells and were fixed in ethanol, incubated with the fluorescent DNA stain DAPI, and visualised using fluorescence microscopy. After 10 hr in sporulation medium, the majority of WT cells had underdone at least one nuclear division, however, the majority of *dmc1*Δ cells remain mononucleate. *pch2*Δ appears to rescue the *dmc1*Δ prophase arrest with at least 80 % of cells having undergone at least one nuclear division by time point 10 hr.

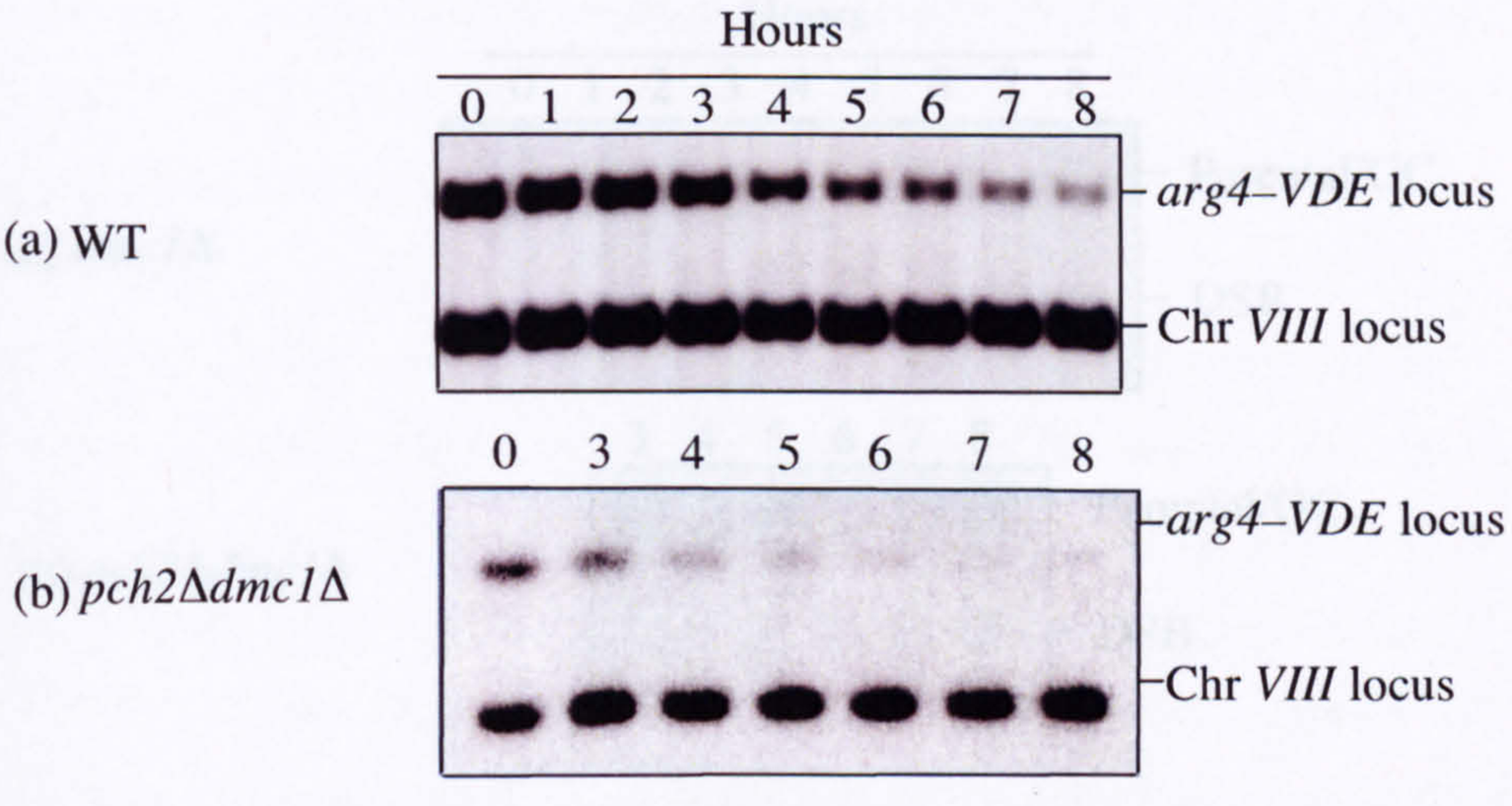

Figure 5.3: Physical analysis and quantification of *arg4–VDE* cleavage in WT and *pch2Δdmc1Δ* cells. Southern analysis using *Bgl*II/*Eco*RV-digested DNA extracted from synchronous meiotic time course of (a) WT and (b) *pch2Δdmc1Δ* cells and processed as for figure 3.4 The scanned images have been cropped to show only the *arg4–VDE* and *arg4–nsp,bgl* (loading control) band. (c) By t = 8 hr nearly all *arg4–VDE* alleles are cut. The cleavage at *arg4-VDE* is the same in WT and *pch2Δdmc1Δ* strains.

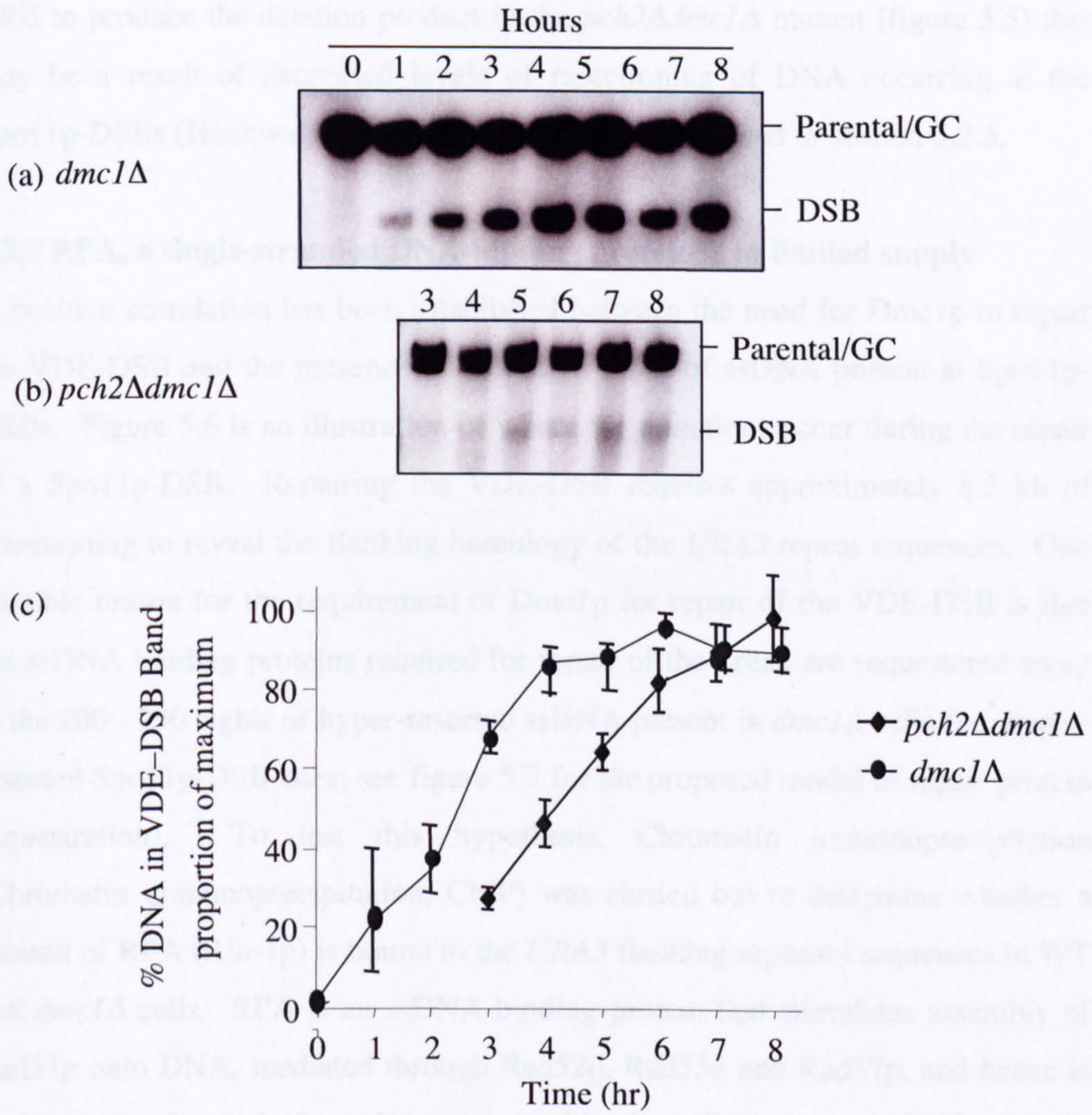

Figure 5.4: Physical analysis and quantification of the VDE–DSB in *dmc1Δ* and *pch2Δdmc1Δ* cells. Southern analysis using *Spe*I-digested DNA extracted from synchronous meiotic time course of (a) *dmc1Δ* and (b) *pch2Δdmc1Δ* cells and processed as for figure 3.5. (c) The VDE-DSB is seen to accumulate to higher levels than in the *dmc1Δ* single mutant, possibly a result of the DSB molecules being hyper-resected in the *dmc1Δ* mutants. The *pch2Δdmc1Δ* mutant is seen to accumulate large levels of VDE-DSBs, suggesting the pachytene arrest of the *dmc1Δ* cells is not the cause of the block of repair.

DSB to produce the deletion product in the *pch2Δdmc1Δ* mutant (figure 5.5) this may be a result of decreased levels of resectioning of DNA occurring at the Spo11p-DSBs (Hochwagen *et al.*, 2005)– an issue discussed in section 5.2.5.

5.2.3 RPA, a single-stranded DNA-binding protein is in limited supply

A positive correlation has been established between the need for Dmc1p to repair the VDE-DSB and the presence of extensive tracts of ssDNA present at Spo11p-DSBs. Figure 5.6 is an illustration of where the mutations occur during the repair of a Spo11p-DSB. Repairing the VDE-DSB requires approximately 8.5 kb of resectioning to reveal the flanking homology of the *URA3* repeat sequences. One possible reason for the requirement of Dmc1p for repair of the VDE-DSB is that the ssDNA binding proteins required for repair of the break are sequestered away to the 200 - 250 sights of hyper-resected ssDNA present in *dmc1Δ* cells (i.e. hyper-resected Spo11p-DSB sites; see figure 5.7 for the proposed model of repair protein sequestration). To test this hypothesis, Chromatin immunoprecipitation (Chromatin immunoprecipitation; ChIP) was carried out to determine whether a subunit of RPA (Rfa-1p) is bound to the *URA3* flanking repeated sequences in WT and *dmc1Δ* cells. RPA is an ssDNA-binding protein that stimulates assembly of Rad51p onto DNA, mediated through Rad52p, Rad55p and Rad57p, and hence is an important factor in homologous recombination (Gasior *et al.*, 2001). RPA's ssDNA-binding property and its many well-documented roles in meiotic recombination make it a good candidate for ChIP experiments throughout this study.

Meiotic time courses were carried out and samples were taken for DNA extraction and DNA-protein cross-linking. Southern analysis was carried out on the meiotic time courses to ensure that the VDE allele had received efficient cutting, cleavage at *arg4-VDE* was found to be as in WT cells (data not shown).

Enrichment of Rfa-1p was determined at the 1) *URA3* repeat region 3′ of the reporter cassette 2) a Spo11-coldspot (a dubious ORF, unlikely to encode a protein, see figure 5.8 for illustration of location) and 3) a Spo11p-hotspot (9% of

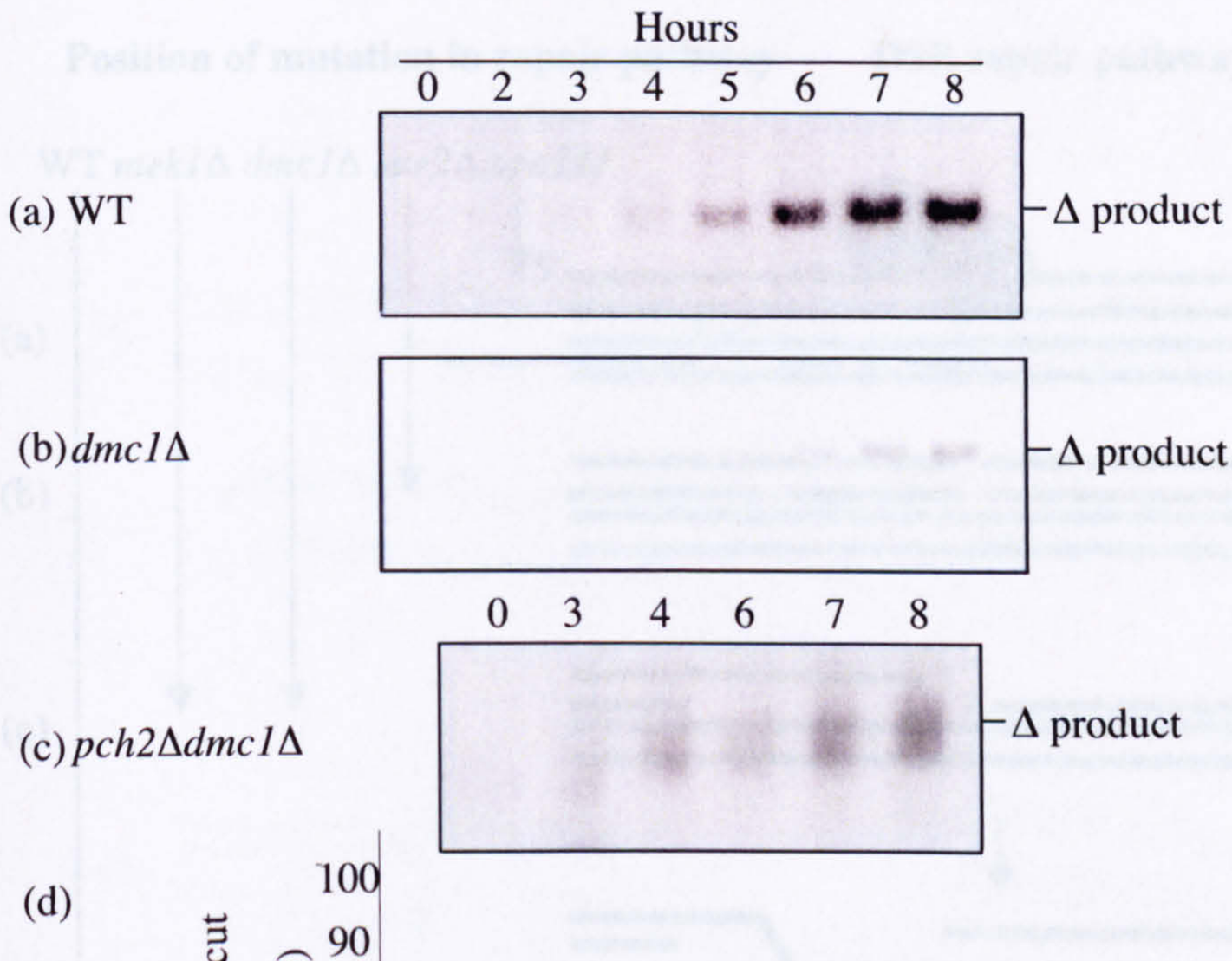

Figure 5.5: Physical analysis and quantification of deletion product formation in WT, *dmc1Δ*, *pch2Δ* and *pch2Δdmc1Δ* cells. Southern analysis using *Spe*I-digested DNA extracted from synchronous meiotic time course of (a) WT, (b) *dmc1*Δ and (c) *pch2Δdmc1*Δ cells and processed as for figure 3.5. (d) By time point 8 hr, there is significantly more repair of the DSB to produce the deletion product in the *pch2Δdmc1Δ* mutant, this may be a result of decreased levels of resection of DNA occurring at the Spo11p-DSBs.

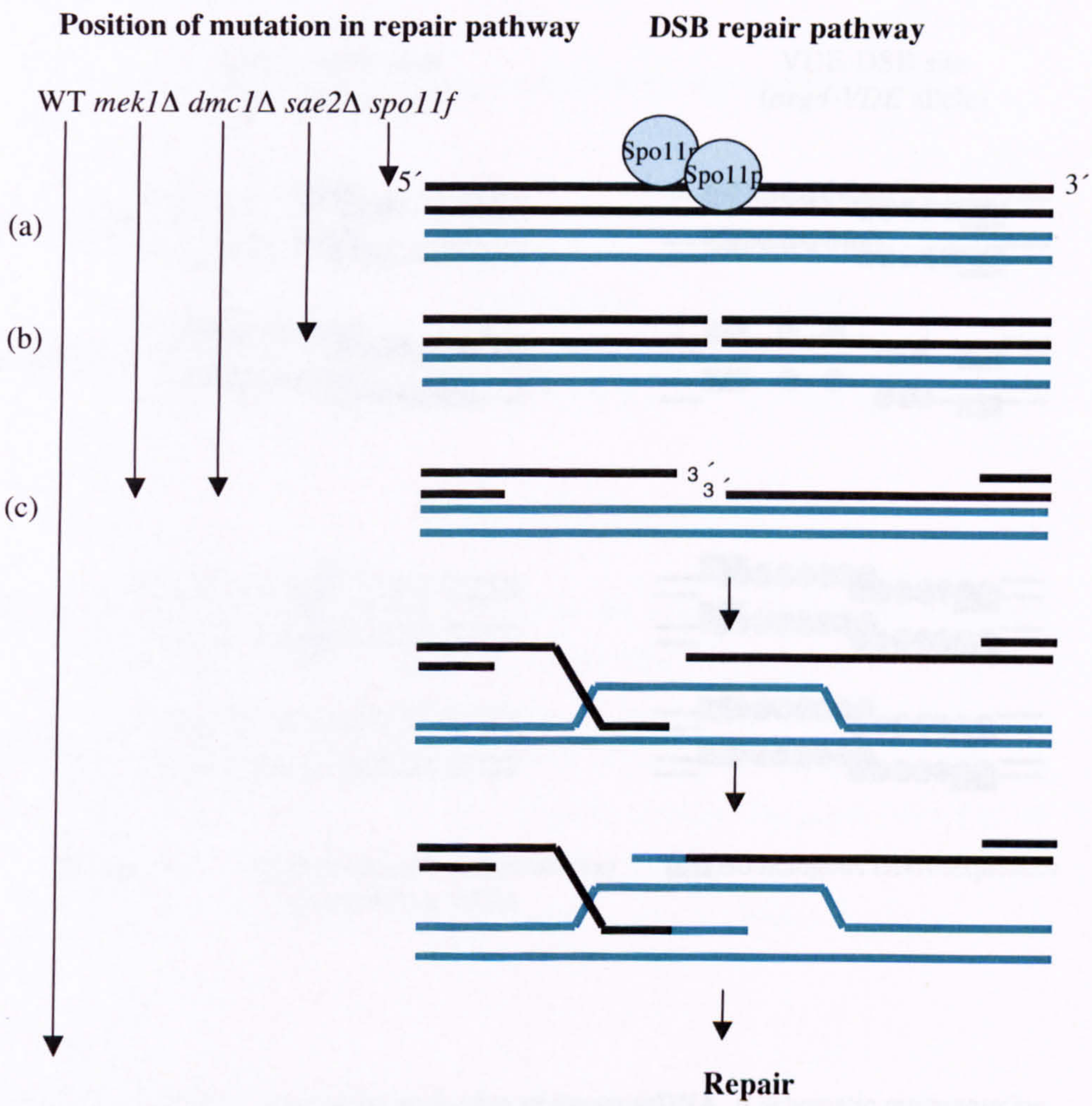

Figure 5.6: DSB repair pathway and position where mutation is apparent. (a) is the stage at which the Spo11p-DSB is created. In *spo11f* mutants, Spo11p-DSB do not form. (b) The removal of the covalently bound Spo11p homodimer form the DNA ends. *sae2*Δ mutants do not remove the Spo11p from the DNA. (c) The 5´ to 3´ resection of the DNA. *dmc1*Δ mutants show excessive resection. *mek1*Δ mutants also show a very rapid processing of the DSB.

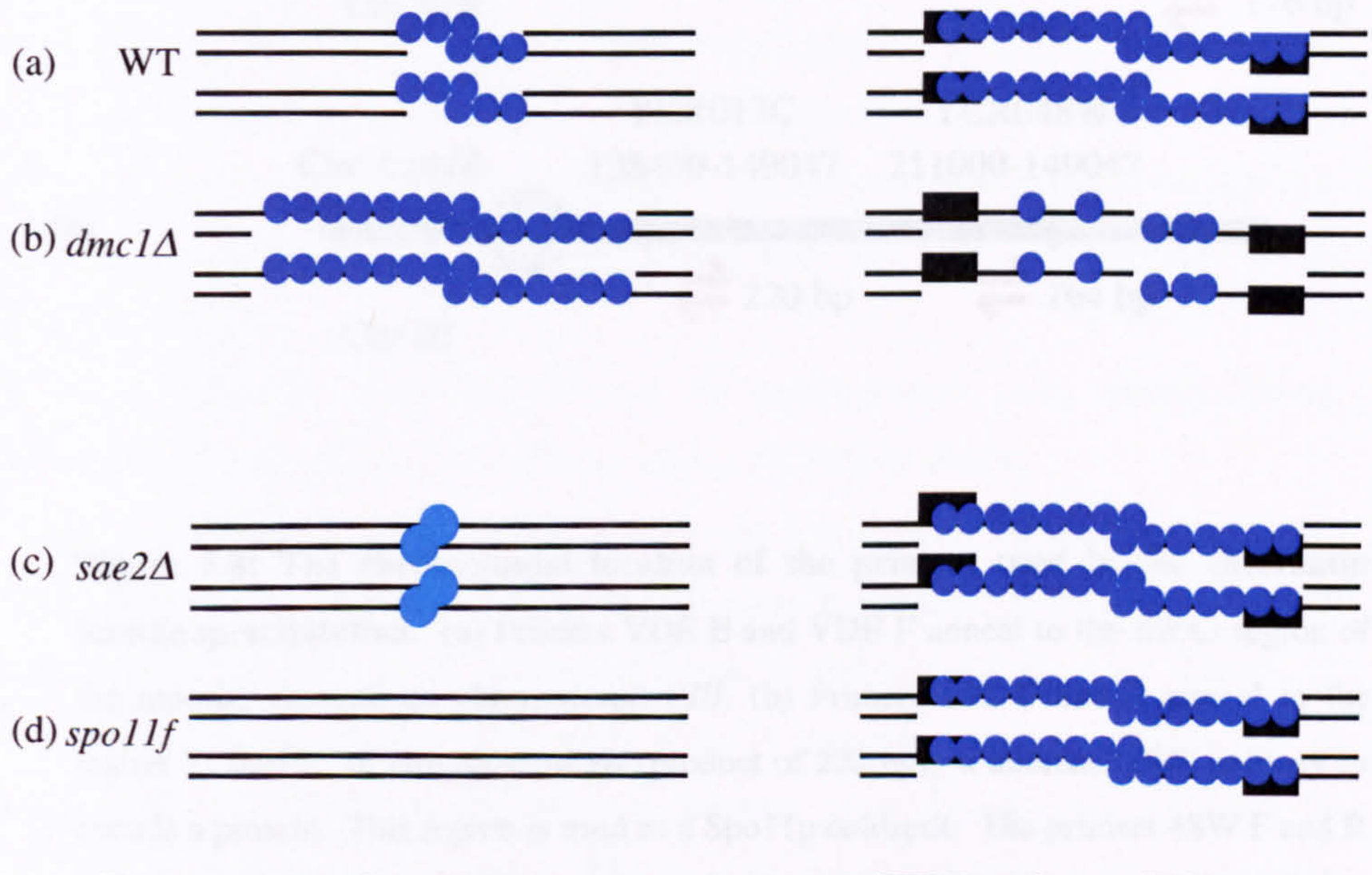

Figure 5.7: Protein sequestration at sites of excess ssDNA. A schematic representation of the events at multiple Spo11p-DSBs and the VDE-DSB site during meiotic DSB repair. Transient ssDNA formation at Spo11p-DSBs in WT cells is not sufficient to sequester the ssDNA binding-proteins proteins away from the VDE-DSB site. In *sae2Δ* and *spo11f* mutants, (and *hop1Δ*, not shown) the absolute lack of ssDNA at Spo11-DSB sites makes available all of the RPA protein to bind the ssDNA at the *arg4-VDE* allele allowing WT repair. In *dmc1Δ* cells, hyper-resection of the accumulating Spo11p-DSBs generates sufficient ssDNA to sequester the ssDNA binding proteins away from the VDE-DSB, therefore impairing SSA repair of the *arg4-VDE* allele.

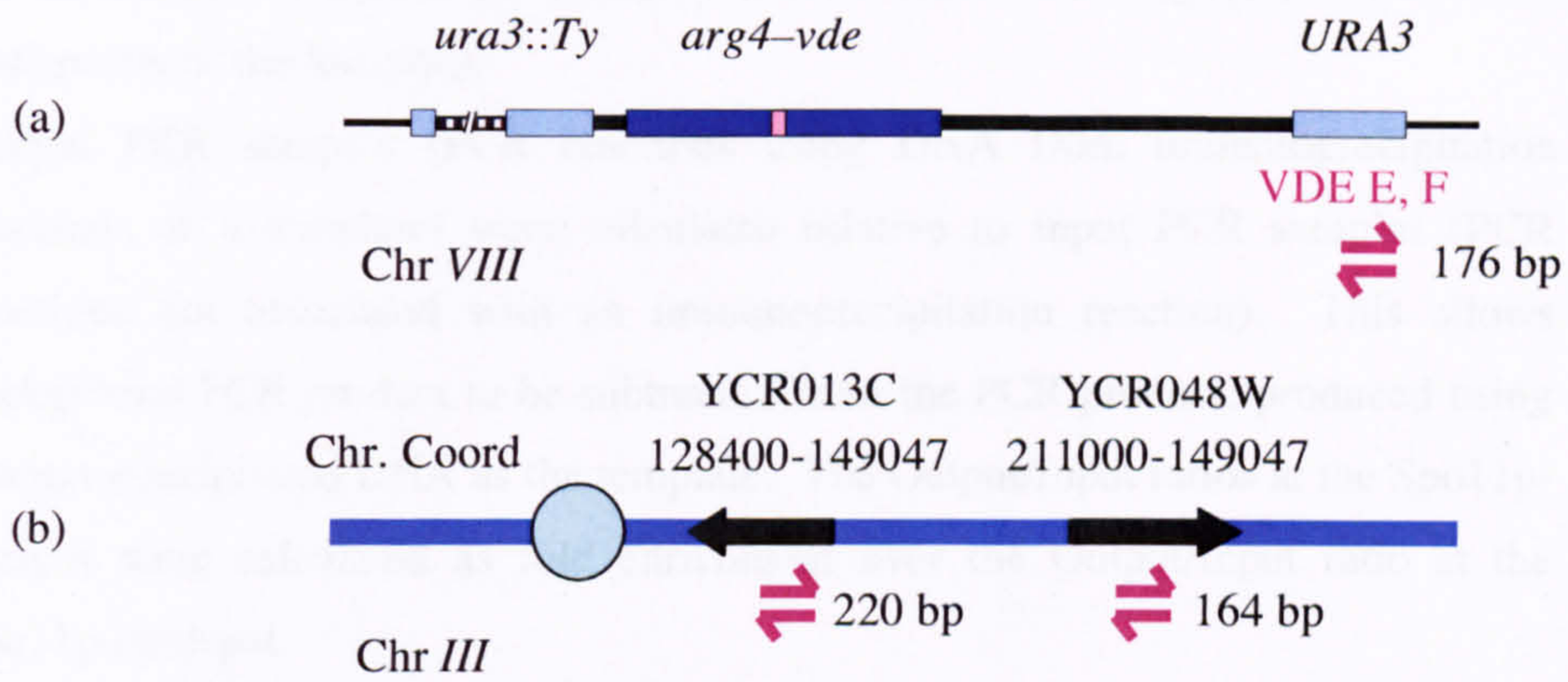

Figure 5.8: The chromosomal location of the primers used in the chromatin immunoprecipitation. (a) Primers VDE E and VDE F anneal to the *URA3* region of the reporter cassette on chromosome *VIII*. (b) Primers 13C F and R anneal to the region YCR013C of chromosome *III* (product of 220 bp), a dubious ORF, unlikely to encode a protein. This region is used as a Spo11p coldspot. The primers 48W F and R anneal to the region YCR048W on chromosome *III* (product of 164 bp). This region is used as a Spo11p hotspot (9 % of all chromosomes receive a break).

all chromosomes receive a break, Borde *et al.*, 2004. Figure 5.8 shows an illustration of the location).

Output PCR samples (PCR reactions using DNA from immunoprecipitation reactions as a template) were calculated relative to input PCR samples (PCR reactions not associated with an immunoprecipitation reaction). This allows background PCR product to be subtracted from the PCR product, produced using immunoprecipitated DNA as the template. The Output/Input ratios at the Spo11p-hotspot were calculated as fold enrichment over the Output/Input ratio at the Spo11p-coldspot.

Initial experiments were carried out in collaboration with Sheila Harris. Experiments were repeated in collaboration with Valerie Borde.

In two independent experiments there was found to be an increase in the enrichment of Rfa-1p at the Spo11p-DSB hotspot in the ChIP from *dmc1Δ* cells in comparison with WT cells, presumably due to the accumulation of ssDNA in *dmc1Δ* cells. In *dmc1Δ* cells, after 8 hr in meiosis, there is an increase in enrichment of Rfa-1p at the Spo11p hotspot over the Spo11p coldspot in comparison with the enrichment of Rfa-1p at the Spo11p hotspot over the Spo11p coldspot in WT cells. This data suggests that there is a significant accumulation of Rfa-1p coating the ssDNA at the Spo11p hotspot in a *dmc1Δ* mutant, which is known to amass significant tracts of ssDNA (see figure 5.9).

There was also found to be an enrichment of Rfa-1 close to the *URA3* repeat sequence of the *ura3::arg4-VDE-URA3* reporter cassette in comparison with the Spo11p coldspot, that is greater in WT cells than in with *dmc1Δ* cells. At the 8 hr time point, there was found to be an increase in the enrichment of Rfa-1p at the *URA3* repeat region of the cassette over the Spo11p coldspot in WT cells in comparison with *dmc1Δ* cells (figure 5.9). This is consistent with the lack of repair in a *dmc1Δ* cell being due to the limitation of available Rfa-1p and again is consistent with the hypothesis that when Dmc1p function is lacking, hyper-resected ssDNA accumulates at Spo11p-DSBs which sequesters away Rfa-1p and

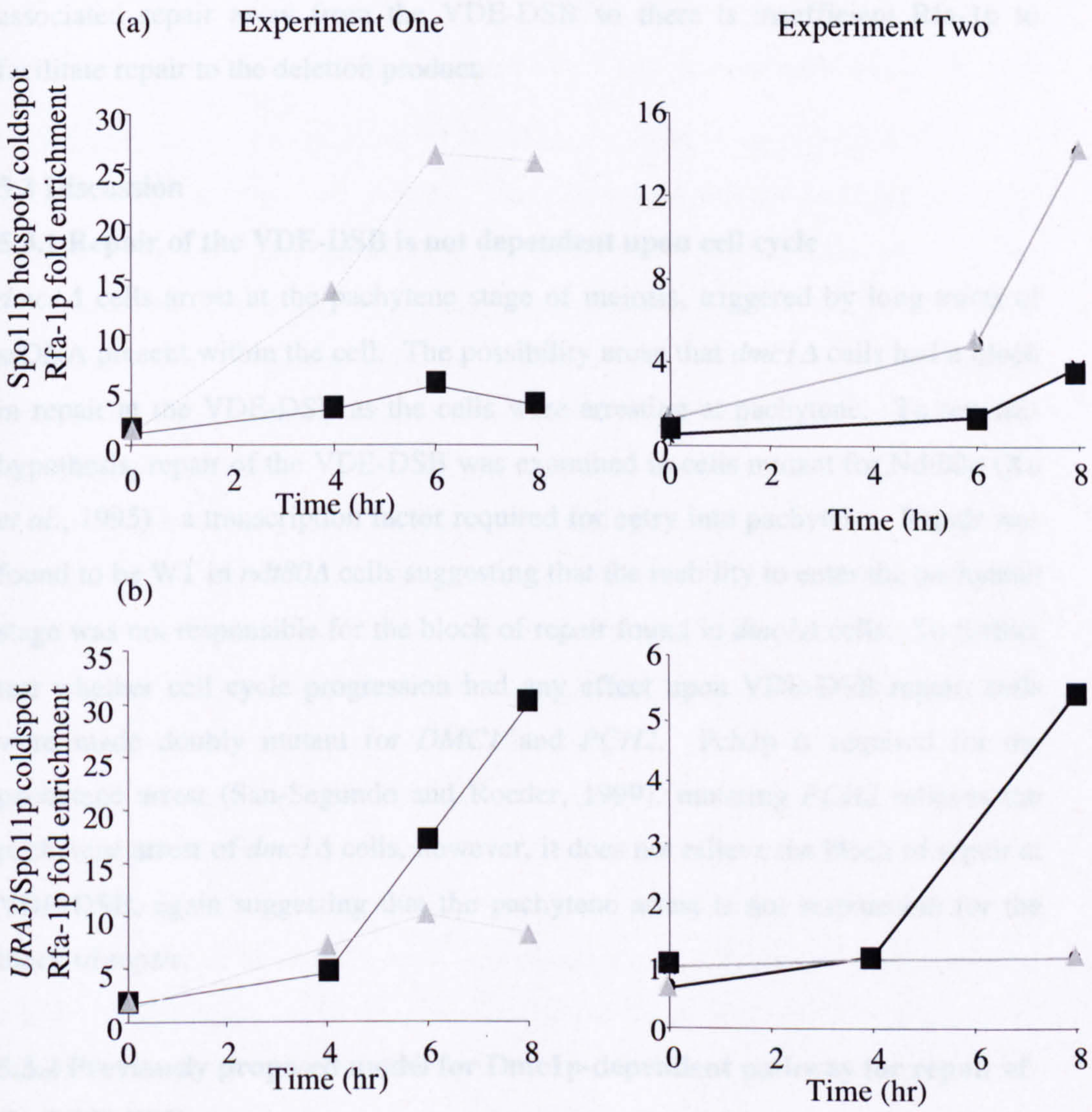

Figure 5.9: Enrichment for Rfa-1p in WT and *dmc1Δ* cells. (a) There is an increase in the enrichment of Rfa-1p at the Spo11p hotspot over the Spo11p coldspot, in *dmc1Δ* cells in comparison with WT cells. WT cells show a 4-fold increase and *dmc1Δ* cells exhibit a 25-fold increase. (b) There was found to be an enrichment of Rfa-1p close to the *URA3* repeat sequence of the *ura3::arg4-VDE-URA3* reporter cassette in comparison with the Spo11p coldspot that is greater in WT cells than in comparison with *dmc1Δ* cells. WT cells exhibit a 31-fold increase and *dmc1Δ* cells show an 8-fold increase. ChIP experiments were performed twice, even though numerical values differed, trends remained consistent. This work was carried out in collaboration with S. Harris and V. Borde. ■ WT ▲ *dmc1Δ*

associated repair away from the VDE-DSB so there is insufficient Rfa-1p to facilitate repair to the deletion product.

5.3 Discussion

5.3.1 Repair of the VDE-DSB is not dependent upon cell cycle

dmc1Δ cells arrest at the pachytene stage of meiosis, triggered by long tracts of ssDNA present within the cell. The possibility arose that *dmc1Δ* cells had a block in repair at the VDE-DSB as the cells were arresting at pachytene. To test this hypothesis, repair of the VDE-DSB was examined in cells mutant for Ndt80p (Xu *et al.*, 1995) - a transcription factor required for entry into pachytene. Repair was found to be WT in *ndt80Δ* cells suggesting that the inability to enter the pachytene stage was not responsible for the block of repair found in *dmc1Δ* cells. To further test whether cell cycle progression had any effect upon VDE-DSB repair, cells were made doubly mutant for *DMC1* and *PCH2*. Pch2p is required for the pachytene arrest (San-Segundo and Roeder, 1999), mutating *PCH2* relieves the pachytene arrest of *dmc1Δ* cells, however, it does not relieve the block of repair at VDE-DSB, again suggesting that the pachytene arrest is not responsible for the block of repair.

5.3.2 Previously proposed model for Dmc1p-dependent pathway for repair of the VDE-DSB

Initial work within this study led to the hypothesis that within a meiotic cell there is an active pathway that leads to meiotic characteristics of repair of the VDE-DSB i.e. Dmc1p-dependent repair which utilises the homologous chromosome as the repair template of choice. This pathway requires that Spo11p-DSBs are present within the cell, even though the break being assayed has been created in a Spo11p-independent manner. Furthermore, this pathway requires that Sae2p is also present within the cell to establish this Dmc1p-dependency. This Dmc1p-dependency is most likely mediated through the Mek1p complex.

5.3.3 A correlation between the amount of ssDNA present within the cell and repair of the VDE-DSB

dmc1Δ cells have been shown to have excessive tracts of resectioning present at Spo11p-DSBs (Bishop *et al.*, 1992b). Many proteins identified as being involved in DSB repair have been shown to bind ssDNA and it became clear that if there was a finite amount of ssDNA binding repair proteins within a cell the available proteins could be sequestered to the approximately 200 – 250 hyper-resected Spo11p-DSBs thus being unable to repair the VDE-DSB. To determine whether the availability of repair proteins *in vivo* was responsible for the block of VDE-DSB repair in *dmc1Δ* cells, Chromatin immunoprecipitation was utilised to identify whether an RPA subunit, Rfa-1p, was limited in supply in mutants differing in the amount of ssDNA present in the cell. The data obtained in the ChIP experiments was consistent with the hypothesis that ssDNA-binding proteins availability is a limiting factor in VDE-DSB repair.

The identification that the presence of vast tracts of ssDNA can influence repair of the VDE-DSB *in trans* has many implications for research outside of this study. The pleiotropic effects of hyper-resectioning at Spo11p-DSBs have a significant impact on VDE-DSB repair. It is important to note that the phenotype of one mutant cannot always imply the exact function of the protein and instead could be the result of an altered biochemistry of the cell, which may have implications for research outside of this study.

The possibility that the block of repair found in the *dmc1Δ* mutant is the result of sequestering away of repair machinery to other break sites elsewhere in the genome, could explain why *pch2Δdmc1Δ* cells show a increased level of deletion product in comparison with *dmc1Δ* cells. *pch2Δ* exhibit reduced levels of DNA resectioning at Spo11p-DSBs (Hochwagen *et al.*, 2005). If there is reduced tracts of ssDNA in *pch2Δ*, this could alleviate some of the sequestered RPA and associated repair proteins so that RPA is available at the VDE-DSB, and facilitate repair to the deletion product.

Chapter Six

Examining the roles of Sae2p, Mre11p and Exo1p during resectioning at *arg4-VDE*

6.1 Introduction

Mre11p forms a complex with two additional proteins; Xrs2p and Rad50p, collectively called the MRX complex. This complex is known to have many distinct roles within DSB processing in all cell types. In meiotic cells, the MRX complex is firstly required for the creation of the Spo11p-DSB itself, as null mutants of any of the complex members are unable to produce Spo11p-DSBs (Moreau *et al.*, 2001), and secondly in the processing of the Spo11p-DSB. Specifically, it has been suggested that the MRX complex unwinds the ends of a DSB, thus providing a substrate for endonuclease activity of Mre11p to remove Spo11p form DSBs (Neale *et al.*, 2005).

Biochemical studies in other labs have previously shown that purified Mre11p exhibits 3′ to 5′ exonuclease activity and endonuclease activity *in vitro* (Furuse *et al.*, 1998; Trujillo *et al.*, 1998; Usui *et al.*, 1998; Tsubouchi and Ogawa, 2000). However, it is implicated in 5′-3′ resectioning of DNA duplex *in vivo* - the first step in the processing of a Spo11p-DSB. This is the wrong polarity if Mre11p were the major resectioning activity. It is more likely that Mre11p is involved in DSB resectioning by being targeted to the 5′ strand by an as yet unknown mechanism (Mirzoeva and Petrini, 2003; Lewis *et al.*, 2004).

Mre11p was an early candidate for the primary resectioning protein in DSB, mutations in any three of the phosphodiesterase domains abolish resectioning at Spo11p-DSBs during meiosis (Nairz and Klein, 1997; Moreau *et al.*, 1999). Studies at clean vegetative breaks, created by the HO-endonuclease, have suggested that Mre11p nuclease activity is not required for resectioning (Llorente

and Symington, 2004). In contrast to *mre11Δ* cells, strains homozygous for *MRE11* separation of function alleles contain WT levels of Spo11p-DSBs, but these breaks do not undergo resectioning and Spo11p remains covalently bound at the break site (Nairz and Klein, 1997; Moreau *et al.*, 1999). Both *MRE11* separation of function alleles used in this study are deficient for nuclease activity, although *mre11*-H125N is reported to form the MRX complex whilst *mre11*-58S apparently does not (Usui *et al.*, 1998; Moreau *et al.*, 1999; Krogh *et al.*, 2005).

EXO1 was also isolated as a highly expressed cDNA that was found to suppress the DNA repair deficiency of *rad50*Δ (Tishkoff *et al.*, 1997). Overexpression of *EXO1* increased the resistance of *rad50*Δ, *mre11*Δ and *xrs2*Δ to ionising radiation or MMS, but not in other mutants defective for homologous recombination (*rad51,52,54,59*) or non-homologous end joining (non-homologous end joining; NHEJ) (Chamankhah *et al.*, 2000).

Exo1p has also been previously shown to be required for WT levels of meiotic crossing over and normal meiotic chromosome segregation, as *exo1Δ* cells were shown to exhibit a 2-fold reduction in crossing over (Symington *et al.*, 2000). Khazanehdari *et al.* have suggested that Exo1p plays a role in DNA resectioning as mutants display reduced levels of gene conversion at some, but not all loci – suggesting possible redundancy with one or more proteins (Khazanehdari and Borts, 2000).

Several observations suggest a certain degree of redundancy between *MRE11* and *EXO1*, however, there still is a large deal of uncertainty. In mitotic cells, Tsubouchi *et al.* have demonstrated that multiple copies of *EXO1* suppress the MMS sensitivity of *mre11*Δ cells and the double mutant *exo1*Δ*mre11*Δ exhibiting increased MMS sensitivity and more severe defects in processing of MMS-induced single-stranded DNA breaks than either single mutant, suggesting Exo1p and Mre11p function independently in DNA damage processing (Tsubouchi and Ogawa, 2000).

It is uncertain whether Mre11p nuclease activity is required for resectioning during repair of many DSBs, or whether the activity is limited to processing fewer,

aberrant DSBs. To answer this, Llorente and Symington (2002) analysed resectioning by ssDNA formation in cells subjected to several DSBs catalysed by HO, or phleomycin treatment, in mitotic cells. The authors found no difference between WT and *mre11*-D56N nuclease-deficient cells, suggesting that Mre11p nuclease activity is not required for extensive 5′ to 3′ resectioning of DSB, in mitotic cells. However, DSB processivity was effected by the number of DSBs, in a dose-dependent manner. Llorente *et al.*, (2004) postulate that the MMS sensitivity in *mre11* strains is due to an inability to process IR-induced DNA damage. *exo1Δ* cells were shown to exhibit reduced processivity of a singular HO-induced DSB, in mitotic cells.

SAE2 was identified from a screen that identified mutants lethal if DSB were formed, but viable if there were no DSBs within the genome (McKee and Kleckner, 1997; Prinz *et al.*, 1997). *sae2Δ* mutants are functional for the formation of DSB; however, the covalently bound Spo11p remains attached to the 5′ end of the DSB (Prinz *et al.*, 1997). As *sae2Δ* cells do not remove the covalently attached Spo11p from the break site, it is impossible to study any downstream roles directly at the Spo11p-break site.

The aim of this chapter is to further characterise the roles of the MRX complex, Exo1p and Sae2p during meiotic DSB repair, in particular during 5′ to 3′ resectioning of DNA. Repair kinetics of *arg4-VDE*, and formation of the deletion product was examined. Loss-of-restriction site assays were also implemented to characterise a detailed profile of resectioning at *arg4-VDE* in *mre11* and *exo1Δ* mutant cells. The use of the VDE reporter cassette allows the functions of MRX downstream of Spo11p-DSB formation and removal of Spo11p, to be elucidated, events not possible to study directly at Spo11p-DSBs.

6.2 Results

6.2.1 Sae2p influences the initiation but not the processivity of resectioning at the VDE-DSB, a site specific DSB that does not have associated covalently bound Spo11p

The number of Spo11p-DSBs present in cells can influence the turnover of the VDE-DSB *in trans*. *sae2Δ* cells exhibit a delay in the turnover of the VDE-DSB and this is independent of the proportion of cells that induce a DSB in the *arg4-VDE* allele (Neale *et al.*, and Chapter Three of this study). This delay in the repair of the VDE-DSB is apparent even though there is no covalently bound protein (which would possibly require Sae2p for its removal) at this break site.

This delay is in the initiation of resectioning in *sae2Δ* cells, and could be an indirect effect of accumulating unresected Spo11p-DSBs e.g. by the sequestration of resectioning complexes engaged in DNA repair at the 200 - 250 blocked Spo11p-DSBs (see Chapter 5). To test this hypothesis, a strain doubly mutant for *sae2Δ* and *spo11f* was constructed and the repair of the VDE-DSB was assessed. If the influence of Sae2p on VDE-DSB repair were an indirect affect of the accumulation of unresected Spo11p-DSBs, the repair in *sae2Δ* and *spo11f* cells would be identical to that of *spo11f* cells. If, on the other hand, Sae2p has a more direct role on resectioning at the VDE-DSB, then the repair in the *sae2Δspo11f* strain would be delayed in comparison with *spo11f* single mutants.

sae2Δspo11f cells show a delay in repair of VDE-DSB similar to _sae2Δ_ but deletion product formation similar to _spo11f_

The efficiency of cleavage at *arg4-VDE* was assessed in cells doubly mutant for *SAE2* and *SPO11*. Similar to all strains, over 95 % of *arg4-VDE* alleles had been cleaved (see figure 6.1).

Standard Southern analysis of *Spe*I-digested DNA, shows that there is a delay in the turnover of the VDE-DSB in *sae2Δspo11f* cells compared to *spo11f*. The relative increase in the height of the peak for *sae2Δ spo11f* cells is similar to that for *sae2Δ* cells in comparison with WT. In essence *sae2Δ* is epistatic to *spo11f*, with regards to the kinetics of the VDE-DSB (see figure 6.2). Repair of the VDE-

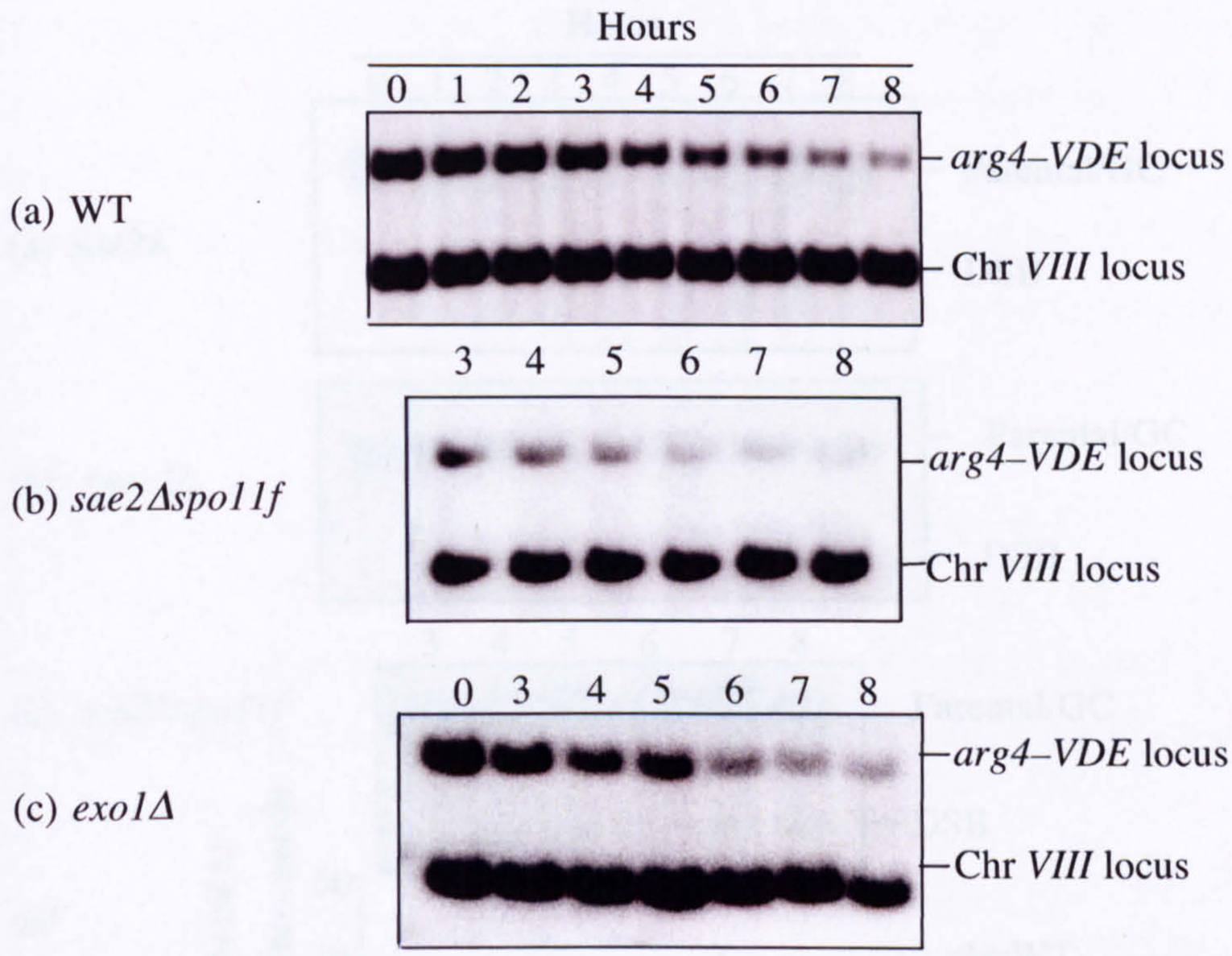

Figure 6.1: Physical analysis and quantification of *arg4–VDE* cleavage in WT, *sae2Δ* *spo11f* and *exo1Δ* cells. Southern analysis using *Bgl*II/*Eco*RV-digested meiotic time course DNA of (a) WT, (b) *sae2Δspo11f* and (c) *exo1Δ cells* and processed as for figure 3.4. WT data is shown for comparison. The scanned images have been cropped to show only the *arg4–VDE* and *arg4–nsp,bgl* (loading control) band. (d) The extent of VDE cleavage was similar in all three strains,

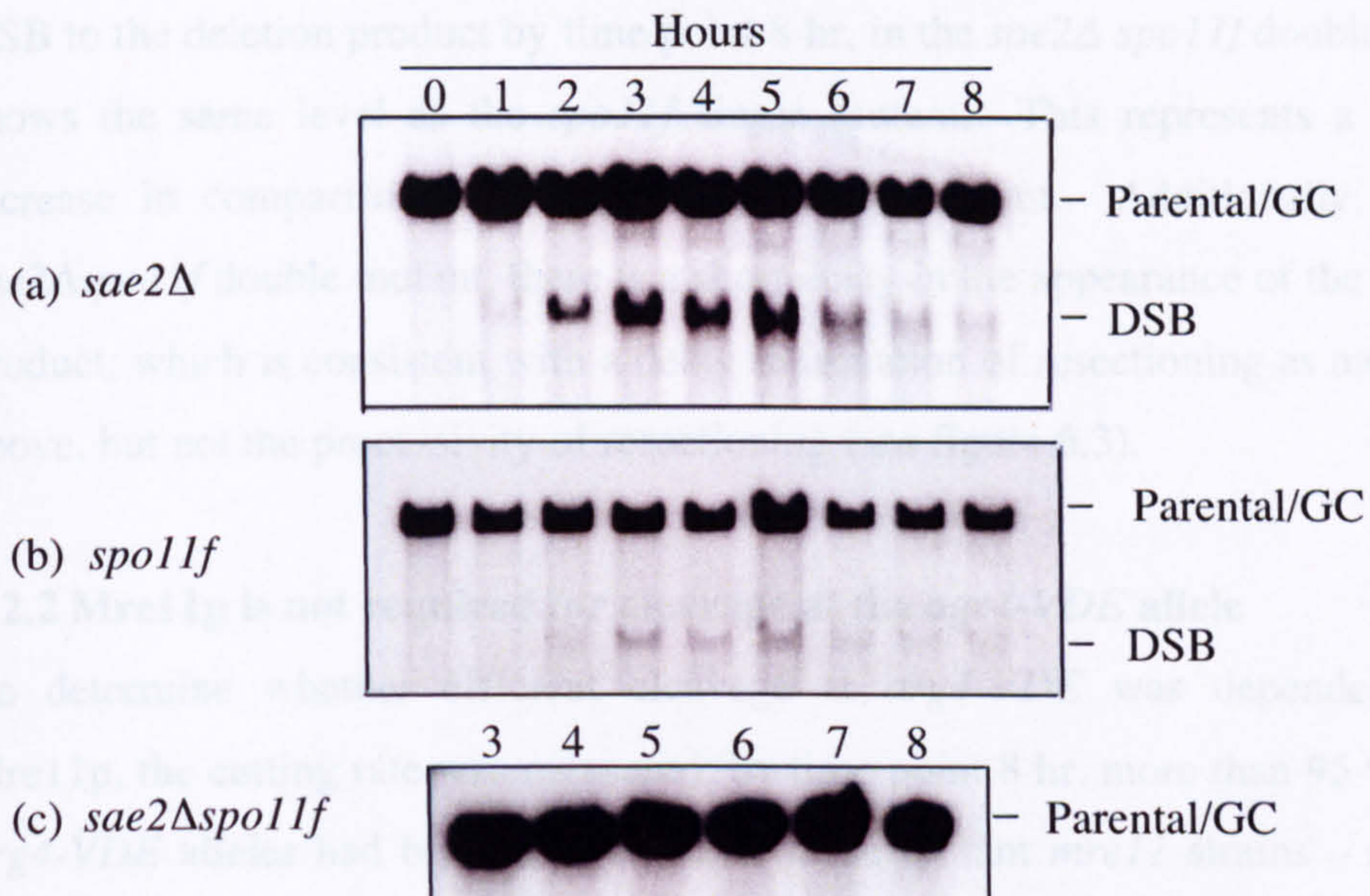

Figure 6.2: Physical analysis and quantification of the VDE–DSB in WT, *sae2Δ*, *spo11f* and *sae2Δspo11f* cells. Southern analysis using *Spe*I-digested meiotic time course DNA of (a) *sae2*, (b) *spo11f* and (c) *sae2Δspo11f* cells and processed as for figure 3.5. WT, *sae2Δ* and *spo11f* data was added for comparison (Chapter Three). Scanned images were cropped to show only Parental/GC and VDE-DSB bands. (d) The VDE-DSB band peaks to a greater maximum value in *sae2Δ* cells suggesting a delay in repair of the break. *sae2Δspo11f* cells show a delay in repair compared with *spo11f* cells, with the break peaking 2 hr later and reaching a greater maximum value.

DSB to the deletion product by time point 8 hr, in the *sae2Δ spo11f* double mutant shows the same level as the *spo11f* single mutant. This represents a 2.5-fold increase in comparison with the *sae2Δ* single mutant. Additionally, for the *sae2Δspo11f* double mutant, there is a short delay in the appearance of the deletion product, which is consistent with a delay in initiation of resectioning as mentioned above, but not the processivity of resectioning (see figure 6.3).

6.2.2 Mre11p is not required for cleavage at the *agr4-VDE* allele

To determine whether efficient cleavage at *arg4-VDE* was dependent upon Mre11p, the cutting rate was measured; by time point 8 hr, more than 95 % of the *arg4-VDE* alleles had been cleaved in all three mutant *mre11* strains – *mre11Δ*, *mre11*-58S and *mre11*-H125N (see figure 6.4).

6.2.3 Mre11p is involved in the initiation of resectioning at the VDE-DSB

The appearance of the VDE-DSB and its disappearance as it repairs varies from WT in all three *MRE11* mutant strains. For both *mre11Δ* and *mre11*-H125N cells, the VDE-DSB band peaks at a later time point than in WT cells, suggesting a delay in the repair of the break. Conversely, the VDE-DSB band in *mre11*-58S appears and disappears with similar kinetics to WT. For *mre11Δ* and *mre11*-H125N the prolonged appearance of the VDE-DSB and its delay in repair implies that they are less efficient at resectioning (see figure 6.5). By 8 hr all three *MRE11* mutant strains have more VDE-DSB left unrepaired than WT (see figure 6.6).

6.2.4 In *MRE11* mutants repair of the VDE-DSB to the deletion product is reduced

There is significantly less repair to form the deletion product, when calculated as a proportion of the *arg4-VDE* chromatids that have received a DSB. This reduced level of deletion product is consistent with a large proportion of VDE-DSB that remains unrepaired by time point 8 hr. There are three potential possibilities for why repair to the deletion product is reduced. Firstly, *MRE11* mutants fail to

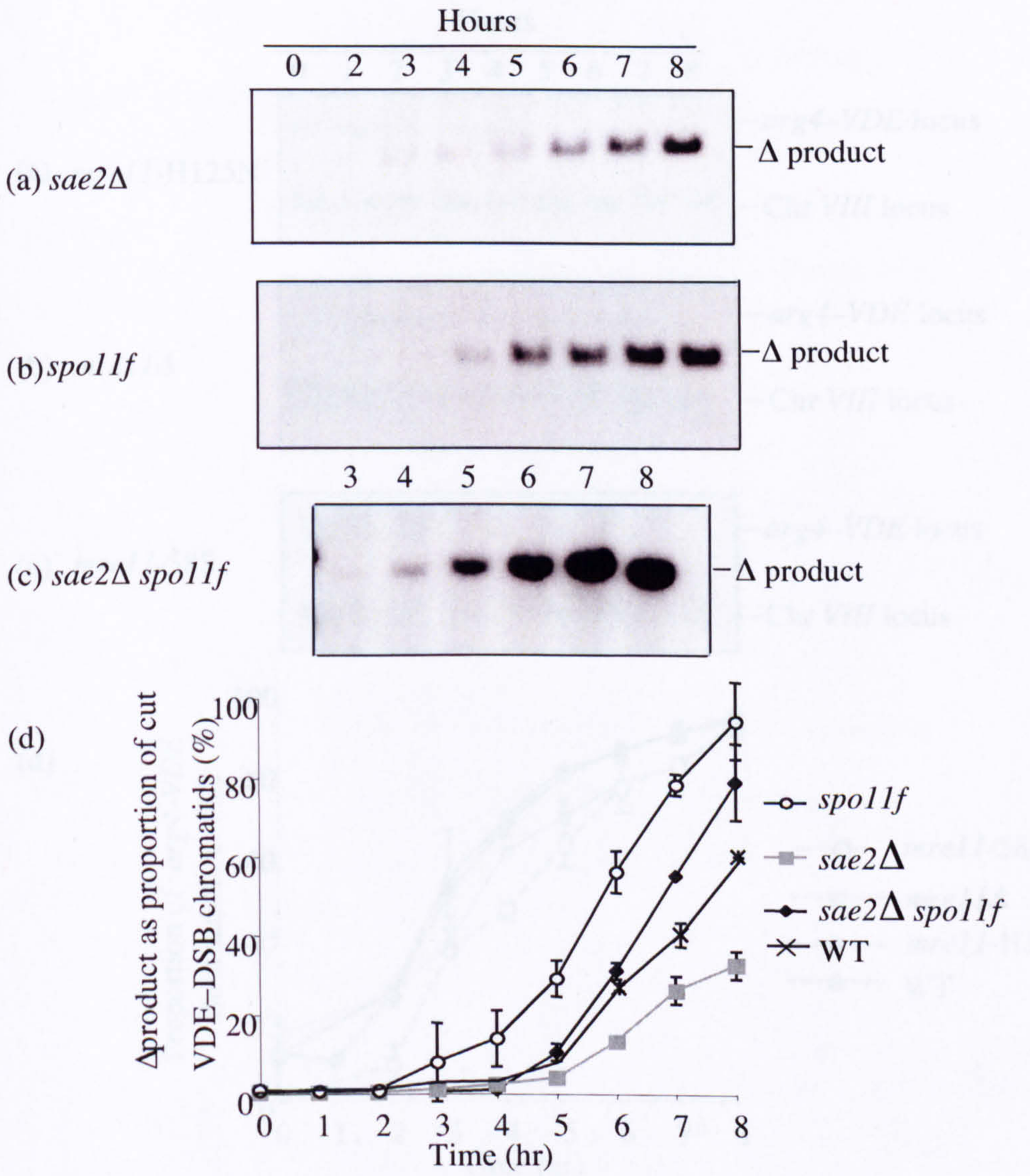

Figure 6.3: Physical analysis and quantification of deletion product formation in WT, *sae2Δ*, *spo11f* and *sae2Δspo11f* cells. Southern analysis using *Spe*I-digested meiotic time course DNA of (a) *sae2*Δ, (b) *spo11f* and (c) *sae2*Δ*spo11f* cells and processed as for figure 3.5. WT,, *sae2*Δ and *spo11f* data was added for comparison (Chapter Three). (d) *sae2Δ* cells delay repair of the VDE-DSBs to the deletion product from the *URA3* repeat regions. The amount of deletion product in the *sae2*Δ*spo11f* double mutant has levels similar to the *spo11f* single mutant.

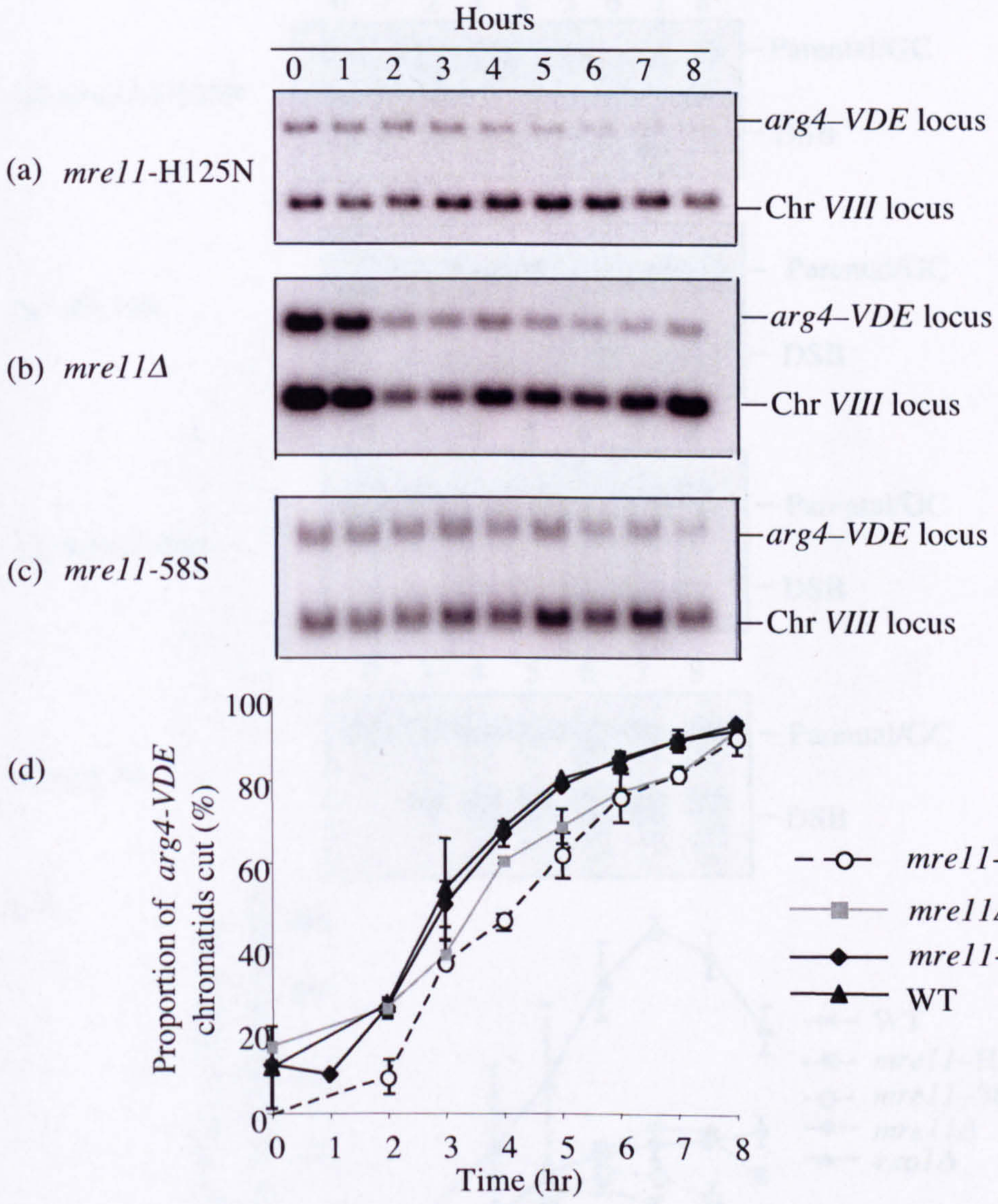

Figure 6.4: Physical analysis and quantification of *arg4–VDE* cleavage in WT, *mre11*-58S, *mre11Δ* and *mre11*-H125N cells. Southern analysis using *Spe*I-digested meiotic time course DNA of (a) *mre11*-H125N, (b) *mre11Δ* and (c) *mre11*-58S, and processed as for figure 3.4 . WT data was added for comparison. The scanned images have been cropped to show only the *arg4–VDE* and *arg4–nsp,bgl* (loading control) band. (d) The extent of VDE cleavage was similar in all four strains.

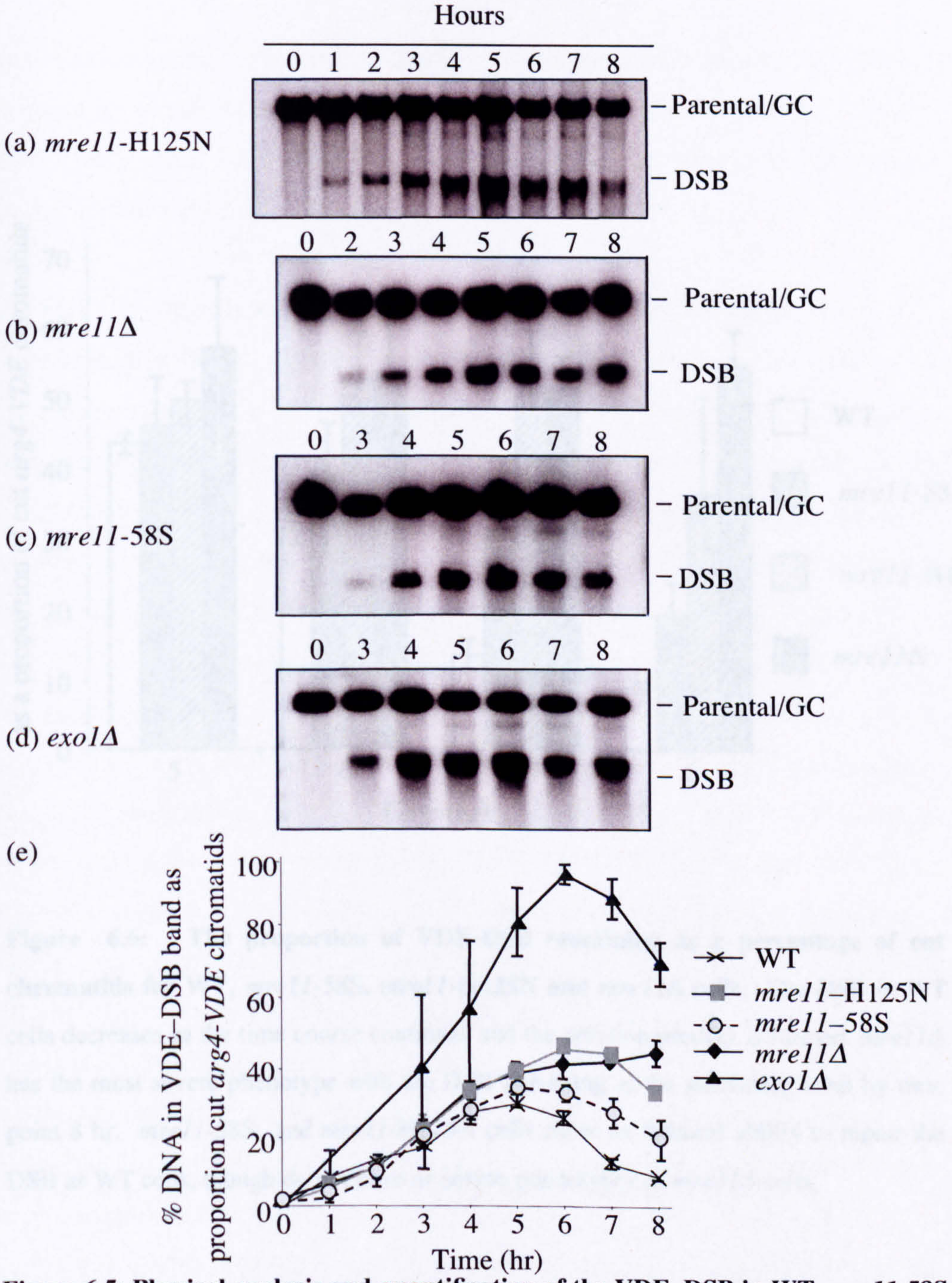

Figure 6.5: Physical analysis and quantification of the VDE–DSB in WT, *mre11*-58S, *mre11*Δ, *mre11*-H125N and *exo1*Δ cells. Southern analysis using *Bgl*II/*Eco*RV-digested meiotic time course DNA of (a) *mre11*-H125N (b) *mre11Δ* (c) *mre11*-58S and (d) *exo1Δ* cells and processed as for figure 3.5. WT data was added for comparison. Scanned images were cropped to only show Parental/GC and VDE-DSB bands. (e) *mre11Δ* and *mre11*-H125N cells show a delay in repair of the VDE-DSB, the *mre11*-58S allele has much less of an impact with near WT levels of VDE-DSB apparent, deleting *EXO1* causes a very strong block to repair.

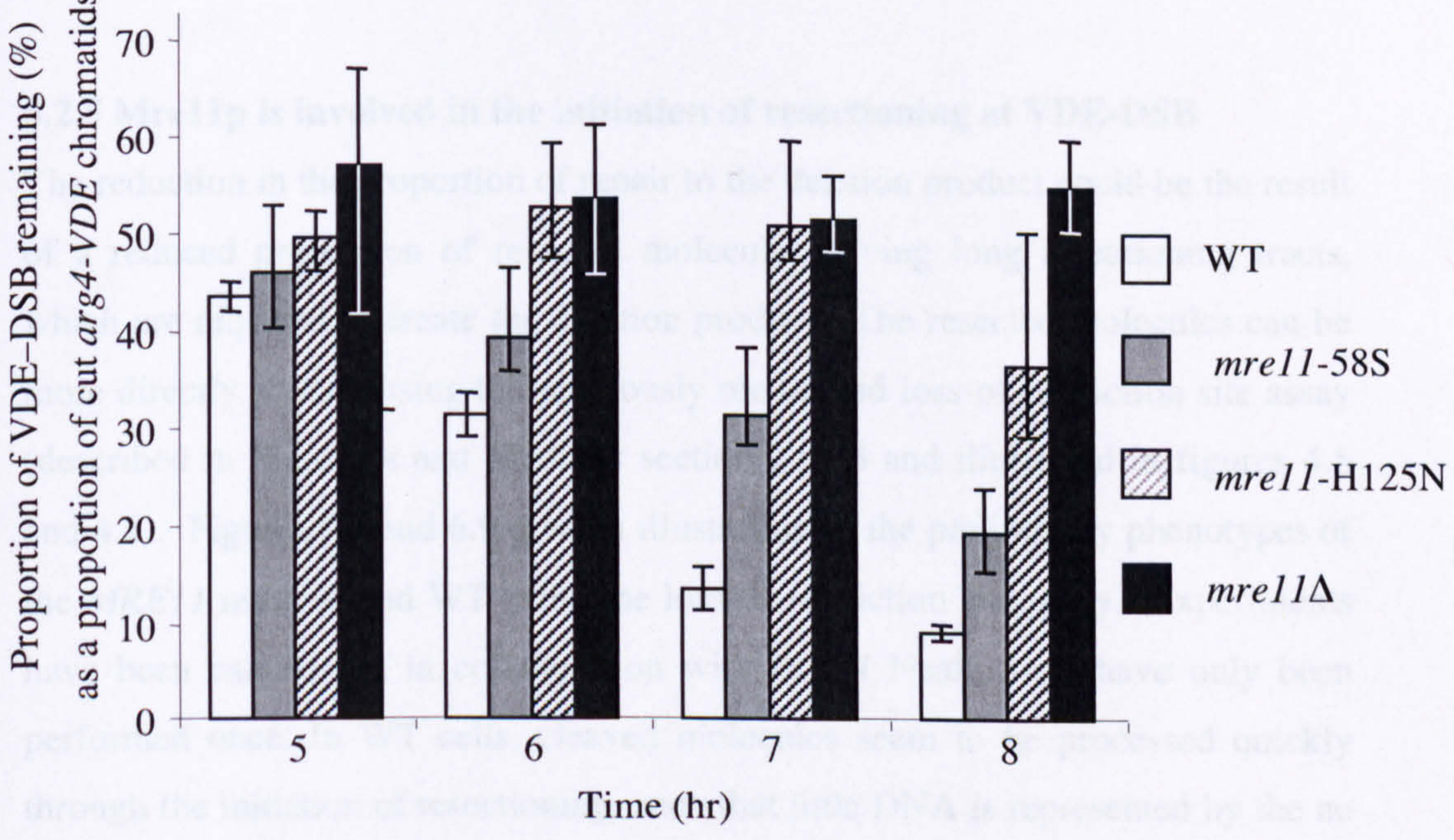

Figure 6.6: The proportion of VDE-DSB remaining as a percentage of cut chromatids for WT, *mre11*-58S, *mre11*-H125N and *mre11Δ* cells. The DSB in WT cells decreases as the time course continues and the deletion product is formed. *mre11Δ* has the most severe phenotype with the DSB persisting at the maximum level by time point 8 hr. *mre11*-58S and *mre11*-H125N cells show an reduced ability to repair the DSB as WT cells, though do not have as severe phenotypes as *mre11Δ* cells.

initiate resectioning. Secondly, *MRE11* mutants exhibit slower or reduced resectioning, which would prevent uncovering flanking repeat sequences. Thirdly, *MRE11* cells could be proficient at resectioning but are unable to convert the resected intermediates into the deletion product (see figure 6.7).

6.2.5 Mre11p is involved in the initiation of resectioning at VDE-DSB

The reduction in the proportion of repair to the deletion product could be the result of a reduced proportion of resected molecules having long resectioning tracts, which are required to create the deletion product. The resected molecules can be more directly studied using the previously mentioned loss-of-restriction site assay (described in Materials and Methods section 2.9.13 and illustrated in figures 4.5 and 4.6). Figures 6.8 and 6.9 give an illustration of the preliminary phenotypes of the *MRE11* mutants and WT using the loss-of-restriction site assay. Experiments have been carried out in collaboration with M.J.N Neale, they have only been performed once. In WT cells, cleaved molecules seem to be processed quickly through the initiation of resectioning, such that little DNA is represented by the no or very short resectioning bands (of 0–400 bases), at all time points (see figure 6.9). Molecules that have undergone 400 bases of resectioning can be removed from the quantified band either by repair to *arg4-bgl* or *ARG4* by gene conversion, or by further resectioning. Bands indicating resectioning up to 1.8 kb (short) and up to 3.6 kb (medium) accrue at 4 h and 6 h to higher levels; implying that at resectioning may slow down after the initial phase. Very small amounts of long (up to 8.5 kb) resectioning tract molecules are visible implying that resectioning speeds up again and/or the conversion to the deletion product it rapid.

In all three strains mutant for *MRE11,* there is a considerable increase in the proportion of DNA trapped in the band representing no, or very short resectioning (see figure 6.9). This observation supports the hypothesis that Mre11p has a role in establishing early resectioning at a VDE–DSB.

In *mre11Δ* cells the amount of deletion product appearing by 8 hr is ~ 30 % of that seen in WT cells (see figure 6.9). Conversely, the amount of DNA detectable in

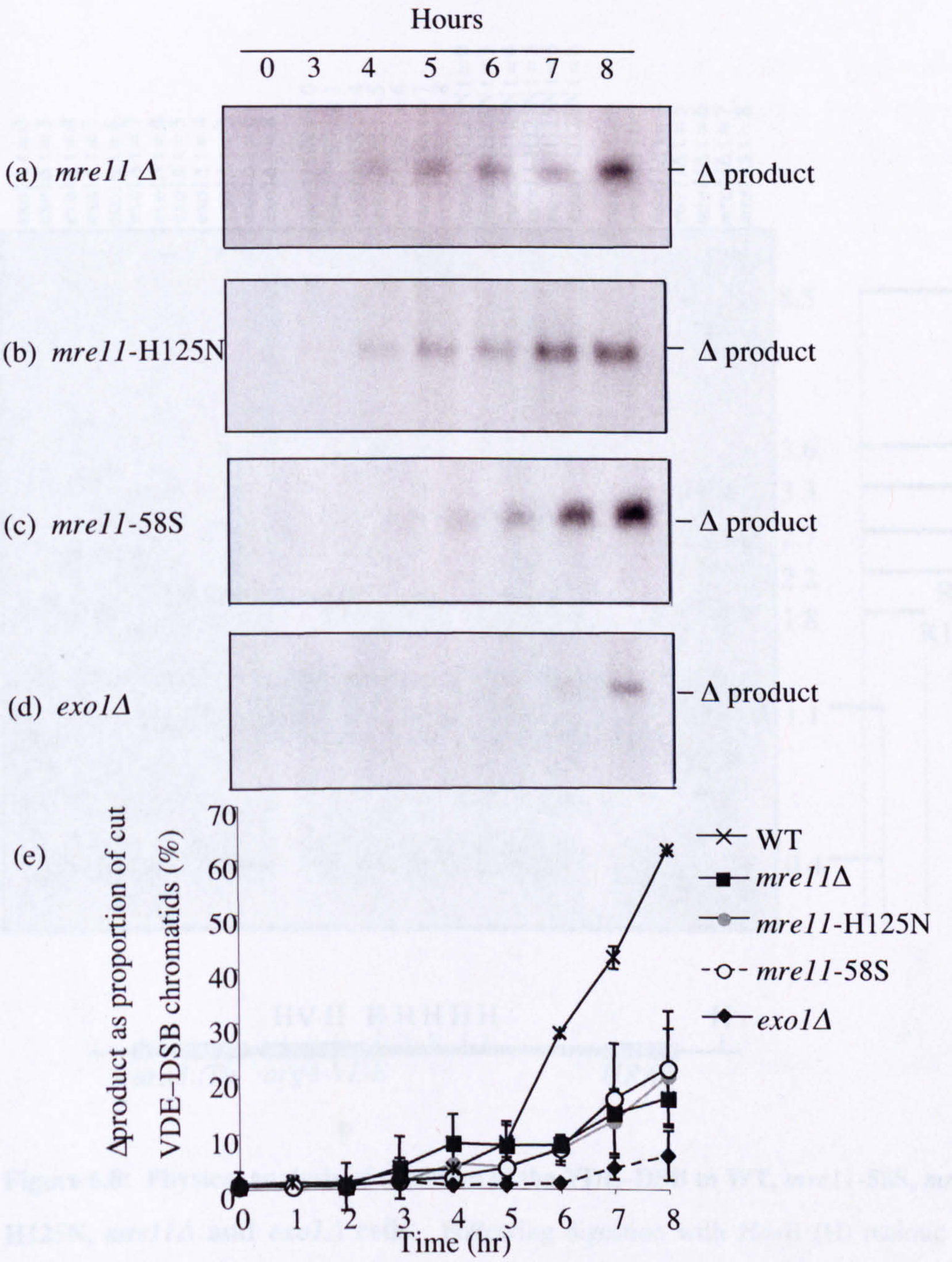

Figure 6.7: Physical analysis and quantification of deletion formation. in WT, *mre11*-58S, *mre11*-H125N, *mre11Δ* and *mre11Δ* cells. Southern analysis using *Spe*I-digested meiotic time course DNA of (a) *mre11*Δ (b) *mre11*-H125N (c) *mre11*-58S and (d) *exo1*Δ cells and processed as for figure 3.5. WT data was included for comparison. Scanned images were cropped to show only the deletion band. (e) All *mre11* and *exo1Δ* mutant strains show a reduced level of deletion product formation in comparison to WT.

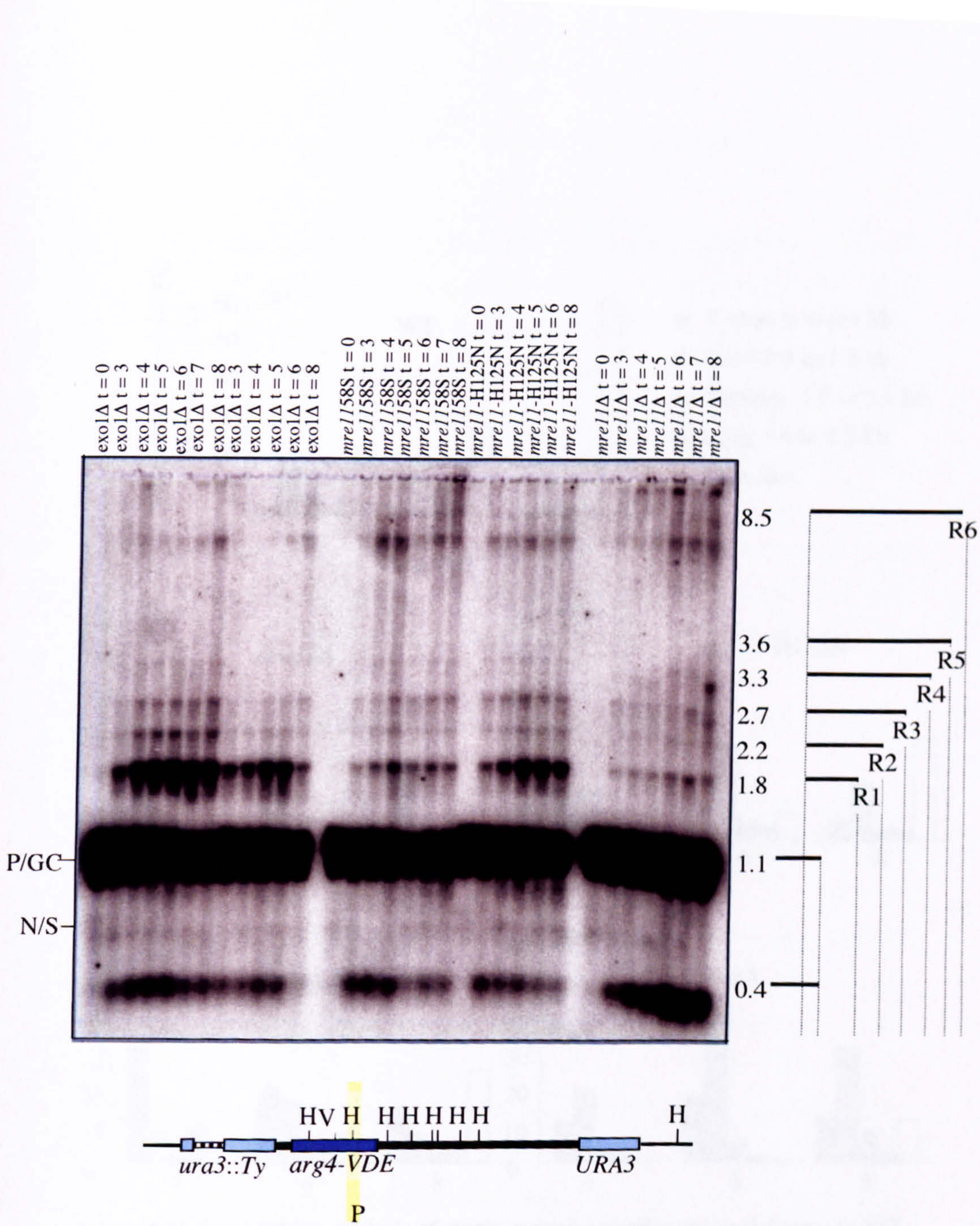

Figure 6.8: Physical analysis of resection at the VDE–DSB in WT, *mre11*-58S, *mre11*-H125N, *mre11Δ* and *exo1Δ* cells. Following digestion with *Hae*II (H) meiotic time course DNA was fractionated in an alkaline 0.7 % agarose gel and hybridised with (P) a ssDNA probe specific to the 3´–end of the unresected strand. (N/S) non–specific hybridisation. P/GC DNA representing parental and gene conversion DNA. R1 – R6 bands correspond to the sequential loss of *Hae*II cleavage at sites downstream of the (V) VDE–DSB were detected at later time points. Such bands indicate the passage of single–stranded resection through an earlier *Hae*II site. This work was carried out in collaboration with M. J. Neale.

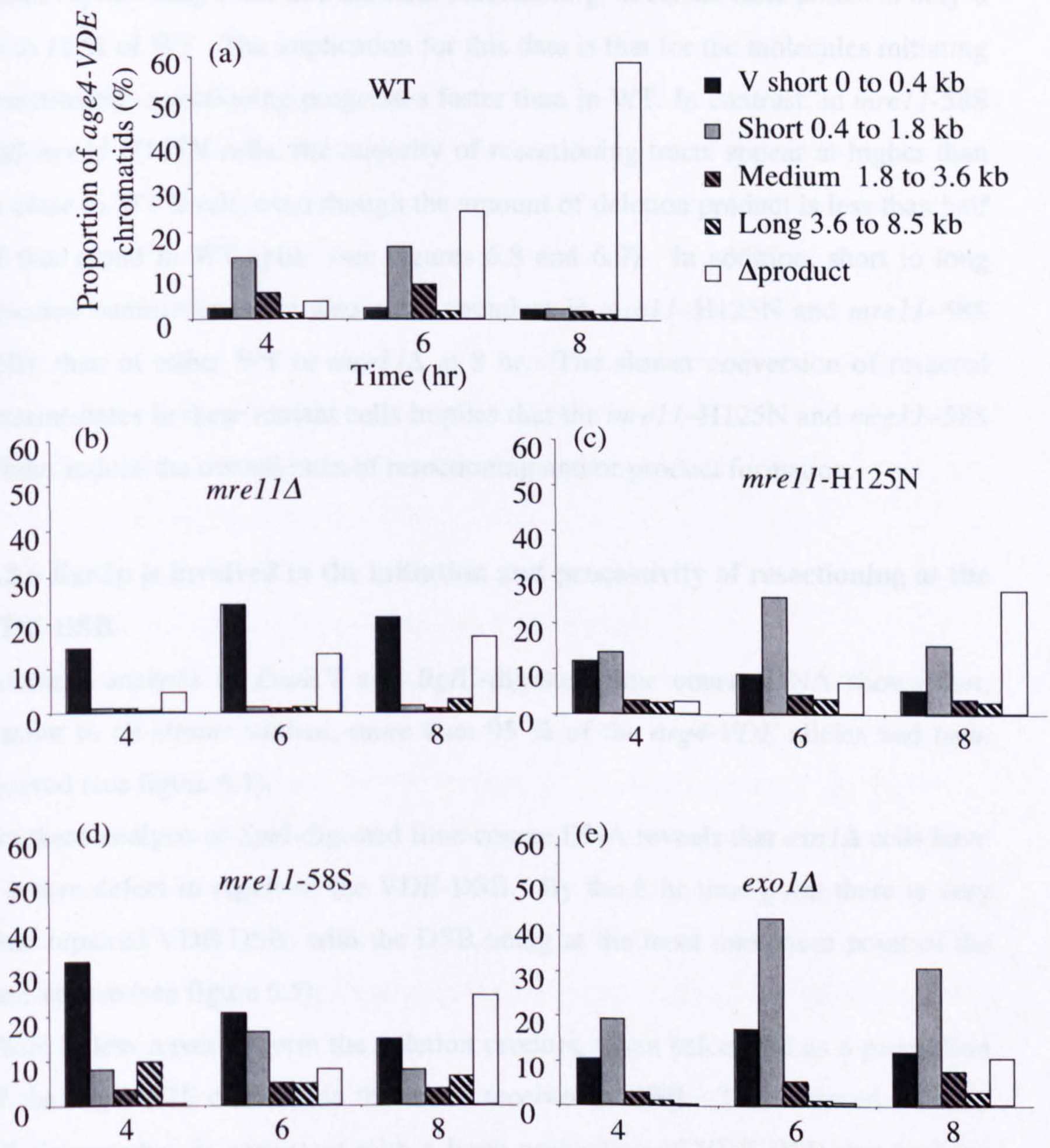

Figure 6.9: Comparative analysis of single–strand resection intermediates in WT, *mre11Δ*, *mre11*-H125N, *mre11*-58s and *exo1Δ* cells. DNA was extracted from a synchronous meiotic cultures of (a) WT, (b) *mre11Δ* , (c) *mre11*-H125N, (d) *mre11*-58S and (e) *exo1Δ* cells, and processed as for Figure 4.6. Scanning densitometry was used to determine the amount of probe hybridising to the resectioning bands representing; very short, short, medium and long resection tracts, and the deletion product, at 4 hr, 6 hr, and 8 hr of meiosis when signals were strongest. Data is expressed as the proportion of signal in the specific resection bands, relative to the total DNA present in the lane. This work was carried out in collaboration with M.J. Neale.

bands representing short and medium resectioning, at earlier time points is only 6 % to 11 % of WT. The implication for this data is that for the molecules initiating resectioning, resectioning progresses faster than in WT. In contrast, in *mre11*-58S and *mre11*-H125N cells, the majority of resectioning tracts appear at higher than or close to WT levels, even though the amount of deletion product is less than half of that found in WT cells (see figures 6.8 and 6.9). In addition, short to long resected intermediates are also more abundant in *mre11*–H125N and *mre11*–58S cells, than in either WT or *mre11*Δ at 8 hr. The slower conversion of resected intermediates in these mutant cells implies that the *mre11*–H125N and *mre11*–58S alleles reduce the overall rates of resectioning and/or product formation.

6.2.6 Exo1p is involved in the initiation and processivity of resectioning at the VDE-DSB

Southern analysis of *Eco*RV and *Bgl*II-digested time course DNA shows that, similar to all strains studied, more than 95 % of the *arg4-VDE* alleles had been cleaved (see figure 6.1).

Southern analysis of *Spe*I-digested time course DNA reveals that *exo1Δ* cells have a severe defect in repair of the VDE-DSB. By the 8 hr time point there is very little repaired VDE-DSB, with the DSB being at the most maximum point of the time course (see figure 6.5).

There is less repair to form the deletion product, when calculated as a proportion of the *arg4-VDE* chromatids that have received a DSB. This reduced level of deletion product is consistent with a large proportion of VDE-DSB that remains unrepaired by time point 8 hr. This reduced level of repair to deletion product could be the result of a deficiency in resectioning of DNA or an inability to repair the resected molecules to form the deletion product. However, this is unlikely as the VDE-DSB repair profile indicates that the majority of the VDE-DSB persists by time point 8 hr (see figure 6.7).

6.2.7 The profile of VDE-DSB shows an accumulation of resected intermediates

The appearance of the VDE-DSB is markedly different in *exo1Δ* cells than in WT cells. A profile of radioisotope signal intensity through the VDE-DSB can be used to assess the proportion of accumulating DSB molecules that are resected. A perfectly symmetrical profile is expected if all molecules are of identical size. A shoulder on the right hand side of the peak, the lower molecular weight side, is indicative of active resected DNA. As figure 6.10 shows, there is a significant shoulder to the right hand side of the peak of the break, when the signal profile is plotted as a proportion of maximum, and when compared to WT. *exo1Δ* and WT data has been overlaid for ease of comparison.

6.2.8 Exo1p is required for progressive resectioning

The loss-of-restriction site assay was employed, as described in Materials and Methods section 2.9.13 and illustrated in figures 4.5 and 4.6, to determine the spectrum of resected intermediates formed in an *exo1Δ* mutant. As figure 6.9 illustrates, alike the *mre11Δ* cells, preliminary results reveal that *exo1Δ* cells accumulate significant amounts of DNA that has undergone either no or very little resectioning (0 to 0.4 kb of resectioning). Furthermore, there was a significant accumulation of DNA in the bands representing short tracts of resectioning (0.4 to 1.8 kb of resectioning). Interestingly, at time points 4 hr and 6 hr, there are WT levels of medium to long resectioning tract DNA, however, this DNA persist at this level up to time point 8 hr. In essence, the loss-of-restriction site data suggests that *exo1Δ* has a deficiency in the initiation of resectioning, but also, once started occurs at a slower rate that WT. Once again, there exists the possibility that *exo1Δ* strains exhibit a reduced ability to repair the resected molecules to form the deletion product. This data is reminiscent, but more severe than *mre11*-H125N and *mre11*-58S and correlates well the lack of deletion product in the *exo1Δ* strain.

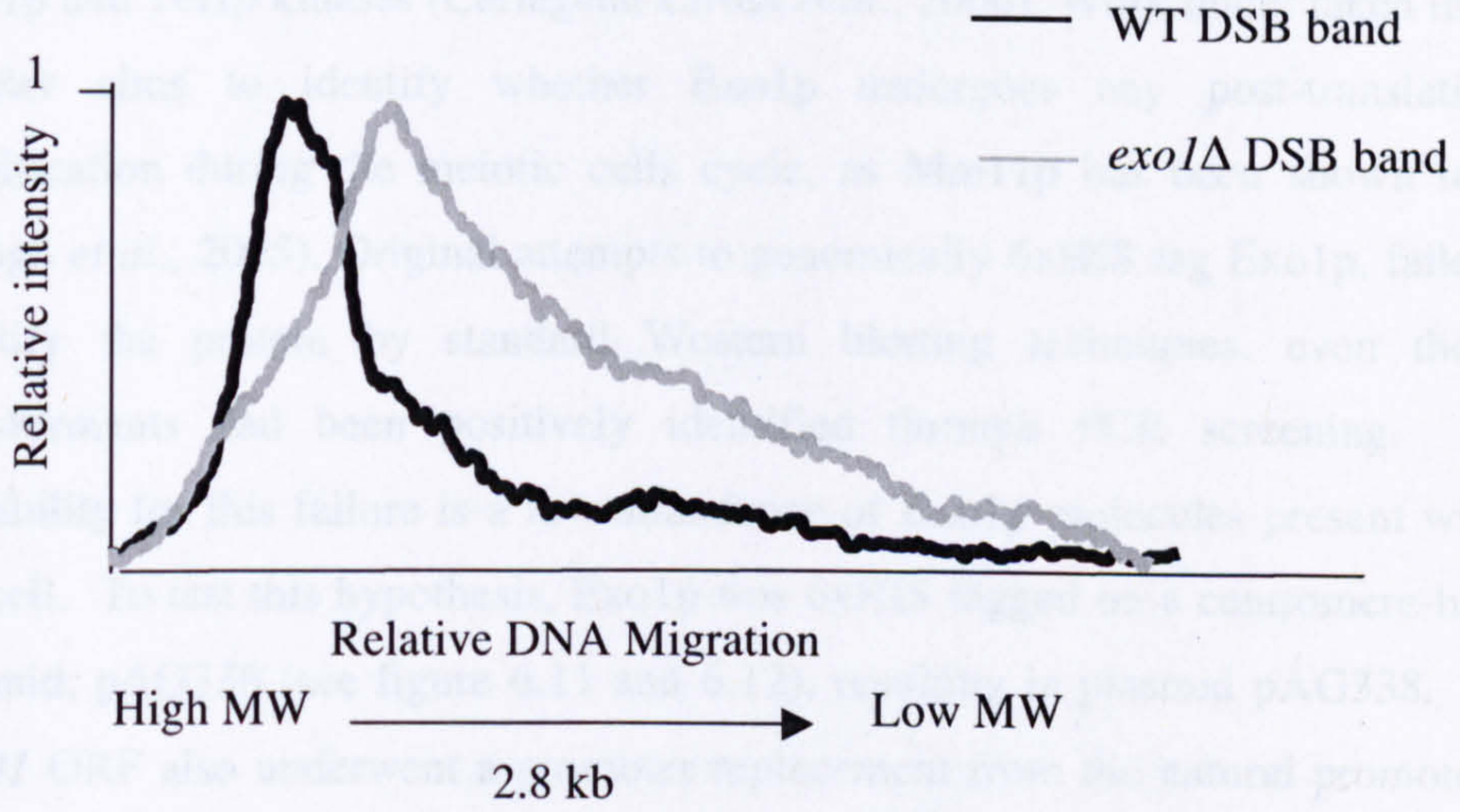

Figure 6.10: Signal Intensities of VDE-DSB bands in WT and *exo1Δ* cells. Profiles of signal intensities running through the VDE-DSB bands of WT and *exo1Δ* cells at t = 4 hr The curves are normalised to the maximum signal within the bands and stacked for comparison. The wide shoulder of the *exo1Δ* graph reflects smearing of the VDE-DSB, whilst the narrower (symmetrical) curve of WT reflects discrete VDE-DSB banding.

6.2.9 The creation of an Exo1p-6xHIS tagged strain

Many proteins undergo post-translational modifications during the meiotic cell cycle. One example of such a protein is Sae2p, which is phosphorylated by the Mec1p and Tel1p kinases (Cartagena-Lirola *et al.*, 2006). Work under taken in this chapter aims to identify whether Exo1p undergoes any post-translational modification during the meiotic cells cycle, as Mre11p has been shown to do (Krogh *et al.*, 2005). Original attempts to genomically 6xHIS tag Exo1p, failed to identify the protein by standard Western blotting techniques, even though transformants had been positively identified through PCR screening. One possibility for this failure is a low abundance of Exo1p molecules present within the cell. To test this hypothesis, Exo1p was 6xHIS tagged on a centromere-based plasmid, pAG336 (see figure 6.11 and 6.12), resulting in plasmid pAG338. The *EXO1* ORF also underwent a promoter replacement from the natural promoter to that of *MET25*, a highly expressed and regulable promoter. Transformants obtained were PCR screened and positive candidates were grown under *MET*-inducible conditions and checked by standard Western analysis. Five transformants were tested and a band present of the correct size, that was missing in the negative control, suggested Exo1p had been successfully tagged and promoter replaced (see figure 6.13). One positive transformant was selected and designated hAG1389. hAG1389 was mated with WT haploid hAG3, and the resulting diploid was termed dAG1432. Meiotic time courses were carried out on dAG1432, and protein samples were analysed by standard Western techniques (see figure 6.13). To determine whether Exo1p undergoes any phosphorylation events, Exo1p was immuno-precipitated from total cell extracts and treated with λ phosphatase. Samples with and without λ phosphatase treatment were analysed by standard Western techniques (see figure 6.13). Unfortunately, as figure 6.13 illustrates, Exo1p runs at the same weight as the IgG chain, masking identification of any phosphorylation modifications of Exo1p.

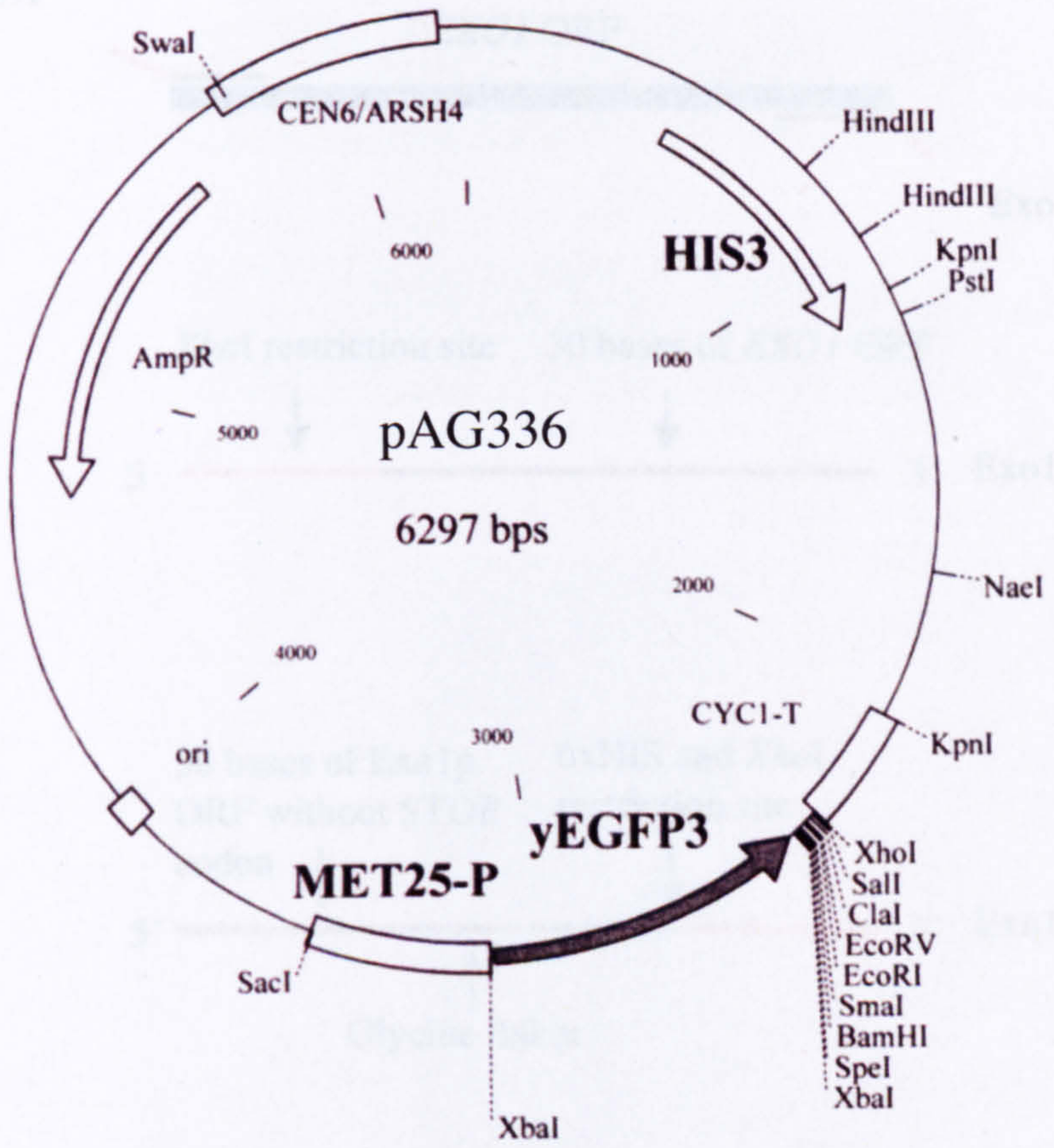

Figure 6.11: Map of plasmid pAG336. Schematic map of pAG336: a centromere based plasmid. The plasmid was digested with restriction sites *Xba*I and *Xho*I to remove the yEGFP3 fragment. Ligated in is the amplified *EXO1* ORF with additional 6xHIS fragment. This results in 6xHIS tagged Exo1p being expressed under the highly active *MET25* promoter, Exo1p-6xHIS is expressed when Methionine is not present in the media. This plasmid is transformed into hAG407, resulting in hAG1389.

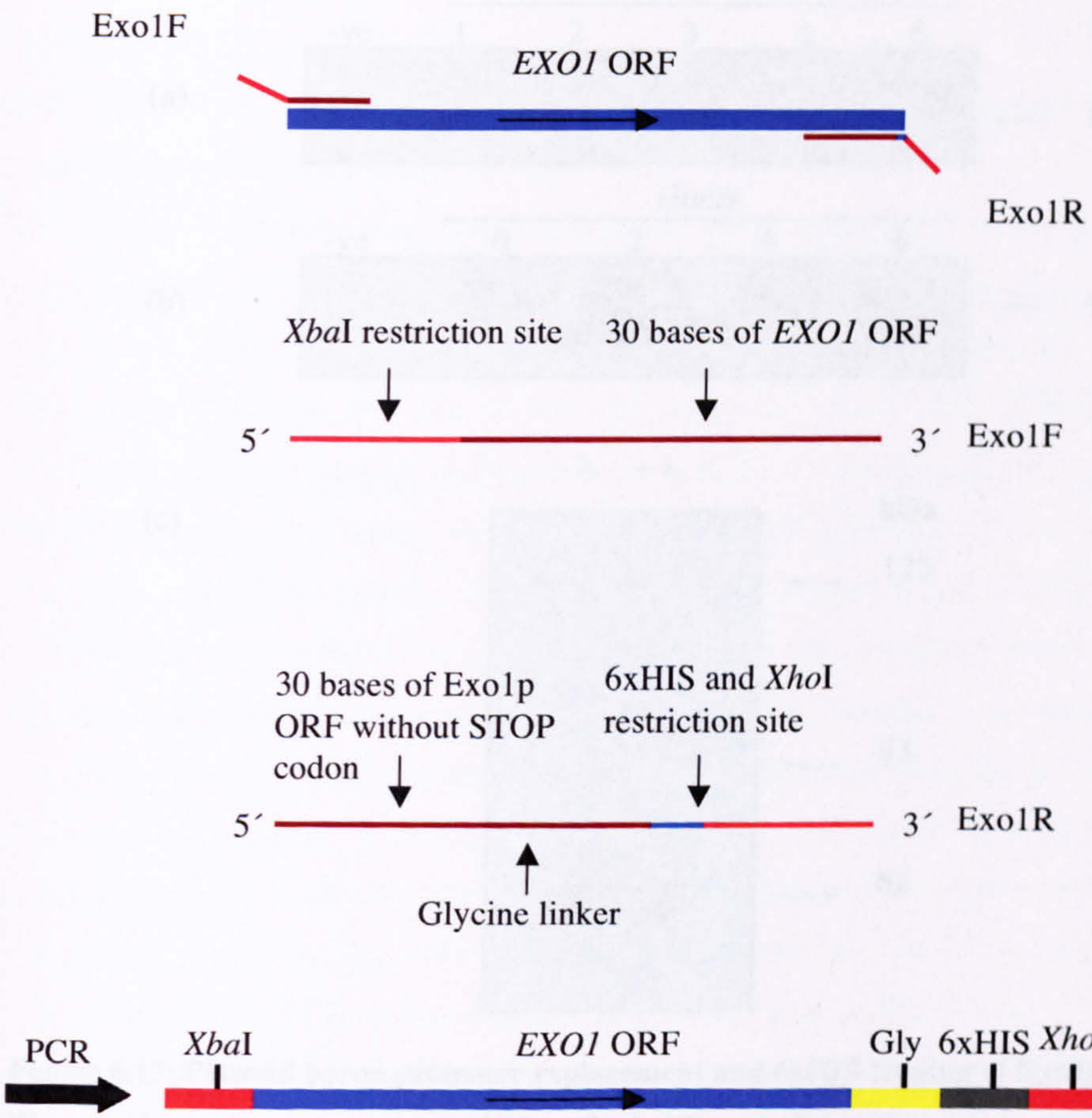

Figure 6.12: Schematic representation of 6xHIS tagging of Exo1p. Schematic representation of the plasmid based 6xHIS tagging of Exo1p. The forward primer, Exo1F, contains additional bases to create an *Xba*I site, which will be complementary with the digested plasmid the fragment is to be ligated into. Following this, there are 30 bases of homology initiating with the START codon of *EXO1* ORF. The reverse plasmid contains the final 30 bases of the *EXO1* ORF without the STOP codon. This is followed by a glycine linker then six Histidine codons, finally there were additional bases added on to create an *Xho*I restrcition site which will be complementary with the digested plasmid.

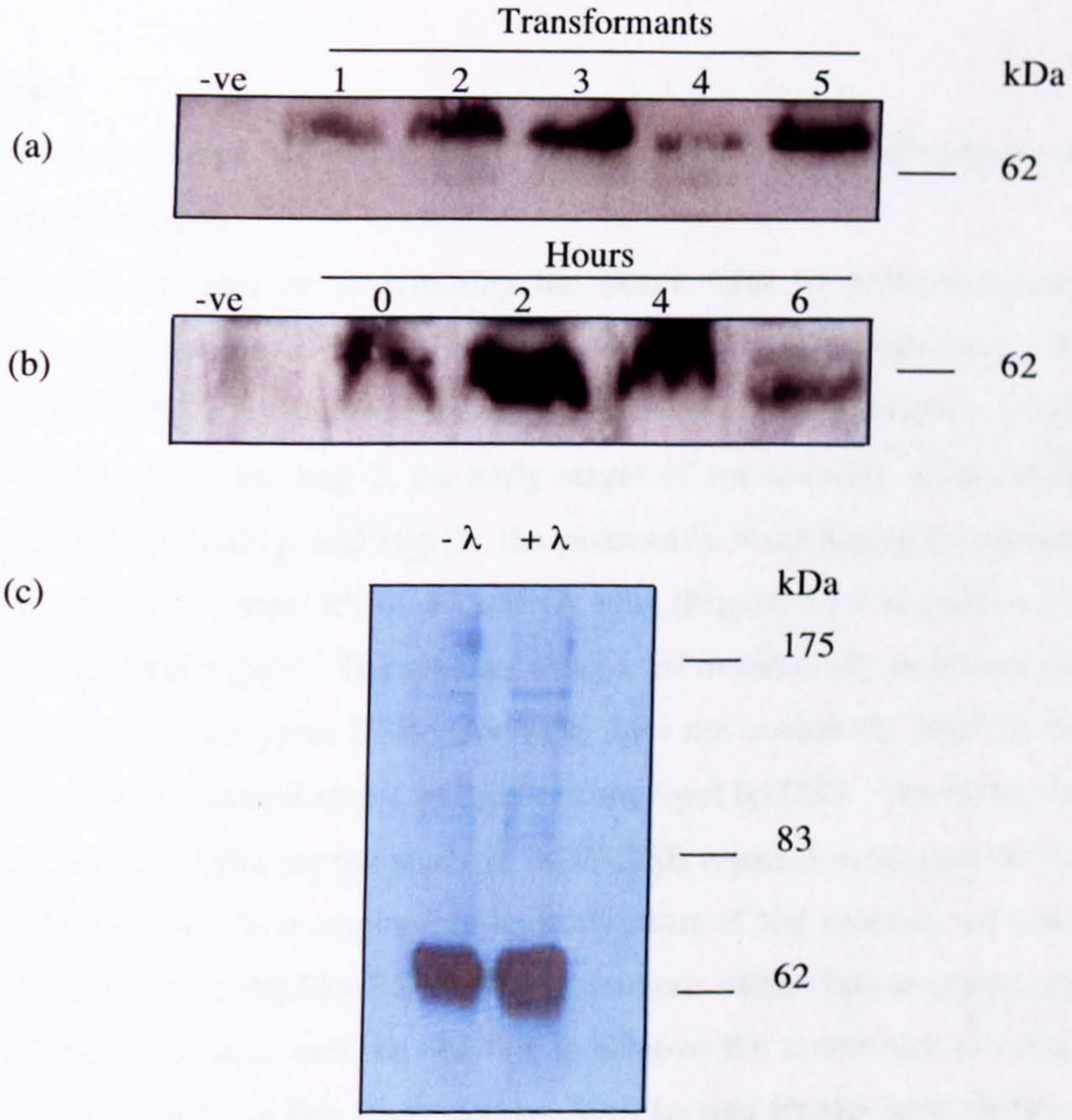

Figure 6.13: Plasmid borne promoter replacement and 6xHIS tagging of Exo1p. (a) A Western blot against α-mouse tetra HIS antibody (Sigma) of negative control (WT) and 5 candidate transformants. A band was detected in the candidate strains of the appropriate size (Exo1p is ~ 80 kDa) which was not present in the negative control lane. (b) Meiotic time course of Exo1p-6xHIS strain. The image has been cropped to show only the band representing the tagged protein. (c) Immunoprecipitation using anti α-mouse tetra His antibody. The Exo1p-6xHIS runs, with and without λ phosphatase treatment, at the same size as the IgG chain, making visualisation of the protein impossible.

6.3 Discussion

6.3.1 The three steps of VDE-DSB repair and the involvement of recombination proteins

This chapter has centered on determining the direct roles of proteins already implicated in resectioning of DNA DSBs. There are three distinct steps during the repair of a Spo11p-DSB, as follows: step 1; the removal of the covalently bound Spo11p from the break site, step 2; the early stages of resectioning immediately after the removal of Spo11p and step 3; the processive resectioning to provide extensive, if necessary, many kb of 3′ ssDNA tails (Figure 6.14 illustrates the three steps during DSB repair). The reporter assay used in this study examines the repair of a Spo11p independent DSB. As VDE does not covalently bind to the DNA the assay cannot address step 1 of repair of the Spo11p-DSB. However, the assay does provide a model for the study of VDE-DSB repair downstream of the removal of the Spo11p. It is impossible to study most of the mutants we have employed directly at the Spo11p-DSB as these mutants either fail to create the DSB in the first place (e.g. *mre11Δ*) or fail to remove the covalently attached Spo11p (e.g. *mre11*-58S). In this study, Sae2p, Mre11p, and Exo1p have all been found to have influences on the initiation of resectioning at VDE-DSB and the subsequent processing of the break site.

6.3.2 Sae2p is involved in the initiation of resectioning

sae2Δ has been previously shown and re-examined in this study, to reduce the overall rate of resectioning at VDE-DSB during meiosis (Neale *et al.*, 2002). One possibility is that the large number of unprocessed Spo11p-DSBs in *sae2Δ* cells sequesters away resectioning apparatus, reducing the amount of resectioning at the VDE-DSB. This study has shown that the *sae2Δ* delay in VDE-DSB is not dependent upon the presence of accumulating Spo11p-DSBs. Thus, Sae2p has a genuine role in initiation of resectioning at the VDE-DSB, step two in the above model of DSB repair, and hence a role downstream of its established involvement in the removal Spo11p. The impact of removing Sae2p function does not appear

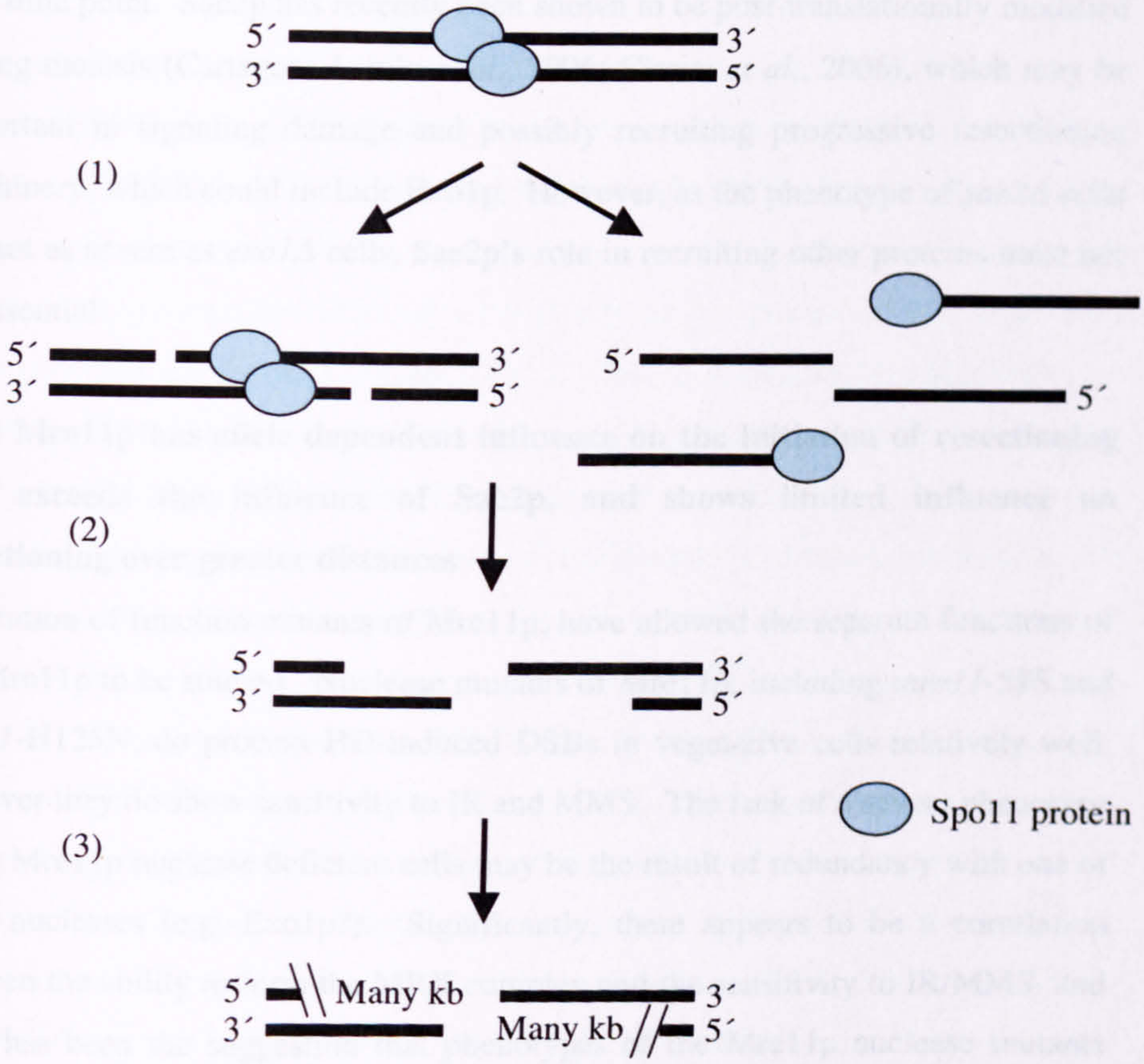

Figure 6.14: The three stages of resection at a Spo11p-DSB. The three steps of DNA resectioning during meiosis are proposed. As Spo11p binds covalently to the break site, the first step of resectioning creates a 'protein free' substrate for nuclease activity, this step is not required at the VDE-DSB as VDE does not covalently bind to the break site. Step1 at the Spo11p-DSB liberates Spo11p covalently attached to an oligonucleotide. Step 2 involves resectioning over a few hundred bases of DNA, usually sufficient tracts of ssDNA to initiate recombination. Step 3, longer tracts of resectioning can arise, covering many kb. Step 3 is required to repair the VDE-DSB to the deletion product.

to have a severe effect upon the cell as the majority of the DSB are repaired by the 8 hr time point. Sae2p has recently been shown to be post-translationally modified during meiosis (Cartagena-Lirola *et al.*, 2006; Clerici *et al.*, 2006), which may be important in signaling damage and possibly recruiting progressive resectioning machinery, which could include Exo1p. However, as the phenotype of *sae2Δ* cells are not as severe as *exo1Δ* cells, Sae2p's role in recruiting other proteins must not be essential.

6.3.3 Mre11p has allele dependent influence on the initiation of resectioning that exceeds the influence of Sae2p, and shows limited influence on resectioning over greater distances

Separation of function mutants of Mre11p, have allowed the separate functions of the Mre11p to be studied. Nuclease mutants of Mre11p, including *mre11*-58S and *mre11*-H125N, do process HO-induced DSBs in vegetative cells relatively well, however they do show sensitivity to IR and MMS. The lack of a severe phenotype in the Mre11p nuclease deficient cells may be the result of redundancy with one or more nucleases (e.g. Exo1p?). Significantly, there appears to be a correlation between the ability to form the MRX complex and the sensitivity to IR/MMS, and there has been the suggestion that phenotypes of the Mre11p nuclease mutants reflects an inability to form the MRX complex, rather than the lack of nuclease activity.

This study has shown that the main role for Mre11p is an early one, step two of the DSB model proposed in figure 6.14. A large proportion of VDE-DSBs remain unrepaired in *mre11Δ*, *mre11*-H125N and less so for *mre11*-58S, suggesting that initiation of resectioning can occur through at least two routes, one of which in Mre11p independent. When Mre11p is absent it appears possible that the VDE-DSBs that can repair are not hindered for long resectioning tracts and may even repair faster than in WT. The evidence for this is the lack of accumulation of bands representing the short to long resectioning tracts in the loss-of-restriction site assay. This observation could be due to the absence of Spo11p-DSBs. It may

also be possible that Mre11p acts as a negative regulator of very long resectioning tracts, possibly by promoting repair (Paull and Gellert, 2000).

In is interesting to note that this study has shown a more severe phenotype for the *mre11*-H125N allele, which is phosphorylated, compared to the *mre11*-58S allele, which is not (M. Khisroon Unpub. and Krogh *et al.*, 2005). Worthy of note is that the phosphorylation of Mre11p is normally associated with the presence of DSBs blocked by a chemical adduct or a covalently bound protein. Usui *et al.* have suggested that the phospho-modification of Mre11p is required for Mre11p to act on blocked DSBs. This study raises the possibility that this modification may be inhibitory to Mre11p function at clean DSBs (Usui *et al.*, 2001).

According to Usui and Krogh the *mre11*-H125N allele is complex forming and the *mre11*-58S allele is not (Tsubouchi and Ogawa, 1998; Usui *et al.*, 1998; Moreau *et al.*, 1999; Moreau *et al.*, 2001; Krogh *et al.*, 2005). This correlates well with the effect of the respective alleles on IR/MMS sensitivity. The less severe phenotype of *mre11*-58S with respect to repair of the VDE-DSB raises the possibility that Mre11p has important function outside of the MRX complex or that analyses of complex formation by immuno-precipitation are not fully representative of the *in vivo* situation. For example, *mre11*-58S may make sufficient MRX complex *in vivo* to handle the VDE-DSB but not enough to reliably act on a genome wide basis in the presence of IR or MMS. An additional possibility is that the dysfunctional MRX complex formed in an *mre11*-H125N mutant has a negative impact on resectioning by blocking recruitment of alternative, functioning repair machinery to the break site. There also exists the possibility that Mre11p has roles outside the context of the MRX complex, and in an *mre11*-H125N allele all of the Mre11p is recruited to a non-functioning MRX complex – inhibiting MRX independent roles of Mre11p.

6.3.4 *mre11*-H125N results suggest a different role for Mre11p in repair of Meiotic versus Mitotic DSB repair

Moreau and colleagues demonstrated in their 1999 and 2001 publications that *mre11*-H125N cells show an accumulation of unprocessed Spo11p-DSBs in meiosis (Moreau *et al.*, 1999; Moreau *et al.*, 2001). This is consistent with other work that suggests Mre11p is required for the removal of the covalently bound Spo11 protein from the break site. In a mitotic study, Moreau *et al.*, have demonstrated that HO-induced DSB repair in *mre11*-H125N cells showed no difference from WT cells. In this chapter it has been shown that *mre11*-H125N cells show a severe phenotype at the VDE-DSB, with a significant inability to repair the DSB. This apparent contradiction suggests that the repair of meiotic and mitotic DSB do vary, and in particular, the role of Mre11p is not the same in both situations.

6.3.5 Exo1p is involved in the initiation of resectioning and in the processivity

In vitro studies have shown that Exo1p possess 5´ to 3´ nuclease activity and so it has been implicated in resectioning. However, in the literature there are conflicting accounts about its involvement in resectioning with dramatically varying severities of phenotypes. The *exo1Δ* mutant showed an extremely severe phenotype with respect to the repair of the VDE-DSB, and the loss-of-restriction site assay showed a lack of molecules with no or very short resectioning tracts, indicative of a contribution to both the initiation of resectioning and to the processive progression of resectioning.

6.3.6 A second, hemizygous VDE reporter cassette, provides support for proposed role of Exo1p identified in this chapter

The hemizygous reporter cassette contains a large region in common with the *arg4-VDE* cassette used in this study, including the immediate context of the VDE-DSB. The homologous chromosome contains a delete region, preventing repair of the VDE-DSB by an inter-homologue mechanism. Repair can occur via

SSA using either proximal or distal repeat regions, resulting in deletion product $_{proximal}$ or deletion product $_{distal}$ respectively, as figure 6.15 illustrates. By comparing the proportion of repair products that are deletion product $_{proximal}$ versus deletion product $_{distal}$ it is possible to look at the influence of candidate genes on resectioning tract length.

Data to support Exo1p's involvement in initiation of resectioning and in the processivity comes from the hemizygous cassette, with very little repair of VDE-DSB occurring. Of the VDE-DSB that is repaired, very little deletion product $_{distal}$ is formed, consistent with a defect in 5′ - 3′ resectioning.

A radioisotope signal intensity through the VDE-DSB of the hemizygous cassette was again employed to assess the proportion of accumulating DSB molecules that are resected. In *exo1Δ* cells the VDE-DSB of the hemizygous cassette appears with lower molecular weight discrete bands, implying that resectioning in this strain is significantly hindered and that there are relatively specific pause sights. This data is consistent with Exo1p being required for WT levels of 5′ - 3′ resectioning (see figure 6.16 A. Bishop-Bailey. Unpub.).

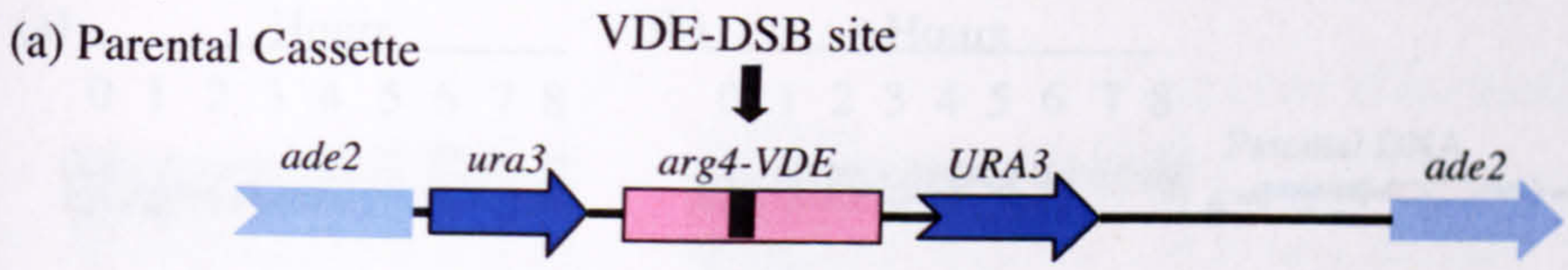

Figure 6.15: Hemizygous *arg4-VDE* reporter cassette and associated deletion products (a) Parental cassette DNA, containing the *arg4–VDE* allele (pink box; black box denotes VDE recognition sequence), flanked proximally by *URA3* and *ura3* direct repeated sequences (dark blue arrows), and distally by *ade2* direct repeated sequences (light blue (part) arrows). When VDE-endonuclease cleaves the *arg4-VDE* allele, the VDE-DSB can be repaired via SSA deletion repair by the generation of: (b) Resectioning tracts of length 2.5kb and 2.5kb (**5kb** total), that uncover the proximal *URA3* repeated sequences, creating first deletion product. (c) Resectioning tracts of length 7kb and 3.5kb (**10.5kb** total), that uncover the distal *ade2* repeated sequences, creating second deletion product.

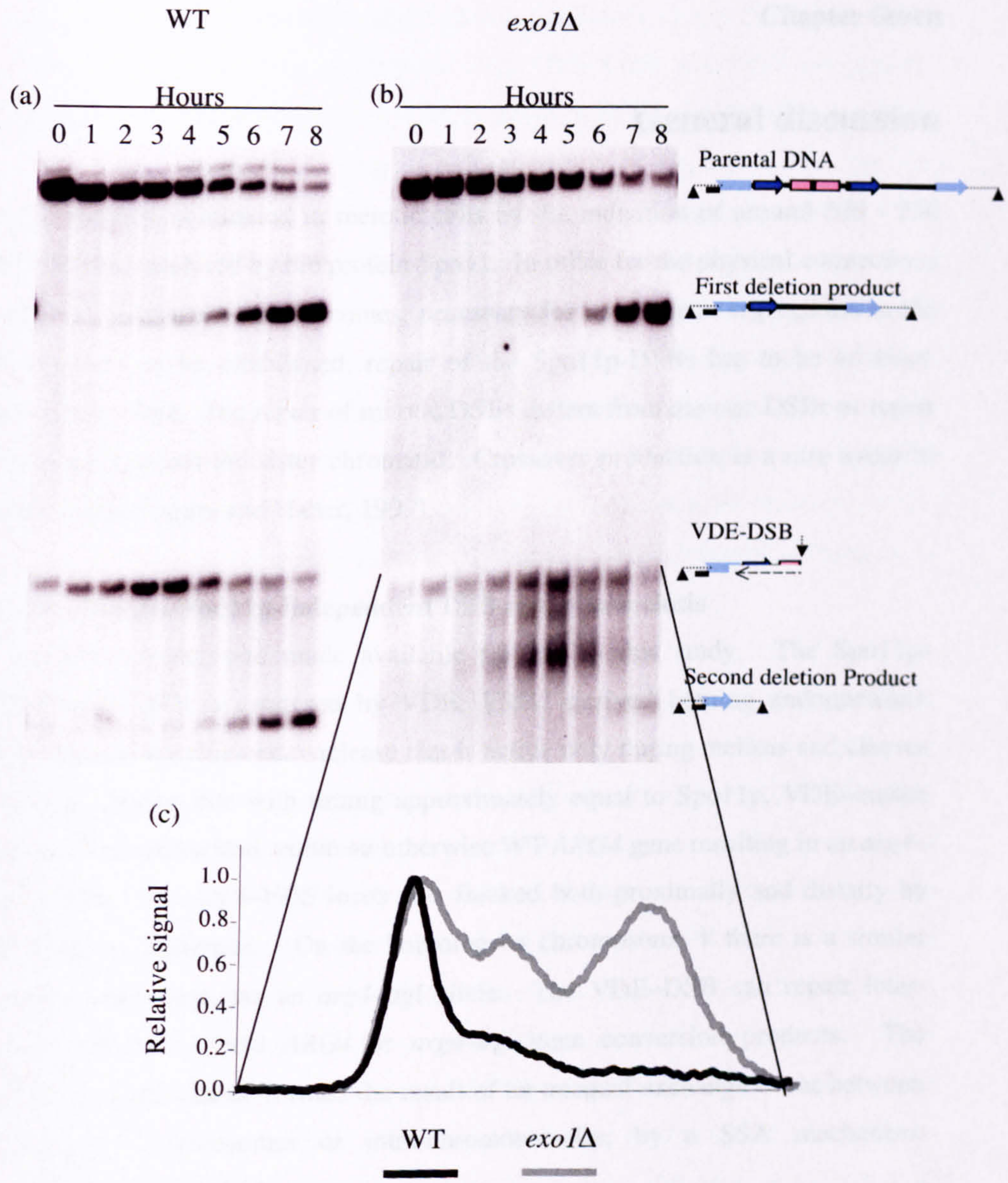

Figure 6.16: Physical analysis of VDE-DSB of hemizygous cassette in WT and *exo1Δ* cells. Physical analysis of VDE-DSB formation and repair to the deletion products in (a) WT and (b) *exo1Δ* cells. (c) A comparison of the radioisotope profile through VDE-DSB of the hemizygous VDE cassette of WT and *exo1Δ*. In *exo1Δ* cells the VDE-DSB of the hemizygous cassette appears with lower molecular weight discrete bands, implying that resectioning in this strain is significantly hindered and that there are relatively specific pause sights. This data is consistent with Exo1p being required for WT levels of 5´ - 3´ resectioning. This data is courtesy of A. Bishop-Bailey, Unpub.

Chapter Seven

General discussion

Recombination is initiated in meiotic cells by the induction of around 200 - 250 DNA DSBs, catalysed by the protein Spo11. In order for the physical connections between homologous chromosomes, necessary for appropriate segregation at the MI division, to be established, repair of the Spo11p-DSBs has to be an inter-homologue event. The repair of mitotic DSBs differs from meiotic DSBs as repair is directed towards the sister chromatid. Crossover production is a rare event in mitotic cells (Paques and Haber, 1999).

7.1 An assay for Spo11p-independent DSB repair in meiosis

A reporter cassette was made available for use in this study. The Spo11p-independent DSB is catalysed by VDE; *VMA1* derived homing endonuclease. VDE is a site–specific endonuclease that is active only during meiosis and cleaves at the recognition site with timing approximately equal to Spo11p. VDE–cutsite sequences are embedded within an otherwise WT *ARG4* gene resulting in an *arg4–VDE* allele. The *arg4–VDE* locus was flanked both proximally and distally by *URA3* repeat sequences. On the homologous chromosome *V* there is a similar cassette, which contains an *arg4–bgl* allele. The VDE–DSB can repair inter-chromosomally to yield *ARG4* or *arg4–bgl* gene conversion products. The deletion product, can be formed the result of an unequal exchange event between homologous chromosomes or intra-chromosomally, by a SSA mechanism involving flanking *URA3* repeats.

7.2 Repeating the work of Neale *et al.*, 2002, confirms that the number of Spo11p-DSBs within a cells influences meiotic DSB *in trans*

The original study carried out by Neale *et al.*, (2002) was repeated on finding that the Kodak Phosphor Screens have to be scanned by the BioRad Personal FX

imager in the dark as the white light dis-proportionally blanks the Southern blot, effectively reducing the quantity of the VDE-DSB and deletion product. Repeating the work of Neale *et al.*, (2002) whilst scanning the phosphor screens in the dark, has confirmed the original findings that the number of Spo11p-DSBs present within a cell, can influence repair of a Spo11p-independent break, VDE-DSB. The trends between WT and mutant strains remained the same as the original study, but the numerical values were altered. *spo11f* and *hop1Δ* cells were found to repair the VDE-DSB to the deletion product significantly more frequently than in WT cells. Furthermore, in *spo11f* and *hop1Δ* cells the turnover of the VDE-DSB peaked to lower levels and peaked earlier than in WT. This modification of repair at the VDE-DSB seen in cells with no (*spo11f*) or few (*hop1Δ*) Spo11p-DSBs is believed to be due to extensive hyper-resectioning at the break site.

7.3 Sae2p has a *bone fide* role in initiation of resectioning but not processivity at VDE-DSB

Repair of the VDE-DSB is delayed in *sae2Δ* cells even though the VDE-DSB does not have a covalently attached Spo11 protein at the break site (Sae2p's primary role in meiotic DSB repair to date has been in the removal of Spo11p from the break site). The delay in repair of the VDE-DSB in *sae2Δ* cells could be an indirect effect of sequestration of repair machinery to the alternative Spo11p-DSBs present elsewhere through out the genome. To test this theory, a strain doubly mutant for *SAE2* and *SPO11* was created. There is a delay in the repair of the VDE-DSB in *sae2Δspo11f* cells with respect to the turnover of the break not found in *spo11f* cells. This suggests that Sae2p has a *bone fide* role in initiation of resectioning, which is not dependent upon the number of Spo11p-DSBs present within the cell. The impact of removing Sae2p function does not appear to have a severe effect upon the cell as the majority of the DSB are repaired by the 8 hr time point. Sae2p has recently been shown to be post-translationally modified during meiosis (Cartagena-Lirola *et al.*, 2006; Clerici *et al.*, 2006), which may be

important in signaling damage and possibly recruiting progressive resectioning machinery, which could include Exo1p. However, as the phenotype of *sae2Δ* cells are not as severe as *exo1Δ* cells, Sae2p's role in recruiting other proteins must not be essential and may have redundancy with an alternative recruiting protein or may be through a different route.

7.4 Mek1p is a negative regulator of resectioning at *arg4-VDE*

This study has presented data that suggests Mek1p acts as a negative regulator of resectioning, as in its absence, resectioning at the VDE-DSB is increased. One possibility is that this function of Mek1p is required to enable inter-homologue recombination to be promoted, reducing resectioning at a meiotic DSB to allow the search for homology to proceed. This could be an additional mechanism to promote inter-homologue repair than the one recently proposed by Wan and colleagues, which implicated Mek1p in blocking inter-sister repair (Wan, de los Santo *et al.*, 2004; Niu, Wan *et al.*, 2005). More specifically, this thesis has identified that the kinase activity of Mek1p is required for the negative regulation of resectioning at VDE-DSB, presumably through the phosphorylation of an as yet unknown target(s) Indeed, evidence in the literature supports the hypothesis that Mek1p is a negative regulator of resectioning. It has been shown by Schwacha, Xu, and co-workers that loss of *MEK1* (or *RED1)* can reduce the presence of Spo11p-DSBs up to 4-fold and furthermore, can enforce recombination down a Dmc1p independent route (Schwacha and Kleckner, 1997; Xu *et al.*, 1997; Hubscher *et al.*, 2000). However, following further research, it was discovered that *mek1Δ* cells do not form fewer Spo11p-DSBs, instead, the breaks in question appear to be resected at a greater rate than in WT, so much so that the apparent number of breaks appears significantly reduced. Evidence for this comes from studies with *mek1rad50S* (*rad50S* cells have blocked break ends, which cannot be resected) cells, which show WT levels (Xu *et al.*, 1997).

7.5 *dmc1Δ* cells prevent repair of the VDE-DSB, even though the break can be repaired by a strand invasion independent mechanism

Repair of the VDE-DSB is prevented in *dmc1Δ* cells, even though the break can be repaired by SSA. This mechanism is independent of a strand invasion step, hence independent of Dmc1p. Three possibilities were tested to account for this Dmc1p-dependency. Firstly, there was the possibility that the pachytene arrest found in *dmc1Δ* cells was responsible for the block of repair at VDE. *NDT80*, a transcription factor required for exit from pachytene stage of meiosis, was mutated to see if this prevented repair of the VDE-DSB. *ndt80Δ* cells were found to repair the VDE-DSB as WT, suggesting that the pachytene arrest in *dmc1Δ* cells was not responsible for the block of repair. A *dmc1Δpch2Δ* double mutant was also created, *PCH2* is required for the pachytene arrest of meiotic cells; mutating *pch2Δ* relieves the pachytene arrest of *dmc1Δ* cells. The *pch2Δdmc1Δ* double mutant did not fully restore repair of the VDE-DSB, again suggesting that the block of repair found in *dmc1Δ* cells is not dependent upon progression of the cell cycle.

Secondly, the possibility existed that Dmc1p had a direct influence on repair of the VDE-DSB, to test this possibility *dmc1Δ* cells were made doubly mutant with genes implicated in meiotic DSB repair. When *dmc1Δ* mutation was coupled with mutations in *SPO11*, *SAE2*, *HOP1* and *MEK1*, the *dmc1Δ* block of VDE-DSB repair was abolished. These observations led to the proposal of a Dmc1p-dependent pathway for repair of a meiotic DSB. The pathway proposed that for the establishment of this Dmc1p-dependent repair; firstly, there have to be Spo11p-DSBs present within the genome, albeit the break in question is Spo11p-independent. The VDE-DSB then has to be processed by Sae2p, again even though the VDE-DSB does not have a covalently attached protein that has to be removed. Finally, the Dmc1p-dependency is then mediated through the Mek1p complex, a complex already implicated by others in directing repair of meiotic DSBs towards the homologue (Niu *et al.*, 2005).

A third possibility is that the block of repair in the *dmc1Δ* mutant was the result of sequestration of repair machinery to the approximately 200 - 250 Spo11p-DSBs, that have undergone extensive resectioning resulting in long tracts of ssDNA. A correlation was identified between block of repair at the VDE-DSB and extensive resectioning at Spo11p-DSBs. The mutations that relieve the *dmc1Δ* block also prevented long tracts of ssDNA being created within the cell. To test this hypothesis, ChIP was utilised to identify whether Rfa-1p, a protein involved in DSB repair in meiosis, was in limited supply in certain mutants.

7.6 RPA availability is a limiting factor in VDE-DSB repair

The enrichment of Rfa-1, a subunit of RPA, was found to be significantly increased at a Spo11p hotspot compared with a Spo11p coldspot in *dmc1Δ* cells. The same enrichment was significantly reduced in WT cells. The difference is believed to be the result of the extensive tracts of ssDNA found in *dmc1Δ* cells. The relationship at the VDE-DSB is reversed with increased enrichment of Rfa-1p close to the *URA3* repeat compared with the Spo11p coldspot, greater in WT than in *dmc1Δ* cells. This supports the hypothesis that the block of repair at the VDE-DSB in *dmc1Δ* cells is the result of sequestered repair machinery to the 200 - 250 hyper-resected Spo11p-DSBs present elsewhere in the genome. The identification that the presence of long tracts of ssDNA at Spo11p-DSBs can influence repair of the VDE-DSB *in trans* has many implications for research outside of this study. The pleiotropic effects of hyper-resectioning at Spo11p-DSBs have a significant impact on VDE-DSB repair. It is important to note that the phenotype of one mutant cannot always imply the exact function of the protein and instead could be the result of an altered biochemistry of the cell.

7.7 Mre11p is involved in initiation and processivity of resectioning at the VDE-DSB

Spo11p-DSB formation has an absolute necessity for Mre11p function. The involvement of Mre11p following Spo11p-DSB formation cannot be studied

directly at Spo11p-DSBs as they do not form in these cells. Examination of break repair at VDE-DSB therefore allows the downstream roles of Mre11p following Spo11p-DSB formation to be elucidated. Separation of function alleles of *MRE11* permit the formation of Spo11p-DSBs, however they remain unprocessed with covalently attached Spo11p at the break site. *mre11*-58S is a separation of function allele that permits the creation of Spo11p-DSBs, however, as a result of the mutation in the phosphodiesterase domain, the protein has lost its nuclease activity. Furthermore, *mre11*-58S has lost the ability to form the MRX complex (Usui *et al.*, 1998). A second *MRE11* separation of function allele is *mre11*-H125N, which again has lost nuclease activity, but is able to form the MRX complex (Usui *et al.*, 1998; Moreau *et al.*, 1999; Krogh *et al.*, 2005). The *mre11Δ* null mutant shows a more severe phenotype of VDE-DSB repair than either separation of function alleles, with a large proportion of the break remaining unrepaired after 8 hr in meiosis. In accord with a defect in 5′ to 3′ resectioning of the VDE-DSB, very little break is converted to form the deletion product in *mre11Δ* cells. Additional support for an involvement in resectioning at the break site came from the loss-of-restriction site assay. *mre11Δ* cells were shown to have very little DNA present within the bands representing resected DNA, with DNA accumulating in the band representing molecules that have undergone no or little resectioning (less than 0.4 kb). Interestingly there is a lack of molecules that have undergone short to long tracts of resectioning, suggesting that molecules than can proceed beyond the initial stages have no defect in resectioning and can rapidly proceed to form the deletion product. It is feasible that Mre11p acts as a negative regulator of very long resectioning tracts, possibly by promoting repair (Paull and Gellert, 2000). The most severe phenotype of the separation of function alleles of *MRE11* is that of the phosphorylated allele, *mre11*-H125N. The phosphorylation of Mre11p has been suggested by others to be necessary for Mre11p to repair DSBs blocked by a chemical adduct or a covalently attached protein (Usui *et al.*, 2001a). Work in this study has led to the suggestion that this modification of Mre11p may actually hinder repair at the clean VDE-DSB. A

further possibility for the differing phenotypes of the *MRE11* separation of function alleles, stems from the ability to form the MRX complex. According to Usui and Krogh (1998; 2005) the *mre11*-H125N allele is complex forming and the *mre11*-58S allele is not. The less severe phenotype of *mre11*-58S with respect to repair of the VDE-DSB raises the possibility that Mre11p has important function outside of the MRX complex. A possibility is that the dysfunctional MRX complex formed in an *mre11*-H125N mutant has a negative impact on resectioning by blocking recruitment of alternative, functioning repair machinery to the break site. There also exists the possibility that Mre11p has roles outside the context of the MRX complex, and in an *mre11*-H125N allele all of the Mre11p is recruited to a non-functioning MRX complex – inhibiting MRX independent roles of Mre11p.

7.8 *mre11*-H125N results suggest a different role for Mre11p in repair of meiotic compared to mitotic DSB repair

Moreau and colleagues have shown that *mre11*-H125N cells show an accumulation of unprocessed Spo11p-DSBs in meiosis (Moreau *et al.*, 2001; Krogh *et al.*, 2005). This is consistent with other work that suggests Mre11p is required for the removal of the covalently bound Spo11p from the break site. However, Moreau *et al.*, have demonstrated that mitotic HO-induced DSB repair in *mre11*-H125N cells showed no difference from WT (Moreau *et al.*, 1999; Moreau *et al.*, 2001). This study has shown that *mre11*-H125N cells show a severe phenotype at the VDE-DSB, with a significant inability to repair the DSB. This apparent contradiction suggests that the repair of meiotic and mitotic DSB do vary, and in particular, the role of Mre11p is not the same in both situations. Furthermore, it supports the model that Mre11p has a role in meiotic DSB repair after the removal of Spo11p from the break site.

7.9 Exo1p is involved in initiation and processivity of resectioning at the VDE-DSB

Others have implicated Exo1p, in the 5´ to 3´ resectioning of DNA (Tishkoff *et al.*, 1997; Tran *et al.*, 2002; Tran *et al.*, 2004). However, in contradiction to the initial *in vitro* findings, there is confusion in the literature as to the involvement of Exo1p in meiotic DSB repair, with varying severities of phenotypes when mutated. The repair at VDE-DSB was the more severe of any *mre11* mutants, with very little repair of the break occurring. Consistent with little resectioning of DNA or repair, very little deletion product is formed in the *exo1Δ* cells. Studies of the loss-of-restriction site assay supports the lack of repair at the VDE-DSB, with significant amounts of DNA having undergone little or no resectioning. Furthermore, what DNA has undergone resectioning persists for longer than WT, suggesting that even when initiated, resectioning proceeds at a slower rate than WT. Exo1p may be the redundant exonuclease that resects meiotic DSBs in the absence of the MRX complex. The next logical step would be to examine repair of the VDE-DSB in an *mre11Δexo1Δ* mutant, where it would be expected that virtually no repair of VDE–DSB would occur.

7.10 Future Work and Further Directions

Creation of an *mre11Δexo1Δ* double mutant – under control of CLB2 promoter. This controllable promoter would allow the double mutant to grow well mitotically, allowing synchronous meiotic time courses to be performed. Is the double mutant phenotype exaggerated, implying separate roles during DSB repair?

Are there any post-translational modifications of Exo1p during meiosis? If so, does the phosphorylation status of Exo1p change when Mre11p is absent?

Employ the return to growth experiments using the reporter cassette to assess whether gene conversion is altered in *mre11* and *exo1Δ* mutant strains

Bibliography

Agarwal, S., and Roeder, G.S. (2000). Zip3 provides a link between recombination enzymes and synaptonemal complex proteins. Cell *102*, 245-255.

Allers, T., and Lichten, M. (2001a). Differential timing and control of non-crossover and crossover recombination during meiosis. Cell *106*, 47-57.

Allers, T., and Lichten, M. (2001b). Intermediates of yeast meiotic recombination contain heteroduplex DNA. Mol Cell *8*, 225-231.

Arbel, A., Zenvirth, D., and Simchen, G. (1999). Sister chromatid-based DNA repair is mediated by *RAD54*, not by *DMC1* or *TID1*. Embo J *18*, 2648-2658.

Bailis, J.M., and Roeder, G.S. (2000). Pachytene exit controlled by reversal of Mek1-dependent phosphorylation. Cell *101*, 211-221.

Baroni, E., Viscardi, V., Cartagena-Lirola, H., Lucchini, G., and Longhese, M.P. (2004). The functions of budding yeast Sae2 in the DNA damage response require Mec1- and Tel1-dependent phosphorylation. Mol Cell Biol *24*, 4151-4165.

Baudat, F., Manova, K., Yuen, J.P., Jasin, M., and Keeney, S. (2000). Chromosome synapsis defects and sexually dimorphic meiotic progression in mice lacking Spo11. Mol Cell *6*, 989-998.

Baudat, F., and Nicolas, A. (1997). Clustering of meiotic double-strand breaks on yeast chromosome *III*. Proc Natl Acad Sci U S A *94*, 5213-5218.

Bergerat, A., de Massy, B., Gadelle, D., Varoutas, P.C., Nicolas, A., and Forterre, P. (1997). An atypical topoisomerase II from Archaea with implications for meiotic recombination. Nature *386*, 414-417.

Bishop, D.K., Nikolski, Y., Oshiro, J., Chon, J., Shinohara, M., and Chen, X. (1999). High copy number suppression of the meiotic arrest caused by a dmc1 mutation: *REC114* imposes an early recombination block and *RAD54* promotes a *DMC1*-independent DSB repair pathway. Genes Cells *4*, 425-444.

Bishop, D.K., Park, D., Xu, L., and Kleckner, N. (1992a). *DMC1:* a meiosis-specific yeast homolog of *E. coli recA* required for recombination, synaptonemal complex formation, and cell cycle progression. Cell *69*, 439-456.

Bishop, D.K., Park, D., Xu, L., and Kleckner, N. (1992b). *DMC1*: a meiosis-specific yeast homolog of *E. coli* recA required for recombination, synaptonemal complex formation, and cell cycle progression. Cell 69, 439-456.

Blat, Y., and Kleckner, N. (1999). Cohesins bind to preferential sites along yeast chromosome III, with differential regulation along arms versus the centric region. Cell *98*, 249-259.

Borde, V., Lin, W., Novikov, E., Petrini, J.H., Lichten, M., and Nicolas, A. (2004). Association of Mre11p with double-strand break sites during yeast meiosis. Mol Cell *13*, 389-401.

Bremer, M.C., Gimble, F.S., Thorner, J., and Smith, C.L. (1992). VDE endonuclease cleaves *S. cerevisiae* genomic DNA at a single site: physical mapping of the *VMA1* gene. Nucleic Acids Res *20*, 5484.

Cao, L., Alani, E., and Kleckner, N. (1990). A pathway for generation and processing of double-strand breaks during meiotic recombination in *S. cerevisiae*. Cell *61*, 1089-1101.

Cartagena-Lirola, H., Guerini, I., Viscardi, V., Lucchini, G., and Longhese, M.P. (2006). Budding Yeast Sae2 is an In Vivo Target of the Mec1 and Tel1 Checkpoint Kinases During Meiosis. Cell Cycle *5*, 1549-1559.

Celerin, M., Merino, S.T., Stone, J.E., Menzie, A.M., and Zolan, M.E. (2000). Multiple roles of Spo11 in meiotic chromosome behavior. Embo J *19*, 2739-2750.

Chamankhah, M., Fontanie, T., and Xiao, W. (2000). The *S. cerevisiae* mre11(ts) allele confers a separation of DNA repair and telomere maintenance functions. Genetics *155*, 569-576.

Champoux, J.J. (2001). DNA topoisomerases: structure, function, and mechanism. Annu Rev Biochem *70*, 369-413.

Chen, Y.K., Leng, C.H., Olivares, H., Lee, M.H., Chang, Y.C., Kung, W.M., Ti, S.C., Lo, Y.H., Wang, A.H., Chang, C.S., Bishop, D.K., Hsueh, Y.P., and Wang, T.F. (2004). Heterodimeric complexes of Hop2 and Mnd1 function with Dmc1 to promote meiotic homolog juxtaposition and strand assimilation. Proc Natl Acad Sci U S A *101*, 10572-10577.

Chu, S., DeRisi, J., Eisen, M., Mulholland, J., Botstein, D., Brown, P.O., and Herskowitz, I. (1998). The transcriptional program of sporulation in budding yeast. Science *282*, 699-705.

Clerici, M., Mantiero, D., Lucchini, G., and Longhese, M.P. (2006). The *S. cerevisiae* Sae2 protein negatively regulates DNA damage checkpoint signalling. EMBO Rep *7*, 212-218.

Conrad, M.N., Dominguez, A.M., and Dresser, M.E. (1997). Ndj1p, a meiotic telomere protein required for normal chromosome synapsis and segregation in yeast [see comments]. Science *276*, 1252-1255.

D'Amours, D., and Jackson, S.P. (2002). The Mre11 complex: at the crossroads of DNA repair and checkpoint signalling. Nat Rev Mol Cell Biol *3*, 317-327.

de los Santos, T., and Hollingsworth, N M. (1999) Red1p, a *MEK1*-dependent phosphoprotein that physically interacts with Hop1 during meiosis in yeast. J Bio Chem *3*, 1783-90.

Dernburg, A.F., McDonald, K., Moulder, G., Barstead, R., Dresser, M., and Villeneuve, A.M. (1998). Meiotic recombination in *C. elegans* initiates by a conserved mechanism and is dispensable for homologous chromosome synapsis. Cell *94*, 387-398.

Di Giacomo, M., Barchi, M., Baudat, F., Edelmann, W., Keeney, S., and Jasin, M. (2005). Distinct DNA-damage-dependent and -independent responses drive the loss of oocytes in recombination-defective mouse mutants. Proc Natl Acad Sci U S A *102*, 737-742.

Downs, J.A., Lowndes, N.F., and Jackson, S.P. (2000). A role for *S. cerevisiae* histone H2A in DNA repair. Nature *408*, 1001-1004.

Enomoto, T. (2001). [Function of RecQ family helicases and Bloom's syndrome]. Tanpakushitsu Kakusan Koso *46*, 1082-1088.

Fan, Q., Xu, F., and Petes, T.D. (1995). Meiosis-specific double-strand DNA breaks at the HIS4 recombination hot spot in the yeast *S. cerevisiae:* control in cis and trans. Mol Cell Biol *15*, 1679-1688.

Fikus, M.U., Mieczkowski, P.A., Koprowski, P., Rytka, J., Sledziewska-Gojska, E., and Ciesla, Z. (2000). The product of the DNA damage-inducible gene of *S. cerevisiae*, *DIN7*, specifically functions in mitochondria. Genetics *154*, 73-81.

Fiorentini, P., Huang, K.N., Tishkoff, D.X., Kolodner, R.D., and Symington, L.S. (1997). Exonuclease I of *S. cerevisiae* functions in mitotic recombination in vivo and in vitro. Mol Cell Biol *17*, 2764-2773.

Fukuda, T., Nogami, S., and Ohya, Y. (2003). VDE-initiated intein homing in *S. cerevisiae* proceeds in a meiotic recombination-like manner. Genes Cells *8*, 587-602.

Fung, J.C., Rockmill, B., Odell, M., and Roeder, G.S. (2004). Imposition of crossover interference through the nonrandom distribution of synapsis initiation complexes. Cell *116*, 795-802.

Furuse, M., Nagase, Y., Tsubouchi, H., Murakami-Murofushi, K., Shibata, T., and Ohta, K. (1998). Distinct roles of two separable in vitro activities of yeast Mre11 in mitotic and meiotic recombination. Embo Journal *17*, 6412-6425.

Gasior, S.L., Olivares, H., Ear, U., Hari, D.M., Weichselbaum, R., and Bishop, D.K. (2001). Assembly of RecA-like recombinases: distinct roles for mediator proteins in mitosis and meiosis. Proc Natl Acad Sci U S A *98*, 8411-8418.

Gerton, J.L., DeRisi, J., Shroff, R., Lichten, M., Brown, P.O., and Petes, T.D. (2000). Inaugural article: global mapping of meiotic recombination hotspots and coldspots in the yeast *S. cerevisiae*. Proc Natl Acad Sci U S A *97*, 11383-11390.

Gerton, J.L., and DeRisi, J.L. (2002). Mnd1p: an evolutionarily conserved protein required for meiotic recombination. Proc Natl Acad Sci U S A *99*, 6895-6900.

Gilbertson, L.A., and Stahl, F.W. (1996). A test of the double-strand break repair model for meiotic recombination in *S. cerevisiae*. Genetics *144*, 27-41.

Gimble, F.S., and Thorner, J. (1992). Homing of a DNA endonuclease gene by meiotic gene conversion in *S. cerevisiae*. Nature *357*, 301-306.

Goldman, A.S., and Lichten, M. (2000). Restriction of ectopic recombination by interhomolog interactions during *S. cerevisiae* meiosis. Proc Natl Acad Sci U S A *97*, 9537-9542.

Goyon, C., and Lichten, M. (1993). Timing of molecular events in meiosis in *S. cerevisiae:* stable heteroduplex DNA is formed late in meiotic prophase. Mol Cell Biol *13;* 373-382.

Guacci, V., Hogan, E., and Koshland, D. (1994). Chromosome condensation and sister chromatid pairing in budding yeast. J Cell Biol *125*, 517-530.

Haber, J.E. (2000a). Partners and pathways repairing a double-strand break. Trends Genet *16*, 259-264.

Haber, J.E. (2000b). Recombination: a frank view of exchanges and vice versa. Curr Opin Cell Biol *12*, 286-292.

Hartung, F., and Puchta, H. (2000). Molecular characterisation of two paralogous SPO11 homologues in Arabidopsis thaliana. Nucleic Acids Res *28*, 1548-1554.

Hassold, T., and Hunt, P. (2001). To err (meiotically) is human: the genesis of human aneuploidy. Nat Rev Genet *2*, 280-291.

Hassold, T., Merrill, M., Adkins, K., Freeman, S., and Sherman, S. (1995). Recombination and maternal age-dependent nondisjunction: molecular studies of trisomy 16. Am J Hum Genet *57*, 867-874.

Hayase, A., Takagi, M., Miyazaki, T., Oshiumi, H., Shinohara, M., and Shinohara, A. (2004). A protein complex containing Mei5 and Sae3 promotes the assembly of the meiosis-specific RecA homolog Dmc1. Cell *119*, 927-940.

Henderson, K.A., and Keeney, S. (2004). Tying synaptonemal complex initiation to the formation and programmed repair of DNA double-strand breaks. Proc Natl Acad Sci U S A *101*, 4519-4524.

Hepworth, S.R., Friesen, H., and Segall, J. (1998). *NDT80* and the meiotic recombination checkpoint regulate expression of middle sporulation-specific genes in *S. cerevisiae*. Mol Cell Biol *18*, 5750-5761.

Heyting, C. (1996). Synaptonemal complexes: structure and function. Curr Opin Cell Biol *8*, 389-396.

Hiraoka, Y., Ding, D.Q., Yamamoto, A., Tsutsumi, C., and Chikashige, Y. (2000). Characterization of fission yeast meiotic mutants based on live observation of meiotic prophase nuclear movement. Chromosoma *109*, 103-109.

Hochwagen, A., Tham, W.H., Brar, G.A., and Amon, A. (2005). The FK506 binding protein Fpr3 counteracts protein phosphatase 1 to maintain meiotic recombination checkpoint activity. Cell *122*, 861-873.

Hollingsworth, N.M., and Ponte, L. (1997). Genetic interactions between *HOP1*, *RED1* and *MEK1* suggest that *MEK1* regulates assembly of axial element components during meiosis in the yeast *S. cerevisiae*. Genetics *147*, 33-42.

Hong, E.J., and Roeder, G.S. (2002). A role for Ddc1 in signaling meiotic double-strand breaks at the pachytene checkpoint. Genes Dev *16*, 363-376.

Hopfner, K.P., Craig, L., Moncalian, G., Zinkel, R.A., Usui, T., Owen, B.A., Karcher, A., Henderson, B., Bodmer, J.L., McMurray, C.T., Carney, J.P., Petrini, J.H., and Tainer, J.A. (2002). The Rad50 zinc-hook is a structure joining Mre11 complexes in DNA recombination and repair. Nature *418*, 562-566.

Hubscher, U., Nasheuer, H.P., and Syvaoja, J.E. (2000). Eukaryotic DNA polymerases, a growing family. Trends Biochem Sci *25*, 143-147.

Hunter, N., and Kleckner, N. (2001). The single-end invasion. An asymmetric intermediate at the double-strand break to double-holliday junction transition of meiotic recombination. Cell *106*, 59-70.

Ivanov, E.L., Sugawara, N., Fishman-Lobell, J., and Haber, J.E. (1996). Genetic requirements for the single-strand annealing pathway of double-strand break repair in *S. cerevisiae*. Genetics *142*, 693-704.

John, B. (1990). Meiosis. Cambridge University Press, Cambridge.

Kane, S.M., and Roth, R. (1974). Carbohydrate metabolism during ascospore development in yeast. J Bacteriol *118*, 8-14.

Katis, V.L., Galova, M., Rabitsch, K.P., Gregan, J., and Nasmyth, K. (2004). Maintenance of cohesin at centromeres after meiosis I in budding yeast requires a kinetochore-associated protein related to MEI-S332. Curr Biol *14*, 560-572.

Keeney, S. (2001). Mechanism and control of meiotic recombination initiation. Curr Top Dev Biol *52*, 1-53.

Keeney, S., Baudat, F., Angeles, M., Zhou, Z.H., Copeland, N.G., Jenkins, N.A., Manova, K., and Jasin, M. (1999). A mouse homolog of the *S. cerevisiae* meiotic recombination DNA transesterase Spo11p. Genomics *61*, 170-182.

Keeney, S., Giroux, C.N., and Kleckner, N. (1997). Meiosis-specific DNA double-strand breaks are catalyzed by Spo11, a member of a widely conserved protein family. Cell *88*, 375-384.

Keeney, S., and Kleckner, N. (1995). Covalent protein-DNA complexes at the 5' strand termini of meiosis-specific double-strand breaks in yeast. Proc Natl Acad Sci U S A *92*, 11274-11278.

Khazanehdari, K.A., and Borts, R.H. (2000). EXO1 and MSH4 differentially affect crossing-over and segregation. Chromosoma *109*, 94-102.

Klein, F., Mahr, P., Galova, M., Buonomo, S.B., Michaelis, C., Nairz, K., and Nasmyth, K. (1999). A central role for cohesins in sister chromatid cohesion, formation of axial elements, and recombination during yeast meiosis. Cell *98*, 91-103.

Kolodkin, A.L., Klar, A.J., and Stahl, F.W. (1986). Double-strand breaks can initiate meiotic recombination in *S. cerevisiae*. Cell *46*, 733-740.

Krogh, B.O., Llorente, B., Lam, A., and Symington, L.S. (2005). Mutations in Mre11 phosphoesterase motif I that impair *S. cerevisiae* Mre11-Rad50-Xrs2 complex stability in addition to nuclease activity. Genetics *171*, 1561-1570.

Lee, J.Y., and Orr-Weaver, T.L. (2001). The molecular basis of sister-chromatid cohesion. Annu Rev Cell Dev Biol *17*, 753-777.

Leu, J.Y., Chua, P.R., and Roeder, G.S. (1998). The meiosis-specific Hop2 protein of *S. cerevisiae* ensures synapsis between homologous chromosomes. Cell *94*, 375-386.

Leu, J.Y., and Roeder, G.S. (1999). The pachytene checkpoint in *S. cerevisiae* depends on Swe1-mediated phosphorylation of the cyclin-dependent kinase Cdc28. Mol Cell *4*, 805-814.

Lewis, L.K., Storici, F., Van Komen, S., Calero, S., Sung, P., and Resnick, M.A. (2004). Role of the nuclease activity of *S. cerevisiae* Mre11 in repair of DNA double-strand breaks in mitotic cells. Genetics *166*, 1701-1713.

Lin, J.J., and Zakian, V.A. (1994). Isolation and characterization of two *S. cerevisiae* genes that encode proteins that bind to (TG1-3)n single strand telomeric DNA in vitro [published erratum appears in Nucleic Acids Res 1994 Dec 11;22(24):5516]. Nucleic Acids Res *22*, 4906-4913.

Llorente, B., and Symington, L.S. (2004). The Mre11 nuclease is not required for 5' to 3' resectioning at multiple HO-induced double-strand breaks. Mol Cell Biol *24*, 9682-9694.

Longhese, M.P., Foiani, M., Muzi-Falconi, M., Lucchini, G., and Plevani, P. (1998). DNA damage checkpoint in budding yeast. Embo J *17*, 5525-5528.

Lustig, A.J. (1998). Mechanisms of silencing in *S. cerevisiae*. Curr Opin Genet Dev *8*, 233-239.

Lydall, D., Nikolsky, Y., Bishop, D.K., and Weinert, T. (1996). A meiotic recombination checkpoint controlled by mitotic checkpoint genes. Nature *383*, 840-843.

Mahadevaiah, S.K., Turner, J.M., Baudat, F., Rogakou, E.P., de Boer, P., Blanco-Rodriguez, J., Jasin, M., Keeney, S., Bonner, W.M., and Burgoyne, P.S. (2001). Recombinational DNA double-strand breaks in mice precede synapsis. Nat Genet *27*, 271-276.

Malkova, A., Ross, L., Dawson, D., Hoekstra, M.F., and Haber, J.E. (1996). Meiotic recombination initiated by a double-strand break in rad50 delta yeast cells otherwise unable to initiate meiotic recombination. Genetics *143*, 741-754.

Mao-Draayer, Y., Galbraith, A.M., Pittman, D.L., Cool, M., and Malone, R.E. (1996). Analysis of meiotic recombination pathways in the yeast *S. cerevisiae*. Genetics *144*, 71-86.

Martini, E., Diaz, R.L., Hunter, N., and Keeney, S. (2006). Crossover homeostasis in yeast meiosis. Cell *126*, 285-295.

McKee, A.H., and Kleckner, N. (1997). A general method for identifying recessive diploid-specific mutations in *S. cerevisiae*, its application to the isolation of mutants blocked at intermediate stages of meiotic prophase and characterization of a new gene SAE2. Genetics *146*, 797-816.

McKim, K.S., and Hayashi-Hagihara, A. (1998). mei-W68 in *Drosophila melanogaster* encodes a spo11 homolog: evidence that the mechanism for initiating meiotic recombination is conserved. Genes Dev *12*, 2932-2942.

Mirzoeva, O.K., and Petrini, J.H. (2003). DNA replication-dependent nuclear dynamics of the Mre11 complex. Mol Cancer Res *1*, 207-218.

Miyazaki, W.Y., and Orrweaver, T.L. (1994). Sister-chromatid cohesion in mitosis and meiosis. Annual Review Of Genetics *28*, 167-187.

Moens, P.B., Pearlman, R.E., Heng, H.H., and Traut, W. (1998). Chromosome cores and chromatin at meiotic prophase. Curr Top Dev Biol *37*, 241-262.

Moreau, S., Ferguson, J.R., and Symington, L.S. (1999). The nuclease activity of Mre11p is required for meiosis but not for mating type switching, end joining, or telomere maintenance. Mol Cell Biol *19*, 556-566.

Moreau, S., Morgan, E.A., and Symington, L.S. (2001). Overlapping functions of the *S. cerevisiae* Mre11, Exo1 and Rad27 nucleases in DNA metabolism. Genetics *159*, 1423-1433.

Moses, M.J., and Solari, A.J. (1976). Positive contrast staining and protected drying of surface spreads: electron microscopy of the synaptonemal complex by a new method. J Ultrastruct Res *54*, 109-114.

Nag, D.K., Scherthan, H., Rockmill, B., Bhargava, J., and Roeder, G.S. (1995). Heteroduplex DNA formation and homolog pairing in yeast meiotic mutants. Genetics *141*, 75-86.

Nairz, K., and Klein, F. (1997). mre11S a yeast mutation that blocks double-strand-break processing and permits nonhomologous synapsis in meiosis. Genes Dev *11*, 2272-2290.

Nakada, D., Hirano, Y., and Sugimoto, K. (2004). Requirement of the Mre11 complex and exonuclease 1 for activation of the Mec1 signaling pathway. Mol Cell Biol *24*, 10016-10025.

Nakada, D., Matsumoto, K., and Sugimoto, K. (2003). ATM-related Tel1 associates with double-strand breaks through an Xrs2-dependent mechanism. Genes Dev *17*, 1957-1962.

Nasmyth, K., Peters, J.M., and Uhlmann, F. (2000). Splitting the chromosome: cutting the ties that bind sister chromatids. Science *288*, 1379-1385.

Neale, M.J., and Keeney, S. (2006). Clarifying the mechanics of DNA strand exchange in meiotic recombination. Nature *442*, 153-158.

Neale, M.J., Pan, J., and Keeney, S. (2005). Endonucleolytic processing of covalent protein-linked DNA double-strand breaks. Nature *436*, 1053-1057.

Neale, M.J., Ramachandran, M., Trelles-Sticken, E., Scherthan, H., and Goldman, A.S. (2002). Wild-type levels of Spo11-induced DSBs are required for normal single-strand resectioning during meiosis. Mol Cell *9*, 835-846.

Nicolas, A., Treco, D., Schultes, N.P., and Szostak, J.W. (1989). An initiation site for meiotic gene conversion in the yeast *S. cerevisiae*. Nature *338*, 35-39.

Niu, H., Wan, L., Baumgartner, B., Schaefer, D., Loidl, J., and Hollingsworth, N.M. (2005). Partner choice during meiosis is regulated by Hop1-promoted dimerization of Mek1. Mol Biol Cell *16*, 5804-5818.

Padmore, R., Cao, L., and Kleckner, N. (1991). Temporal comparison of recombination and synaptonemal complex formation during meiosis in *S. cerevisiae*. Cell *66*, 1239-1256.

Paques, F., and Haber, J.E. (1999). Multiple pathways of recombination induced by double-strand breaks in *S. cerevisiae*. Microbiology and Molecular Biology Reviews *63*, 349-404.

Pastink, A., Eeken, J.C., and Lohman, P.H. (2001). Genomic integrity and the repair of double-strand DNA breaks. Mutat Res *480-481*, 37-50.

Paull, T.T., and Gellert, M. (2000). A mechanistic basis for Mre11-directed DNA joining at microhomologies. Proc Natl Acad Sci U S A *97*, 6409-6414.

Petrini, J.H. (1999). The mammalian Mre11-Rad50-nbs1 protein complex: integration of functions in the cellular DNA-damage response. American Journal of Human Genetics *64*, 1264-1269.

Petukhova, G., Sung, P., and Klein, H. (2000). Promotion of Rad51-dependent D-loop formation by yeast recombination factor Rdh54/Tid1. Genes Dev *14*, 2206-2215.

Petukhova, G.V., Pezza, R.J., Vanevski, F., Ploquin, M., Masson, J.Y., and Camerini-Otero, R.D. (2005). The Hop2 and Mnd1 proteins act in concert with Rad51 and Dmc1 in meiotic recombination. Nat Struct Mol Biol *12*, 449-453.

Prinz, S., Amon, A., and Klein, F. (1997). Isolation of *COM1*, a new gene required to complete meiotic double-strand break-induced recombination in *S. cerevisiae*. Genetics *146*, 781-795.

Rasmussen, S.W. (1986). Chromosome interlocking during synapsis--a transient disorder. Tokai J Exp Clin Med *11*, 437-451.

Ritchie, K.B., and Petes, T.D. (2000). The Mre11p/Rad50p/Xrs2p complex and the Tel1p function in a single pathway for telomere maintenance in yeast. Genetics *155*, 475-479.

Rockmill, B., Engebrecht, J.A., Scherthan, H., Loidl, J., and Roeder, G.S. (1995). The yeast MER2 gene is required for chromosome synapsis and the initiation of meiotic recombination. Genetics *141*, 49-59.

Rockmill, B., Fung, J.C., Branda, S.S., and Roeder, G.S. (2003). The Sgs1 helicase regulates chromosome synapsis and meiotic crossing over. Curr Biol *13*, 1954-1962.

Roeder, G.S. (1997). Meiotic chromosomes: it takes two to tango. Genes Dev *11*, 2600-2621.

Roeder, G.S., and Bailis, J.M. (2000). The pachytene checkpoint. Trends Genet *16*, 395-403.

Rogakou, E.P., Boon, C., Redon, C., and Bonner, W.M. (1999). Megabase chromatin domains involved in DNA double-strand breaks in vivo. J Cell Biol *146*, 905-916.

Rogakou, E.P., Pilch, D.R., Orr, A.H., Ivanova, V.S., and Bonner, W.M. (1998). DNA double-stranded breaks induce histone H2AX phosphorylation on serine 139. J Biol Chem *273*, 5858-5868.

Rouse, J., and Jackson, S.P. (2002). Lcd1p recruits Mec1p to DNA lesions in vitro and in vivo. Mol Cell *9*, 857-869.

San-Segundo, P.A., and Roeder, G.S. (1999). Pch2 links chromatin silencing to meiotic checkpoint control. Cell *97*, 313-324.

San-Segundo, P.A., and Roeder, G.S. (2000). Role for the silencing protein Dot1 in meiotic checkpoint control. Mol Biol Cell *11*, 3601-3615.

Scherthan, H., Weich, S., Schwegler, H., Heyting, C., Harle, M., and Cremer, T. (1996). Centromere and telomere movements during early meiotic prophase of mouse and man are associated with the onset of chromosome pairing. J Cell Biol *134*, 1109-1125.

Schmekel, K., Skoglund, U., and Daneholt, B. (1993). The three-dimensional structure of the central region in a synaptonemal complex: a comparison between rat and two insect species, *Drosophila melanogaster* and *Blaps cribrosa*. Chromosoma *102*, 682-692.

Schwacha, A., and Kleckner, N. (1994). Identification of joint molecules that form frequently between homologs but rarely between sister chromatids during yeast meiosis. Cell *76*, 51-63.

Schwacha, A., and Kleckner, N. (1997). Interhomolog bias during meiotic recombination: meiotic functions promote a highly differentiated interhomolog-only pathway. Cell *90*, 1123-1135.

Sears, D.D., Hegemann, J.H., and Hieter, P. (1992). Meiotic recombination and segregation of human-derived artificial chromosomes in *S. cerevisiae*. Proc Natl Acad Sci U S A *89*, 5296-5300.

Sehorn, M.G., Sigurdsson, S., Bussen, W., Unger, V.M., and Sung, P. (2004). Human meiotic recombinase Dmc1 promotes ATP-dependent homologous DNA strand exchange. Nature *429*, 433-437.

Shimomura, T., Ando, S., Matsumoto, K., Sugimoto, K. (1998). Functional and physical interaction between Rad24 and Rfc5 in the yeast checkpoint pathways. Mol Cell Biol. *18*. 5485-5491

Shinohara, M., Shita-Yamaguchi, E., Buerstedde, J.M., Shinagawa, H., Ogawa, H., and Shinohara, A. (1997). Characterization of the roles of the *S. cerevisiae* RAD54 gene and a homologue of RAD54, RDH54/TID1, in mitosis and meiosis. Genetics *147*, 1545-1556.

Shiomi, y., Shinozaki, A., Nakada, D., Sugimoto, K., Usukura, J., Obuse, C., Tsurimoto, T. (2002). Clamp and clamp loader structures of the human checkpoint protein complexes, Rad9-1-1 and Rad17-RFC. Genes Cells. *7*. 861-868

Shuster, E.O., and Byers, B. (1989). Pachytene arrest and other meiotic effects of the start mutations in *S. cerevisiae*. Genetics *123*, 29-43.

Signon, L., Malkova, A., Naylor, M.L., Klein, H., and Haber, J.E. (2001). Genetic requirements for RAD51- and RAD54-independent break-induced replication repair of a chromosomal double-strand break. Mol Cell Biol *21*, 2048-2056.

Smith, A.V., and Roeder, G.S. (1997). The yeast Red1 protein localizes to the cores of meiotic chromosomes. J Cell Biol *136*, 957-967.

Stahl, F.W., Foss, H.M., Young, L.S., Borts, R.H., Abdullah, M.F., and Copenhaver, G.P. (2004). Does crossover interference count in *S. cerevisiae*? Genetics *168*, 35-48.

Stewart, G.S., Maser, R.S., Stankovic, T., Bressan, D.A., Kaplan, M.I., Jaspers, N.G., Raams, A., Byrd, P.J., Petrini, J.H., and Taylor, A.M. (1999). The DNA double-strand break repair gene hMRE11 is mutated in individuals with an ataxia-telangiectasia-like disorder. Cell *99*, 577-587.

Sugawara, N., and Haber, J.E. (1992a). Characterization of double-strand break-induced recombination: homology requirements and single-stranded DNA formation. Molecular and Cellular Biology *12*, 563-575.

Sugawara, N., and Haber, J.E. (1992b). Characterization of double-strand break-induced recombination: homology requirements and single-stranded DNA formation. Mol Cell Biol *12*, 563-575.

Sugawara, N., Ira, G., and Haber, J.E. (2000). DNA length dependence of the single-strand annealing pathway and the role of *S. cerevisiae RAD59* in double-strand break repair. Mol Cell Biol *20*, 5300-5309.

Sung, P., Krejci, L., Van Komen, S., and Sehorn, M.G. (2003). Rad51 recombinase and recombination mediators. J Biol Chem *278*, 42729-42732.

Svoboda, A., Bahler, J., and Kohli, J. (1995). Microtubule-driven nuclear movements and linear elements as meiosis-specific characteristics of the fission yeasts *Schizosaccharomyces versatilis* and *Schizosaccharomyces pombe*. Chromosoma *104*, 203-214.

Symington, L.S., Kang, L.E., and Moreau, S. (2000). Alteration of gene conversion tract length and associated crossing over during plasmid gap repair in nuclease-deficient strains of *S. cerevisiae*. Nucleic Acids Res *28*, 4649-4656.

Szankasi, P., and Smith, G.R. (1995). A role for exonuclease I from S. pombe in mutation avoidance and mismatch correction. Science *267*, 1166-1169.

Thompson, D.A., and Stahl, F.W. (1999). Genetic control of recombination partner preference in yeast meiosis. Isolation and characterization of mutants elevated for meiotic unequal sister-chromatid recombination. Genetics *153*, 621-641.

Tishkoff, D.X., Boerger, A.L., Bertrand, P., Filosi, N., Gaida, G.M., Kane, M.F., and Kolodner, R.D. (1997). Identification and characterization of *S. cerevisiae* EXO1, a gene encoding an exonuclease that interacts with MSH2. Proc Natl Acad Sci U S A *94*, 7487-7492.

Tong, A.H., Lesage, G., Bader, G.D., Ding, H., Xu, H., Xin, X., Young, J., Berriz, G.F., Brost, R.L., Chang, M., Chen, Y., Cheng, X., Chua, G., Friesen, H., Goldberg, D.S., Haynes, J., Humphries, C., He, G., Hussein, S., Ke, L., Krogan, N., Li, Z., Levinson, J.N., Lu, H., Menard, P., Munyana, C., Parsons, A.B., Ryan, O., Tonikian, R., Roberts, T., Sdicu, A.M., Shapiro, J., Sheikh, B., Suter, B., Wong, S.L., Zhang, L.V., Zhu, H., Burd, C.G., Munro, S., Sander, C., Rine, J., Greenblatt, J., Peter, M., Bretscher, A., Bell, G., Roth, F.P., Brown, G.W., Andrews, B., Bussey, H., and Boone, C. (2004). Global mapping of the yeast genetic interaction network. Science *303*, 808-813.

Tran, P.T., Erdeniz, N., Dudley, S., and Liskay, R.M. (2002). Characterization of nuclease-dependent functions of Exo1p in *S. cerevisiae*. DNA Repair (Amst) *1*, 895-912.

Tran, P.T., Erdeniz, N., Symington, L.S., and Liskay, R.M. (2004). EXO1-A multi-tasking eukaryotic nuclease. DNA Repair (Amst) *3*, 1549-1559.

Trelles-Sticken, E., Dresser, M.E., and Scherthan, H. (2000). Meiotic telomere protein Ndj1p is required for meiosis-specific telomere distribution, bouquet formation and efficient homologue pairing. J Cell Biol *151*, 95-106.

Trujillo, K.M., Roh, D.H., Chen, L., Van Komen, S., Tomkinson, A., and Sung, P. (2003). Yeast xrs2 binds DNA and helps target rad50 and mre11 to DNA ends. J Biol Chem *278*, 48957-48964.

Trujillo, K.M., and Sung, P. (2001). DNA structure-specific nuclease activities in the *S. cerevisiae* Rad50-Mre11 complex. J Biol Chem *276*, 35458-35464.

Trujillo, K.M., Yuan, S.S., Lee, E.Y., and Sung, P. (1998). Nuclease activities in a complex of human recombination and DNA repair factors Rad50, Mre11, and p95. Journal of Biological Chemistry *273*, 21447-21450.

Tsubouchi, H., and Ogawa, H. (1998). A novel mre11 mutation impairs processing of double-strand breaks of DNA during both mitosis and meiosis. Mol Cell Biol *18*, 260-268.

Tsubouchi, H., and Ogawa, H. (2000). Exo1 roles for repair of DNA double-strand breaks and meiotic crossing over in *S. cerevisiae*. Mol Biol Cell *11*, 2221-2233.

Tsubouchi, H., and Roeder, G.S. (2002). The Mnd1 protein forms a complex with hop2 to promote homologous chromosome pairing and meiotic double-strand break repair. Mol Cell Biol *22*, 3078-3088.

Tsubouchi, H., and Roeder, G.S. (2003). The importance of genetic recombination for fidelity of chromosome pairing in meiosis. Dev Cell *5*, 915-925.

Tsubouchi, H., and Roeder, G.S. (2004). The budding yeast mei5 and sae3 proteins act together with dmc1 during meiotic recombination. Genetics *168*, 1219-1230.

Tsukuda, T., Fleming, A.B., Nickoloff, J.A., and Osley, M.A. (2005). Chromatin remodelling at a DNA double-strand break site in *S. cerevisiae*. Nature *438*, 379-383.

Usui, T., Ogawa, H., and Petrini, J.H. (2001a). A DNA damage response pathway controlled by Tel1 and the Mre11 complex. Mol Cell *7*, 1255-1266.

Usui, T., Ohta, T., Oshiumi, H., Tomizawa, J., Ogawa, H., and Ogawa, T. (1998). Complex formation and functional versatility of Mre11 of budding yeast in recombination. Cell *95*, 705-716.

Varon, R., Vissinga, C., Platzer, M., Cerosaletti, K.M., Chrzanowska, K.H., Saar, K., Beckmann, G., seemanova, E., Cooper, P.R., Nowak, N.J., Stumm, M., Weemaes, C.M., Gatti, R.A., Wilson, R.K., Digweed, M., Rosenthal, A., Sperling, K., Concannon, P., and Reis, A. (1998). Nibrin, a novel DNA double-strand break repair protein, is mutated in Nijmegen breakage syndrome. Cell *93*, 467-476.

Vaze, M.B., Pellicioli, A., Lee, S.E., Ira, G., Liberi, G., Arbel-Eden, A., Foiani, M., and Haber, J.E. (2002). Recovery from checkpoint-mediated arrest after repair of a double-strand break requires Srs2 helicase. Mol Cell *10*, 373-385.

Villeneuve, A.M. (2001). Development. How to stimulate your partner. Science *291*, 2099-2101.

Villeneuve, A.M., and Hillers, K.J. (2001). Whence meiosis? Cell *106*, 647-650.

Waga, S., and Stillman, B. (1998). The DNA replication fork in eukaryotic cells. Annu Rev Biochem *67*, 721-751.

Wan, L., de los Santos, T., Zhang, C., Shokat, K., and Hollingsworth, N.M. (2004). Mek1 kinase activity functions downstream of RED1 in the regulation of meiotic double strand break repair in budding yeast. Mol Biol Cell *15*, 11-23.

Wang, T.F., Kleckner, N., and Hunter, N. (1999). Functional specificity of MutL homologs in yeast: evidence for three Mlh1-based heterocomplexes with distinct roles during meiosis in recombination and mismatch correction. Proc Natl Acad Sci U S A *96*, 13914-13919.

Wei, K., Clark, A.B., Wong, E., Kane, M.F., Mazur, D.J., Parris, T., Kolas, N.K., Russell, R., Hou, H., Jr., Kneitz, B., Yang, G., Kunkel, T.A., Kolodner, R.D., Cohen, P.E., and Edelmann, W. (2003). Inactivation of Exonuclease 1 in mice results in DNA mismatch repair defects, increased cancer susceptibility, and male and female sterility. Genes Dev *17*, 603-614.

Weiner, B.M., and Kleckner, N. (1994). Chromosome pairing via multiple interstitial interactions before and during meiosis in yeast. Cell *77*, 977-991.

Woltering, D., Baumgartner, B., Bagchi, S., Larkin, B., Loidl, J., de los Santos, T., and Hollingsworth, N.M. (2000). Meiotic segregation, synapsis, and recombination checkpoint functions require physical interaction between the chromosomal proteins Red1p and Hop1p. Mol Cell Biol *20*, 6646-6658.

Xu, L., Ajimura, M., Padmore, R., Klein, C., and Kleckner, N. (1995). NDT80, a meiosis-specific gene required for exit from pachytene in *S. cerevisiae*. Mol Cell Biol *15*, 6572-6581.

Xu, L., Weiner, B.M., and Kleckner, N. (1997). Meiotic cells monitor the status of the interhomolog recombination complex. Genes Dev *11*, 106-118.

Yokobayashi, S., Yamamoto, M., and Watanabe, Y. (2003). Cohesins determine the attachment manner of kinetochores to spindle microtubules at meiosis I in fission yeast. Mol Cell Biol *23*, 3965-3973.

Yu, J., Marshall, K., Yamaguchi, M., Haber, J.E., and Weil, C.F. (2004). Microhomology-Dependent End Joining and Repair of Transposon-Induced DNA Hairpins by Host Factors in *S. cerevisiae*. Mol Cell Biol *24*, 1351-1364.

Zetka, M.C., Kawasaki, I., Strome, S., and Muller, F. (1999). Synapsis and chiasma formation in *Caenorhabditis elegans* require HIM-3, a meiotic chromosome core component that functions in chromosome segregation. Genes Dev *13*, 2258-2270.

Zickler, D., and Kleckner, N. (1998). The leptotene-zygotene transition of meiosis. Annu Rev Genet *32*, 619-697.

Zickler, D., and Kleckner, N. (1999). Meiotic chromosomes: integrating structure and function. Annu Rev Genet *33*, 603-754.

Zierhut, C., Berlinger, M., Rupp, C., Shinohara, A., and Klein, F. (2004). Mnd1 is required for meiotic interhomolog repair. Curr Biol *14*, 752-762.

Zou, L., and Elledge, S.J. (2003). Sensing DNA damage through ATRIP recognition of RPA-ssDNA complexes. Science *300*, 1542-1548.